ISSN 2572-5505

Journal of Exploratory Research in Pharmacology

2023 Volume 8 Issue 2
April / May / June

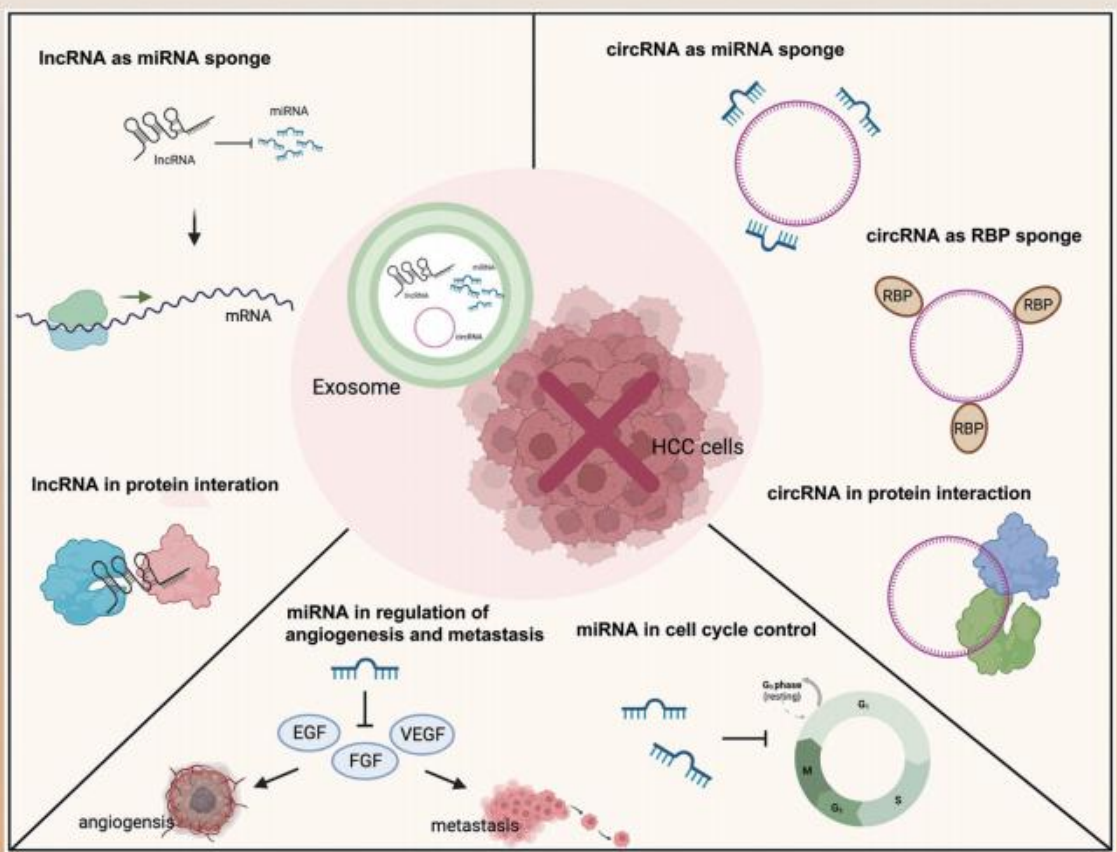

Therapeutic Potential of Extracellular Vesicles as Vehicles to Deliver Druggable Molecules for Hepatocellular Carcinoma page 164

JERP

PUBLISHED BY XIA & HE PUBLISHING INC.
eISSN: 2572-5505
Frequency: Quarterly
Launch date: November 10, 2016 (Volume 1, Issue 1)

Contact Information

Editorial Office

Managing Editor: Lisa Li Chen
Telephone: +1-409-420-2868
E-mail: jerp@xiahepublishing.com
Postal Address: 14090 Southwest Freeway, Suite 300, Sugar Land, Texas, 77478, USA

Publisher

Xia & He Publishing Inc.
Website: www.xiahepublishing.com
E-mail: service@xiahepublishing.com
Postal Address: 14090 Southwest Freeway, Suite 300, Sugar Land, Texas, 77478, USA

Current Issue: Volume 8, Issue 2

Publication date: June 25, 2023

Aims and Scope

Journal of Exploratory Research in Pharmacology (JERP) publishes original innovative exploratory research articles, state-of-the-art reviews, editorials, short communications that focus on novel findings and the most recent advances in basic and clinical pharmacology, covering topics from drug research, drug development, clinical trials and application. Topics included, but not limited to the following areas will be considered for publication in JERP: drug composition and properties; synthesis and design of drugs and potential drugs; molecular/cellular and organ/system mechanisms; signal transduction/cellular communications/interactions; toxicology; chemical biology; molecular/biomarker diagnostics; therapeutics; medical applications; interventional (phases I-IV) clinical trials; observational (post-marketing) clinical studies on investigational new drugs; pharmacogenetics; pharmacoepigenetics; pharmacokinetics; pharmacodynamics; molecular pharmacology; transgenic models.

Indexing & Archiving

JERP is now included in Dimensions, Directory of Research Journals Indexing (DRJI), Google Scholar, Index Copernicus, Naver Academic, Publons, ResearchGate, Road, ScienceGate, Scilit, Semantic Scholar.

Open Access

Disclaimer

Links

Journal Home: https://www.xiahepublishing.com/journal/jerp
Editorial Board: https://www.xiahepublishing.com/journal/jerp/editors
Archive: https://www.xiahepublishing.com/journal/jerp/archive
Instructions for Authors: https://www.xiahepublishing.com/journal/jerp/instruction
Online Submission System: https://www.publinexh.com/

Editorial Board

JERP

Associate Editors

Editorial Board Members

Editorial Board Members

JOURNAL OF EXPLORATORY RESEARCH IN PHARMACOLOGY

CONTENTS

2023 8(2):93–179

Journal of Exploratory Research in Pharmacology **2023** vol. 8(2) | 93–94
DOI: 10.14218/JERP.2023.00025

Editorial

Detriments of Antioxidant Oversupply and Determination of the Oxidative Status

Wei-Zheng Zhang*

VIDRL and The Peter Doherty Institute for Infection and Immunity, Melbourne, Australia

Received: March 31, 2023 | **Revised:** May 08, 2023 | **Accepted:** May 30, 2023 | **Published online:** June 12, 2023

The recent review article "Antioxidants for the treatment of non-communicable diseases" discussed the benefits of antioxidants in treating certain diseases.[1] Although the authors briefly mentioned the roles of oxidants in cell metabolism and defense, they may not have emphasized the potential detriments of an oversupply of antioxidants. The cellular antioxidant defense mechanism plays an important role in maintaining *in vivo* metabolism with a U-shaped dose-response relationship to health outcomes, meaning that both excessive and insufficient levels of antioxidants can cause metabolic disorders (details have been reviewed by Zhang).[2]

While antioxidants are often viewed as beneficial, it is important to recognize their double-edged nature and not overlook their detrimental effects. The market is saturated with over-the-counter antioxidant products and exaggerated advertising that lacks any proper indication of detrimental effects leading to the unrestrained use, and possible misuse, of these products, resulting in metabolic diseases. Supplemental antioxidants can only be effective in treating diseases when cells produce excessive reactive oxygen species that the endogenous antioxidant defense mechanism cannot counterbalance resulting in imbalanced oxidant homeostasis. However, over-supplementing with antioxidants can also disturb the homeostasis and induce metabolic diseases by excessively lowering levels of reactive oxygen species (ROS). Moreover, it can disrupt the body's innate antioxidant defenses by interacting with enzymes such as superoxide dismutase, glutathione peroxidase, and catalase. Adequate levels of ROS are necessary for vital physiological functions such as signaling pathways and immune system responses. In some populations, excessive selenium supplementation may increase the likelihood of developing type 2 diabetes and metabolic syndrome.[3] Moreover, vitamin E and A supplements have been found to disrupt cell metabolism in a peculiar manner, which may result in an elevated risk of type 2 diabetes, cardiovascular diseases, and even some cancers.[4] It has also been indicated that excessive intake of selenium may hinder insulin signaling and associated glucose metabolism as well as dyslipidemia, contributing to metabolic syndrome. Similarly, an overabundance of vitamin E or A, or both, can impede the immune system's capacity to identify and eliminate cancer cells, potentially promoting their growth. To ensure the safe effective administration of antioxidants, it is essential to evaluate an individual's oxidative status before providing antioxidant supplementation.

A recent publication suggests that before taking antioxidant supplements, an individual's oxidative status should be determined as a baseline for correcting imbalanced oxidative homeostasis and avoiding a potential oversupply of antioxidants.[2] However, selecting a biomarker for the quantification of oxidative stress can be challenging due to the instability of oxidant molecules. To address this, the author developed a simple and reliable method for determining blood-free 3-Nitrotyrosine (3NT) as an oxidative stress marker and recommended it for clinical applications.[5] 3NT is formed proportionally by the nitration of protein-bound and free tyrosine residues under oxidative stress through the reactive peroxynitrite molecules formed from the reaction between reactive oxygen and nitrogen species. An integrative panel of multi-markers for oxidative stress is also proposed for more extensive measurement in humans.[6] By implementing the measurement, individuals should be able to safely and efficiently supplement with antioxidants without exerting significant detrimental effects.

In conclusion, while antioxidants have beneficial effects, it is important to recognize their potential detrimental effects. Timely measuring an individual's oxidative status is essential for accurate supplementation of antioxidants and avoiding adverse effects.

Acknowledgments

None.

Funding

None.

Conflict of interest

None.

Abbreviations: 3NT, 3-Nitrotyrosine.

***Correspondence to:** Wei-Zheng Zhang, VIDRL and The Peter Doherty Institute for Infection and Immunity, Melbourne 3000, Australia. ORCID: https://orcid.org/0000-0002-8509-3490. Tel: +61413144193, Fax: +61 3 9342 2666, E-mail: weizzhang@hotmail.com

How to cite this article: Zhang WZ. Detriments of Antioxidant Oversupply and Determination of the Oxidative Status. *J Explor Res Pharmacol* 2023;8(2):93–94. doi: 10.14218/JERP.2023.00025.

References

[1] Ayoka TO, Ezema BO, Eze CN, Nnadi CO. Antioxidants for the Preven-

tion and Treatment of Non-communicable Diseases. J Explor Res Pharmacol 2022;7(3):178–188. doi:10.14218/JERP.2022.00028.
[2] Zhang WZ. The Double-edged Sword of Antioxidant Supplements on Metabolic Diseases, A Necessity for Quantification of Oxidative Status. Archives of Epidemiology & Public Health Research 2023;2(1):168–171. doi:10.33140/aephr.02.01.06.
[3] Yuan Z, Xu X, Ye H, Jin L, Zhang X, Zhu Y. High levels of plasma selenium are associated with metabolic syndrome and elevated fasting plasma glucose in a Chinese population: A case-control study. J Trace Elem Med Biol 2015;32:189–194. doi:10.1016/j.jtemb.2015.07.009, PMID:26302928.
[4] Sharifi-Rad M, Anil Kumar NV, Zucca P, Varoni EM, Dini L, Panzarini E, *et al*. Lifestyle, Oxidative Stress, and Antioxidants: Back and Forth in the Pathophysiology of Chronic Diseases. Front Physiol 2020;11:694. doi:10.3389/fphys.2020.00694, PMID:32714204.
[5] Zhang WZ, Lang C, Kaye DM. Determination of plasma free 3-nitrotyrosine and tyrosine by reversed-phase liquid chromatography with 4-fluoro-7-nitrobenzofurazan derivatization. Biomed Chromatogr 2007;21(3):273–278. doi:10.1002/bmc.750, PMID:17236239.
[6] Squillacioti G, Guglieri F, Colombi N, Ghelli F, Berchialla P, Gardois P, *et al*. Non-Invasive Measurement of Exercise-Induced Oxidative Stress in Response to Physical Activity. A Systematic Review and Meta-Analysis. Antioxidants (Basel) 2021;10(12):2008. doi:10.3390/antiox10122008, PMID:34943111.

Journal of Exploratory Research in Pharmacology **2023** vol. 8(2) | 95–106
DOI: 10.14218/JERP.2022.00061

Original Article

Virtual Screening of Shuanghuanglian Components for the Binding to the Proteinases of SARS-CoV-2

Yu-Shun Yang[1,2,3*], Dilimulati Ainiwaer[2], Xiao Wang[1], Chao-Yue Wang[1] and Jie Yang[2*]

[1]*Jinhua Advanced Research Institute, Jinhua, China;* [2]*State Key Laboratory of Pharmaceutical Biotechnology, School of Life Sciences, Nanjing University, Nanjing, China;* [3]*Research Center of Sensors and Functional Materials, Hi-Techjig Co. Ltd., Zhenjiang, China*

Received: July 22, 2022 | **Revised:** September 06, 2022 | **Accepted:** October 19, 2022 | **Published online:** November 23, 2022

Abstract

Background and objectives: Coronavirus disease 2019 (COVID-19), a global pandemic disease caused by SARS-CoV2 infection, has existed for nearly three years. However, there are currently only a few therapeutic drugs available. The objective of this study attempted to explore the potential therapeutic actions of Shuanghuanglian, a traditional Chinese medicine, using molecular docking simulation technology.

Methods: The ingredients of Shuanghuanglian and the approved drugs were structurally evaluated. The potential bindings of the individual ingredients in Shuanghuanglian to the PLPro and Mpro of the SARS-CoV2 were evaluated by molecular docking simulation according to the energy parameters. The corresponding binding patterns into each defined site were analyzed. The pharmacokinetics of the individual ingredients were predicted to preliminarily evaluate their oral bioavailability.

Results: There were 482 unique natural products in the categories of fatty acids, aromatic compounds, glycosides, and sterols. The successfully docked rates of the Shuanghuanglian components binding to the PLPro and Mpro were all higher than those of the compounds in the Food and Drug Administration-approved Drug Library. In general, Shuang and Lian took the primary status in providing the top hits via the hydrogen bonds, while Huang acted as an important supplement to the global activity. Though the selected hits faced the common difficulty of polarity, the deglycosylation and the package by the carriers could also be practical to overcome the pharmacokinetic violation.

Conclusions: Shuang and Lian retain the potential ability to interact with the PLPro and Mpro of SARS-CoV2, and other herbs seem to have the potential to be involved.

Keywords: Coronavirus disease 2019; Natural products; Virtual screening; Potential interactions; Traditional Chinese medicine.

Abbreviations: ADME, absorption, distribution, metabolism, and excretion; CoV, coronavirus; FDA, Food and Drug Administration, USA; HSA, human serum albumin; MERS, Middle East respiratory syndrome; MOF, metal-organic framework; Mpro, main protease; PLPro, papain-like protease; RdRP, RNA-dependent RNA polymerase; SARS, severe acute respiratory syndrome; SMILE, simplified molecular input line entry system; TCMSP, traditional Chinese medicine systems pharmacology database and analysis platform; TPSA, topological polar surface area.

***Correspondence to:** Yu-Shun Yang, Jinhua Advanced Research Institute, Jinhua 321019, China. ORCID: https://orcid.org/0000-0001-5424-8202. Tel: +86 25-8968-2572, Fax: +86 25-8968-2572, E-mail: ys_yang@nju.edu.cn; Jie Yang, State Key Laboratory of Pharmaceutical Biotechnology, School of Life Sciences, Nanjing University, Nanjing 210023, China. ORCID: https://orcid.org/0000-0002-5983-6414. Tel: +86 25-8359-4060, Fax: +86 25-8359-4605, E-mail: yangjie@nju.edu.cn

How to cite this article: Yang YS, Ainiwaer D, Wang X, Wang CY, Yang J. Virtual Screening of Shuanghuanglian Components for the Binding to the Proteinases of SARS-CoV-2. *J Explor Res Pharmacol* 2023;8(2):95–106. doi: 10.14218/JERP.2022.00061.

Introduction

It has been nearly three years since the Coronavirus (CoV) disease 2019 (COVID-19) was first detected in December 2019 in Wuhan, Hubei Province, China.[1] COVID-19 was caused by an infection with a new CoV named severe acute respiratory syndrome coronavirus 2 (SARS-CoV-2),[2] which was the third highly pathogenic virus in addition to the SARS-CoV in 2003,[3] and the Middle East respiratory syndrome coronavirus (MERS-CoV) in 2012.[4] COVID-19 spread to all countries around the world and was declared a pandemic disease by the World Health Organization.[5,6] The SARS-CoV-2, particularly for the recent dominant Omicron strains, seems to be less fatal (~5% *vs.* ~10% and ~40%, respectively) but is more contagious (R_0 = 2.0–6.5) than SARS and MERS.[7–10] Currently, there are a few drugs that have been approved for the treatment of COVID-19 although different types of vaccines have demonstrated to limit the severity of COVID-19 around the world. Hence,

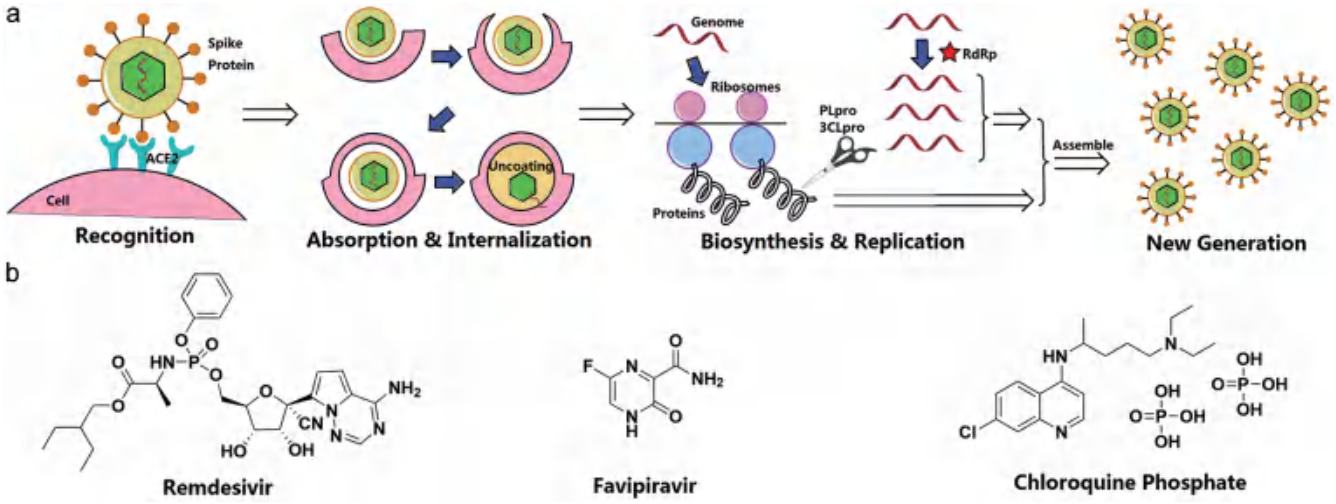

Fig. 1. The life cycle of the SARS-CoV-2 and current potential drugs for COVID-19. (a) The illustration of the SARS-CoV-2 life-cycle following its infection. (b) The potential drugs for treating COVID-19.

understanding the molecular pathogenesis of COVID-19 and the discovery of new therapies are urgently needed (Fig. 1).[11–13] During the life cycle of SARS-CoV-2, four major proteins have been regarded as the potential targets, including the Spike protein for the recognition onto the host, the RNA-dependent RNA polymerase (RdRP) for the replication of RNA, the papain-like protease (PL-Pro), and main protease (Mpro) for preparing the biosynthesis of the next generation of the virus.

At present, the highly restricted policies, immediate isolation of individuals with a positive SARS-CoV2 infection and extensive screening, as well as effective therapies have controlled the spreading of COVID-19 in China.[14,15] In 2020, potential drug candidates, such as Remdesivir, Favipiravir and Chloroquine/Hydroxychloroquine, were chosen for the treatment of COVID-19 patients.[16–19] Recently, Paxlovid and Molnupiravir were approved by the Food and Drug Administration (FDA) of the USA for treatment of patients with early stages of COVID-19 and other biological drugs, such as specific neutralization antibodies that had also been approved for the treatment of patients with severe COVID-19.[20–22] Furthermore, Chinese medicinal herbs, such as Shuanghuanglian, Lianhua Qingwen capsules, Qingfei Paidu decoction, and other modified prescriptions have been recommended for the treatment of patients with mild COVID-19.[16,23,24] However, the pharmacological actions of these Chinese medicinal herbs, particularly for Shuanghuanglian, the first recommended Chinese medicinal herb, have not yet been clarified.[25]

This study explored the potential bindings of the ingredients in Shuanghuanglian to the PLPro and Mpro of SARS-CoV2 according to their crystal structures available in the literature.[26] Shuanghuanglian contains three major ingredients: *Lonicerae Japonicae Flos* (Shuang means Shuanghua also called honeysuckle), *Scutellariae Radix* (Huang means Huangqin), and *Forsythiae Fructus* (Lian means Lianqiao).[27–29] A previous study has reported that miR2911 in honeysuckle inhibits the SARS-CoV-2 replication and accelerates the negative conversion of infected patients.[30–32] Accordingly, we attempted to explore the therapeutic potential of abundant natural products in Chinese medicinal herbs.[33–35] Based on its therapeutic efficiency, the relatively clear compositions, available reference value of other prescriptions, and our previous experience, Shuanghuanglian was chosen for the *in silico* analysis. We scanned the database of the traditional Chinese herbs, analyzed the natural products of each ingredient, conducted the molecular docking simulation, and gave further discussion on the practical potential. Our findings could aid in the design of new medical herbs and help in internationally standardized research on traditional Chinese medicines.[36–38]

Materials and methods

General system and software information

The investigation was mainly conducted on a workstation with the following system configurations: Intel CORE i7-9800X CPU @3.80 GHz processor, system memory: 32 GB RAM, system type: 64-bit operating system, and Windows 10 as the operating system. The data library was mainly summed up and analyzed by the *in silico* simulation in the Windows system using Python and Cygwin. The two-dimensional structure of the compounds was drawn using Chemdraw 14.0 software (ChemBioOffice, CambridgeSoft). The preparation and molecular docking simulation were performed using Discovery Studio 3.5 and Discovery Studio Visualizer 2016 (Accelrys Software, Inc).

Selection of the natural products

The natural products of the corresponding herbs were obtained from the traditional Chinese medicine systems pharmacology database and analysis platform (TCMSP) Version 2.3 launched by the Lab of Systems Pharmacology at Northwest University, Xi'an, Shaanxi Province, China.[39] All the compounds were collected with the Mol ID in this database. The structures in the mol2 format were identified using Chemdraw 14.0 software (ChemBioOffice, CambridgeSoft). The comparison on the percentage of the pass was performed using the FDA-approved Drug Library (2,747 compounds) supported by Selleck (China) (Shanghai, China).

Ligand preparation

All the compounds were prepared with the "Prepare Ligands" modules in Discovery Studio 3.5 (Accelrys Software, Inc). Each prepared ligand was identified to confirm that the conformation agreed with the one in the original database.

Receptor preparation

Based on the topic of the specific treatment instead of the prevention or broad-spectrum therapy, we mainly investigated PLPro and Mpro for preparing the biosynthesis of the next generation virus in the life cycle of SARS-CoV-2. To avoid the same nationality of the initial report,[26] the recent released protein structures by the National Institutes of Health, Bethesda, Maryland, USA or National Science Foundation, Alexandria, Virginia USA were used. Accordingly, the crystal structures of the wild type SARS-CoV-2 PLPro (PDB code: 7JRN),[40] and SARS-CoV-2 Mpro (PDB code: 7CWC) were chosen.[41] Subsequently, we prepared the protein structures with the "Prepare Protein" modules in Discovery Studio 3.5 (Accelrys Software, Inc). During the automatic procedure, the water molecules were eliminated if they did not participate in the interactions, the polar hydrogen was added, and the incomplete loops were repaired. The preparation was performed under a CHARMm minimization.[42]

Afterwards, the hierarchy view of the prepared proteins was unfolded. For PLPro, the binding site was defined as one of GRL0617 (a selective inhibitor of SARS-CoV PLPro).[43] For Mpro, the definition of the binding sites was more complex according to our findings. Basically, the most important site was the N3-binding site as reported.[26] When we studied the receptor cavities more carefully, we defined five binding sites which were more suitable for small molecules. All the binding sites were investigated in this work. Among them, Sites I and II were separated from the N3-binding site, which was near the α-helix-rich region of Mpro; Sites III and IV were independent on the beta (β)-sheet-rich region; while Site V was at the linking position of the two regions.

Molecular docking simulation protocol

Molecular docking simulation was carried out using Discovery Studio 3.5 (Accelrys Software, Inc), and visualization was performed using Discovery Studio Visualizer 2016 (Accelrys Software, Inc). Since the involved ligands bore structural diversity, we chose the graphical user interface CDOCKER protocol, a CHARMm force field-based molecular docking tool with a half-flexible receptor, to implement the simulation.[44] The major steps were as follows:

1. Initially, the conformations of the ligands were generated through high temperature molecular dynamics with different random seeds.
2. In each defined binding site, the original ligands were removed. Subsequently, translating the center of each ligand to a specified position within the receptor active site and performing a series of random rotations led to random orientations of the conformations. During the generation of the random orientations, each time when the calculated softened energy was lower than the set limit, the orientation was recorded. This step was repeated until the desired number (here we set three to improve the accuracy as well as to avoid unnecessary crosses in order) of the low-energy orientations was achieved, or the test times of the bad orientations had reached the maximum number.
3. Afterwards, each recorded orientation was subjected to simulated annealing molecular dynamics. The simulation experienced a heated process and was cooled down to the target temperature. The final energy minimization of each ligand in the rigid receptor using non-softened potential was conducted. The heating steps were 2,000 with 700 of the heating target temperature; while the cooling steps were 5,000 with 300 cooling target temperature.
4. Finally, the CHARMm energy (interaction energy plus ligand strain) and the interaction energy alone of each recorded pose were calculated. Three (as we set) poses saved for each ligand were ranked according to the CHARMm energy and the dock scores (more negative, thus more favorable for binding).

Pharmacokinetic properties and Lipinski's rule of five

The pharmacokinetic properties comprising absorption, distribution, metabolism, and excretion (ADME) were predicted using the Swiss ADME protocol (http://www.swissadme.ch/).[45,46] The predicted data from this source were checked with the data from the TCMSP Version 2.3.[39] We also checked the top hits with the Lipinski's oral drug likeliness properties consisting of: 1) the molecular weight (<500 Daltons), 2) number of hydrogen bond donors (<5), 3) number of hydrogen bond acceptors (<10), 4) log P (<5), and 5) molar refractivity (<140).[47]

Results and discussion

Preliminary analysis of the natural products

Shuanghuanglian contained three major ingredients: *Lonicerae Japonicae Flos* (Shuang), *Scutellariae Radix* (Huang), and *Forsythiae Fructus* (Lian). The natural products of the corresponding herbs were obtained from the TCMSP system Version 2.3.[39] From this database, the structures were downloaded and named with their Mol ID. In Table S1, the Mol ID of the compounds from all three herbs were listed. A general analysis of these natural products led to some hints. First, the reported number of natural products in Shuang, Huang, and Lian were 236, 143 and 150, respectively. They were all rich in diversity because a random sampling of 10 herbs in the database indicated that all 10 herbs had fewer than 50 natural products. Secondly, some of the components of the herbs were repeated. As colored in Table S1 and shown in Figure 2, 20 compounds in Shuang and Huang, 21 compounds in Shuang and Lian, 10 compounds in Huang and Lian, were the same. There were four compounds (MOL000069, MOL000254, MOL000357, and MOL000358) that appeared in all three herbs. Interestingly, they covered the categories of fatty acids, aromatic compounds, glycosides, and sterols. Moreover, there were 482 distinguished natural products in Shuanghuanglian.

Molecular docking simulation

Focusing on specific treatment, we chose the crystal structures of the wild type SARS-CoV-2 PLPro (PDB code: 7JRN),[40] and SARS-CoV-2 Mpro (PDB code: 7CWC),[41] respectively. For the other two enzymes, because the Spike protein might be for prevention and RdRP for the broad-spectrum treatment, which could also be helped by miR2911,[32] the binding sites of the PLPro and Mpro were identified. As shown in Figure 3, the binding site in PLPpro was that of the original ligand GRL0617, while the binding sites in Mpro were complex. The basic site was that of ligand N3 together with another five binding sites. Sites I and II were separated from the N3-binding site, which was near the alpha (α)-helix-rich region of the Mpro; Sites III and IV were independent in the β-sheet-rich region, while Site V was at the linking position of the two regions. All of the natural products could have binding sites according to the steric and electronic surroundings. We chose the CDOCKER protocol considering the structural diversity of the ligands. Accordingly, the "-CDOCKER Interaction Energy" was selected as the basic index to evaluate the possibility of the interaction between each ligand and the binding site, while the "-CDOCKER Energy" was chosen as the reference index to evaluate the possible steadiness of the ligand-receptor complex.

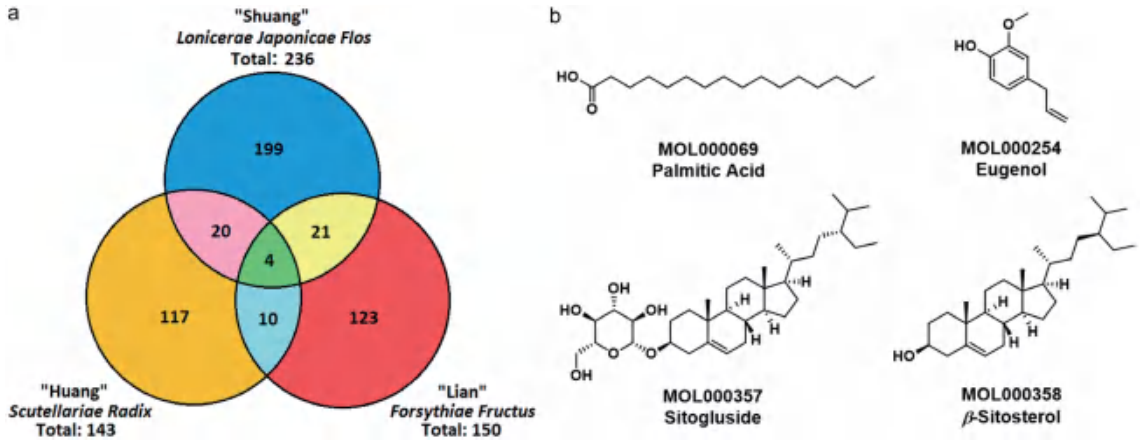

Fig. 2. The number of ingredients in Lonicerae Japonicae Flos (Shuang), Scutellariae Radix (Huang), and Forsythiae Fructus (Lian), and four compounds in all three herbs. (a) The numbers of natural products in the three herbs. (b) The compounds that appeared in all three herbs.

From the simple object to the complex one, we chose to analyze the results from SARS-CoV-2 PLPro. Among the 482 natural products, 438 were docked into this site while 255 reached the basic requirement of potential interactions (we set as -CDOCKER Interaction Energy >30.0 kcal/mol). We listed the MOL IDs of the 255 compounds in Table S2 and illustrated the 2D binding patterns of the top 15 hits in Figure S1. The top 15 hits were also compared in Table 1. First, Shuanghuanglian seemed to have potential for SARS-CoV-2 PLPro because 90.87% (438 out of 482) of its investigated components were docked into the PLPro, which was higher than that of the compounds in the FDA-approved Drug Library supported by Selleck (China) (Shanghai, China) (81.14%; 2,229 out of 2,747). Simultaneously, the "-CDOCKER Interaction Energy" of the top hits were almost in the rational range of 40.0–60.0 kcal/mol, which was almost the most potential situation of CDOCKER before further modification and evaluation. Secondly, the flavones, glycosides, and polyphenols were preferred in the top hits, while long chain fatty acid esters also appeared. Specially, among the top hits, long chain fatty acid esters were all from Huang. Thirdly, Shuang and Lian were more important than Huang for binding to the PLPro. Additionally, the repeated compounds did not appear frequently (two out of 15; 13.33%). In particular, as shown in the 3D binding pattern of MOL003130 (Fig. 4a) and MOL002037 (Fig. 4b), the major key residues for the hydrogen bonds were Lys157, Leu162, Asp164, Arg166, Glu167, Gly266, Asn267, Tyr268, Gln269, Tyr273, and Thr301, respectively. We then chose the top three to evaluate their possible druggability.

Actually, with higher homology with SARS-CoV, Mpro has been widely investigated.[26] Here, we also analyzed the results in the N3-binding site before that of the further defined ones. Among the 482 natural products, 451 were docked into this site, while 246 could be potential for interactions with the Mpro. We listed the MOL ID of the 246 compounds in Table S3 and illustrated the 2D binding patterns of the top 15 hits in Figure S2. The hints from the docking results in SARS-CoV-2 Mpro were different (Table 2). Initially, compared with that in PLPro, the success rate of docking was even as high as 93.57% (451 out of 482), which was also higher than that of the compounds in the FDA-approved Drug Library (83.25%; 2,287 out of 2,747). However, one questionable point was that the "-CDOCKER Interaction Energy" of the top hits was all beyond 60.0 kcal/mol, thus suggesting that the N3-binding site could be too large for the investigated ligands. Accordingly, we subsequently divided it into smaller sites. Secondly, flavones, glycosides, and polyphenols were preferred. Simultaneously, the long chain species were alkanes. The long chain compounds were all from Huang, and they were not favorable for generating hydrogen bonds. Thirdly, though Shuang and Lian still covered a majority of the top hits, their compounds were quite different from those

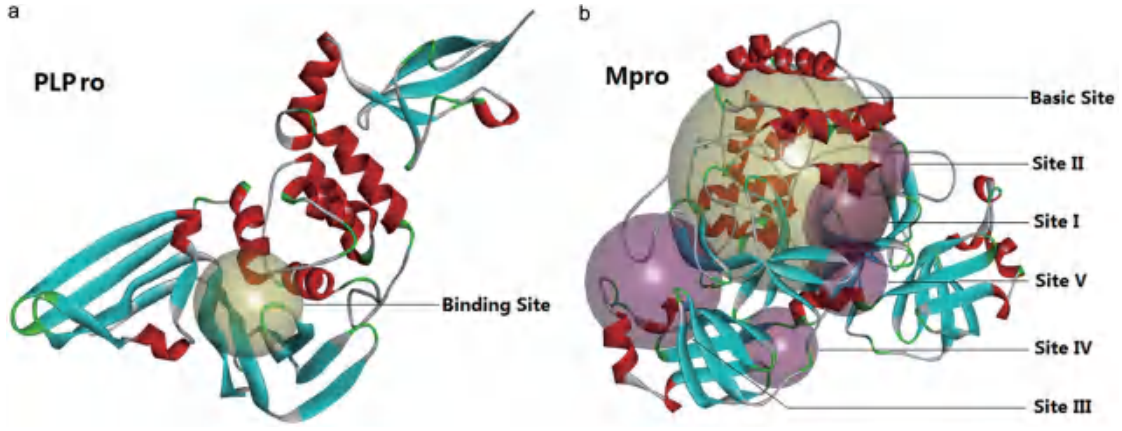

Fig. 3. The defined binding sites in SARS-CoV-2 PLPro (a) and Mpro (b). Mpro, main protease; PLPro, papain-like protease.

Table 1. The comparison of the top 15 hits in SARS-CoV-2 PLPro

MOL ID	-CDOCKER interaction energy (kcal/mol)	-CDOCKER energy (kcal/mol)	Source	Number of H-bonds	General name
MOL003130	−6.29035	63.3313	Shuang	10	Madreselvin A
MOL002037	41.0151	60.9759	Lian	7	Amentoflavone
MOL000010	−3.98465	58.1761	Shuang	7	Rhoifolin
MOL001875	44.3396	57.8812	Shuang	4	Isochlorogenic acid
MOL003051	−1.68697	56.8953	Shuang	1	Scolymoside
MOL003309	38.3745	56.5246	Lian	6	Plantainoside A
MOL003076	35.8932	56.4097	Shuang	2	3,5-Di-O-caffeoylquinic acid methyl ester
MOL003284	31.5003	56.2757	Lian	5	Caleolarioside A
MOL003077	38.4369	56.182	Shuang	8	4,5-Di-O-caffeoylquinic acid methyl ester
MOL003334	−3.93747	55.5806	Lian	7	Forsythoside D
MOL000415	−2.95525	55.0801	Shuang & Lian	3	Rutin
MOL013161	51.9647	54.8761	Huang	1	Methyl Hexacosanoate
MOL007792	8.65799	54.3395	Huang	4	Isomartynoside
MOL009734	49.455	53.8073	Huang	1	Methyl lignocerate
MOL000007	14.4816	53.6873	Shuang & Huang	4	Cosmetin

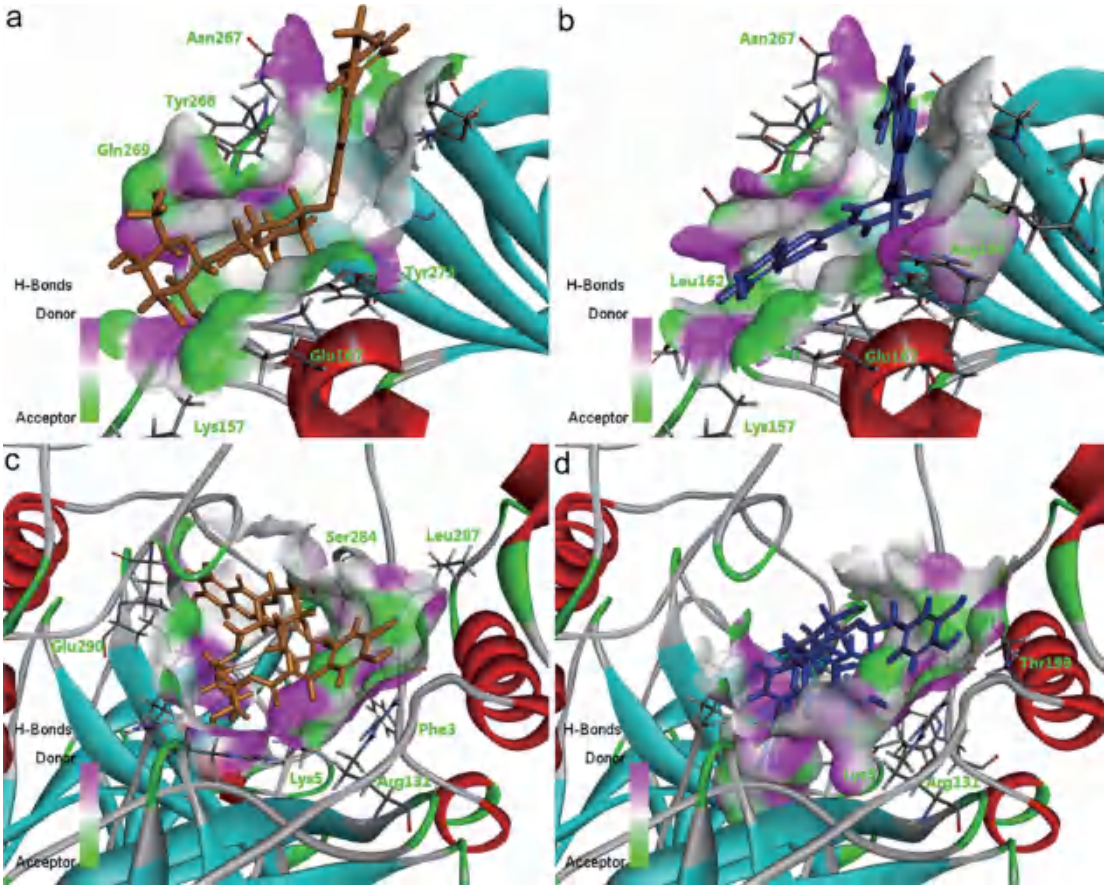

Fig. 4. The 3D binding patterns of the top hits in the detailed binding sites with the H-bond surface comprising MOL003130 in PLPro (a), MOL002037 in PLPro (b), MOL003008 in Mpro (c), and MOL003337 in Mpro (d).

Table 2. The comparison of the top 15 hits in SARS-CoV-2 Mpro at the N3-binding site

MOL ID	-CDOCKER interaction energy (kcal/mol)	-CDOCKER energy (kcal/mol)	Source	Number of H-bonds	General name
MOL003008	17.0653	74.3945	Shuang	9	Madreselvin B
MOL003337	13.6612	74.0027	Lian	6	Forsythoside F
MOL003332	29.1808	71.6769	Lian	7	Forsythoside C
MOL003110	−52.6021	71.2342	Shuang	5	Centauroside
MOL003130	0.355922	68.1028	Shuang	7	Madreselvin A
MOL000870	54.4467	64.6227	Huang	0	Hexatriacontane
MOL007792	20.8246	63.9904	Huang	5	Isomartynoside
MOL003331	24.3554	63.6139	Lian	4	Forsythiaside
MOL003285	−5.4399	63.3833	Lian	9	N/A
MOL003333	27.1839	62.5565	Lian	7	Acteoside
MOL003316	28.799	61.8015	Lian	5	*β*-Hydroxyacteoside
MOL003013	12.6776	61.1352	Shuang	4	Secologanic dibutylacetal
MOL003313	13.6329	60.7986	Lian	4	Suspensaside A
MOL000522	14.5554	60.2791	Lian	4	Arctiin
MOL005224	57.0222	60.1095	Huang	0	Tetratetracintane

docked in the PLPro because only two out of 15 (MOL003130 and MOL007792) were the same. All the top hits were unique herbs. We illustrated the 3D patterns of MOL003008 (Fig. 4c) and MOL003337 (Fig. 4d) to infer the key residues for the hydrogen bonds as Phe3, Arg4, Lys5, Arg131, Thr199, Ser284, Leu287, Glu288, and Glu290, respectively.

In addition, it could be possible that smaller binding sites could be more rational than the N3-binding site for the prepared ligands. Instead of simply reducing the radius, we identified the new sites according to the real cavities. Preliminarily, we compared the feasibility of the five divided sites. The successful docked and interaction possible ligands were Site I: 339 and 21; Site II: 436 and 257; Site III: 390 and 173; Site IV: 367 and 169; Site V: 412 and 221. Because the top hit (MOL003283) in Site I indicated the "-CDOCKER Interaction Energy" of merely 36.0175 kcal/mol, we reasonably believed that Site I did not have the potential for the prepared ligands from Shuanghuanglian. The top 50 hits in each site were listed in Table S4, and the 2D binding patterns of the top 15 hits were illustrated in Figures S3-S6. Site II was similar too, but smaller than the N3-binding site. From the energy index in Table 3, Site II was also more rational than the N3-binding site, which realized our purpose of defining the divided sites. The top hits were all formed from flavones, glycosides, and polyphenols. Shuang and Lian contributed to 14 out of 15 top hits, except the one that appeared in both herbs. Since Site II was similar to the N3-binding site, a high percentage of ligands (33.3%, five out of 15, were marked in Table 3) appeared in the top hits in both sites. We compared the detailed binding patterns of MOL003130 in both sites (Fig. 5a, b, and d), and found that these two conformations interacted with the different residues in the Mpro. Coincidently, MOL003130 also appeared in the top hits in PLPro. Other repeated ligands in both the Mpro Site II and PLPro included MOL000415, MOL001875, MOL003051, MOL000010, and MOL003334. For each repeat, we picked the top three from the previously unpicked ones for further evaluation. They were MOL003316, MOL003313, MOL003013, MOL000415, MOL001875, and MOL003051.

When we divided the sites, we thought that Sites III and IV were not typical for the small molecular ligands because they were surrounded mainly by the *β*-sheet and their successfully docked ligands were relatively fewer (<400). Though the energy index was also less favorable, these two sites could have potential because the "-CDOCKER Interaction Energy" of the top hits was almost in the rational range of 40.0–60.0 kcal/mol (Tables 4 and 5). Interestingly, the compounds from Huang, regardless of their chain lengths, appeared more frequently in the top hits. Accordingly, we could not ignore the possibility that Huang might interact at these binding sites and act as an important supplement to the overall activity of Shuanghuanglian.

Although the surrounding of Site V contained both the *α*-helix and *β*-sheet, the top hits seemed more similar to the ones in Site II, which were in an *α*-helix-rich region. As shown in Table 6, four out of the top five hits (in total five out of 15 as marked) repeated the top hits in Site II or the N3-binding site. We noticed that MOL003130 appeared again in the leading position with the potential energy values. Given that Site V was close to the N3-binding site, we illustrated the detailed binding patterns of MOL003130 in Site V (Fig. 5c) and compared its relative position in Mpro (Fig. 5d). Because these two conformations were both bound near the center of the corresponding sites, there seemed no key residues to interact with both of the conformations of MOL003130. Alternatively, MOL003130 could bind to the different sites of the Mpro simultaneously. We also selected the top three unpicked ligands from this site (MOL003336, MOL003284, and MOL003334).

Pharmacokinetic potential

We picked 15 hits to predict their pharmacokinetic potential by checking the ADME properties and the violation with Lipinski's rule of five. The major properties were listed in Table S5 with the corresponding simplified molecular input line entry system

Table 3. The comparison of the top 15 hits in the SARS-CoV-2 Mpro Site II

MOL ID	-CDOCKER interaction energy (kcal/mol)	-CDOCKER energy (kcal/mol)	Source	Number of H-bonds	General name
MOL000415	6.83568	64.3218	Shuang & Lian	11	Rutin
MOL003130	−8.23777	63.2077	Shuang	8	Madreselvin A
MOL001875	34.2741	61.9011	Shuang	7	Isochlorogenic acid
MOL003051	1.79757	61.1418	Shuang	7	Scolymoside
MOL002921	11.635	59.2781	Huang	9	N/A
MOL003316	21.7516	59.1990	Lian	7	*β*-Hydroxyacteoside
MOL000010	5.53976	59.0876	Shuang	6	Rhoifolin
MOL003118	37.2258	58.1035	Shuang	9	Isochlorogenic acid C
MOL003332	15.5971	58.0757	Lian	5	Forsythoside C
MOL003334	12.9183	56.2545	Lian	8	Forsythoside D
MOL006370	30.5446	55.3136	Huang	7	5-O-Caffeoylquinic acid
MOL003313	4.35655	55.2171	Lian	4	Suspensaside A
MOL003013	−17.4498	55.1203	Shuang	3	Secologanic dibutylacetal
MOL003010	22.1107	54.5034	Shuang	6	Quercetin-3-O-*β*-D-glu
MOL003336	15.8194	53.9310	Lian	8	Forsythoside E

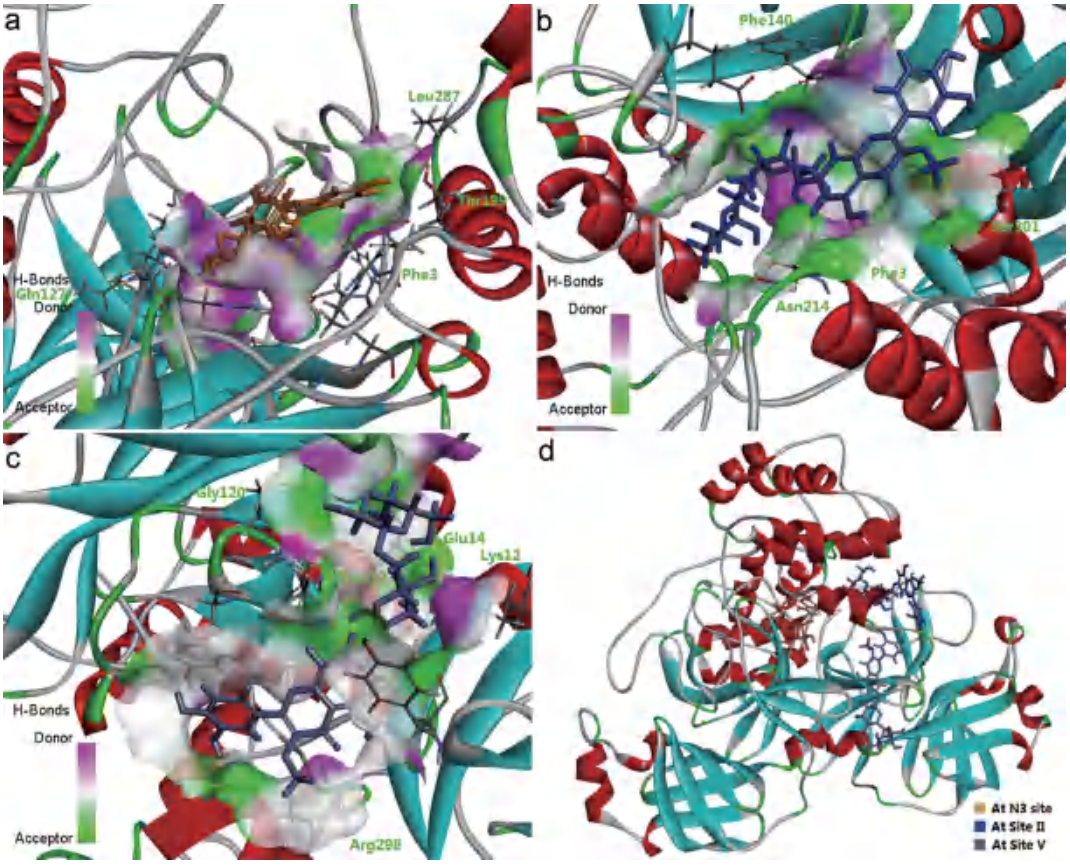

Fig. 5. The 3D binding patterns of MOL003130 to SARS-CoV-2 detailed in the N3-binding site (a), Sites II (b) and V (c), and in the relative positions of the above sites (d).

Table 4. The comparison of the top 15 hits in the SARS-CoV-2 Mpro Site III

MOL ID	-CDOCKER interaction energy (kcal/mol)	-CDOCKER energy (kcal/mol)	Source	Number of H-bonds	General name
MOL000870	42.1147	48.0156	Huang	0	Hexatriacontane
MOL008595	42.8505	46.4620	Huang	1	Methyl henicosanoate
MOL005368	41.4543	45.0270	Huang	2	Methyl tricosanoate
MOL003284	27.3505	44.9463	Lian	3	Caleolarioside A
MOL003290	19.0479	44.4435	Lian	3	N/A
MOL003010	16.5869	43.5525	Shuang	6	Quercetin-3-O-*β*-D-glu
MOL000702	10.2468	43.2031	Lian	5	Guajavarin
MOL009730	29.8744	42.6731	Huang	1	Methyl icos-11-enoate
MOL000663	43.3447	42.6685	Shuang	1	Lignoceric acid
MOL002879	41.0219	42.5431	Huang	1	Diop
MOL003322	−1.69405	42.5174	Lian	4	Forsythinol
MOL005224	31.3177	42.3766	Huang	0	Tetratetracintane
MOL002027	38.0839	42.3339	Huang	0	Methyl behenate
MOL003030	33.7532	42.3317	Shuang	0	Ginnol
MOL002934	16.9542	42.2364	Huang	5	Neobaicalein

(SMILES) codes in Table S6, and the oral bioavailability radar maps were presented in Figure 6. For treating COVID-19, we analyzed the oral bioavailability. For all of the selected hits, all the natural products had the most common difficulty of polarity. Given the major structural moieties were flavones, glycosides, and polyphenols, their topological polar surface area (TPSA) went beyond the limit of 130 $Å^2$.[48] Moreover, a majority of the hits faced the problem of size (11 out of 15), which could result from the fact that these compounds contained one or more glycosides. Several hits needed improvement on flexibility (five out of 15). Actually, two possible approaches could be applied to improve the oral bioavailability. One was modifying the deglycosylated metabolites of these natural products. As shown in Figure 6, deglycosylated MOL003130 exhibited no violations of Lipinski's rules. Further modification could improve the potential of the interaction with its targets in the binding sites. The others were packaging the drug-like compounds in certain carriers, such as human serum albumin (HSA), metal-organic framework (MOF),

Table 5. The comparison of the top 15 hits in the SARS-CoV-2 Mpro Site IV

MOL ID	-CDOCKER interaction energy (kcal/mol)	-CDOCKER energy (kcal/mol)	Source	Number of H-bonds	General name
MOL003309	32.9477	55.5423	Lian	6	Plantainoside A
MOL000009	18.7637	51.3359	Shuang	5	Luteolin-7-O-glucoside
MOL003345	13.0808	50.3323	Lian	5	N/A
MOL000561	15.2567	50.2364	Shuang & Lian	4	Astragalin
MOL000437	15.4088	49.6075	Lian	5	Hirsutrin
MOL000007	15.1167	49.0453	Shuang & Huang	5	Cosmetin
MOL002935	15.7847	48.0702	Huang	4	Baicalin
MOL002912	22.8402	47.9820	Huang	3	Dihydrobaicalin
MOL002931	25.8930	47.8252	Huang	4	Scutellarin
MOL003284	30.3906	46.1796	Lian	4	Caleolarioside A
MOL003297	−5.35172	46.0809	Lian	3	N/A
MOL003010	18.5803	45.6709	Shuang	6	Quercetin-3-O-*β*-D-glu
MOL000702	9.11693	44.8240	Lian	3	Guajavarin
MOL003128	2.8717	44.7907	Shuang	3	Dinethylsecologanoside
MOL003119	−8.58632	44.5271	Shuang	6	Loniceracetalide A

Table 6. The comparison of the top 15 hits in the SARS-CoV-2 Mpro Site V

MOL ID	-CDOCKER interaction energy (kcal/mol)	-CDOCKER energy (kcal/mol)	Source	Number of H-bonds	General name
MOL003130	−3.17177	62.6809	Shuang	6	Madreselvin A
MOL003336	−3.49283	57.1383	Lian	7	Forsythoside E
MOL003284	34.4530	56.6149	Lian	8	Caleolarioside A
MOL003334	2.75989	55.4900	Lian	8	Forsythoside D
MOL003285	−13.2275	54.0015	Lian	4	N/A
MOL000536	13.0390	53.3301	Lian	3	Matairesinoside
MOL003309	31.5105	52.9643	Lian	6	Plantainoside A
MOL002702	49.0094	52.6923	Shuang	1	Nonacosanol
MOL003030	48.1793	52.3531	Shuang	2	Ginnol
MOL003020	7.01853	51.5526	Shuang	3	Secologanoside 7-methylester
MOL003118	31.1981	51.4023	Shuang	6	Isochlorogenic acid C
MOL009734	50.1233	51.1693	Huang	1	Methyl lignocerate
MOL003327	17.7518	51.0608	Lian	5	Rengyoside C
MOL000357	−50.5619	50.5453	All	2	Sitogluside
MOL003292	−11.9878	50.4217	Lian	3	(+)-Epipinoresinol-4′-O-D-glucoside

and aptamers. Consequently, it could be practical to overcome one or two violations.

Future directions

Similarity in the compounds and ingredients

There were some common compounds among the top hits in the different binding sites, including MOL003130, MOL000415, MOL 001875, MOL003051, MOL000010, and MOL003334. They shared some similar moieties, such as phenylpropanoids, flavones, and glycosides. Their ADME properties had advantages in insaturation and flexibility, as well as disadvantages in size and polarity.

Among the relevant efficacious Chinese medicines, there was also similarity in the ingredients. Lianhua Qingwen capsules, supplied during the COVID-19 pandemic in Shanghai in 2022, shared the major ingredients of Shuang and Lian, while Qingfei Paidu decoction shared the major ingredient of Huang.[49,50] Moreover, the involved ingredients, such as *Atractylodes macrocephala* Koidz, *Belamcanda chinensis* (L.) Redouté, and *Citrus reticulata* Blanco, contained similar components as those found in Shuanghuanglian.

Significance of the components and substitutability

Subsequently, we intended to define the sites in the Mpro, especially the separation of Sites I and II. According to the experience of the structural analysis, the analysis of the released structure of Mpro revealed the reported binding site was bulky. The so-called N3-binding site was bound with a small peptide, which was consistent with our recognition.[26] However, we believed that the evolution of the species obeyed the natural rules, thus inferring that the binding site could be composed of two or more known sites. Although the major topic of this work was analyzing the natural products, we also conducted virtual screening during the beginning months of the pandemic and reported the separation of the binding site as public information instead of a research paper. Sites I and II, respectively had the unique features of the previous CoV site and angiotensin receptor. This result was consistent with the clinical characteristics of SARS-CoV2.[11–13] Furthermore, some of the main components of Shuang and Lian were originally applied for inhibiting the similar sites.

Subsequently, the analysis of the prepared ligands in each binding site unveiled the substitutability of the herbs. Initially, Huang could be the supplement to the overall activity of Shuanghuanglian, and Huang could be de-emphasized considering the main bioactivity of the prescription. The herb resources of the selected hits are listed in Table S7. Among the 15 natural products, three were unique for Shuang and seven in Lian, hence inferring that these two herbs were irreplaceable. Several herbs also had five other hits and included *Chrysanthemi Flos* (359 compounds), *Aurantii Fructus Immaturus* (65 compounds), *Ginkgo Semen* (80 compounds), *Herbahypericiperforati* (37 compounds), *Canarii Fructus* (56 compounds), and *Saussureae Involucratae Herba* (55 compounds). These herbs could provide possible substitutability in urgent situations.

Conclusions

This study screened the potential binding of natural products in Shuanghuanglian to the the PLPro and Mpro of SARS-CoV2 by molecular docking simulation. There were 482 distinguished natural products in Shuanghuanglian that were categorized in the fatty acids, aromatic compounds, glycosides, and sterols. These compounds in these three herbs had certain repetition. The N3-binding site of the Mpro was further divided into five detailed sites. The successfully docked rates of the Shuanghuanglian components to these proteins were all higher than that of the compounds in the FDA-approved Drug Library. A majority of the top hits might interact with the binding sites via hydrogen bonds. In general, Shuang

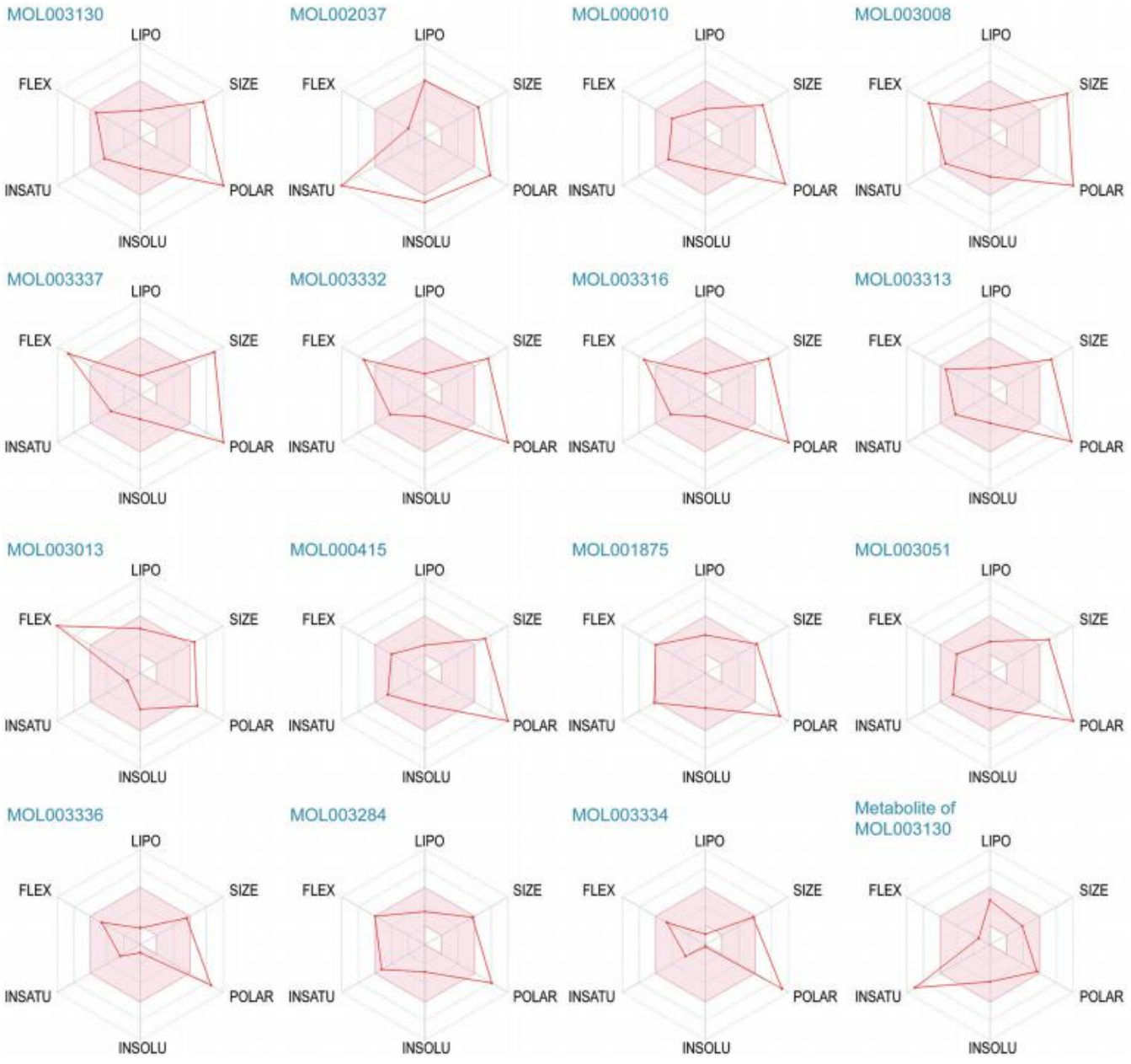

Fig. 6. The oral bioavailability radar maps of the selected hits and the metabolite of MOL003130. The colored zone was the suitable physiochemical space for oral bioavailability limited by LIPO (lipophility), SIZE, POLAR (polarity), INSO (insolubility), INSA (insaturation) and FLEX (flexibility).

and Lian took the primary status in providing the top hits, while Huang could act as an important supplement to their overall activity. Moreover, we checked the pharmacokinetic potential of the top hits. Though the selected hits faced the common difficulty of polarity, the deglycosylation and the package by the carriers could also be practical to overcome the violation. The substitutability of these herbs indicated that Shuang and Lian were irreplaceable, while other herbs seemed to have potential to be involved after further evaluation and analysis of the diversity and risks in the future. The findings from this work could open an avenue for international and standardized research on traditional Chinese medicines, thus contributing to global public health.

Supporting information

Supplementary material for this article is available at https://doi.org/10.14218/JERP.2022.00061.

Table S1. The natural products from the three major ingredients of Shuanghuanglian.

Table S2. The docked natural products which reached the basic requirement of potential interactions with SARS-CoV-2 PLPro (Ranked from left to right in each line).

Table S3. The docked natural products which reached the basic

requirement of potential interactions with SARS-CoV-2 Mpro N3-binding site (Ranked from left to right in each line).

Table S4. The top 50 hits in each binding site in SARS-CoV-2 Mpro.

Table S5. The predicted ADME properties of the selected hits and the Metabolite.

Table S6. The SMILE codes of the selected hits and the Metabolite.

Table S7. The herb resources of the selected hits.

Figure S1. The 2D binding patterns of the top 15 hits in SARS-CoV-2 PLPro.

Figure S2. The 2D binding patterns of the top 15 hits in SARS-CoV-2 Mpro at N3-binding site.

Figure S3. The 2D binding patterns of the top 15 hits in SARS-CoV-2 Mpro Site II.

Figure S4. The 2D binding patterns of the top 15 hits in SARS-CoV-2 Mpro Site III.

Figure S5. The 2D binding patterns of the top 15 hits in SARS-CoV-2 Mpro Site IV.

Figure S6. The 2D binding patterns of the top 15 hits in SARS-CoV-2 Mpro Site V.

Acknowledgments

We thank Prof. Yang Zhou and Dr. Peng-Fei Qi from Ningbo Institute of Materials Technology and Engineering, Chinese Academy of Sciences for their help in checking the parameters of the virtual screening.

Funding

This work was supported by the grants from the Innovation Fund for Technology of Nanjing University (2021), Research Project of Jinhua Traditional Chinese Medicine Science and Technology (2022KY33), and Scientific Research Project of Jinhua Advanced Research Institute (GYY202108 and GYY202104).

Conflict of interest

Yu-Shun Yang is a part-time academic consultant of Hi-Techjig Co. Ltd. (Zhenjiang, China). The authors have no other conflicts of interest to declare.

Author contributions

Conceptualization: YSY; formal analysis: YSY, DA, XW, and CYW; methodology: YSY and JY; writing the original draft: YSY; reviewing and editing: XW, CYW, and JY. All authors read and agreed to the published version of the manuscript.

Data sharing statement

The data from this study are available within the article and its supplementary files. Other corresponding details can be shared by requesting from the corresponding authors.

References

[1] Huang C, Wang Y, Li X, Ren L, Zhao J, Hu Y, *et al*. Clinical features of patients infected with 2019 novel coronavirus in Wuhan, China. Lancet 2020;395(10223):497–506. doi:10.1016/S0140-6736(20)30183-5, PMID:31986264.

[2] Li H, Liu L, Zhang D, Xu J, Dai H, Tang N, *et al*. SARS-CoV-2 and viral sepsis: observations and hypotheses. Lancet 2020;395(10235):1517–1520. doi:10.1016/S0140-6736(20)30920-X, PMID:32311318.

[3] van Doremalen N, Bushmaker T, Morris DH, Holbrook MG, Gamble A, Williamson BN, *et al*. Aerosol and Surface Stability of SARS-CoV-2 as Compared with SARS-CoV-1. N Engl J Med 2020;382(16):1564–1567. doi:10.1056/NEJMc2004973, PMID:32182409.

[4] de Groot RJ, Baker SC, Baric RS, Brown CS, Drosten C, Enjuanes L, *et al*. Middle East respiratory syndrome coronavirus (MERS-CoV): announcement of the Coronavirus Study Group. J Virol 2013;87(14):7790–7792. doi:10.1128/JVI.01244-13, PMID:23678167.

[5] Remuzzi A, Remuzzi G. COVID-19 and Italy: what next? Lancet 2020;395(10231):1225–1228. doi:10.1016/S0140-6736(20)30627-9, PMID:32178769.

[6] Bhatraju PK, Ghassemieh BJ, Nichols M, Kim R, Jerome KR, Nalla AK, *et al*. Covid-19 in Critically Ill Patients in the Seattle Region - Case Series. N Engl J Med 2020;382(21):2012–2022. doi:10.1056/NEJMoa2004500, PMID:32227758.

[7] Li R, Pei S, Chen B, Song Y, Zhang T, Yang W, *et al*. Substantial undocumented infection facilitates the rapid dissemination of novel coronavirus (SARS-CoV-2). Science 2020;368(6490):489–493. doi:10.1126/science.abb3221, PMID:32179701.

[8] Paules CI, Marston HD, Fauci AS. Coronavirus Infections-More Than Just the Common Cold. JAMA 2020;323(8):707–708. doi:10.1001/jama.2020.0757, PMID:31971553.

[9] Obermeyer F, Jankowiak M, Barkas N, Schaffner SF, Pyle JD, Yurkovetskiy L, *et al*. Analysis of 6.4 million SARS-CoV-2 genomes identifies mutations associated with fitness. Science 2022;376(6599):1327–1332. doi:10.1126/science.abm1208, PMID:35608456.

[10] Wilder-Smith A, Chiew CJ, Lee VJ. Can we contain the COVID-19 outbreak with the same measures as for SARS? Lancet Infect Dis 2020;20(5):e102–e107. doi:10.1016/S1473-3099(20)30129-8, PMID:32145768.

[11] Jiang S. Don't rush to deploy COVID-19 vaccines and drugs without sufficient safety guarantees. Nature 2020;579(7799):321. doi:10.1038/d41586-020-00751-9, PMID:32179860.

[12] Li G, De Clercq E. Therapeutic options for the 2019 novel coronavirus (2019-nCoV). Nat Rev Drug Discov 2020;19(3):149–150. doi:10.1038/d41573-020-00016-0, PMID:32127666.

[13] DeGrace MM, Ghedin E, Frieman MB, Krammer F, Grifoni A, Alisoltani A, *et al*. Defining the risk of SARS-CoV-2 variants on immune protection. Nature 2022;605(7911):640–652. doi:10.1038/s41586-022-04690-5, PMID:35361968.

[14] Xu X, Han M, Li T, Sun W, Wang D, Fu B, *et al*. Effective treatment of severe COVID-19 patients with tocilizumab. Proc Natl Acad Sci U S A 2020;117(20):10970–10975. doi:10.1073/pnas.2005615117, PMID:32350134.

[15] Shen C, Wang Z, Zhao F, Yang Y, Li J, Yuan J, *et al*. Treatment of 5 Critically Ill Patients With COVID-19 With Convalescent Plasma. JAMA 2020;323(16):1582–1589. doi:10.1001/jama.2020.4783, PMID:32219428.

[16] Wang M, Cao R, Zhang L, Yang X, Liu J, Xu M, *et al*. Remdesivir and chloroquine effectively inhibit the recently emerged novel coronavirus (2019-nCoV) in vitro. Cell Res 2020;30(3):269–271. doi:10.1038/s41422-020-0282-0, PMID:32020029.

[17] Du YX, Chen XP. Favipiravir: Pharmacokinetics and Concerns About Clinical Trials for 2019-nCoV Infection. Clin Pharmacol Ther 2020;108(2):242–247. doi:10.1002/cpt.1844, PMID:32246834.

[18] Gautret P, Lagier JC, Parola P, Hoang VT, Meddeb L, Mailhe M, *et al*. Hydroxychloroquine and azithromycin as a treatment of COVID-19: results of an open-label non-randomized clinical trial. Int J Antimicrob

Agents 2020;56(1):105949. doi:10.1016/j.ijantimicag.2020.105949, PMID:32205204.
[19] Sanders JM, Monogue ML, Jodlowski TZ, Cutrell JB. Pharmacologic Treatments for Coronavirus Disease 2019 (COVID-19): A Review. JAMA 2020;323(18):1824–1836. doi:10.1001/jama.2020.6019, PMID:32282022.
[20] Fernando K, Menon S, Jansen K, Naik P, Nucci G, Roberts J, *et al*. Achieving end-to-end success in the clinic: Pfizer's learnings on R&D productivity. Drug Discov Today 2022;27(3):697–704. doi:10.1016/j.drudis.2021.12.010, PMID:34922020.
[21] Hashemian SMR, Pourhanifeh MH, Hamblin MR, Shahrzad MK, Mirzaei H. RdRp inhibitors and COVID-19: Is molnupiravir a good option? Biomed Pharmacother 2022;146:112517. doi:10.1016/j.biopha.2021.112517, PMID:34902743.
[22] Mohamed Y, El-Maradny YA, Saleh AK, Nayl AA, El-Gendi H, El-Fakharany EM. A comprehensive insight into current control of COVID-19: Immunogenicity, vaccination, and treatment. Biomed Pharmacother 2022;153:113499. doi:10.1016/j.biopha.2022.113499, PMID:36076589.
[23] Zhu Z, Lu Z, Xu T, Chen C, Yang G, Zha T, *et al*. Arbidol monotherapy is superior to lopinavir/ritonavir in treating COVID-19. J Infect 2020;81(1):e21–e23. doi:10.1016/j.jinf.2020.03.060, PMID:32283143.
[24] Xiao M, Tian J, Zhou Y, Xu X, Min X, Lv Y, *et al*. Efficacy of Huoxiang Zhengqi dropping pills and Lianhua Qingwen granules in treatment of COVID-19: A randomized controlled trial. Pharmacol Res 2020;161:105126. doi:10.1016/j.phrs.2020.105126, PMID:32781283.
[25] Ni L, Zhou L, Zhou M, Zhao J, Wang DW. Combination of western medicine and Chinese traditional patent medicine in treating a family case of COVID-19. Front Med 2020;14(2):210–214. doi:10.1007/s11684-020-0757-x, PMID:32170559.
[26] Jin Z, Du X, Xu Y, Deng Y, Liu M, Zhao Y, *et al*. Structure of M^{pro} from SARS-CoV-2 and discovery of its inhibitors. Nature 2020;582(7811):289–293. doi:10.1038/s41586-020-2223-y, PMID:32272481.
[27] Shi Z, Liu Z, Liu C, Wu M, Su H, Ma X, *et al*. Spectrum-Effect Relationships Between Chemical Fingerprints and Antibacterial Effects of Lonicerae Japonicae Flos and Lonicerae Flos Base on UPLC and Microcalorimetry. Front Pharmacol 2016;7:12. doi:10.3389/fphar.2016.00012, PMID:26869929.
[28] Li C, Lin G, Zuo Z. Pharmacological effects and pharmacokinetics properties of Radix Scutellariae and its bioactive flavones. Biopharm Drug Dispos 2011;32(8):427–445. doi:10.1002/bdd.771, PMID:21928297.
[29] Jiao J, Fu YJ, Zu YG, Luo M, Wang W, Zhang L, *et al*. Enzyme-assisted microwave hydro-distillation essential oil from Fructus forsythia, chemical constituents, and its antimicrobial and antioxidant activities. Food Chem 2012;134(1):235–243. doi:10.1016/j.foodchem.2012.02.114.
[30] Zhou Z, Li X, Liu J, Dong L, Chen Q, Liu J, *et al*. Honeysuckle-encoded atypical microRNA2911 directly targets influenza A viruses. Cell Res 2015;25(1):39–49. doi:10.1038/cr.2014.130, PMID:25287280.
[31] Zhou LK, Zhou Z, Jiang XM, Zheng Y, Chen X, Fu Z, *et al*. Absorbed plant MIR2911 in honeysuckle decoction inhibits SARS-CoV-2 replication and accelerates the negative conversion of infected patients. Cell Discov 2020;6(1):54. doi:10.1038/s41421-020-00197-3, PMID:32802404.
[32] Zhou Z, Zhou Y, Jiang XM, Wang Y, Chen X, Xiao G, *et al*. Decreased HD-MIR2911 absorption in human subjects with the SIDT1 polymorphism fails to inhibit SARS-CoV-2 replication. Cell Discov 2020;6:63. doi:10.1038/s41421-020-00206-5, PMID:32934821.
[33] Ho LTF, Chan KKH, Chung VCH, Leung TH. Highlights of traditional Chinese medicine frontline expert advice in the China national guideline for COVID-19. Eur J Integr Med 2020;36:101116. doi:10.1016/j.eujim.2020.101116, PMID:32292529.
[34] Li Y, Li J, Zhong D, Zhang Y, Zhang Y, Guo Y, *et al*. Clinical practice guidelines and experts' consensuses of traditional Chinese herbal medicine for novel coronavirus (COVID-19): protocol of a systematic review. Syst Rev 2020;9(1):170. doi:10.1186/s13643-020-01432-4, PMID:32746913.
[35] Zhang D, Zhang B, Lv JT, Sa RN, Zhang XM, Lin ZJ. The clinical benefits of Chinese patent medicines against COVID-19 based on current evidence. Pharmacol Res 2020;157:104882. doi:10.1016/j.phrs.2020.104882, PMID:32380051.
[36] Qiu J. China plans to modernize traditional medicine. Nature 2007;446(7136):590–591. doi:10.1038/446590a, PMID:17410143.
[37] Leonti M, Casu L. Traditional medicines and globalization: current and future perspectives in ethnopharmacology. Front Pharmacol 2013;4:92. doi:10.3389/fphar.2013.0009, PMID:23898296.
[38] Li DD, Yu P, Xiao W, Wang ZZ, Zhao LG. Berberine: A Promising Natural Isoquinoline Alkaloid for the Development of Hypolipidemic Drugs. Curr Top Med Chem 2020;20(28):2634–2647. doi:10.2174/1568026620666200908165913, PMID:32901585.
[39] Ru J, Li P, Wang J, Zhou W, Li B, Huang C, *et al*. TCMSP: a database of systems pharmacology for drug discovery from herbal medicines. J Cheminform 2014;6:13. doi:10.1186/1758-2946-6-13, PMID:24735618.
[40] Ma C, Sacco MD, Xia Z, Lambrinidis G, Townsend JA, Hu Y, *et al*. Discovery of SARS-CoV-2 Papain-like Protease Inhibitors through a Combination of High-Throughput Screening and a FlipGFP-Based Reporter Assay. ACS Cent Sci 2021;7(7):1245–1260. doi:10.1021/acscentsci.1c00519, PMID:34341772.
[41] DeMirci H. Ambient-Temperature Serial Femtosecond X-ray Crystal structure of SARS-CoV-2 Main Protease at 2.1 A Resolution (P212121). doi:10.2210/pdb7cwc/pdb.
[42] Brooks BR, Bruccoleri RE, Olafson BD, States DJ, Swaminathan S, Karplus M. CHARMm - A program for macromolecular energy, minimization, and dynamics calculation. J Comput Chem 1983;4:187–217. doi:10.1002/jcc.540040211.
[43] Ratia K, Pegan S, Takayama J, Sleeman K, Coughlin M, Baliji S, *et al*. A noncovalent class of papain-like protease/deubiquitinase inhibitors blocks SARS virus replication. Proc Natl Acad Sci U S A 2008;105(42):16119–16124. doi:10.1073/pnas.0805240105, PMID:18852458.
[44] Wu G, Robertson DH, Brooks CL 3rd, Vieth M. Detailed analysis of grid-based molecular docking: A case study of CDOCKER-A CHARMm-based MD docking algorithm. J Comput Chem 2003;24(13):1549–1562. doi:10.1002/jcc.10306, PMID:12925999.
[45] Daina A, Michielin O, Zoete V. SwissADME: a free web tool to evaluate pharmacokinetics, drug-likeness and medicinal chemistry friendliness of small molecules. Sci Rep 2017;7:42717. doi:10.1038/srep42717, PMID:28256516.
[46] Daina A, Michielin O, Zoete V. iLOGP: a simple, robust, and efficient description of n-octanol/water partition coefficient for drug design using the GB/SA approach. J Chem Inf Model 2014;54(12):3284–3301. doi:10.1021/ci500467k, PMID:25382374.
[47] Lipinski CA, Lombardo F, Dominy BW, Feeney PJ. Experimental and computational approaches to estimate solubility and permeability in drug discovery and development settings. Adv Drug Deliv Rev 2001;46(1-3):3–26. doi:10.1016/s0169-409x(00)00129-0.
[48] Ertl P, Rohde B, Selzer P. Fast calculation of molecular polar surface area as a sum of fragment-based contributions and its application to the prediction of drug transport properties. J Med Chem 2000;43(20):3714–3717. doi:10.1021/jm000942e, PMID:11020286.
[49] Shen X, Yin F. The mechanisms and clinical application of Traditional Chinese Medicine Lianhua-Qingwen capsule. Biomed Pharmacother 2021;142:111998. doi:10.1016/j.biopha.2021.111998, PMID:34385103.
[50] Zhang L, Ma Y, Shi N, Tong L, Liu S, Ji X, *et al*. Effect of Qingfei Paidu decoction combined with Western medicine treatments for COVID-19: A systematic review and meta-analysis. Phytomedicine 2022;102:154166. doi:10.1016/j.phymed.2022.154166, PMID:35636170.

Journal of Exploratory Research in Pharmacology **2023** vol. 8(2) | 107–120
DOI: 10.14218/JERP.2022.00068

Original Article

Network Pharmacology Analysis of Potential Mechanisms Underlying the Action of *Radix Salviae* in Preventing In-stent Restenosis After Percutaneous Coronary Intervention

Lu-Jing Zheng[1], Zhen Zhao[2], Da-Wei Wang[2,3], Rong-Yuan Yang[2] and Qing Liu[2*]

[1]*Hebei Provincial Hospital of Traditional Chinese Medicine, Hebei Provincial Institute of Traditional Chinese Medicine Preparation Industry Technology, Shijiazhuang, China;* [2]*Guangdong Provincial Hospital of Chinese Medicine, The Second Clinical School of Medicine, Guangzhou University of Chinese Medicine, Guangdong, China;* [3]*Shunde Hospital of Guangzhou University of Chinese Medicine, Guangdong, China*

Received: August 18, 2022 | **Revised:** September 21, 2022 | **Accepted:** October 25, 2022 | **Published online:** December 20, 2022

Abstract

Background and objectives: In-stent restenosis (ISR) is a common complication after percutaneous coronary intervention. This study aimed to investigate the mechanisms of *Radix Salviae* in preventing ISR based on network pharmacology.

Methods: The bioactive compounds were searched from natural product databases. The related targets were collected from the databases and screened. The drug-compound-target-disease network was then constructed by Venny and Cytoscape software, and the intersection targets were further investigated in the STRING database. Functional enrichment analysis was performed in the DAVID database by conducting gene ontology and Kyoto Encyclopaedia of Genes and Genomes analyses. The software AutoDock Vina was used to conduct the molecular docking simulation.

Results: A total of 33 bioactive compounds, including Luteolin, Tanshinone iia, and Dihydrotanshinlactone of *Radix Salviae*, were predicted with 53 targets as the compound-related targets in the ISR disease. Then the protein-protein interaction analysis discovered three key nodes, i.e., STAT3, JUN, and TP53. Moreover, functional enrichment of the gene ontology analysis demonstrated that the main biological processes included the response to the drug and regulation of the transcription from the RNA polymerase II promoter. The main molecular functions included protein binding, etc. The Kyoto Encyclopaedia of Genes and Genomes analysis revealed that the signaling pathways were mainly related to the PI3K-Akt signaling pathway, lipid-atherosclerosis signaling pathway, etc. Further investigation by molecular docking simulation between the ligands of the *Radix Salviae* compounds and target proteins revealed great probability binding activities between Luteolin-STAT3 (−7.4 kcal/mol), Tanshinone iia-TP53 (−7.2 kcal/mol), and Luteolin-TP53 (−6.2 kcal/mol).

Conclusions: This study indicated that the bioactive compounds like Tanshinone in *Radix Salviae* could modulate ISR via PI3K-Akt and lipid-atherosclerosis pathways, and the targets probably included STAT3, JUN, and TP53.

Keywords: Coronary atherosclerotic heart disease (CHD); Network pharmacology; In-stent Restenosis; *Radix Salviae*; Percutaneous coronary intervention (PCI).

Abbreviations: CHD, coronary atherosclerotic heart disease; DAVID, database for annotation visualization and integrated discovery; DL, drug-likeness; EC, endothelial cells; GO, gene ontology; ISR, in-stent restenosis; KEGG, Kyoto Encyclopaedia of Genes and Genomes; NCBI gene, National Center for Biotechnology Information gene; NIRS, near-infrared spectroscopy; OB, oral bioavailability; OCT, optical coherence tomography; PCI, percutaneous coronary intervention; PPI, protein-protein interaction; TTD, Therapeutic Target Database; VSMC, vascular smooth muscle cells.

***Correspondence to:** Qing Liu, Guangdong Provincial Hospital of Chinese Medicine, The Second Clinical School of Medicine, Guangzhou University of Chinese Medicine, Guangdong 510120, China. ORCID: https://orcid.org/0000-0002-2199-2999. Tel: +86 13631223512, Fax: +86 0756-3325088, E-mail: 851757626@qq.com

How to cite this article: Zheng LJ, Zhao Z, Wang DW, Yang RY, Liu Q. Network Pharmacology Analysis of Potential Mechanisms Underlying the Action of *Radix Salviae* in Preventing In-stent Restenosis After Percutaneous Coronary Intervention. *J Explor Res Pharmacol* 2023;8(2):107–120. doi: 10.14218/JERP.2022.00068.

Introduction

Coronary atherosclerotic heart disease (CHD) is a common global disease, which leads to the narrowing or occlusion of the blood vessels resulting in myocardial ischemia, hypoxia, and necrosis.[1] Although improving the symptoms of CHD, percutaneous coronary intervention (PCI) also injures the vascular endothelium, induces or aggravates the vascular inflammatory response, and leads to postoperative in-stent restenosis (ISR).[2] *Radix Salviae* and its bioactive compounds in different dosage forms are widely used in clinics in many Asian countries to treat CHD, and it has been reported that extracts from *Radix Salviae* are helpful in preventing

injury-activated neointimal hyperplasia[3] and the occurrence of ISR that follows.[4,5]

Network pharmacology has been increasingly applied in Chinese medicine research, including the study of the herb *Radix Salviae*.[6,7] Furthermore, the network pharmacology of Chinese medicine has been developed into a new interdisciplinary subject, which has combined the methods of network science, bioinformatics, computer science, and mathematics into the study of Chinese medicine pharmacology, and elucidated Chinese medicine from the molecular level and the functions of molecular network regulation.[8] However, the underlying mechanisms of *Radix Salviae* and its bioactive compounds in regulating the occurrence of ISR after PCI in patients with CHD have not yet been intensively studied Thus, this study was designed to investigate the potential mechanisms of *Radix Salviae* in preventing the occurrence of ISR after PCI based on network pharmacological techniques.

Methods

Bioactive compounds of Radix Salviae and compound-target prediction

The compounds of *Radix Salviae* were mainly searched from three natural product databases, i.e., Lab of Systems Pharmacolog (TCMSP; https://old.tcmsp-e.com/tcmsp.php, https://pubmed.ncbi.nlm.nih.gov/24735618/), a Bioinformatics Analysis Tool of Molecular Mechanism of Traditional Chinese Medicine (BATMAN, http://bionet.ncpsb.org.cn/batman-tcm/), and TCM@Taiwan (http:// tcm.cmu.edu.tw). The compounds were collected and any duplications were removed. To identify the compounds that could exert bioactive activities, the bioactive compound candidates were screened with the criteria of Lipinski's rule,[9] including oral bioavailability (OB) ≥30%, drug-likeness (DL) ≥0.18, and HL ≥4. In this study, we selected the three commonly used webservers (i.e., TCMSP, BATMAN, and TCM@Taiwan) to collect the predicted targets for the compounds. The compound-related targets were further screened by setting the prediction score of ≥50 where there was a threshold.

ISR disease-related targets

The disease-related targets were collected by searching the keyword "In-stent restenosis" and target species "Homo sapiens". ISR-target genes were obtained from the three databases: Gene cards (www.genecards.org/), National Centre for Biotechnology Information gene (NCBI genes, www.ncbi.nlm.nih.gov/gene), and Therapeutic Target Database (TTD; http://db.idrblab.net/ttd). Duplications of the ISR targets from the different databases were removed, and the overlapping target genes from these databases were collected.

Drug-compound-target-disease network

The targets of the *Radix Salviae* compounds related to the ISR disease were demonstrated and constructed by the drug-compound-target-disease network. The intersection of the *Radix Salviae* compound-related targets and the ISR disease-related targets were obtained and plotted as a Venn diagram by Venny2.1 (https://bioinfogp.cnb.csic.es/tools/venny/). Then the network of the *Radix Salviae* compound targets related to the ISR disease was constructed by the Cytoscape software version 3.6.1 (www.cytoscape.org).

Protein-protein interaction (PPI) network construction

The interaction network among the screened target candidates was helpful to determine the core regulatory genes. Here the STRING database (https://string-db.org/) was used for this analysis by uploading the identifiers or sequences of the proteins from the intersection of the drug-compound-target-disease network. The specific settings in this system were performed by selecting "Homo sapiens" in the organism, selecting "Evidence" in the meaning of the network edges, selecting the "highest confidence (0.900)" in the minimum required interaction score, hiding disconnected nodes in the network, and obtaining the correlation data among the targets, then importing the acquired data into the Cytoscape software for the PPI network construction. The nodes with a degree more than twice of the average number of neighbors were regarded as the key nodes in the PPI network, and nodes with a degree more than the median number were collected.

Functional enrichment analysis

The Database for Annotation Visualization and Integrated Discovery version 2021 (DAVID; https://david.ncifcrf.gov/home.jsp) database was used to enrich the functions of the intersection targets. The DAVID database integrated the gene ontology (GO) biological process and Kyoto Encyclopaedia of Genes and Genomes (KEGG) pathway to annotate the biological processes and pathway analysis. The screening criteria of $p < 0.05$ was set by Bonferroni correction in the GO analysis, and the criteria of $p < 0.05$ and the Kappa Score ≥0.4 were set in the KEGG analysis. Additionally, the biological processes or pathways with the count of enrolled genes more than the median count and enrichment factor >1.5 were collected and ranked, then they were grouped according to the similarity of their members. The functional items with a degree more than the median number were regarded as key functional items. The top-ranked pathways were selected and mapped by the KEGG database, and the key genes enrolled in the selected pathways were labeled by red stars. The histogram of the top-ranked GO biological processes and bubble chart of the top-ranked KEGG signaling pathways were plotted.

Molecular docking verification

The database of the Research Collaboratory for Structural Bioinformatics PDB (RCSR PDB) (www.rcsb.org) was used to check the target protein structures, and the database of NCBI PubChem (https://pubchem.ncbi.nlm.nih.gov) was used to find the docking ligand of the *Radix Salviae* compounds like Luteolin, Tanshinone iia, and Cryptotanshinone. After obtaining the molecular structures of the target proteins and ligand compounds, the PyMOL software was used to remove H_2O and ligands. Then the molecular docking stimulation of the target proteins and ligand compounds was conducted in the software of AutoDock Vina. The binding energy of less than −5.0 kcal/mol was characterized as good binding activity, and the lower binding energy indicated the greater probability of binding activity.[10]

Results

Bioactive compounds and candidate targets

A total of 326 components of *Radix Salviae* were collected from the three main databases of TCM. The bioactive compound candidates were screened by Lipinski's rule. Then, the duplications were removed and a total of 45 bioactive compounds were finally included for further analysis. The candidate targets of each compound were searched in the databases above with the name of the compound or its molecular ID. Not all of the screened compounds

Table 1. The top-ranked bioactive ingredients in *Radix Salviae* with Lipinski's Rule from the database

Mol ID	Molecule name	MW	AlogP	Hdon	Hacc	OB (%)	Caco-2	BBB	DL	FASA-	HL
MOL007154	Tanshinone iia	294.37	4.66	0	3	49.89	1.05	0.7	0.4	0.31	23.56
MOL007156	Tanshinone VI	296.34	2.44	2	4	45.64	0.48	−0.28	0.3	0.38	15.21
MOL007151	Tanshindiol b	312.34	2.34	2	5	42.67	0.05	−0.63	0.45	0.33	22.25
MOL007079	Tanshinaldehyde	308.35	3.83	0	4	52.47	0.57	−0.07	0.45	0.32	23.49
MOL002222	Sugiol	300.48	4.99	1	2	36.11	1.14	0.7	0.28	0.27	14.62
MOL007077	Sclareol	308.56	4.27	2	2	43.67	0.84	0.51	0.21	0.27	4.71
MOL007085	Salvilenone	292.4	4.26	0	2	30.38	1.46	1.07	0.38	0.35	20.81
MOL007071	Przewaquinone f	312.34	2.07	2	5	40.31	−0.09	−0.9	0.46	0.29	22.45
MOL007152	Przewaquinone e	312.34	2.34	2	5	42.85	−0.04	−0.65	0.45	0.32	22.44
MOL007069	Przewaquinone c	296.34	3.31	1	4	55.74	0.42	−0.3	0.4	0.32	23.7
MOL007068	Przewaquinone b	292.3	2.99	1	4	62.24	0.39	−0.45	0.41	0.38	24.94
MOL007130	Prolithospermic acid	314.31	2.77	4	6	64.37	0.1	−0.75	0.31	0.42	8.82
MOL007124	Neocryptotanshinone ii	270.35	3.61	1	3	39.46	0.76	0.16	0.23	0.32	26.98
MOL007125	Neocryptotanshinone	314.41	3.01	2	4	52.49	0.35	−0.13	0.32	0.28	14.46
MOL007122	Miltirone	282.41	4.73	0	2	38.76	1.23	0.87	0.25	0.32	14.82
MOL007119	Miltionone I	312.39	3.33	1	4	49.68	0.35	−0.11	0.32	0.35	41.49
MOL007061	Methylenetanshinquinone	278.32	4.26	0	3	37.07	1.03	0.46	0.36	0.36	24.33
MOL000006	Luteolin	286.25	2.07	4	6	36.16	0.19	−0.84	0.25	0.39	15.94
MOL007111	Isotanshinone ii	294.37	4.66	0	3	49.92	1.03	0.45	0.4	0.3	24.73
MOL007108	Isocryptotanshi-none	296.39	3.59	0	3	54.98	0.93	0.34	0.39	0.3	31.92
MOL007058	Formyltanshinone	290.28	3.36	0	4	73.44	0.54	−0.28	0.42	0.41	24.12
MOL007101	Dihydrotanshinone I	278.32	2.86	0	3	45.04	0.95	0.43	0.36	0.4	18.32
MOL007100	Dihydrotanshinlactone	266.31	2.77	0	3	38.68	1.26	0.81	0.32	0.38	5.42
MOL007098	Deoxyneocryptotanshinone	298.41	4.32	1	3	49.4	0.85	0.24	0.29	0.3	27.17
MOL002651	Dehydrotanshinone ii a	292.35	4.22	0	3	43.76	1.02	0.52	0.4	0.33	23.71
MOL007093	Dan-shexinkum d	336.41	2.83	1	4	38.88	0.67	−0.15	0.55	0.35	30
MOL007094	Danshenspiroketallactone	282.36	3.24	0	3	50.43	0.88	0.51	0.31	0.34	15.19
MOL007081	Danshenol b	354.48	2.59	1	4	57.95	0.53	0.11	0.56	0.3	4.28
MOL007082	Danshenol a	336.41	2.01	1	4	56.97	0.33	−0.01	0.52	0.34	5.15
MOL007088	Cryptotanshinone	296.39	3.44	0	3	52.34	0.95	0.51	0.4	0.29	17.3
MOL001601	1,2,5,6-tetrahydrotanshinone	280.34	2.98	0	3	38.75	0.96	0.39	0.36	0.33	18.05
MOL007049	4-methylenemiltirone	266.36	4.33	0	2	34.35	1.25	0.87	0.23	0.38	14.6
MOL007045	3α-hydroxytanshinone IIa	310.37	3.56	1	4	44.93	0.53	0.22	0.44	0.3	23.78

AlogP, octanol-water partition coefficient; BBB, blood-brain barrier; DL, drug-likeness; FASA-, fractional negative accessible surface area; hacc, hydrogen bond acceptor count; hdon, hydrogen bond donor count; HL, half-life; MW, molecular weight; OB, oral bioavailability.

had targets, and 12 compounds with no target were removed. Thus, 33 bioactive compounds of *Radix Salviae* with 122 candidate targets were predicted (Table 1).

Compound-target network related to ISR

In total, 528 ISR-related targets from three main databases of human genomes were collected, and the duplications were removed. Then 461 ISR-related targets were used for the intersection analysis with 122 candidate targets related to the compounds screened from *Radix Salviae*. A Venn diagram showed that 53 targets (about 10% of the combined targets) were selected as the *Radix Salviae* compound-related targets in the ISR disease (Fig. 1a).

Drug-compound-target-disease network

In order to display the relationship among the *Radix Salviae* compounds and their potential targets in ISR development, the drug-compound-target-disease network was composed with the software Cytoscape. The degree term was used to screen the hub compounds and hub targets in the compound-target network, and the results could reflect the importance of the nodes through their numbers of

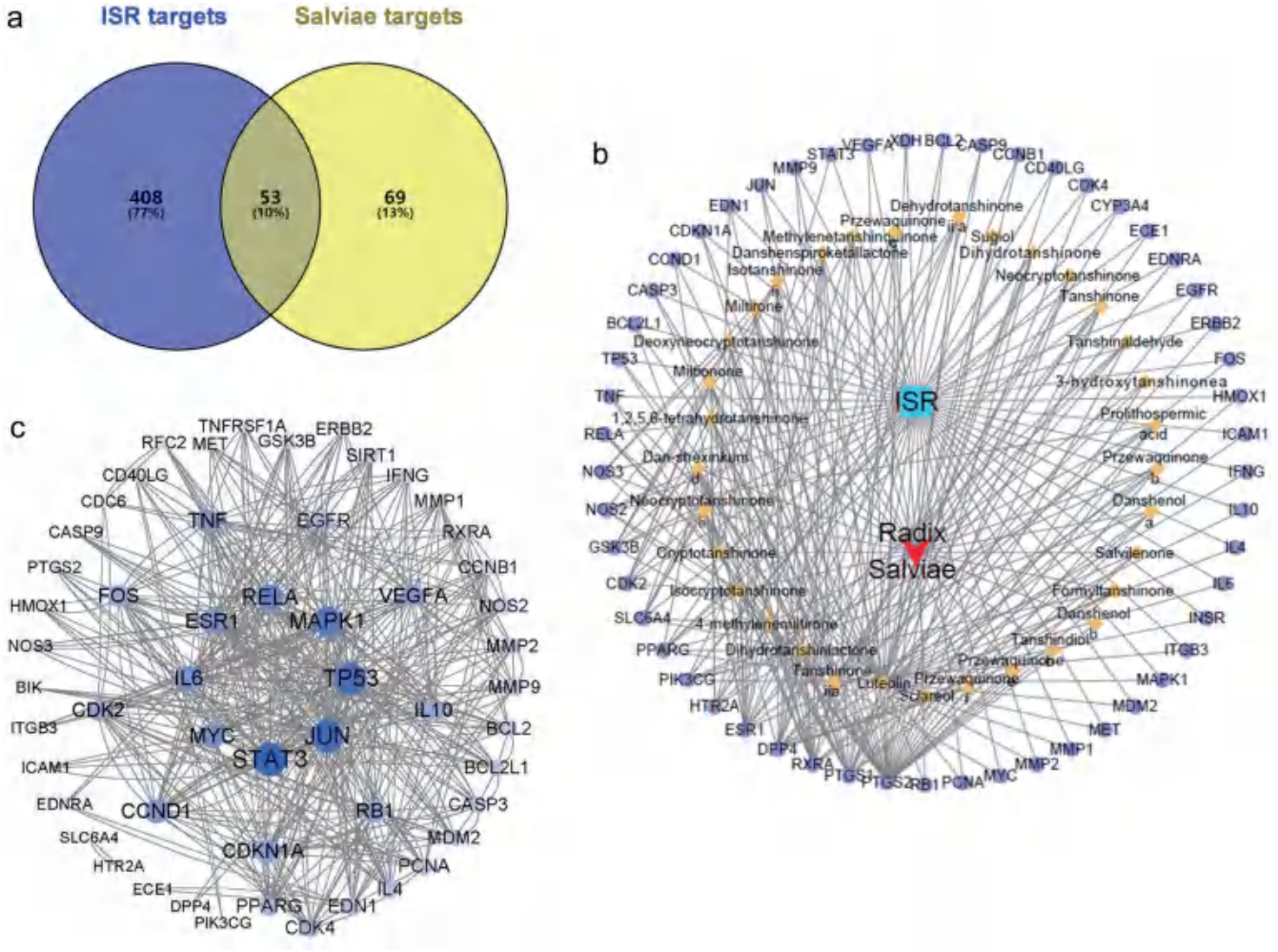

Fig. 1. Screening the hub targets and interacted proteins from Radix Salviae for the ISR disease. (a) The Venn diagram indicated the number of intersection targets of the ISR-related genes and targets of the bioactive compounds from *Radix Salviae*. (b) The drug-compound-target-disease network showed the intersection targets of the ISR-related genes and targets of the bioactive compounds from *Radix Salviae*. The circle size indicated the degree of the interacted targets. (c) The protein-protein interaction network from STRING database showed the interaction among the hub targets of the drug-compound-target-disease network. The circle size and transparency indicated the degree of the interacted targets. ISR, in-stent restenosis.

connections to other nodes.[11] Our results showed the hub compounds with a criteria of degree of ≥30 were Luteolin, Tanshinone iia, Dihydrotanshinlactone, 4-methylenemiltirone, Isocryptotanshinone, Cryptotanshinone, Neocryptotanshinone ii, Dan-shexinkum d, and 1,2,5,6-tetrahydrotanshinone. The active compounds screened from *Radix Salviae* were further verified by the published papers, and we found that some of the above-mentioned compounds (e.g. Luteolin,[12,13] Tanshinone iia,[14] and Cryptotanshinone[15]) were reported to be potential therapeutic drugs for ISR prevention and treatment. The hub targets with a degree ≥5 were PTGS2, PTGS1, RXRA, DPP4, ESR1, HRT2A, PIK3CG, PPARG, SLC6A4, CDK2, and GSK3B. The intersection targets of the ISR-related genes and targets of the bioactive compounds from *Radix Salviae* are described in Figure 1b and Table 2.

Protein-protein interaction network

To further study the interactions among the target proteins of the *Radix Salviae* compounds in the ISR development and explore the hub target proteins in the PPI, the STRING database was used to construct the PPI network. The 53 potential targets for *Radix Salviae* in the treatment of ISR were uploaded to the STRING database. Finally, three key nodes with a degree more than twice of the average number of neighbors in the network[16] were obtained (Fig. 1c), i.e., STAT3 (degree 23), JUN (degree 22), and TP53 (degree 21). Nodes with a degree more than the median number of the degree are listed in Table 3. The results suggested that these targets of *Radix Salviae* probably affected the ISR pathology.

Functional enrichment analysis

The cluster of the *Radix Salviae* compound-related targets in the ISR disease was subsequently uploaded to the DAVID database. The enrichment analysis of the targets for *Radix Salviae* in regulating the ISR pathology was then performed, and we obtained 454 GO biological processes, 42 GO cellular components, 88 GO molecular functions, and 142 KEGG signaling pathways. The top-ranked items in GO and KEGG are listed in Tables 4–7. For the GO items, Figure 2 showed that the main biological processes in

Table 2. The top-ranked gene targets in the intersection of the *Radix Salviae* ingredients-related genes and ISR-related genes

Target name	Degree	Average shortest path length	Betweenness centrality	Closeness centrality	Neighborhood connectivity	Number of directed edges	Radiality	Stress	Topological coefficient
PTGS2	34	1.93960924	0.05423601	0.51556777	34.38235294	34	0.76509769	548920	0.06310464
PTGS1	20	2.01776199	0.02779512	0.49559859	47.75	20	0.7455595	359378	0.08973129
RXRA	18	2.04618117	0.02385006	0.48871528	50.33333333	18	0.73845471	317668	0.09579288
DPP4	17	2.02841918	0.02218696	0.49299475	48.17647059	17	0.7428952	245162	0.09054985
ESR1	15	2.09236234	0.01899042	0.47792869	54.53333333	15	0.72690941	251874	0.1060066
PPARG	8	2.07815275	0.00985313	0.48119658	84	8	0.73046181	132576	0.16085271
PIK3CG	8	2.09591474	0.00880962	0.47711864	78.125	8	0.72602131	96164	0.15092955
HTR2A	8	2.13854352	0.00932818	0.46760797	81.5	8	0.71536412	135092	0.16132265
SLC6A4	7	2.14920071	0.00810756	0.46528926	91.85714286	7	0.71269982	126928	0.18281115
GSK3B	7	2.13854352	0.00779648	0.46760797	91.85714286	7	0.71536412	122358	0.18171429
CDK2	7	2.14564831	0.00775917	0.4660596	91.14285714	7	0.71358792	121972	0.18100975
NOS2	6	2.14564831	0.0066054	0.4660596	99.66666667	6	0.71358792	92324	0.19772879
NOS3	5	2.1740675	0.00560859	0.45996732	116.2	5	0.70648313	83560	0.23414634

ISR included the response to the drug, regulation of the transcription from the RNA polymerase II promoter, regulation of the cell proliferation, regulation of the DNA-templated transcription, and regulation of the gene expression. The main cellular components included the nucleus, cytosol, nucleoplasm, cytoplasm, and plasma membrane. The main molecular functions included protein binding, identical protein binding, enzyme binding, and macromolecular complex binding. Additionally, the KEGG pathway enrichment results suggested that the mechanisms of the *Radix Salviae* compounds in affecting ISR were mainly related to the PI3K-Akt signaling pathway, lipid and atherosclerosis, endocrine resistance, AGE-RAGE signaling pathway in diabetic complications, HIF-1 signaling pathway, fluid shear stress and atherosclerosis, IL-17 signaling pathway, and MAPK signaling pathway (Fig. 3). For the

Table 3. The top-ranked hub targets in the protein-protein interaction network for the ISR from the STRING database

Target name	Degree	Betweenness centrality	Closeness centrality	Clustering coefficient	Degree layout	Neighborhood connectivity	Number of directed edges	Radiality	Stress	Topological coefficient
STAT3	23	0.16854	0.607143	0.280632	46	10.65217	23	0.870588	1984	0.231569
JUN	22	0.133907	0.614458	0.324675	44	11.72727	22	0.87451	1608	0.244318
TP53	21	0.147607	0.579545	0.280952	42	10.14286	21	0.854902	1688	0.239229
MAPK1	19	0.137273	0.607143	0.28655	38	11.42105	19	0.870588	1474	0.232009
RELA	17	0.087643	0.573034	0.419118	34	12.58824	17	0.85098	1086	0.267835
IL6	15	0.039766	0.520408	0.409524	30	11.53333	15	0.815686	610	0.288333
MYC	15	0.033492	0.56044	0.504762	30	13.86667	15	0.843137	510	0.295035
ESR1	15	0.053931	0.566667	0.380952	30	12.6	15	0.847059	722	0.2625
TNF	14	0.038757	0.51	0.43956	28	11.35714	14	0.807843	534	0.291209
CCND1	14	0.039052	0.542553	0.527473	28	13.5	14	0.831373	580	0.3
VEGFA	13	0.033573	0.485714	0.358974	26	9.461538	13	0.788235	352	0.260684
CDKN1A	13	0.03638	0.525773	0.487179	26	12.46154	13	0.819608	512	0.283217
FOS	12	0.018025	0.53125	0.545455	24	14.66667	12	0.823529	286	0.325926
RB1	12	0.018022	0.5	0.484848	24	12.16667	12	0.8	276	0.304167
IL10	11	0.022195	0.455357	0.436364	22	9.545455	11	0.760784	246	0.289256
CDK2	11	0.037222	0.46789	0.527273	22	11.54545	11	0.772549	528	0.339572
EGFR	10	0.039183	0.504951	0.4	20	12.2	10	0.803922	480	0.283721

MW, molecular weight; OB, oral bioavailability; BBB, blood-brain barrier; DL, drug-likeness; FASA-, fractional negative accessible surface area; HL, half-life; ISR, in-stent restenosis.

Table 4. The top-ranked biological process in the GO analysis of the *Radix Salviae*-targeted genes in the ISR disease

GO #	Term	Count	%	P value	Genes	Fold enrichment	FDR
GO:0042493	Response to the drug	20	37.73584906	8.46E−22	IL10, CDKN1A, JUN, STAT3, FOS, HTR2A, PTGS2, RELA, SLC6A4, ICAM1, CCNB1, CCND1, CDK4, MYC, CASP3, MDM2, BCL2, HMOX1, PPARG, TP53	24.67254814	1.19E−18
GO:0045944	Positive regulation of the transcriptions from the RNA polymerase II promoter	19	35.8490566	8.82E−10	IL10, RB1, JUN, EDN1, STAT3, FOS, ESR1, TNF, EGFR, RELA, VEGFA, IL4, IL6, RXRA, MYC, MDM2, PPARG, MET, TP53	5.795446222	8.86E−08
GO:0000122	Negative regulation of the transcriptions from the RNA polymerase II promoter	18	33.96226415	2.53E−10	RB1, JUN, EDN1, PCNA, STAT3, ESR1, TNF, RELA, VEGFA, IL4, RXRA, IFNG, CCND1, MYC, CDK2, MDM2, PPARG, TP53	6.834192167	3.23E−08
GO:0008284	Positive regulation of the cell proliferation	17	32.0754717	4.37E−13	EDN1, INSR, HTR2A, EGFR, RELA, VEGFA, DPP4, IL4, IL6, IFNG, CDK4, MYC, ERBB2, CDK2, MDM2, BCL2, BCL2L1	11.50692531	1.53E−10
GO:0045893	Positive regulation of the DNA-templated transcriptions	17	32.0754717	1.10E−11	IL10, JUN, INSR, STAT3, FOS, ESR1, TNF, EGFR, RELA, IL4, IL6, RXRA, MYC, CDK2, MAPK1, PPARG, TP53	9.296063711	1.93E−09
GO:0010628	Positive regulation of the gene expression	16	30.18867925	3.44E−12	GSK3B, NOS3, STAT3, TNF, RELA, SLC6A4, VEGFA, IL4, IL6, IFNG, MYC, ERBB2, MDM2, MAPK1, PPARG, TP53	11.36197502	8.05E−10
GO:0043066	Negative regulation of the apoptotic processes	16	30.18867925	4.06E−12	IL10, GSK3B, CDKN1A, MMP9, EGFR, RELA, VEGFA, IL4, IL6, CD40LG, MYC, CASP3, MDM2, BCL2, TP53, BCL2L1	11.22960249	8.16E−10
GO:0009410	Response to the xenobiotic stimulus	14	26.41509434	4.48E−14	IL10, JUN, MMP2, FOS, HTR2A, PTGS2, TNF, SLC6A4, CCND1, CDK4, MYC, CASP3, BCL2, HMOX1	21.44211705	3.15E−11
GO:0010629	Negative regulation of the gene expression	13	24.52830189	2.80E−11	RB1, GSK3B, CDKN1A, EDN1, NOS2, ESR1, TNF, VEGFA, CCNB1, IFNG, MYC, PPARG, XDH	15.25612595	3.94E−09
GO:0006357	Regulation of the transcription from the RNA polymerase II promoter	13	24.52830189	0.001647095	RB1, JUN, STAT3, FOS, ESR1, TNF, RELA, VEGFA, RXRA, MYC, MDM2, PPARG, TP53	2.765677924	0.015647401
GO:0043065	Positive regulation of the apoptotic process	12	22.64150943	1.05E−09	CASP9, IL6, JUN, CDK4, CASP3, MMP2, HMOX1, PPARG, PTGS2, TNF, TP53, MMP9	13.18368985	9.81E−08
GO:0007165	Signal transduction	12	22.64150943	3.37E−04	IL10, GSK3B, EDNRA, CDK4, ERBB2, STAT3, CDK2, MAPK1, PPARG, ESR1, MET, EGFR	3.581696088	0.004733706
GO:0071456	Cellular response to hypoxia	11	20.75471698	1.96E−12	EDN1, CCNB1, MYC, MDM2, BCL2, HMOX1, PPARG, PTGS2, TP53, ICAM1, VEGFA	30.35100101	5.50E−10
GO:0006468	Protein phosphorylation	11	20.75471698	9.00E−07	GSK3B, EDN1, EDNRA, CCNB1, CCND1, CDK4, INSR, ERBB2, CDK2, MAPK1, PIK3CG	7.842171858	3.61E−05
GO:0007568	Aging	10	18.86792453	1.96E−09	IL10, CASP9, JUN, MMP2, STAT3, MAPK1, FOS, HTR2A, PTGS2, RELA	19.02383317	1.62E−07
GO:0051726	Regulation of the cell cycle	10	18.86792453	1.47E−07	RB1, CDKN1A, JUN, IFNG, CCND1, CDK4, MYC, STAT3, MDM2, TP53	11.54801374	6.66E−06
GO:0006954	Inflammatory response	10	18.86792453	1.22E−06	IL6, CD40LG, NOS2, STAT3, FOS, PTGS2, TNF, RELA, PIK3CG, PTGS1	8.969052858	4.40E−05

GO, gene ontology; ISR, in-stent restenosis.

Table 5. The top-ranked cellular component in the GO analysis of the *Radix Salviae*-targeted genes in the ISR disease

GO#	Term	Count	%	P value	Genes	Fold enrichment	FDR
GO:0005634	Nucleus	29	54.71698113	1.48E−04	RB1, GSK3B, CDKN1A, PCNA, ITGB3, RELA, EGFR, CASP9, CCNB1, RXRA, CCND1, MYC, CASP3, ERBB2, MAPK1, HMOX1, JUN, NOS2, NOS3, MMP2, STAT3, FOS, ESR1, CDK4, CDK2, BCL2, MDM2, PPARG, TP53	1.886557	0.002572
GO:0005829	Cytosol	28	52.83018868	9.64E−05	RB1, GSK3B, CDKN1A, HTR2A, RELA, PIK3CG, CASP9, CCNB1, RXRA, CCND1, CASP3, ERBB2, MAPK1, HMOX1, XDH, JUN, NOS2, NOS3, STAT3, FOS, ESR1, CDK4, CDK2, BCL2, MDM2, PPARG, TP53, BCL2L1	1.977014	0.00188
GO:0005654	Nucleoplasm	24	45.28301887	2.96E−05	RB1, GSK3B, CDKN1A, JUN, PCNA, NOS2, ITGB3, STAT3, FOS, ESR1, RELA, CCNB1, RXRA, CCND1, CDK4, MYC, CASP3, CDK2, MDM2, BCL2, MAPK1, HMOX1, PPARG, TP53	2.370921	7.70E−04
GO:0005737	Cytoplasm	24	45.28301887	0.004653505	GSK3B, EDN1, NOS2, NOS3, STAT3, CYP3A4, PTGS2, ESR1, EGFR, PIK3CG, RELA, PTGS1, VEGFA, CASP9, CCNB1, CCND1, CASP3, CDK2, MDM2, BCL2, MAPK1, PPARG, TP53, BCL2L1	1.698682	0.034569
GO:0005886	Plasma membrane	23	43.39622642	0.003955116	GSK3B, JUN, NOS2, NOS3, ITGB3, MMP2, INSR, STAT3, ECE1, HTR2A, ESR1, TNF, EGFR, PIK3CG, SLC6A4, ICAM1, DPP4, EDNRA, CD40LG, ERBB2, MDM2, MAPK1, MET	1.757377	0.032474
GO:0016020	Membrane	16	30.18867925	0.001302967	INSR, ECE1, FOS, ESR1, TNF, EGFR, PIK3CG, ICAM1, VEGFA, DPP4, CCNB1, CD40LG, CCND1, BCL2, HMOX1, MET	2.417372	0.013551
GO:0005615	Extracellular space	14	26.41509434	8.69E−04	IL10, EDN1, MMP2, TNF, MMP9, EGFR, ICAM1, VEGFA, IL4, IL6, CD40LG, IFNG, HMOX1, XDH	2.794373	0.010429
GO:0005576	Extracellular region	13	24.52830189	0.006594857	IL10, EDN1, MMP1, MMP2, TNF, MMP9, VEGFA, DPP4, IL4, IL6, IFNG, MAPK1, MET	2.33726	0.042867
GO:0032991	Macromolecular complex	12	22.64150943	1.19E−06	CASP9, CDKN1A, MYC, ITGB3, MDM2, BCL2, MAPK1, PTGS2, ESR1, TNF, TP53, EGFR	6.606668	6.17E−05
GO:0000785	Chromatin	12	22.64150943	5.23E−05	RB1, JUN, RXRA, PCNA, CDK4, MYC, STAT3, PPARG, FOS, ESR1, TP53, RELA	4.423651	0.001165
GO:0005887	Integral component of the plasma membrane	11	20.75471698	0.00347907	EDNRA, CD40LG, ITGB3, INSR, ERBB2, HTR2A, TNF, MET, EGFR, SLC6A4, ICAM1	2.890037	0.030152
GO:0005667	Transcription factor complex	10	18.86792453	6.23E−09	RB1, JUN, RXRA, CDK4, STAT3, CDK2, FOS, ESR1, TP53, RELA	16.6857	9.71E−07

GO, gene ontology; ISR, in-stent restenosis.

Table 6. The top-ranked molecular function in the GO analysis of the *Radix Salviae*-targeted genes in the ISR disease

GO#	Term	Count	%	P value	Genes	Fold enrichment	FDR
GO:0005515	Protein binding	52	98.11321	1.87E−08	RB1, GSK3B, CDKN1A, ITGB3, ECE1, HTR2A, TNF, PIK3CG, SLC6A4, ICAM1, CASP9, EDNRA, CCND1, MYC, CASP3, IL10, EDN1, MMP2, FOS, MMP9, IFNG, PPARG, MET, TP53, PCNA, CYP3A4, PTGS2, EGFR, RELA, PTGS1, DPP4, CCNB1, RXRA, ERBB2, MAPK1, HMOX1, XDH, JUN, NOS2, NOS3, INSR, STAT3, ESR1, VEGFA, IL4, IL6, CD40LG, CDK4, CDK2, BCL2, MDM2, BCL2L1	1.470875	1.45E−06
GO:0042802	Identical protein binding	28	52.83019	2.61E−15	RB1, PCNA, ITGB3, HTR2A, TNF, RELA, EGFR, PIK3CG, SLC6A4, CASP9, DPP4, RXRA, ERBB2, MAPK1, HMOX1, JUN, INSR, STAT3, FOS, MMP9, ESR1, VEGFA, BCL2, MDM2, PPARG, MET, TP53, BCL2L1	5.855632	6.06E−13
GO:0019899	Enzyme binding	15	28.30189	1.45E−12	RB1, JUN, PCNA, ITGB3, CYP3A4, PTGS2, ESR1, EGFR, RELA, RXRA, CCND1, MDM2, HMOX1, PPARG, TP53	13.90275	1.69E−10
GO:0044877	Macromolecular complex binding	11	20.75472	1.62E−07	CDKN1A, JUN, PCNA, CCND1, CDK4, MYC, CASP3, INSR, FOS, HTR2A, RELA	9.452968	7.52E−06
GO:0019901	Protein kinase binding	11	20.75472	9.38E−07	CASP9, GSK3B, CDKN1A, CCNB1, CCND1, STAT3, ESR1, TP53, RELA, EGFR, BCL2L1	7.804855	2.72E−05
GO:0042803	Protein homodimerization activity	11	20.75472	1.99E−05	DPP4, NOS2, STAT3, BCL2, HMOX1, ECE1, PTGS2, XDH, RELA, BCL2L1, VEGFA	5.524287	3.30E−04
GO:0003677	DNA binding	10	18.86792	0.008017786	JUN, PCNA, MYC, STAT3, MAPK1, PPARG, FOS, ESR1, TP53, RELA	2.763908	0.048951
GO:0008134	Transcription factor binding	9	16.98113	9.50E−08	RB1, JUN, CCND1, MYC, STAT3, PPARG, FOS, ESR1, TP53	15.39377	5.51E−06
GO:0031625	Ubiquitin protein ligase binding	9	16.98113	1.75E−06	RB1, GSK3B, CDKN1A, JUN, MDM2, BCL2, TP53, RELA, EGFR	10.48194	4.52E−05
GO:0003700	Transcription factor activity; sequence-specific DNA binding	9	16.98113	1.30E−04	JUN, RXRA, MYC, STAT3, PPARG, FOS, ESR1, TP53, RELA	5.762223	0.001673
GO:0008270	Zinc ion binding	9	16.98113	0.0024518	RXRA, MMP1, MMP2, MDM2, ECE1, PPARG, ESR1, TP53, MMP9	3.683826	0.021067
GO:0000978	RNA polymerase II core promoter proximal region sequence-specific DNA binding	9	16.98113	0.017078706	JUN, RXRA, MYC, STAT3, PPARG, FOS, ESR1, TP53, RELA	2.644406	0.077691
GO:0000981	RNA polymerase II transcription factor Activity, sequence-specific DNA binding	9	16.98113	0.023549822	JUN, RXRA, MYC, STAT3, PPARG, FOS, ESR1, TP53, RELA	2.491407	0.098682
GO:0005125	Cytokine activity	8	15.09434	8.89E−07	IL10, IL4, IL6, EDN1, CD40LG, IFNG, TNF, VEGFA	14.90765	2.72E−05
GO:0000976	Transcription regulatory region sequence-specific DNA binding	8	15.09434	3.76E−06	JUN, RXRA, STAT3, PPARG, FOS, TNF, TP53, RELA	12.00192	7.94E−05
GO:0004672	Protein kinase activity	8	15.09434	7.80E−05	GSK3B, CCND1, CDK4, ERBB2, CDK2, MET, EGFR, PIK3CG	7.493261	0.001065
GO:0004712	Protein serine/threonine/tyrosine kinase activity	8	15.09434	1.74E−04	GSK3B, CDK4, INSR, ERBB2, CDK2, MET, EGFR, PIK3CG	6.5871	0.002119
GO:0003682	Chromatin binding	8	15.09434	2.80E−04	JUN, PCNA, PPARG, FOS, ESR1, TP53, RELA, EGFR	6.091296	0.003191

GO, gene ontology; ISR, in-stent restenosis.

Table 7. The top-ranked cell signaling pathways in the KEGG analysis of the *Radix Salviae*-targeted genes in the ISR disease

Hsa #	Term	Count	%	P value	Genes	Fold enrichment	FDR
hsa04151	PI3K-Akt signaling pathway	24	45.28301887	1.46E−18	GSK3B, CDKN1A, NOS3, ITGB3, INSR, EGFR, PIK3CG, RELA, VEGFA, CASP9, IL4, IL6, RXRA, CCND1, CDK4, MYC, ERBB2, CDK2, MDM2, BCL2, MAPK1, MET, TP53, BCL2L1	10.61538462	4.28E−17
hsa05417	Lipid and atherosclerosis	20	37.73584906	1.03E−17	GSK3B, JUN, NOS3, MMP1, STAT3, FOS, TNF, MMP9, RELA, ICAM1, CASP9, IL6, RXRA, CD40LG, CASP3, BCL2, MAPK1, PPARG, TP53, BCL2L1	14.56529517	2.26E−16
hsa01522	Endocrine resistance	15	28.30188679	4.50E−16	RB1, CDKN1A, JUN, MMP2, FOS, ESR1, MMP9, EGFR, CCND1, CDK4, ERBB2, MDM2, BCL2, MAPK1, TP53	23.96585557	5.65E−15
hsa04933	AGE-RAGE signaling pathway in diabetic complications	15	28.30188679	6.03E−16	JUN, EDN1, NOS3, MMP2, STAT3, TNF, RELA, ICAM1, VEGFA, IL6, CCND1, CDK4, CASP3, BCL2, MAPK1	23.48653846	5.75E−15
hsa04066	HIF-1 signaling pathway	15	28.30188679	2.21E−15	CDKN1A, EDN1, NOS2, NOS3, INSR, STAT3, EGFR, RELA, VEGFA, IL6, IFNG, ERBB2, BCL2, MAPK1, HMOX1	21.54728299	1.62E−14
hsa05418	Fluid shear stress and atherosclerosis	15	28.30188679	6.95E−14	JUN, EDN1, NOS3, ITGB3, MMP2, FOS, TNF, MMP9, RELA, ICAM1, VEGFA, IFNG, BCL2, HMOX1, TP53	16.89679026	3.60E−13
hsa04657	IL-17 signaling pathway	13	24.52830189	2.99E−13	GSK3B, JUN, MMP1, FOS, PTGS2, TNF, MMP9, RELA, IL4, IL6, IFNG, CASP3, MAPK1	21.65425532	1.46E−12
hsa04010	MAPK signaling pathway	13	24.52830189	1.76E−07	JUN, INSR, FOS, TNF, EGFR, RELA, VEGFA, MYC, CASP3, ERBB2, MAPK1, MET, TP53	6.923469388	3.11E−07
hsa04926	Relaxin signaling pathway	12	22.64150943	2.86E−10	EDN1, JUN, NOS2, MMP1, NOS3, MMP2, MAPK1, FOS, MMP9, RELA, EGFR, VEGFA	14.56529517	8.98E−10
hsa04218	Cellular senescence	12	22.64150943	2.21E−09	RB1, IL6, CDKN1A, CCNB1, CCND1, CDK4, MYC, CDK2, MDM2, MAPK1, TP53, RELA	12.0443787	5.25E−09
hsa04115	p53 signaling pathway	11	20.75471698	1.69E−11	CASP9, CDKN1A, CCNB1, CCND1, CDK4, CASP3, CDK2, MDM2, BCL2, TP53, BCL2L1	23.59378293	6.48E−11
hsa04660	T cell receptor signaling pathway	11	20.75471698	6.16E−10	IL10, IL4, GSK3B, JUN, CD40LG, IFNG, CDK4, MAPK1, FOS, TNF, RELA	16.56102071	1.81E−09
hsa04668	TNF signaling pathway	11	20.75471698	1.29E−09	IL6, EDN1, JUN, CASP3, MAPK1, FOS, PTGS2, TNF, MMP9, RELA, ICAM1	15.37809066	3.24E−09
hsa04110	Cell cycle	11	20.75471698	4.11E−09	RB1, GSK3B, CDKN1A, CCNB1, PCNA, CCND1, CDK4, MYC, CDK2, MDM2, TP53	13.66941392	9.51E−09
hsa04068	FoxO signaling pathway	11	20.75471698	6.01E−09	IL10, IL6, CDKN1A, CCNB1, CCND1, INSR, STAT3, CDK2, MDM2, MAPK1, EGFR	13.14768056	1.32E−08
hsa04630	JAK-STAT Signaling pathway	11	20.75471698	4.66E−08	IL10, IL4, IL6, CDKN1A, IFNG, CCND1, MYC, STAT3, BCL2, EGFR, BCL2L1	10.63176638	9.03E−08
hsa01521	EGFR tyrosine kinase inhibitor resistance	10	18.86792453	1.05E−09	GSK3B, IL6, ERBB2, STAT3, BCL2, MAPK1, MET, EGFR, BCL2L1, VEGFA	19.81986368	2.71E−09
hsa04919	Thyroid hormone signaling pathway	10	18.86792453	4.72E−08	CASP9, GSK3B, RXRA, CCND1, MYC, ITGB3, MDM2, MAPK1, ESR1, TP53	12.94024158	9.03E−08
hsa04210	Apoptosis	10	18.86792453	1.30E−07	CASP9, JUN, CASP3, BCL2, MAPK1, FOS, TNF, TP53, RELA, BCL2L1	11.51300905	2.34E−07
hsa04510	Focal adhesion	10	18.86792453	3.53E−06	GSK3B, JUN, CCND1, ITGB3, ERBB2, BCL2, MAPK1, MET, EGFR, VEGFA	7.78989667	5.09E−06

KEGG, Kyoto Encyclopaedia of Genes and Genomes; ISR, in-stent restenosis.

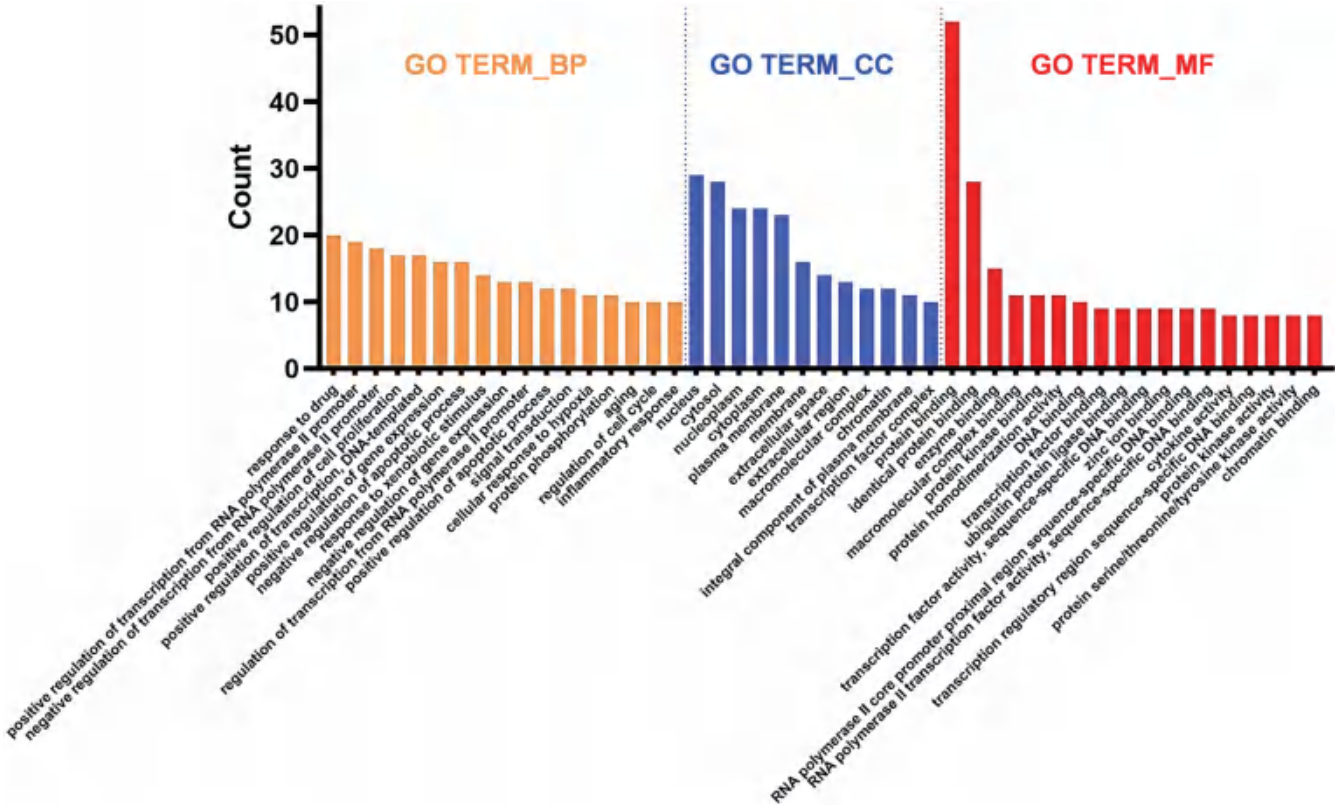

Fig. 2. Histogram of the enriched items of the biological process, cellular components, and molecular function in the GO analysis of the *Radix Salviae*-targeted genes in the ISR disease. GO, gene ontology; ISR, in-stent restenosis.

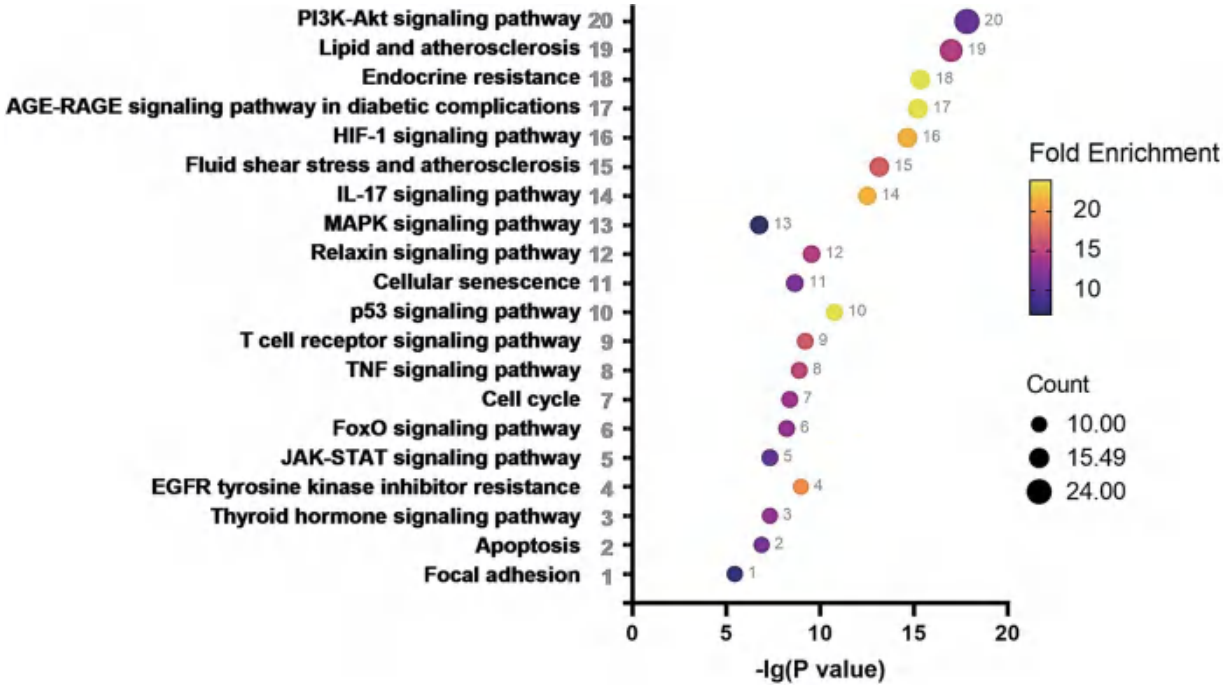

Fig. 3. The enriched items in the KEGG pathways of the *Radix Salviae*-targeted genes in the ISR disease. The size of the dots represents the number of targets in the corresponding pathway, and the color of the dots represents the fold enrichment value in the corresponding pathway. KEGG, Kyoto Encyclopaedia of Genes and Genomes; ISR, in-stent restenosis.

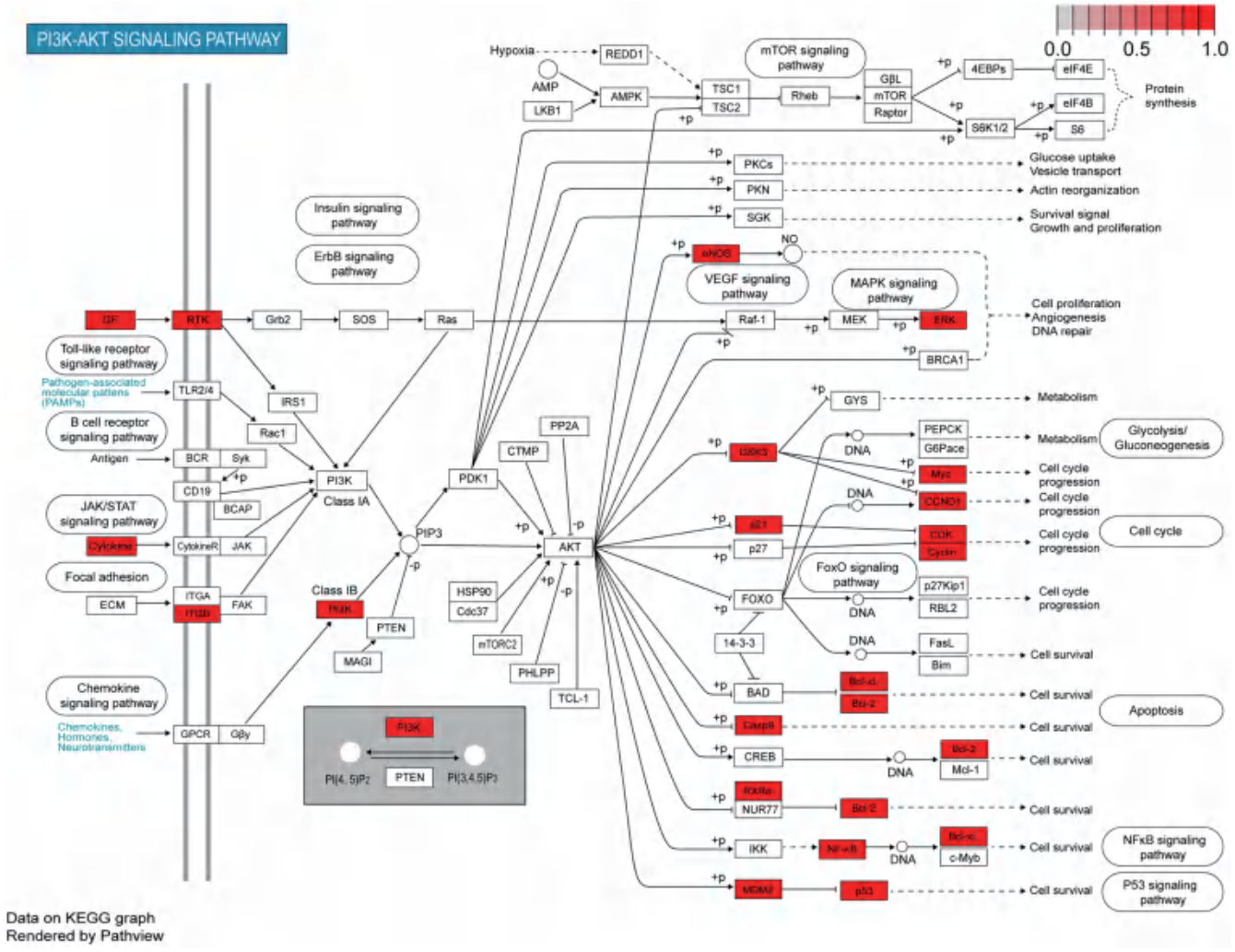

Fig. 4. The representative pathway of the PI3K-Akt signal in the *Radix Salviae*-targeted genes in the ISR disease. The red star labeled genes indicate the targets enriched in this pathway. ISR, in-stent restenosis.

specific targets involved in the representative signaling pathways, Figure 4 and Supplementary Figures 1-3 demonstrate the labeled genes in detail.

Molecular docking simulation

Based on the above analysis, we found that the hub targets (i.e., STAT3, JUN, and TP53) were enrolled in several important cell signaling pathways, including the PI3K-Akt signaling pathway, and the lipid and atherosclerosis pathway. Thus, we tried three compounds from *Radix Salviae* (i.e., Luteolin, Tanshinone iia, and Cryptotanshinone), which had been reported in the literature, for further molecular docking simulation in the AutoDock Vina software. The results showed that the binding energy between Luteolin-STAT3 (−7.4 kcal/mol), Tanshinone iia-TP53 (−7.2 kcal/mol), and Luteolin-TP53 (−6.2 kcal/mol) was less than −5 kcal/mol, consequently indicating a high probability of binding activities between these ligand compounds and target proteins. The visualized binding sites between these docking pairs are presented in Figure 5, and the binding energy has been evaluated and listed in Table 8.

Discussion

This study was designed to investigate the potential mechanisms of *Radix Salviae* in the pathogenesis of ISR. Our results showed that 33 bioactive compounds were predicted by the databases, and 53 targets were selected as the compound-related targets in ISR. There were key nodes discovered in the PPI network, i.e., STAT3, JUN, and TP53. Moreover, the functional enrichment of the GO analysis demonstrated that the main biological processes in ISR included the response to the drug, regulation of the transcription from the RNA polymerase II promoter, and the main molecular functions, which included protein binding. The KEGG analysis revealed that the cell signaling pathways of *Radix Salviae* were mainly related to the PI3K-Akt, lipid and atherosclerosis signals, etc.

Network pharmacology is a powerful tool to reveal the mechanisms of TCM in the prevention and treatment of various diseases, including CHD.[17–19] *Radix Salviae* is a commonly used herbal medicine in treating CHD,[20] and it was reported that extracts from *Radix Salviae* were helpful in the prevention of the occurrence of ISR.[4,21] Here we screened the bioactive compound candidates of *Radix Salviae* with Lipinski's rule based on the biochemical data-

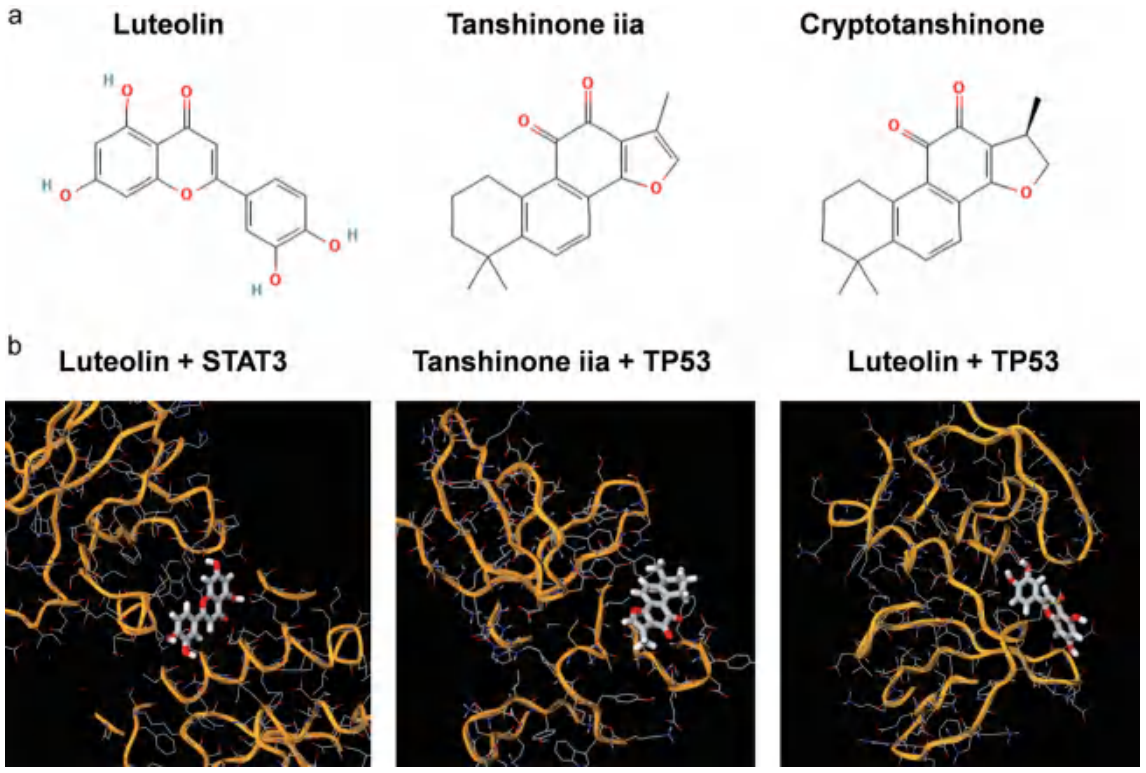

Fig. 5. The representative molecular docking pairs between the ligands of the *Radix Salviae* compounds and target proteins. (a) The chemical structures of the *Radix Salviae* compounds. (b) The docking sites between the ligand compounds and target proteins.

bases.[22] Tanshinone was reported to be effective in inhibiting intimal thickening and inflammation in a rat carotid artery restenosis model,[23] thus suggesting that Tanshinone could be an important bioactive compound in preventing ISR.

The occurrence and development of ISR involved the co-regulation of multiple genes. The PPI network was then used to analyze the protein-protein target interactions, which helped to interpret the relationships among the target proteins of *Radix Salviae* and highlight the hub targets in the ISR pathology. The PPI results showed that STAT3, JUN, and TP53 were the top-ranked targets with high neighborhood connectivity. The activation or high expression of STAT3 was found in the development of ISR after the stent implantation,[24] and treatment with sirolimus or a high-nitrogen low-nickel coronary stent could inhibit STAT3 activation or expression in preclinical studies.[25] JUN was also reported to mediate the proliferation of vascular smooth muscle cells (VSMC) in the pathogenesis of ISR.[26,27] Hence, modulating the activation or expression of the key targets (e.g., STAT3 or JUN) of the ISR pathogenesis that could help to interpret the mechanisms of *Radix Salviae* in preventing ISR development.

Table 8. The top-ranked pairs of ligand compounds and target proteins evaluated by the binding energy

Ligand compounds	Target proteins	Binding energy (kcal/mol)
Luteolin	STAT3	−7.4
Tanshinone iia	TP53	−7.2
Luteolin	TP53	−6.2
Tanshinone iia	STAT3	−4.5

Furthermore, functional enrichment analysis was conducted by the GO and KEGG analyses. Our results showed that the PI3K-Akt and lipid-atherosclerosis signals were highlighted. The PI3K-Akt signaling pathway was reported to mediate both the endothelial cells (EC) proliferation and VSMC proliferation as well as migration, which was involved in the ISR pathogenesis,[28,29] and treatment with the compound Cantharidin, extracted from traditional Chinese medicine, could inhibit the phosphorylation of Akt (P-Akt).[30] Our results indicated that TP53 was also enrolled in the PI3K-Akt signaling in mediating the ISR pathology. Similar predictions and reports could be found in both cancer development and non-cancer diseases, and agents targeting TP53 could regulate the PI3K-Akt signaling-mediated diseases.[31–33] These data provided a possibility of *Radix Salviae* in preventing ISR development via PI3K-Akt signaling and TP53. Additionally, the lipid-atherosclerosis signaling was a series of classical pathways, and our data revealed that this signaling included the STAT3, JUN, and TP53 genes.

In addition to the roles of the STAT3, JUN, and TP53 genes in the ISR pathogenesis, lipid and lipid-mediated atherosclerosis signals were also essential in the ISR development. It was reported that the degree of neointimal proliferation in ISR was proportional to the amount of injury, the intensity of the inflammatory infiltrate, and the association of stent struts with lipid-filled plaque;[34] moreover, the in-stent neointima formation could be identified as a lipid rich part by both near-infrared spectroscopy (NIRS) and optical coherence tomography (OCT) in the clinic.[35] Our results indicated that *Radix Salviae* had the potential to prevent ISR development via modulating the lipid and atherosclerosis signaling pathways.

Molecular docking simulation could also be used to examine

and screen the possibility of the binding activity between the compounds and targets.[36,37] Therefore, further investigation by molecular docking simulation between the ligand of the *Radix Salviae* compounds and target proteins were performed. As the lower binding energy indicated the greater probability of the binding activity, our results revealed a high probability of binding activities between Luteolin-STAT3 (−7.4 kcal/mol), Tanshinone iia-TP53 (−7.2 kcal/mol), and Luteolin-TP53 (−6.2 kcal/mol). This preliminary result would be helpful for experimental validation in the future.

Thus, these above-mentioned data provided network pharmacological evidence for exploring the potential mechanisms underlying the action of *Radix Salviae* in preventing ISR after PCI.

Limitations and prospects

The network pharmacology investigation in this study would help to elucidate the mechanisms of *Radix Salviae* in preventing ISR development in the clinic. However, the major limitation of this study was the lack of experimental confirmation although some of the published studies could support our network pharmacological exploratory results to some extent. Thus, further experimental studies with cultured cells and animals of ISR models treated by the screened active compounds from *Radix Salviae* should be designed to validate the network pharmacological findings of this study in the future.

Conclusions

Overall, this study indicated that bioactive compounds like Tanshinone in *Radix Salviae* could modulate ISR via the PI3K-Akt and lipid-atherosclerosis pathways, and the targets probably included STAT3, JUN, and TP53, which could help to elucidate the mechanisms of *Radix Salviae* in preventing ISR.

Supporting information

Supplementary material for this article is available at https://doi.org/10.14218/JERP.2022.00068.

Supplementary Fig. 1. The representative pathway of Lipid and Atherosclerosis in *Radix Salviae*-targeted genes in ISR disease. The red star-labeled genes indicate the targets enriched in this pathway.

Supplementary Fig. 2. The representative pathway of HIF-1 signal in *Radix Salviae*-targeted genes in ISR disease. The red star-labeled genes indicate the targets enriched in this pathway.

Supplementary Fig. 3. The representative pathway of IL-17 signal in *Radix Salviae*-targeted genes in ISR disease. The red star-labeled genes indicate the targets enriched in this pathway.

Acknowledgments

None.

Funding

This study was supported by the Guangdong Medical Science and Technology Research Fund Project (No. B2020155, to Q.L.), National Natural Science Foundation of China (No. 8227427, to Q.L.), Guangdong Provincial Bureau of Traditional Chinese Medicine Fund Project (No. 20221360, to Q.L.), Zhuhai Medical Science and Technology Research Fund Project (No. ZH24013310210002P-WC, to Q.L.), Special Funding for TCM Science and Technology Research of Guangdong Provincial Hospital of Chinese Medicine (No. YN2020QN10, to Q.L.), and Municipal School (College) Joint Funding Project of the Guangzhou Science and Technology Bureau (No. SL2023A03J00081, to Q.L.).

Conflict of interest

The authors declared that there is no conflict of interest in the authorship and publication of this contribution.

Author contributions

Contributed to study concept and design (QL), acquisition and analysis of the data (LJ-Z and ZZ), drafting of the manuscript (QL), critical revision of the manuscript, and supervision (DWW and RYY).

Data sharing statement

The authors confirm that the data supporting the findings of this study are available within the article and its supplementary materials, and these data are also available from the corresponding author, upon reasonable request.

References

[1] Buccheri D, Piraino D, Andolina G, Cortese B. Understanding and managing in-stent restenosis: a review of clinical data, from pathogenesis to treatment. J Thorac Dis 2016;8(10):E1150–E1162. doi:10.21037/jtd.2016.10.93, PMID:27867580.

[2] Alraies MC, Darmoch F, Tummala R, Waksman R. Diagnosis and management challenges of in-stent restenosis in coronary arteries. World J Cardiol 2017;9(8):640–651. doi:10.4330/wjc.v9.i8.640, PMID:28932353.

[3] Sun L, Zhao R, Zhang L, Zhang W, He G, Yang S, *et al*. Prevention of vascular smooth muscle cell proliferation and injury-induced neointimal hyperplasia by CREB-mediated p21 induction: An insight from a plant polyphenol. Biochem Pharmacol 2016;103:40–52. doi:10.1016/j.bcp.2016.01.015, PMID:26807478.

[4] Cho YH, Ku CR, Hong ZY, Heo JH, Kim EH, Choi DH, *et al*. Therapeutic effects of water soluble danshen extracts on atherosclerosis. Evid Based Complement Alternat Med 2013;2013:623639. doi:10.1155/2013/623639, PMID:23401716.

[5] Song J, Zeng J, Zhang Y, Li P, Zhang L, Chen C. Effect of compound Danshen dripping pills combined with atorvastatin on restenosis after angioplasty in rabbits (in Chinese). Nan Fang Yi Ke Da Xue Xue Bao 2014;34(9):1337–1341. PMID:25263371.

[6] Shao M, Guo D, Lu W, Chen X, Ma L, Wu Y, *et al*. Identification of the active compounds and drug targets of Chinese medicine in heart failure based on the PPARs-RXRα pathway. J Ethnopharmacol 2020;257:112859. doi:10.1016/j.jep.2020.112859, PMID:32294506.

[7] Hong M, Li S, Wang N, Tan HY, Cheung F, Feng Y. A Biomedical Investigation of the Hepatoprotective Effect of Radix salviae miltiorrhizae and Network Pharmacology-Based Prediction of the Active Compounds and Molecular Targets. Int J Mol Sci 2017;18(3):620. doi:10.3390/ijms18030620, PMID:28335383.

[8] Wu XM, Wu CF. Network pharmacology: a new approach to unveiling Traditional Chinese Medicine. Chin J Nat Med 2015;13(1):1–2. doi:10.1016/S1875-5364(15)60001-2, PMID:25660283.

[9] Shahid M, Azfaralariff A, Law D, Najm AA, Sanusi SA, Lim SJ, *et al*. Comprehensive computational target fishing approach to identify Xanthorrhizol putative targets. Sci Rep 2021;11(1):1594. doi:10.1038/s41598-021-81026-9, PMID:33452398.

[10] To KI, Zhu ZX, Wang YN, Li GA, Sun YM, Li Y, *et al*. Integrative network pharmacology and experimental verification to reveal the anti-inflammatory mechanism of ginsenoside Rh4. Front Pharmacol 2022;13:953871. doi:10.3389/fphar.2022.953871, PMID:36120306.
[11] Li F, Duan J, Zhao M, Huang S, Mu F, Su J, *et al*. A network pharmacology approach to reveal the protective mechanism of Salvia miltiorrhiza-Dalbergia odorifera coupled-herbs on coronary heart disease. Sci Rep 2019;9(1):19343. doi:10.1038/s41598-019-56050-5, PMID:31852981.
[12] Hsuan CF, Lu YC, Tsai IT, Houng JY, Wang SW, Chang TH, *et al*. Glossogyne tenuifolia Attenuates Proliferation and Migration of Vascular Smooth Muscle Cells. Molecules 2020;25(24):5832. doi:10.3390/molecules25245832, PMID:33321921.
[13] Kim TJ, Kim JH, Jin YR, Yun YP. The inhibitory effect and mechanism of luteolin 7-glucoside on rat aortic vascular smooth muscle cell proliferation. Arch Pharm Res 2006;29(1):67–72. doi:10.1007/BF02977471, PMID:16491846.
[14] Jin UH, Suh SJ, Chang HW, Son JK, Lee SH, Son KH, *et al*. Tanshinone IIA from Salvia miltiorrhiza BUNGE inhibits human aortic smooth muscle cell migration and MMP-9 activity through AKT signaling pathway. J Cell Biochem 2008;104(1):15–26. doi:10.1002/jcb.21599, PMID:17979138.
[15] Wu L, Li X, Li Y, Wang L, Tang Y, Xue M. Proliferative inhibition of danxiongfang and its active ingredients on rat vascular smooth muscle cell and protective effect on the VSMC damage induced by hydrogen peroxide. J Ethnopharmacol 2009;126(2):197–206. doi:10.1016/j.jep.2009.08.045, PMID:19735709.
[16] He S, Wang T, Shi C, Wang Z, Fu X. Network pharmacology-based approach to understand the effect and mechanism of Danshen against anemia. J Ethnopharmacol 2022;282:114615. doi:10.1016/j.jep.2021.114615, PMID:34509606.
[17] Jia LY, Cao GY, Li J, Gan L, Li JX, Lan XY, *et al*. Investigating the Pharmacological Mechanisms of SheXiang XinTongNing Against Coronary Heart Disease Based on Network Pharmacology and Experimental Evaluation. Front Pharmacol 2021;12:698981. doi:10.3389/fphar.2021.698981, PMID:34335263.
[18] Wang J, Zhang Y, Liu YM, Yang XC, Chen YY, Wu GJ, *et al*. Uncovering the protective mechanism of Huoxue Anxin Recipe against coronary heart disease by network analysis and experimental validation. Biomed Pharmacother 2020;121:109655. doi:10.1016/j.biopha.2019.109655, PMID:31734577.
[19] Zhang YQ, Guo QY, Li QY, Ren WQ, Tang SH, Wang SS, *et al*. Main active constituent identification in Guanxinjing capsule, a traditional Chinese medicine, for the treatment of coronary heart disease complicated with depression. Acta Pharmacol Sin 2018;39(6):975–987. doi:10.1038/aps.2017.117, PMID:28858293.
[20] Wu D, Huo M, Chen X, Zhang Y, Qiao Y. Mechanism of tanshinones and phenolic acids from Danshen in the treatment of coronary heart disease based on co-expression network. BMC Complement Med Ther 2020;20(1):28. doi:10.1186/s12906-019-2712-4, PMID:32020855.
[21] Hung HH, Chen YL, Lin SJ, Yang SP, Shih CC, Shiao MS, *et al*. A salvianolic acid B-rich fraction of Salvia miltiorrhiza induces neointimal cell apoptosis in rabbit angioplasty model. Histol Histopathol 2001;16(1):175–183. doi:10.14670/HH-16.175, PMID:11193193.
[22] Chen X, Li H, Tian L, Li Q, Luo J, Zhang Y. Analysis of the Physicochemical Properties of Acaricides Based on Lipinski's Rule of Five. J Comput Biol 2020;27(9):1397–1406. doi:10.1089/cmb.2019.0323, PMID:32031890.
[23] Li X, Du JR, Wang WD, Zheng XY, Sun W, Zong X, *et al*. Experimental study of effect of tanshinone on artery restenosis in rat carotid injury model (in Chinese). Zhongguo Zhong Yao Za Zhi 2006;31(7):580–584. PMID:16780164.
[24] Lim SY, Kim YS, Ahn Y, Jeong MH, Rok LS, Kim JH, *et al*. The effects of granulocyte-colony stimulating factor in bare stent and sirolimus-eluting stent in pigs following myocardial infarction. Int J Cardiol 2007;118(3):304–311. doi:10.1016/j.ijcard.2006.07.018, PMID:17052793.
[25] Wang J, Song C, Xiao Y, Liu B. In vivo and in vitro analyses of the effects of a novel high-nitrogen low-nickel coronary stent on reducing in-stent restenosis. J Biomater Appl 2018;33(1):64–71. doi:10.1177/0885328218773306, PMID:29720017.
[26] Tian M, Sheng L, Huang P, Li J, Zhang CH, Yang J, *et al*. Agonistic autoantibodies against the angiotensin AT1 receptor increase in unstable angina patients after stent implantation. Coron Artery Dis 2014;25(8):691–697. doi:10.1097/MCA.0000000000000146, PMID:25025993.
[27] Klocke R, Hasib L, Nikol S. Recently patented applications of homologous cellular and extracellular agents as therapeutics or targets for the prevention of restenosis post-angioplasty. Recent Pat Cardiovasc Drug Discov 2006;1(1):57–66. doi:10.2174/157489006775244272, PMID:18221074.
[28] Liu TF, Lin T, Ren LH, Li GP, Peng JJ. Association of *CMTM5* gene expression with the risk of in-stent restenosis in patients with coronary artery disease after drug-eluting stent implantation and the effects and mechanisms of *CMTM5* on human vascular endothelial cells (in Chinese). Beijing Da Xue Xue Bao Yi Xue Ban 2020;52(5):856–862. doi:10.19723/j.issn.1671-167X.2020.05.010, PMID:33047719.
[29] Thiel WH, Esposito CL, Dickey DD, Dassie JP, Long ME, Adam J, *et al*. Smooth Muscle Cell-targeted RNA Aptamer Inhibits Neointimal Formation. Mol Ther 2016;24(4):779–787. doi:10.1038/mt.2015.235, PMID:26732878.
[30] Qiu L, Xu C, Jiang H, Li W, Tong S, Xia H. Cantharidin Attenuates the Proliferation and Migration of Vascular Smooth Muscle Cells through Suppressing Inflammatory Response. Biol Pharm Bull 2019;42(1):34–42. doi:10.1248/bpb.b18-00462, PMID:30393274.
[31] Liu H, Yang H, Qin Z, Chen Y, Yu H, Li W, *et al*. Exploration of the Danggui Buxue Decoction Mechanism Regulating the Balance of ESR and AR in the TP53-AKT Signaling Pathway in the Prevention and Treatment of POF. Evid Based Complement Alternat Med 2021;2021:4862164. doi:10.1155/2021/4862164, PMID:35003302.
[32] Li KW, Wang SH, Wei X, Hou YZ, Li ZH. Mechanism of miR-122-5p regulating the activation of PI3K-Akt-mTOR signaling pathway on the cell proliferation and apoptosis of osteosarcoma cells through targeting TP53 gene. Eur Rev Med Pharmacol Sci 2020;24(24):12655–12666. doi:10.26355/eurrev_202012_24163, PMID:33378012.
[33] Chappell WH, Candido S, Abrams SL, Akula SM, Steelman LS, Martelli AM, *et al*. Influences of TP53 and the anti-aging DDR1 receptor in controlling Raf/MEK/ERK and PI3K/Akt expression and chemotherapeutic drug sensitivity in prostate cancer cell lines. Aging (Albany NY) 2020;12(11):10194–10210. doi:10.18632/aging.103377, PMID:32492656.
[34] Scott NA. Restenosis following implantation of bare metal coronary stents: pathophysiology and pathways involved in the vascular response to injury. Adv Drug Deliv Rev 2006;58(3):358–376. doi:10.1016/j.addr.2006.01.015, PMID:16733073.
[35] Roleder T, Karimi Galougahi K, Chin CY, Bhatti NK, Brilakis E, Nazif TM, *et al*. Utility of near-infrared spectroscopy for detection of thin-cap neoatherosclerosis. Eur Heart J Cardiovasc Imaging 2017;18(6):663–669. doi:10.1093/ehjci/jew198, PMID:27679596.
[36] Fatoki TH, Ibraheem O, Ogunyemi IO, Akinmoladun AC, Ugboko HU, Adeseko CJ, *et al*. Network analysis, sequence and structure dynamics of key proteins of coronavirus and human host, and molecular docking of selected phytochemicals of nine medicinal plants. J Biomol Struct Dyn 2021;39(16):6195–6217. doi:10.1080/07391102.2020.1794971, PMID:32686993.
[37] Meng XY, Zhang HX, Mezei M, Cui M. Molecular docking: a powerful approach for structure-based drug discovery. Curr Comput Aided Drug Des 2011;7(2):146–157. doi:10.2174/157340911795677602, PMID:21534921.

Journal of Exploratory Research in Pharmacology **2023** vol. 8(2) | 121–130
DOI: 10.14218/JERP.2022.00062

Review Article

Potential Applications of Cannabis Plant Extracts and Phytochemicals as Natural Antimicrobials

Hebah M.S. AL Ubeed[1*], Asgar Farahnaky[1], Emma L. Beckett[2,3], Momena Khandaker[4] and Christopher J. Pillidge[1]

[1]School of Science, STEM College, RMIT University, VIC, Australia; [2]School of Environmental and Life Sciences, University of Newcastle, NSW, Australia; [3]Hunter Medical Research Institute, New Lambton Heights, NSW, Australia; [4]School of Environmental and Rural Sciences, University of New England, NSW, Australia

Received: July 27, 2022 | **Revised:** October 09, 2022 | **Accepted:** October 24, 2022 | **Published online:** December 05, 2022

Abstract

Cannabis has a long history of use in treating human diseases, but scientific research on its properties has only recently gained momentum. The increasing prevalence of antibiotic resistance in human and animal pathogens has sparked renewed interest in exploring alternative antimicrobial therapies from *Cannabis* and other plant sources. There is also potential for *Cannabis* extracts or purified cannabinoids to be applied in novel medical contexts. Industrial hemp extracts may find applications in food manufacturing, veterinary purposes, and microbial control in cleaners and sanitizers. This review highlights the latest discoveries regarding *Cannabis* plant extracts and phytochemicals as potent antimicrobial agents against various microorganisms, including Gram-positive and Gram-negative bacteria. More importantly, the challenges of using cannabinoids as effective and affordable natural antimicrobial agents are reviewed. While antimicrobial and other applications of *Cannabis* extracts and phytochemicals appear promising, concerns about possible toxic side effects exist. Therefore, future research should focus on addressing the safety of these compounds, evaluating their *in vivo* activity, and understanding structural changes that influence their pharmacokinetic properties. Standardized tests will be crucial for facilitating valid inter-laboratory comparisons. The review article also discusses future research directions aimed at developing novel broad-spectrum antibiotics based on *Cannabis*.

Keywords: *Cannabis*; Antibacterial; Antifungal; Antiviral; Natural phytochemicals; Medicinal Cannabis extract.

Abbreviations: Δ^8-THC, Delta-8-Tetrahydrocannabinol; ABTS, 2,2′-Azinobis [3-ethylbenzothiazoline-6-sulfonic acid]-diammonium salt; ACE-2, Angiotensin-converting enzyme-2; $AgNP_S$, Silver nanoparticles; *B. cereus*, *Bacillus cereus*; *B. longum*, *Bifidobacterium longum*; *B. subtilis*, *Bacillus subtilis*; CBC, Cannabichromene; CBCA, Cannabichromene acid; CBD, Cannabidiol; CBDA, Cannabidiol acid; CBDV, Cannabidivarin; CBDVA, Cannabidivarin acid; CBG, Cannabigerol; CBGA, Cannabigerolic acid; CBL, Cannabicyclol; CBN, Cannabinol; CBNA, Cannabinol acid; CLSI, Clinical Laboratory and standards Institute; COVID-19, Human coronavirus; SARS-CoV2, severe acute respiratory syndrome coronavirus 2; DPPH, 2,2-diphenyl-1-picrylhydrazyl; *E. coli*, *Escherichia coli*; *E. faecalis*, *Enterococcus faecalis*; EOs, Essential Oils; GC-MS, Gas Chromatography Mass Spectrometry; GI, Gastrointestinal; GOT, Geranyl pyrophosphate, Olivetolate geranyltransferase; GPP, Geranyl pyrophosphate; HBV, Hepatitis B virus; HCV, Hepatitis C virus; *K. pneumoniae*, *Klebsiella pneumoniae*; KSHV, Kaposi's sarcoma-associated herpesvirus; *L. donovani*, *Leishmania donovani*; *M. smegmatis*, *Mycobacterium smegmatis*; MBC, minimum bactericidal concentration; MIC, minimum inhibitory concentration; MRSA, Methicillin-resistant *Staphylococcus aureus*; NCs, Nanocarriers; OLA, olivetol acid; *P. aeruginosa*, *Pseudomonas aeruginosa*; *P. falciparum*, *Plasmodium falciparum*; *P. guajava*, *Psidium guajava*; *S. aureus*, *Staphylococcus aureus*; *S. milleri*, *Streptococcus milleri*; *S. mutans*, *Streptococcus mutans*; *S. pyogenes*, *Streptococcus pyogenes*; *SFE-CO_2*, Supercritical fluid extraction with carbon dioxide; THC, Tetrahydrocannabinol; THCA, Tetrahydrocannabinolic acid; THCAA, Delta9-tetrahydrocannabinolic acid-A; THCAS, Tetrahydrocannabinolic acid synthase; THCV, Tetrahydrocannabivarin; THCVA, Tetrahydrocannabivarin acid; TMPRSS2, Transmembrane serine protease 2; $ZnNP_S$, Zinc Nanoparticles; Δ^9-THC, Delta-9-trans-Tetrahydrocannabinol.

***Correspondence to:** Hebah M.S. AL Ubeed, School of Science, STEM College, RMIT University, Bundoora, Melbourne, VIC 3083, Australia. ORCID: https://orcid.org/0000-0003-4344-9513. Tel: +61 3 9925 3347, Fax: RITM0806372, E-mail: hebah.al.ubeed@rmit.edu.au

How to cite this article: AL Ubeed HMS, Farahnaky A, Beckett EL, Khandaker M, Pillidge CJ. Potential Applications of Cannabis Plant Extracts and Phytochemicals as Natural Antimicrobials. *J Explor Res Pharmacol* 2023;8(2):121–130. doi: 10.14218/JERP.2022.00062.

Introduction

Cannabis sativa L. or marijuana, is a flowering plant that has been used for millennia for food, drugs (both legal and illegal), textile (hemp), and religious purposes.[1] Selective breeding has resulted in numerous *C. sativa* strains (cultivars) with different properties. For example, hemp strains are fibrous and low in cannabinoids, while medicinal strains are highly flowering and contain both phytonutrients and phytochemicals.[2–4] Bioactive compounds can be extracted from oils or as aqueous phases from seeds, flowers, leaves, and stems using traditional techniques such as cold-pressing and solvent extraction or by contemporary procedures like ultrasound.[5] Supercritical fluid extraction with carbon dioxide (SFE-CO_2) is another technology used in industry to extract phytochemical compounds.[6,7] This is no different from other plant products, which have been historically used as rich sources of natural products for human health.[8]

Potential therapeutic applications and bioactive mechanisms

of crude *Cannabis* extracts and purified compounds derived from *C. sativa* have been investigated in various pharmacological scenarios, including their use as anti-convulsive, analgesic, anti-anxiety, and anti-emetic therapeutic drugs.[9] While much research has centered around the psychoactive properties of cannabinoids,[10] the antimicrobial properties of compounds extracted from *C. sativa* are now becoming of particular interest due to the emergence of antimicrobial resistance as a vital threat to human health globally.[11] Mitigating the human and economic impacts of this problem, and more broadly, the emergence of new microbial pathogens,[12] requires identifying and elucidating new antimicrobial therapies.

One possibility to combat such infections, apart from antibiotics, is to use phage-based therapies, including lysin therapy and engineered phage enzymes.[13,14] Another alternative is to use plant-derived compounds or extracts with antimicrobial properties (bacterial, fungal, and viral). Among these, *Cannabis* extracts and (more specifically) cannabinoids show colossal promise, especially towards multi-drug resistant microorganisms like MRSA (methicillin-resistant *Staphylococcus aureus*), which can be very difficult to treat.[15] While there is much anecdotal evidence on the efficacy of *Cannabis* compounds or extracts, controlled laboratory investigations of these novel antimicrobial agents, their mode of action, efficacy, and safety, together with the development of safe and approved disease treatment therapies, is certainly needed. *In vitro* antifungal, antibacterial, antimalarial, antileishmanial, and cytotoxic properties of *C. sativa* extracts and compounds have been investigated since the early 2000s.[13,16–19] However, significant challenges exist in assessing the efficacy of these agents (both impure phytochemical extracts and purified compounds), determining their safety, and implementing research findings. These challenges include high variability in cannabinoid content in different *C. sativa* strains; also for different parts of plants and in the extraction methods;[5] a lack of uniform methods for antimicrobial screening assays; diversity in microbial targets (strain variability); failure to consider the stability of extracts or the effects of additional compounds (impurities), both in cell culture experiments and animal trials. Furthermore, challenges regarding the negative perception of *Cannabis*, its safety and potential side effects, variable delivery methods, local and systemic effects, and synergistic effects need to be addressed.[20,21]

This review will describe the potential uses of agents found in medicinal *Cannabis* extracts as antimicrobials, the current knowledge on their mechanism of action, the challenges around phytochemicals' stability and bioavailability, optimized extraction protocols, and isolation of active antibiotic compounds. Also, the prospect of using new formulations containing 'old' antibiotics combined with therapeutic plant compounds to provide a synergistic killing effect is noted. Such combined treatments could more effectively kill or inhibit antibiotic-resistant bacteria causing local and systemic infections.

New classes of potent antimicrobial agents

It has been known for decades that *Cannabis* plant extracts can be effective antimicrobial agents.[22,23] More than 525 phytochemicals have been extracted and isolated in *C. sativa*.[24–26] The most important classes of *Cannabis* phytochemicals are the C21 terpenes, phenolics, and cannabinoids. The respective antimicrobial properties of these compounds will be discussed in this report.

There are many benefits for isolated cannabinoids, including antifungal, antibacterial, antimalarial, antileishmanial, and cytotoxic properties.[26] Active cannabinoids like CBG,[27,28] CBN, CBC,[29] and psychoactive cannabinoids delta-9-trans-tetrahydrocannabinol (Δ^9-THC)[17] (summarized in Table 1 and Fig. 1) and their precursors have a high level of antimicrobial activity.[16,26,30,31] Synthesis of cannabinoids is complex; essentially, they are derived from cannabigerolic acid (CBGA), which is the precursor of olivetol acid (OLA) and geranyl pyrophosphate (GPP), and is induced by the prenyltransferase geranyl pyrophosphate: olivetolategeranyltransferase (GOT).[32] There are some examples of co-enzymes involvement like tetrahydrocannabinolic acid synthase (THCAS), cannabidiolic acid synthase (CBDAS), or cannabichromeneacid synthase (CBCAS). With the assistance of the co-enzyme, CBGA is finally converted to tetrahydrocannabinolic acid (THCA), cannabidiolic acid (CBDA), and cannabichromenic acid (CBCA). Then, oxidation of THCA occurs to produce cannabinolic acid (CBNA) in the buds.[33,34] Cannabinoids Δ^9-THC, CBD, CBG, CBC, and CBN displayed anti-staphylococcal activity with even greater antibiotic effect than traditional antibiotics like norfloxacin, erythromycin, tetracycline, and oxacillin.[3] CBG exhibits antibacterial activities against *Streptococcus mutans (S.mutans)*.[35,36]

Both compounds Δ^9-THC and CBD showed significant antibacterial activity towards *S. aureus*, *Streptococcus pyogenes* (*S. pyogenes*), *Streptococcus milleri* (*S. milleri*), *Enterococcus faecalis* (*E. faecalis*), *E. coli*, *Salmonella typhi,* and *Proteus vulgaris*.[37] Farha, *et al.*[37] further described the antibacterial activity of specific cannabinoids CBC, CBCA, CBD, CBDV, CBDA, CBDVA, CBG, CBGA, CBN, CBL, THC, Δ^8-THC, exo-tetrahydrocannabinol (exo-THC), Δ^9-tetrahydrocannabinolic acid-A (THCAA), THCV, (±) 11-nor-9-carboxy-Δ^9 – THC, and (±) 11-hydroxy-Δ^9-THC against MRSA to inhibit its ability to form biofilms and stationary phase cells' resistance to antibiotics. CBD also showed potent activity against various MRSA strains.[38] A detailed paper on the antimicrobial activity of CBD, including mechanistic mode-of-action studies, was later provided by Blaskovich *et al*.[17] They showed that cannabidiol has a superior effect against biofilms. This cannabinoid could potentially treat Gram-negative bacteria infections, including *Neisseria gonorrhoeae* and Gram-positive bacterial infections. CBD was also shown to be a bigger inhibitor of membrane vesicle emission from *E. coli* (strain VCS257) compared to *S. aureus*. Whenever CBD was used in combination with selected antibiotics, it caused higher inhibition action against Gram-negative bacteria.[39] Similar to terpenes, cannabinoids show synergistic effects with antibiotics. Grassi *et al*.[40] demonstrated that when cannabinoids were combined with polymyxin B, there was an effective inhibition against Gram-negative bacteria.

Apart from cannabinoids, geranyl pyrophosphate is the precursor in synthesizing the terpenoids, leading to the creation of monoterpenoids in secretory cell plastids.[41] For instance, volatile oil fractions incorporate monoterpenoids (C10)[42] or sesquiterpenoids and triterpenoids in the cytoplasm.[43,44] Sesquiterpenes (C15) are major compounds in hemp extracts.[42] After harvest, *Cannabis* buds must be dried to remove the carboxylic acid functional group to extract high-purity CBD, CBC, and CBG. Then, oxidization of THC yields delta-8-tetrahydrocannabinol (Δ^8-THC, the main psychoactive compound) and CBN.[26,45,46]

Many factors affect the quality and consistency of these antibacterial extracts, including environmental and climatic conditions for the growth of leaves, flowers, and seeds. Also, Muscarà *et al.*[47] studied two standardized hexane extracts for their phytonutrients and antibiotic activities. The first extract consisted of cannabidivarinic acid (CBDVA) and tetrahydrocannabivarinic acid (THCVA). The second extract contained cannabidivarin (CBDV)

Table 1. Cannabinoids from *Cannabis sativa L*. with antimicrobial activity

Active compound	Organism	Mode of action	References
CBD	*S. aureus*; *B. subtilis*	CBD is more active than CBDA due to exchanged positions of the one hydroxyl group and lipophilic side chain.	3,89,100
	Hepatitis C virus	CBD interacts with the CB_2 receptor and stimulates apoptosis in thymocytes and splenocytes, then inhibiting the proliferation of T-cells and macrophages as such mechanism cause to indirectly slows the pathogenic process of the HBV virus.	
	SARS-CoV-2	CBD additive or synergic effect with terpene control viral replication or clonal stable conformations with the binding of the transmembrane protease serine 2 (SARS-CoV-2) and angiotensin-converting enzyme-2 (ACE2).	
CBG	*Mycobacterium; Leishmania donovani; S. mutans; S. sanguis; S. sobrinus; S. salivarius;* MRSA	CBG alters membrane structures of treated bacteria and disorders of the cytoplasm activity.	70
CBC	*S.aureus; B.Subtils; C. albicans; Mycobacterium smegmatis; Saccharomyces cerevisiae; Trichophyton mentagrophytes*	The activity of CBC due to bearing the lipophilic side chain and one hydroxyl group in exchanged positions displayed similarly potent activity.	3,74
CBN	Anti-MRSA; antileishmanial; *Plasmodium falciparum*	Decreased or increased esterification or methylation of the carboxylic acid moieties were detrimental to the activity and additional hydroxy function in the lipophilic side chain.	3,76
Δ^9-THC	*S. aureus, Streptococcus pyogenes, Streptococcus. milleri, Enterococcus faecalis, E. coli, Salmonella typhi, Proteus vulgaris,* MRSA	Decreased or increased esterification or methylation of the carboxylic acid moieties were detrimental to the activity.	3,16

ACE-2, Angiotensin-converting enzyme-2; CBD, Cannabidiol; CBDA, Cannabidiol acid; CBG, Cannabigerol; CBN, Cannabinol; MRSA, Methicillin-resistant *Staphylococcus aureus*; SARS-CoV-2, severe acute respiratory syndrome coronavirus 2; Δ^9-THC, Delta-9-trans-Tetrahydrocannabinol.

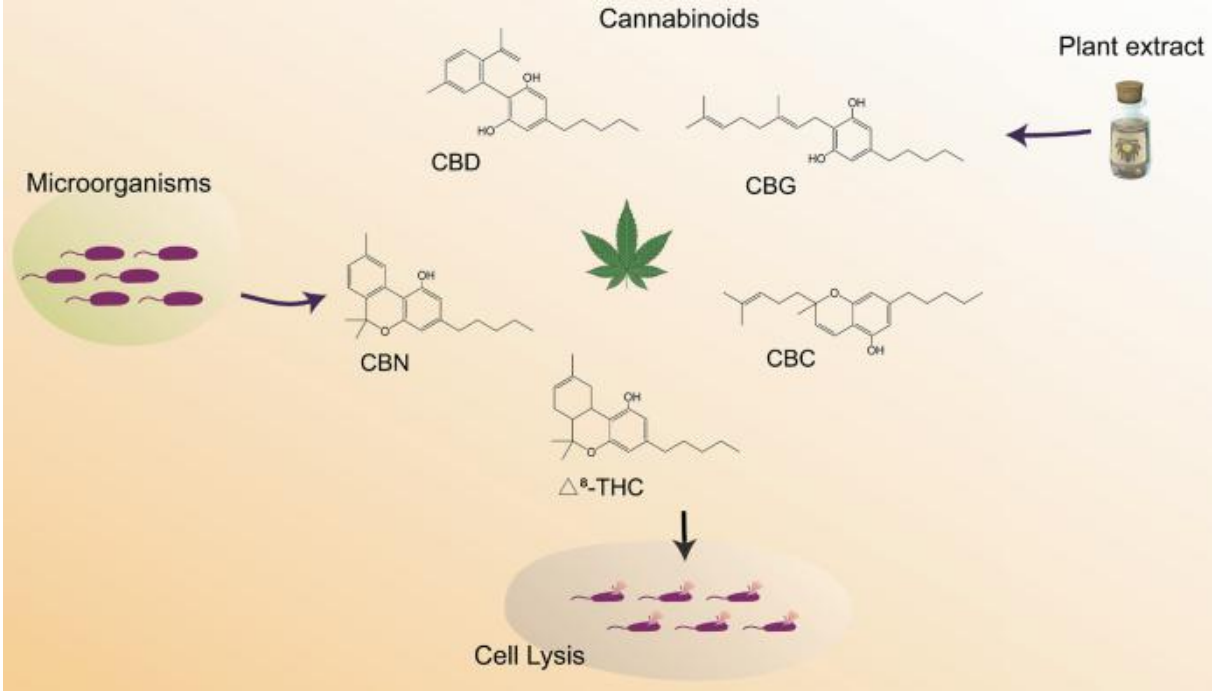

Fig. 1. Antimicrobial activity of cannabinoids like cannabidiol (CBD), cannabigerol (CBG), cannabichromene (CBC), cannabinol (CBN), and delta-8-tetrahydrocannabinol (Δ^8-THC).

and tetrahydrocannabivarin (THCV) from a new Chinese *C.sativa* variety and other non-psychoactive strains. Both extracts showed extraordinary antioxidant activity and antimicrobial and antifungal properties against clinical strains of MRSA and other microorganisms.[28] Various methods have been applied to extract and isolate these and other antimicrobial agents, such as solvent extraction, physical methods, and supercritical fluid extraction, giving different results.[5,6]

Other *Cannabis* compounds with antimicrobial activity include terpenoids. These form a large percentage of essential oils.[48–51] Some 120 terpenoids have been found in marijuana and hemp,[52] but relatively few terpenes have been isolated, purified, and tested.[53] Hemp seed oil was also effective in controlling spoilage of food and phytopathogenic microorganisms.[16,54] An *in vitro* or cell culture study by Nostro *et al*.[55] considered a range of plant extracts, potentially inhibiting biofilms in food. They found that extracts were effective against *S. aureus*, including MRSA strains, *Escherichia coli* (*E. coli)*, and *Pseudomonas aeruginosa (P. aeruginosa*). Another study focused on linalool and α-Phellandrene, which were investigated due to their very low toxicity and ease of use and were registered as a potential new therapeutic.[47,56] Another type of active compound extracted from *Cannabis* seeds are the flavonoids, also effective against bacteria and yeast.[57]

Another active compound class that can be extracted from *Cannabis* and used as an antibiotic alone or in combination with other compounds is *Cannabis* alkaloids. Natural alkaloids accumulate to differing extents in particular parts of the plant, such as barks, roots, and leaves.[58,59] These alkaloids can be chemically modified to produce synthetic and semi-synthetic smart drugs. However, natural compounds are generally safer and cheaper than alternative synthetic compounds.[60] Currently, natural alkaloids are used as a therapeutic compound for human disease and as pesticides in agriculture.[61] Natural alkaloids and phenolic compounds have potential antimicrobial activity due to their ability to alter the structure of the bacterial wall.[62]

In summary, the most valuable compounds in *Cannabis,* besides cannabinoids, include its alkaloids, terpenoids, steroids, phenols, glycosides, and tannins.[63]

A novel mode of action

The most active compounds in *C. sativa* with antimicrobial potential are THC, CBD, CBG, and CBC.[56,64–66] These compounds may also effectively treat psychological and physiological disorders.[67,68] Medicinal *Cannabis* phytochemicals applied to specific medical devices were active against biofilms composed of Gram-positive and Gram-negative bacteria, and their mode of action was to alter and penetrate the bacteria cells[69] are summarized in Table 1. Various methods like scanning electron microscopy, transmission electron microscopy, Nile Red membrane staining, and laurdan membrane fluidity assays have shown that CBG inhibits bacteria via alterations to the bacterial cell structure by inducing membrane hyperpolarization and decreasing the membrane fluidity.[70] CBG exhibited moderate antimicrobial activity towards *Mycobacterium*[25] and *Leishmania donovani* (*L. donovani*).[3] Not only CBG but also its derivative iso-CBG-C1 showed potential activity against *S. aureus* and *Bacillus subtilis* (*B. subtilis*), and *Mycobacterium smegmatis* (*M. smegmatis*).[27]

Other studies found that CBD has a higher effect against Gram-positive bacteria than their acid form due to differences in lipophilicity.[27,71,72] Studies have shown that CBD and CBG have a higher antimicrobial effect than their precursors (acidic cannabinoids or raw material before drying) due to exchanged positions of a hydroxyl group and lipophilic side chain.[3]

While CBD and CBG are effective against Gram-positive bacteria, Krejci *et al.*[73] reported that both cannabinoids were inactive against Gram-negative bacteria. Moreover, compared to other natural cannabinoids and antibiotics like streptomycin, CBC has the highest activity against *S. aureus* and *B. subtilis*,[74] and similar effects were confirmed with iso-CBC due to connecting with the lipophilic side chain and a hydroxyl group in interchanged positions.[75] Furthermore, a cannabinol derivative CBN[76,77] showed moderate anti-MRSA, antileishmanial, and anti-*Plasmodium falciparum* (*P. falciparum*) activity. However, both Δ^9-THCVA and CBDVA showed lower anti-staphylococcal activity based on deleting a side chain compared to Δ^9-THCV and CBDV.[78,79] The primary action of CBG against MRSA is the disordering of the principal activity of the cytoplasm.[37] Recent structure-function studies have helped to determine the most effective cannabinoids.[80] Cannabinoids showed significant differences in antimicrobial activity due to a decrease or increase in methylation or esterification. The most active antimicrobial cannabinoids are Δ^9-THC, CBN, and CBG.[16,70]

No significant antifungal activity has been observed yet for cannabinoids.[19] However, the antiviral potential of CBD has received some attention.[81–86] CBD was effective against hepatitis C virus (HCV),[87–92] which causes liver inflammation.[93] In contrast, CBD was ineffective against the hepatitis B virus (HBV). CBD was more efficient than sofosbuvir and had a less cytotoxic effect.[94] Other research indirectly showed that CBD could effectively work and inhibit Kaposi's sarcoma-associated herpesvirus (KSHV).[95]

One key research target is control of the human coronavirus (COVID-19).[96–99] In a recent article, CBD in combination with terpenes showed antiviral effects against Human Coronavirus E229.[100] Also, in an earlier investigation, terpenes were found to show an antiviral effect on severe acute respiratory syndrome coronavirus 1 (SARS-CoV-1).[101] However, while such compounds show promise, most of these antivirals have not been trialed on humans or undergone controlled clinical trials.[102,103] According to Chatow *et al*.,[100] the combined possibility of plant terpenes with CBD against a human coronavirus strain could be seen using a tissue cell culture model.

Although such studies are a good start, they cannot determine side effects or potential cytotoxicity as *in vivo* animal model studies. Recent studies showed phytochemicals have stable conformations with the binding enzyme of severe acute respiratory syndrome coronavirus 2 (SARS-CoV-2), which has a vital role in viral replication, cloning, suppressing viral entry and activation, and down-regulating ACE2 receptor and TMPRSS2 enzyme.[104–106] Further investigation on developing new vaccines or antivirals will be needed to address strain variability, i.e., target all strains of COVID-19. This needs more intensive research in the future, together with studies giving mechanistic insights into their action.

Challenges in applications of cannabinoids as an antimicrobial agent

As noted earlier, the spread of antibiotic resistance genes is common among many pathogens, and with little or no pending discovery or development of new classes of antibiotics, the need to find other agents for combating infections is vital.[37,107,108] Recently, the World Health Organization announced an archive of 12 microorganisms that have developed antibacterial resistance and are now considered a severe threat to health care. Eight of these pathogens

are Gram-negative and are spectacularly hard to cure, while the other four Gram-positive microorganisms are the most significant threat.[109] The antimicrobial activity of *Cannabis* derives from essential oils (Eos) and purified cannabinoids, the latter receiving increased attention in recent years as possible therapeutic agents.[16,19,56,110] This section will first consider the antimicrobial effects of impure extracts and Eos, then discuss studies on purified cannabinoids.

The disc diffusion assay and the two-fold serial broth dilution assay, which generate a MIC value in a 96-well microtiter plate, are the most commonly used methods to measure antimicrobial effects.[111] The methodology for the MIC assay is standard and specified by the Clinical Laboratory and Standards Institute (CLSI).[112] However, a problem highlighted by Sadgrove and Jones[113] is that MIC values are normally quoted in µg/ml, which does not take into account molarity. The authors also noted that antimicrobial outcomes might be naively extrapolated beyond any reasonable systemic concentration level to show an effect. Even with method standardization, caution must be exercised when comparing inter-laboratory results to ensure that results cross-comparisons are valid. In one study, even though there was the bactericidal effect of both cannabinoids like THC and CBD against staphylococci and streptococci tested in broth media, the impact was much higher in horse blood agar or with 4% horse serum.[109]

Even though essential oils (Eos) can be extracted from low-THC *Cannabis* varieties cultivated without legal restrictions, relatively few studies have considered these Eos or extracts in terms of their antimicrobial activities. The use of *Cannabis* in this way strengthens the idea of growing hemp as a multi-use crop.[54] A fundamental challenge in medical *Cannabis* and hemp research requires production methods or post-harvesting processes that maintain the uniform quality of the product. Also, drying, extraction, isolation, and purification techniques must be optimized to obtain pure chemical composition and pharma grade for different products.[6,114–116]

One problem with assessing multiple studies is that *Cannabis* extracts vary enormously in composition and contain multiple different compounds, making result comparisons extremely difficult. Some key variables that make inter-laboratory comparisons difficult include the absence of standardized antimicrobial testing methodologies; microbiological media components in disk diffusion tests reacting with or modifying extracts; plant extracts containing unstable compounds making accurate quantitative analysis impossible; synergistic or antagonistic effects between multiple compounds; different cultivars or parts of plants used in different studies; and extraction protocols of varying efficiency leading to different outcomes. In one study, *C. sativa* and *Psidium guajava* extracts contained various active compounds like alkaloids, saponins, flavonoids, steroids, cardiac glycosides, terpenes, resins, tannins, and phenols. However, steroids, resins, and cardiac glycosides were absent in another medicinal plant, *Thuja orientalis*. Furthermore, hemp essential oils demonstrated high antimicrobial activity against Gram-positive bacteria.[20,54]

Some studies have focused on extracts of seeds of *Cannabis* plants.[117] Hemp seed extracts show good antimicrobial activity due to their composition of polyphenols, essentially caffeoyltyramine and cannabisin.[118] In another study,[117] *C. sativa L.* seed extracts inhibited biofilm formation by *S. aureus* ATCC 35556. In contrast, adding hemp seed extract to media stimulated the growth of Bifidobacterium and Lactobacillus probiotic strains.[117] The increased growth of *Bifidobacterium Longum* (*B. longum)* in the presence of hemp extract was due to protection from oxidative stress.[119]

Most studies on the effects of extracts use classical disc diffusion methods. However, recently, the study reported by Frassinetti *et al*.[117] was to determine the lowest concentrations with activity via MIC and a biofilm production and inhibition assay. A further study by Iseppi *et al.*[120] aimed to standardize the antibacterial method and provided better designs for experiments. Firstly, the separation of essential oils (EO) compounds was done by gas chromatography mass spectrometry (GC-MS). The EOs were tested via an agar well-diffusion assay, and MIC testing was done against multiple Gram-positive bacteria. The EOs and purified compounds were highly effective against *Enterococcus*, an opportunistic pathogen. These authors also found that two EOs and two purified compounds had lower MICs than amoxicillin or ampicillin against *Bacillus cereus* (*B. cereus)*.

Another active compound extracted from the seed was flavonoids; these were shown to be active against *Candida albicans*, *S. aureus*, and *P. aeruginosa*.[57] EOs of fiber-type hemp have also been applied to prevent food spoilage, incorporating antimicrobial extracts into food packaging. Further studies are needed on pure compounds.[28]

An exciting use of *Cannabis* extracts has been forming silver or zinc nanoparticles (Ag NPs and Zn NPs) with antimicrobial activity. Chouhan and Guleria,[18] Chauhan *et al.*[121] used *C. sativa* extracts to form stable nanoparticle emulsions with Ag-doped, Zn, and ZnO nanoparticles; AgNPs revealed an excellent antioxidant capacity and significant antibiotic activity against several human infection diseases by disc diffusion test, including *E. coli*, *Klebsiella pneumoniae* (*K. pneumoniae*), MRSA, *P. aeruginosa, S. typhi*, and *S.aureus,* and as an antifungal against *Fusarium* spp. *Rosellinia necatrix C. sativa* aqueous leaf extract (CSE) derived AgNPs also had antifungal and α-amylase inhibitory activity. There was minor activity against *Bacillus subtilis*, *S. aureus,* and *K. pneumoniae* tested by a well-diffusion assay with increasing concentrations of AgNPs. Other researchers[122] suggested a synergistic or symbiotic effect between terpenes, flavonoids, and cannabinoids in industry hemp strains to improve the effect of silver nanoparticles (AgNPs). Other studies showed the effective use of hemp extracts to produce nanoparticles effective against biofilms.[123] The main challenge with using nanoparticles based on *C. sativa* extracts is to develop suitable technologies for obtaining nanoparticles with specific properties used in pharmaceutical products. For recent reviews see.[124,125]

Synergistic effects between *Cannabis sativa* and plants such as *Allium sativum* (Garlic) have been shown.[126] Further research is required to study the impact of terpenes, in particular, as antimicrobial agents.[127] There may also be a synergistic effect when these compounds are applied with antibiotics simultaneously, as demonstrated for other plant extracts by Blesson *et al.*[128] In comparative testing, the presence of other compounds must be considered.

Several reviews have summarized the antimicrobial properties of the major cannabinoids against essential pathogenic microorganisms or viruses, including Gram-negative pathogens, MRSA, and SARS-CoV-2.[3,19,22,129,130] From this extensive compilation of data, there is a need for standardization of methodology and approaches so that valid comparisons and conclusions between laboratories can be made. This includes how *in vitro* results can be extrapolated to determine *in vivo* efficacy, determined (usually) by using animal models.[37] However, further *in vivo* or animal model investigation is required to determine how the body reacts and responds to cannabinoids, including side effects.

Another challenge for using cannabinoids in terms of antimi-

crobial activity is to control their stability and bioavailability once introduced into the body. Cannabinoids have significant pharmacological activities but may show poor water solubility and become labile during processing and storage.[131] A commonly used method for the delivery of cannabinoids and improvements in bioavailability is using nanocarriers (NCs) to protect core materials from degradation during passage through the gastrointestinal (GI) tract.[132] Transmucosal oral routes of delivery offer distinct advantages.[5] Determining dosage forms for any medicinal product must consider product instability, such as at room temperature. In this regard, CBD is highly unstable and sensitive to oxidation.[133]

Future directions

For the potential of *Cannabis* plant extracts and phytochemicals to be applied as natural antimicrobials, further work is required to standardize and harmonize research. As is genuine for all-natural extracts, variability in natural bioactive contents between plants, parts of plants, and extracts needs to be addressed with assessment and clear transparent reporting of properties. Additional research to identify active compounds (in isolation and synergistic applications) will potentially circumvent these issues by refining test substances. However, challenges persist regarding stability, delivery, safety, non-uniform testing procedures, and negative perceptions of these products. A multi-disciplinary approach is required to facilitate the progress from promising potential antimicrobials to pharmacological success, with roles for biological sciences, pharmacology, chemistry, and social and other sciences.

Conclusions

The evolution of antibiotic-resistant bacteria and the emergence of new viruses such as COVID-19 have stimulated the search for non-traditional antimicrobial or antiviral treatments. In the case of bacteria, this includes alternatives to using antibiotics. While the use of *Cannabis* as a medicinal agent has been known for thousands of years, there is now great interest in discovering and analyzing potent antimicrobial agents derived from this plant, including its cannabinoids, terpenes, phenolics, and alkaloids. While this is welcome, inter-laboratory comparisons of results showing antimicrobial or antiviral activities are complex, as many variables affect results (such as plant-to-plant variations, differences in extraction protocols, synergistic/antagonistic effects of other compounds, and differences in antimicrobial assay protocols). There are also challenges for commercial applications, such as finding the best method for extraction and isolation of the active compound, not to mention understanding the stability and bioavailability of the cannabinoids and their pharmacokinetics once introduced into the body. Also, more study is necessary to determine the synergic effect of natural therapeutic plants in combination with *Cannabis*, to design functional nanoparticle delivery devices, and to test the safety and efficacy of an experimental new antibiotic in clinical trials.

Acknowledgments

None.

Funding

HMSAU and AF were funded by MGC Pharmaceuticals Limited, Australia.

Conflict of interest

Funding received from a commercial company (MGC Pharmaceuticals Limited) is a potential conflict.

Author contributions

Conceptualization and design (HMSAU); writing original draft preparation, Abstract, New classes of potent antimicrobial agents, A novel mode of action, Conclusion (HMSAU); Introduction and future research directions (ELB); A novel mode of action (MK); Abstract, Introduction, Challenges on applications of Cannabinoids as an antimicrobial agent (CP); Figure design (HMSAU); writing a review, and editing (AF, CP, ELB, HMSAU). All authors have read and agreed to the published version of the manuscript.

References

[1] Bonini SA, Premoli M, Tambaro S, Kumar A, Maccarinelli G, Memo M, *et al*. Cannabis sativa: A comprehensive ethnopharmacological review of a medicinal plant with a long history. J Ethnopharmacol 2018;227:300–315. doi:10.1016/j.jep.2018.09.004, PMID:30205181.

[2] Fischedick JT, Hazekamp A, Erkelens T, Choi YH, Verpoorte R. Metabolic fingerprinting of Cannabis sativa L., cannabinoids and terpenoids for chemotaxonomic and drug standardization purposes. Phytochemistry 2010;71(17-18):2058–2073. doi:10.1016/j.phytochem.2010.10.001, PMID:21040939.

[3] Klahn P. Cannabinoids-Promising Antimicrobial Drugs orIntoxicants with Benefits? Antibiotics (Basel) 2020;9(6):E297. doi:10.3390/antibiotics9060297, PMID:32498408.

[4] Simiyu DC, Jang JH, Lee OR. Understanding *Cannabis sativa* L.: Current Status of Propagation, Use, Legalization, and Haploid-Inducer-Mediated Genetic Engineering. Plants (Basel) 2022;11(9):1236. doi:10.3390/plants11091236, PMID:35567237.

[5] Fathordoobady F, Singh A, Kitts DD, Pratap Singh A. Hemp (*Cannabis Sativa* L.) extract: anti-microbial properties, methods of extraction, and potential oral delivery. Food Rev Int 2019;35(7):664–684. doi:10.1080/87559129.2019.1600539.

[6] Al Ubeed HMS, Bhuyan DJ, Alsherbiny MA, Basu A, Vuong QV. A Comprehensive Review on the Techniques for Extraction of Bioactive Compounds from Medicinal Cannabis. Molecules 2022;27(3):604. doi:10.3390/molecules27030604, PMID:35163863.

[7] Rosenthal E, Zeman G. CO2 extraction. Beyond buds: Next generation-marijuana extracts and cannabis infusions. CA: Quick American Archives; 2018:149–167.

[8] Dias DA, Urban S, Roessner U. A historical overview of natural products in drug discovery. Metabolites 2012;2(2):303–336. doi:10.3390/metabo2020303, PMID:24957513.

[9] Baker D, Pryce G, Giovannoni G, Thompson AJ. The therapeutic potential of cannabis. Lancet Neurol 2003;2(5):291–298. doi:10.1016/s1474-4422(03)00381-8, PMID:12849183.

[10] Andre CM, Hausman JF, Guerriero G. Cannabis sativa: The Plant of the Thousand and One Molecules. Front Plant Sci 2016;7:19. doi:10.3389/fpls.2016.00019, PMID:26870049.

[11] Ferri M, Ranucci E, Romagnoli P, Giaccone V. Antimicrobial resistance: A global emerging threat to public health systems. Crit Rev Food Sci Nutr 2017;57(13):2857–2876. doi:10.1080/10408398.2015.1077192, PMID:26464037.

[12] Vouga M, Greub G. Emerging bacterial pathogens: the past and beyond. Clin Microbiol Infect 2016;22(1):12–21. doi:10.1016/j.cmi.2015.10.010, PMID:26493844.

[13] Danis-Wlodarczyk KM, Wozniak DJ, Abedon ST. Treating Bacterial Infections with Bacteriophage-Based Enzybiotics: In Vitro, In Vivo and Clinical Application. Antibiotics (Basel) 2021;10(12):1497. doi:10.3390/antibiotics10121497, PMID:34943709.

[14] Rios AC, Moutinho CG, Pinto FC, Del Fiol FS, Jozala A, Chaud MV, *et al*. Alternatives to overcoming bacterial resistances: State-of-the-art. Microbiol Res 2016;191:51–80. doi:10.1016/j.micres.2016.04.008, PMID:27524653.

[15] David MZ, Dryden M, Gottlieb T, Tattevin P, Gould IM. Recently approved antibacterials for methicillin-resistant Staphylococcus aureus (MRSA) and other Gram-positive pathogens: the shock of the new. Int J Antimicrob Agents 2017;50(3):303–307. doi:10.1016/j.ijantimicag.2017.05.006, PMID:28666751.
[16] Appendino G, Gibbons S, Giana A, Pagani A, Grassi G, Stavri M, *et al*. Antibacterial cannabinoids from Cannabis sativa: a structure-activity study. J Nat Prod 2008;71(8):1427–1430. doi:10.1021/np8002673, PMID:18681481.
[17] Blaskovich MAT, Kavanagh AM, Elliott AG, Zhang B, Ramu S, Amado M, *et al*. The antimicrobial potential of cannabidiol. Commun Biol 2021;4(1):7. doi:10.1038/s42003-020-01530-y, PMID:33469147.
[18] Chouhan S, Guleria S. Green synthesis of AgNPs using Cannabis sativa leaf extract: Characterization, antibacterial, anti-yeast and α-amylase inhibitory activity. Materials Science for Energy Technologies 2020;3:536–544. doi:10.1016/j.mset.2020.05.004.
[19] Karas JA, Wong LJM, Paulin OKA, Mazeh AC, Hussein MH, Li J, *et al*. The Antimicrobial Activity of Cannabinoids. Antibiotics (Basel) 2020;9(7):E406. doi:10.3390/antibiotics9070406, PMID:32668669.
[20] Chakraborty S, Afaq N, Singh N, Majumdar S. Antimicrobial activity of Cannabis sativa, Thuja orientalis and Psidium guajava leaf extracts against methicillin-resistant Staphylococcus aureus. J Integr Med 2018;16(5):350–357. doi:10.1016/j.joim.2018.07.005, PMID:30120078.
[21] Nashra A, Sujatha R, Sameer D, Bagoliwal A, Mishra V, Kumar A, *et al*. Comparative Evaluation of Antibacterial Efficacy of Cannabis sativa, Allium sativum, Allium cepa, Thuja orientalis and Psidium guajava against Drug Resistance Pathogens. International Journal of Health Sciences and Research 2018;8(8):89–97.
[22] Mahmud MS, Hossain MS, Ahmed ATMF, Islam MZ, Sarker ME, Islam MR. Antimicrobial and Antiviral (SARS-CoV-2) Potential of Cannabinoids and *Cannabis sativa*: A Comprehensive Review. Molecules 2021;26(23):7216. doi:10.3390/molecules26237216, PMID:34885798.
[23] Salami SA, Martinelli F, Giovino A, Bachari A, Arad N, Mantri N. It Is Our Turn to Get Cannabis High: Put Cannabinoids in Food and Health Baskets. Molecules 2020;25(18):E4036. doi:10.3390/molecules25184036, PMID:32899626.
[24] Elsohly MA, Slade D. Chemical constituents of marijuana: the complex mixture of natural cannabinoids. Life Sci 2005;78(5):539–548. doi:10.1016/j.lfs.2005.09.011, PMID:16199061.
[25] Radwan MM, Ross SA, Slade D, Ahmed SA, Zulfiqar F, Elsohly MA. Isolation and characterization of new Cannabis constituents from a high potency variety. Planta Med 2008;74(3):267–272. doi:10.1055/s-2008-1034311, PMID:18283614.
[26] Radwan MM, Elsohly MA, Slade D, Ahmed SA, Wilson L, El-Alfy AT, *et al*. Non-cannabinoid constituents from a high potency Cannabis sativa variety. Phytochemistry 2008;69(14):2627–2633. doi:10.1016/j.phytochem.2008.07.010, PMID:18774146.
[27] Eisohly HN, Turner CE, Clark AM, Eisohly MA. Synthesis and antimicrobial activities of certain cannabichromene and cannabigerol related compounds. J Pharm Sci 1982;71(12):1319–1323. doi:10.1002/jps.2600711204, PMID:7153877.
[28] Khan BA, Warner P, Wang H. Antibacterial properties of hemp and other natural fibre plants: a review. BioResources 2014;9(2):3642–3659. doi:10.15376/biores.9.2.3642-3659.
[29] Turner CE, Elsohly MA. Biological activity of cannabichromene, its homologs and isomers. J Clin Pharmacol 1981;21(S1):283S–291S. doi:10.1002/j.1552-4604.1981.tb02606.x, PMID:7298870.
[30] Ahmed SA, Ross SA, Slade D, Radwan MM, Zulfiqar F, Matsumoto RR, *et al*. Cannabinoid ester constituents from high-potency Cannabis sativa. J Nat Prod 2008;71(4):536–542. doi:10.1021/np070454a, PMID:18303850.
[31] Molnár J, Csiszár K, Nishioka I, Shoyama Y. The effects of cannabispiro compounds and tetrahydrocannabidiolic acid on the plasmid transfer and maintenance in Escherichia coli. Acta Microbiol Hung 1986;33(3):221–231. PMID:3551476.
[32] Fellermeier M, Zenk MH. Prenylation of olivetolate by a hemp transferase yields cannabigerolic acid, the precursor of tetrahydrocannabinol. FEBS Lett 1998;427(2):283–285. doi:10.1016/s0014-5793(98)00450-5, PMID:9607329.
[33] Sirikantaramas S, Morimoto S, Shoyama Y, Ishikawa Y, Wada Y, Shoyama Y, *et al*. The gene controlling marijuana psychoactivity: molecular cloning and heterologous expression of Delta1-tetrahydrocannabinolic acid synthase from Cannabis sativa L. J Biol Chem 2004;279(38):39767–39774. doi:10.1074/jbc.M403693200, PMID:15190053.
[34] Taura F, Morimoto S, Shoyama Y, Mechoulam R. First direct evidence for the mechanism of. DELTA. 1-tetrahydrocannabinolic acid biosynthesis. J Am Chem Soc 1995;117(38):9766–9767. doi:10.1021/ja00143a024.
[35] Feng J, Gu Y, Quan Y, Gao W, Dang Y, Cao M, *et al*. Construction of energy-conserving sucrose utilization pathways for improving poly-γ-glutamic acid production in Bacillus amyloliquefaciens. Microb Cell Fact 2017;16(1):98. doi:10.1186/s12934-017-0712-y, PMID:28587617.
[36] Feldman M, Sionov RV, Mechoulam R, Steinberg D. Anti-Biofilm Activity of Cannabidiol against *Candida albicans*. Microorganisms 2021;9(2):441. doi:10.3390/microorganisms9020441, PMID:33672633.
[37] Farha MA, El-Halfawy OM, Gale RT, MacNair CR, Carfrae LA, Zhang X, *et al*. Uncovering the Hidden Antibiotic Potential of Cannabis. ACS Infect Dis 2020;6(3):338–346. doi:10.1021/acsinfecdis.9b00419, PMID:32017534.
[38] Centers for Disease Control and Prevention (U.S.); National Center for Emerging Zoonotic and Infectious Diseases (U.S.). Division of Healthcare Quality Promotion. Antibiotic Resistance Coordination and Strategy Unit. Antibiotic resistance threats in the United States, 2019. https://stacks.cdc.gov/view/cdc/82532.
[39] Kosgodage US, Matewele P, Awamaria B, Kraev I, Warde P, Mastroianni G, *et al*. Cannabidiol Is a Novel Modulator of Bacterial Membrane Vesicles. Front Cell Infect Microbiol 2019;9:324. doi:10.3389/fcimb.2019.00324, PMID:31552202.
[40] Grassi L, Maisetta G, Esin S, Batoni G. Combination Strategies to Enhance the Efficacy of Antimicrobial Peptides against Bacterial Biofilms. Front Microbiol 2017;8:2409. doi:10.3389/fmicb.2017.02409, PMID:29375486.
[41] Loza-Tavera H. Monoterpenes in essential oils. Biosynthesis and properties. Adv Exp Med Biol 1999;464:49–62. doi:10.1007/978-1-4615-4729-7_5, PMID:10335385.
[42] Bertoli A, Tozzi S, Pistelli L, Angelini LG. Fibre hemp inflorescences: From crop-residues to essential oil production. Industrial Crops Products 2010;32(3):329–337. doi:10.1016/j.indcrop.2010.05.012.
[43] Dewick PM. The biosynthesis of C5-C25 terpenoid compounds. Nat Prod Rep 2002;19(2):181–222. doi:10.1039/b002685i, PMID:12013278.
[44] Russo EB. Taming THC: potential cannabis synergy and phytocannabinoid-terpenoid entourage effects. Br J Pharmacol 2011;163(7):1344–1364. doi:10.1111/j.1476-5381.2011.01238.x, PMID:21749363.
[45] Gagne SJ, Stout JM, Liu E, Boubakir Z, Clark SM, Page JE. Identification of olivetolic acid cyclase from Cannabis sativa reveals a unique catalytic route to plant polyketides. Proc Natl Acad Sci U S A 2012;109(31):12811–12816. doi:10.1073/pnas.1200330109, PMID:22802619.
[46] Thomas BF, Elsohly M. The analytical chemistry of cannabis: Quality assessment, assurance, and regulation of medicinal marijuana and cannabinoid preparations. Elsevier; 2015.
[47] Muscarà C, Smeriglio A, Trombetta D, Mandalari G, La Camera E, Occhiuto C, *et al*. Antioxidant and antimicrobial activity of two standardized extracts from a new Chinese accession of non-psychotropic Cannabis sativa L. Phytother Res 2021;35(2):1099–1112. doi:10.1002/ptr.6891, PMID:33034400.
[48] McPartland JM, Russo EB. Cannabis and cannabis extracts: greater than the sum of their parts? Journal of Cannabis Therapeutics 2001;1(3-4):103–132. doi:10.1300/J175v01n03_08.
[49] Nagy DU, Cianfaglione K, Maggi F, Sut S, Dall'Acqua S. Chemical Characterization of Leaves, Male and Female Flowers from Spontaneous Cannabis (Cannabis sativa L.) Growing in Hungary. Chem Biodivers 2019;16(3):e1800562. doi:10.1002/cbdv.201800562, PMID:30548994.
[50] Novak J, Franz C. Composition of the essential oils and extracts of two populations of Cannabis sativa L. ssp. spontanea from Austria. J Essent Oil Res 2003;15(3):158–160. doi:10.1080/10412905.2003.9712100.
[51] Ross SA, ElSohly MA. The volatile oil composition of fresh and air-dried buds of Cannabis sativa. J Nat Prod 1996;59(1):49–51. doi:10.1021/np960004a, PMID:8984153.

[52] Turner CE, Elsohly MA, Boeren EG. Constituents of Cannabis sativa L. XVII. A review of the natural constituents. J Nat Prod 1980;43(2):169–234. doi:10.1021/np50008a001, PMID:6991645.
[53] Chen F, Tholl D, Bohlmann J, Pichersky E. The family of terpene synthases in plants: a mid-size family of genes for specialized metabolism that is highly diversified throughout the kingdom. Plant J 2011;66(1):212–229. doi:10.1111/j.1365-313X.2011.04520.x, PMID:21443633.
[54] Nissen L, Zatta A, Stefanini I, Grandi S, Sgorbati B, Biavati B, *et al*. Characterization and antimicrobial activity of essential oils of industrial hemp varieties (Cannabis sativa L.). Fitoterapia 2010;81(5):413–419. doi:10.1016/j.fitote.2009.11.010, PMID:19969046.
[55] Nostro A, Guerrini A, Marino A, Tacchini M, Di Giulio M, Grandini A, *et al*. In vitro activity of plant extracts against biofilm-producing food-related bacteria. Int J Food Microbiol 2016;238:33–39. doi:10.1016/j.ijfoodmicro.2016.08.024, PMID:27591384.
[56] Schofs L, Sparo MD, Sánchez Bruni SF. The antimicrobial effect behind Cannabis sativa. Pharmacol Res Perspect 2021;9(2):e00761. doi:10.1002/prp2.761, PMID:33822478.
[57] Onsare JG, Arora DS. Antibiofilm potential of flavonoids extracted from Moringa oleifera seed coat against Staphylococcus aureus, Pseudomonas aeruginosa and Candida albicans. J Appl Microbiol 2015;118(2):313–325. doi:10.1111/jam.12701, PMID:25410525.
[58] Das B, Mishra P. Antibacterial analysis of crude extracts from the leaves of Tagetes erecta and Cannabis sativa. International Journal of Environmental Sciences 2012;2(3):1605–1608. doi:10.6088/ijes.00202030045.
[59] Sambasivam S, Karpagam G, Chandran R, Khan SA. Toxicity of leaf extract of yellow oleander Thevetia nerifolia on Tilapia. J Environ Biol 2003;24(2):201–204. PMID:12974464.
[60] Kayser O, Kiderlen AF, Croft SL. Natural products as potential antiparasitic drugs. Studies in Natural Products Chemistry 2002;26:779–848. doi:10.1016/S1572-5995(02)80019-9.
[61] Varma J, Dubey N. Prospectives of botanical and microbial products as pesticides of tomorrow. Current Science 1999;76(2):172–179.
[62] Cowan MM. Plant products as antimicrobial agents. Clin Microbiol Rev 1999;12(4):564–582. doi:10.1128/CMR.12.4.564, PMID:10515903.
[63] Audu B, Ofojekwu P, Ujah A, Ajima M. Phytochemical, proximate composition, amino acid profile and characterization of marijuana (Cannabis sativa L.). The Journal of Phytopharmacology 2014;3(1):35–43. doi:10.31254/phyto.2014.3106.
[64] Pollastro F, Minassi A, Fresu LG. Cannabis Phenolics and their Bioactivities. Curr Med Chem 2018;25(10):1160–1185. doi:10.2174/0929867324666170810164636, PMID:28799497.
[65] Zagožen M, Čerenak A, Kreft S. Cannabigerol and cannabichromene in Cannabis sativa L. Acta Pharmaceutica 2021;71(3):355–364. doi:10.2478/acph-2021-0021.
[66] Sampson PB. Phytocannabinoid Pharmacology: Medicinal Properties of *Cannabis sativa* Constituents Aside from the "Big Two". J Nat Prod 2021;84(1):142–160. doi:10.1021/acs.jnatprod.0c00965, PMID:33356248.
[67] Gildea L, Ayariga JA, Ajayi OS, Xu J, Villafane R, Samuel-Foo M. *Cannabis sativa* CBD Extract Shows Promising Antibacterial Activity against *Salmonella typhimurium* and *S. newington*. Molecules 2022;27(9):2669. doi:10.3390/molecules27092669, PMID:35566019.
[68] Gray RA, Whalley BJ. The proposed mechanisms of action of CBD in epilepsy. Epileptic Disord 2020;22(S1):10–15. doi:10.1684/epd.2020.1135, PMID:32053110.
[69] Cannabinoids as antimicrobial agents. New York: LAVVAN; 2022. Available from: https://www.lavvan.com/cannabinoids-as-antimicrobial-agents. Accessed May 9, 2022.
[70] Aqawi M, Sionov RV, Gallily R, Friedman M, Steinberg D. Anti-Bacterial Properties of Cannabigerol Toward *Streptococcus mutans*. Front Microbiol 2021;12:656471. doi:10.3389/fmicb.2021.656471, PMID:33967995.
[71] Bucekova M, Jardekova L, Juricova V, Bugarova V, Di Marco G, Gismondi A, *et al*. Antibacterial Activity of Different Blossom Honeys: New Findings. Molecules 2019;24(8):E1573. doi:10.3390/molecules24081573, PMID:31010070.
[72] Martinenghi LD, Jønsson R, Lund T, Jenssen H. Isolation, Purification, and Antimicrobial Characterization of Cannabidiolic Acid and Cannabidiol from *Cannabis sativa* L. Biomolecules 2020;10(6):E900. doi:10.3390/biom10060900, PMID:32545687.
[73] Krejci Z, Horok M, Santavy F. Hanf (cannabis sativa)-antibiotishes heilmittel. 3. Mitteilung: Isolierung und Konstitution zweier aus Cannabis sativa gewonnener sauren. Die Pharmazie 1959;14:349–355.
[74] Izzo AA, Borrelli F, Capasso R, Di Marzo V, Mechoulam R. Non-psychotropic plant cannabinoids: new therapeutic opportunities from an ancient herb. Trends Pharmacol Sci 2009;30(10):515–527. doi:10.1016/j.tips.2009.07.006, PMID:19729208.
[75] Dalzell HC, Uliss DB, Handrick GR, Razdan RK. Hashish. 26. Factors influencing double-bond stability in cannabinoids. The Journal of Organic Chemistry 1981;46(5):949–953. doi:10.1021/jo00318a021.
[76] Clarke H, Roychoudhury P, Narouze SN. Other Phytocannabinoids. In: Narouze SN (ed). Cannabinoids and Pain. Cham: Springer; 2021:87–92. doi:10.1007/978-3-030-69186-8_12.
[77] Tahsin KN, Watson D, Rizkalla A, Heinrichs D, Charpentier P. Antimicrobial Studies of Cannabidiol as Biomaterials against superbug MRSA. CMBES Proc 2021;44.
[78] Palomares Cañero B. Non psychotropic cannabinoids for the treatment of inflammatory diseases [Dissertation]. Universidad de Córdoba, UCO Press; 2020. Available from: http://hdl.handle.net/10396/19632. Accessed May 9, 2022.
[79] Mnekin L, Ripoll L. Topical Use of Cannabis sativa L. Biochemicals. Cosmetics 2021;8(3):85. doi:10.3390/cosmetics8030085.
[80] Khameneh B, Iranshahy M, Soheili V, Fazly Bazzaz BS. Review on plant antimicrobials: a mechanistic viewpoint. Antimicrob Resist Infect Control 2019;8:118. doi:10.1186/s13756-019-0559-6, PMID:31346459.
[81] Sytar O, Brestic M, Hajihashemi S, Skalicky M, Kubeš J, Lamilla-Tamayo L, *et al*. COVID-19 Prophylaxis Efforts Based on Natural Antiviral Plant Extracts and Their Compounds. Molecules 2021;26(3):727. doi:10.3390/molecules26030727, PMID:33573318.
[82] Pitakbut T, Nguyen GN, Kayser O. Activity of THC, CBD, and CBN on Human ACE2 and SARS-CoV1/2 Main Protease to Understand Antiviral Defense Mechanism. Planta Med 2022;88(12):1047–1059. doi:10.1055/a-1581-3707, PMID:34638139.
[83] Onay A, Ertaş A, Süzerer V, Yener İ, Yilmaz MA, Ayaz-Tilkat E, *et al*. Cannabinoids for SARS-CoV-2 and is there evidence of their therapeutic efficacy? Turk J Biol 2021;45(4):570–587. doi:10.3906/biy-2105-73, PMID:34803455.
[84] Yadav V, Kaushik P. Phytochemicals against COVID-19 and a gap in clinical investigations: An outlook. Indian Journal of Biochemistry Biophysics 2021;58(5):403–407.
[85] Zhao L, Yan Y, Dai Q, Wang Z, Yin J, Xu Y, *et al*. The CDK1 inhibitor, Ro-3306, is a potential antiviral candidate against influenza virus infection. Antiviral Res 2022;201:105296. doi:10.1016/j.antiviral.2022.105296, PMID:35367281.
[86] Mabou Tagne A, Pacchetti B, Sodergren M, Cosentino M, Marino F. Cannabidiol for Viral Diseases: Hype or Hope? Cannabis Cannabinoid Res 2020;5(2):121–131. doi:10.1089/can.2019.0060, PMID:32656344.
[87] Stieltjes N, Ounnoughene N, Sava E, Paugy P, Roussel-Robert V, Rosenberg AR, *et al*. Interest of transjugular liver biopsy in adult patients with haemophilia or other congenital bleeding disorders infected with hepatitis C virus. Br J Haematol 2004;125(6):769–776. doi:10.1111/j.1365-2141.2004.04968.x, PMID:15180867.
[88] Leopold SJ, Grady BP, Lindenburg CE, Prins M, Beuers U, Weegink CJ. Common bile duct dilatation in drug users with chronic hepatitis C is associated with current methadone use. J Addict Med 2014;8(1):53–58. doi:10.1097/ADM.0000000000000006, PMID:24394497.
[89] Lowe HI, Toyang NJ, McLaughlin W. Potential of Cannabidiol for the Treatment of Viral Hepatitis. Pharmacognosy Res 2017;9(1):116–118. doi:10.4103/0974-8490.199780, PMID:28250664.
[90] Bachmetov L, Gal-Tanamy M, Shapira A, Vorobeychik M, Giterman-Galam T, Sathiyamoorthy P, *et al*. Suppression of hepatitis C virus by the flavonoid quercetin is mediated by inhibition of NS3 protease activity. J Viral Hepat 2012;19(2):e81–e88. doi:10.1111/j.1365-2893.2011.01507.x, PMID:22239530.
[91] Edmunds BL, Miller ER, Tsourtos G. The distribution and socioeconomic burden of Hepatitis C virus in South Australia: a cross-sectional study 2010-2016. BMC Public Health 2019;19(1):527. doi:10.1186/s12889-019-6847-5, PMID:31068170.

[92] de Paula Farah K, Carmo RA, de Figueiredo Antunes CM, Serufo JC, Nobre Júnior VA, Fonseca de Castro LP, *et al*. Hepatitis C, HCV genotypes and hepatic siderosis in patients with chronic renal failure on haemodialysis in Brazil. Nephrol Dial Transplant 2007;22(7):2027–2031. doi:10.1093/ndt/gfm028, PMID:17309883.

[93] Hegde VL, Nagarkatti PS, Nagarkatti M. Role of myeloid-derived suppressor cells in amelioration of experimental autoimmune hepatitis following activation of TRPV1 receptors by cannabidiol. PLoS One 2011;6(4):e18281. doi:10.1371/journal.pone.0018281, PMID:21483776.

[94] Lowe H, Steele B, Bryant J, Fouad E, Toyang N, Ngwa W. Antiviral Activity of Jamaican Medicinal Plants and Isolated Bioactive Compounds. Molecules 2021;26(3):607. doi:10.3390/molecules26030607, PMID: 33503834.

[95] Maor Y, Yu J, Kuzontkoski PM, Dezube BJ, Zhang X, Groopman JE. Cannabidiol inhibits growth and induces programmed cell death in kaposi sarcoma-associated herpesvirus-infected endothelium. Genes Cancer 2012;3(7-8):512–520. doi:10.1177/1947601912466556, PMID: 23264851.

[96] Camacho-Rivera M, Islam JY, Rodriguez DL, Vidot DC. Cannabis Use among Cancer Survivors amid the COVID-19 Pandemic: Results from the COVID-19 Cannabis Health Study. Cancers (Basel) 2021;13(14):3495. doi:10.3390/cancers13143495, PMID:34298708.

[97] Beasley MB. Acute lung injury-from cannabis to COVID. Mod Pathol 2022;35(Suppl 1):1–7. doi:10.1038/s41379-021-00915-6, PMID:34504310.

[98] van Laar MW, Oomen PE, van Miltenburg CJA, Vercoulen E, Freeman TP, Hall WD. Cannabis and COVID-19: Reasons for Concern. Front Psychiatry 2020;11:601653. doi:10.3389/fpsyt.2020.601653, PMID:33408655.

[99] Chong WW, Acar ZI, West ML, Wong F. A Scoping Review on the Medical and Recreational Use of Cannabis During the COVID-19 Pandemic. Cannabis Cannabinoid Res 2022;7(5):591–602. doi:10.1089/can.2021.0054, PMID:34981958.

[100] Chatow L, Nudel A, Nesher I, Hayo Hemo D, Rozenberg P, Voropaev H, *et al*. In Vitro Evaluation of the Activity of Terpenes and Cannabidiol against Human Coronavirus E229. Life (Basel) 2021;11(4):290. doi:10.3390/life11040290, PMID:33805385.

[101] Loizzo MR, Saab AM, Tundis R, Menichini F, Bonesi M, Piccolo V, *et al*. In vitro inhibitory activities of plants used in Lebanon traditional medicine against angiotensin converting enzyme (ACE) and digestive enzymes related to diabetes. J Ethnopharmacol 2008;119(1):109–116. doi:10.1016/j.jep.2008.06.003, PMID:18601990.

[102] Nguyen LC, Yang D, Nicolaescu V, Best TJ, Ohtsuki T, Chen SN, *et al*. Cannabidiol Inhibits SARS-CoV-2 Replication and Promotes the Host Innate Immune Response. bioRxiv 2021. doi:10.1101/2021.03.10.432967, PMID:33758843.

[103] Perry E, Howes MJ. Medicinal plants and dementia therapy: herbal hopes for brain aging? CNS Neurosci Ther 2011;17(6):683–698. doi:10.1111/j.1755-5949.2010.00202.x, PMID:22070157.

[104] Astuti I, Ysrafil. Severe Acute Respiratory Syndrome Coronavirus 2 (SARS-CoV-2): An overview of viral structure and host response. Diabetes Metab Syndr 2020;14(4):407–412. doi:10.1016/j.dsx.2020.04.020, PMID:32335367.

[105] Davidson AM, Wysocki J, Batlle D. Interaction of SARS-CoV-2 and Other Coronavirus With ACE (Angiotensin-Converting Enzyme)-2 as Their Main Receptor: Therapeutic Implications. Hypertension 2020;76(5):1339–1349. doi:10.1161/HYPERTENSIONAHA.120.15256, PMID:32851855.

[106] Sallenave JM, Guillot L. Innate Immune Signaling and Proteolytic Pathways in the Resolution or Exacerbation of SARS-CoV-2 in Covid-19: Key Therapeutic Targets? Front Immunol 2020;11:1229. doi:10.3389/fimmu.2020.01229, PMID:32574272.

[107] Anand U, Jacobo-Herrera N, Altemimi A, Lakhssassi N. A Comprehensive Review on Medicinal Plants as Antimicrobial Therapeutics: Potential Avenues of Biocompatible Drug Discovery. Metabolites 2019;9(11):E258. doi:10.3390/metabo9110258, PMID:31683833.

[108] Cooper MA, Shlaes D. Fix the antibiotics pipeline. Nature 2011;472(7341):32. doi:10.1038/472032a, PMID:21475175.

[109] WHO. The Burden of Health Care-Associated Infection Worldwide. A Summary; 2010: Geneva.

[110] Datta S, Ramamurthy PC, Anand U, Singh S, Singh A, Dhanjal DS, *et al*. Wonder or evil?: Multifaceted health hazards and health benefits of *Cannabis sativa* and its phytochemicals. Saudi J Biol Sci 2021;28(12):7290–7313. doi:10.1016/j.sjbs.2021.08.036, PMID:34867033.

[111] Eloff JN. A sensitive and quick microplate method to determine the minimal inhibitory concentration of plant extracts for bacteria. Planta Med 1998;64(8):711–713. doi:10.1055/s-2006-957563, PMID:9933989.

[112] CLSI Performance Standards for Antimicrobial Disk Susceptibility Tests. 12th Edition ed. Wayne, PA: Clinical and Laboratory Standards Institute; 2017.

[113] Sadgrove NJ, Jones GL. From Petri Dish to Patient: Bioavailability Estimation and Mechanism of Action for Antimicrobial and Immunomodulatory Natural Products. Front Microbiol 2019;10:2470. doi:10.3389/fmicb.2019.02470, PMID:31736910.

[114] Al Ubeed HMS, Wills RBH, Chandrapala J. Post-Harvest Operations to Generate High-Quality Medicinal Cannabis Products: A Systemic Review. Molecules 2022;27(5):1719. doi:10.3390/molecules27051719, PMID:35268820.

[115] Challa SKR, Misra N, Martynenko A. Drying of cannabis—state of the practices and future needs. Drying Technology 2021;39(14):2055–2064.

[116] Chasiotis V, Tsakirakis A, Termentzi A, Machera K, Filios A. Drying and quality characteristics of Cannabis sativa L. Inflorescences under constant and time-varying convective drying temperature schemes. Thermal Science and Engineering Progress 2022;28:101076. doi:10.1016/j.tsep.2021.101076.

[117] Frassinetti S, Gabriele M, Moccia E, Longo V, Di Gioia D. Antimicrobial and antibiofilm activity of Cannabis sativa L. seeds extract against Staphylococcus aureus and growth effects on probiotic Lactobacillus spp. LWT 2020;124:109149. doi:10.1016/j.lwt.2020.109149.

[118] Patnaik T, Dey R, Gouda P. Antimicrobial Activity of Friedelan-3 [beta]-ol and trans-N-Caffeoyltyramine Isolated from the Root of Vitis trifolia. Asian Journal of Chemistry 2008;20(1):417–421.

[119] Di Gioia D, Gaggia F, Baffoni L, Stenico VJB. Role of bifidobacteria in the production of bioactive compounds and detoxification of harmful compounds. Beneficial microbes in fermented functional foods. 2014:291–308.

[120] Iseppi R, Brighenti V, Licata M, Lambertini A, Sabia C, Messi P, *et al*. Chemical Characterization and Evaluation of the Antibacterial Activity of Essential Oils from Fibre-Type *Cannabis sativa* L. (Hemp). Molecules 2019;24(12):E2302. doi:10.3390/molecules24122302, PMID:31234360.

[121] Chauhan A, Verma R, Kumari S, Sharma A, Shandilya P, Li X, *et al*. Photocatalytic dye degradation and antimicrobial activities of Pure and Ag-doped ZnO using Cannabis sativa leaf extract. Sci Rep 2020;10(1):7881. doi:10.1038/s41598-020-64419-0, PMID:32398650.

[122] Csakvari AC, Moisa C, Radu DG, Olariu LM, Lupitu AI, Panda AO, *et al*. Green Synthesis, Characterization, and Antibacterial Properties of Silver Nanoparticles Obtained by Using Diverse Varieties of *Cannabis sativa* Leaf Extracts. Molecules 2021;26(13):4041. doi:10.3390/molecules26134041, PMID:34279380.

[123] Singh P, Pandit S, Garnæs J, Tunjic S, Mokkapati VR, Sultan A, *et al*. Green synthesis of gold and silver nanoparticles from *Cannabis sativa* (industrial hemp) and their capacity for biofilm inhibition. Int J Nanomedicine 2018;13:3571–3591. doi:10.2147/IJN.S157958, PMID:29950836.

[124] Ying S, Guan Z, Ying S, Ofoegbu PC, Clubb P, Rico C, *et al*. Green synthesis of nanoparticles: Current developments and limitations. Environmental Technology & Innovation. 2022:102336. doi:10.1016/j.eti.2022.102336.

[125] Pal G, Rai P, Pandey A. Green synthesis of nanoparticles: A greener approach for a cleaner future. Green synthesis, characterization and applications of nanoparticles. Elsevier; 2019:1–26. doi:10.1016/B978-0-08-102579-6.00001-0.

[126] Chakarborty PS, Sapkota H, Prabhakar PK. Synergistic interaction of cannabis and garlic with commercial antibiotics. International Journal of Pharmacognosy Phytochemical Research 2015;7(1):193–196.

[127] Nuutinen T. Medicinal properties of terpenes found in Cannabis sativa and Humulus lupulus. Eur J Med Chem 2018;157:198–228. doi:10.1016/j.ejmech.2018.07.076, PMID:30096653.

[128] Blesson J, Saji C, Nivya R, Kumar R. Synergism of antibiotics and plant extracts in antibacterial activity against methicillin resistant Staphylococcus aureus. Journal of Bioavailability & Bioequivalence 2014;6(5):.
[129] Janecki M, Graczyk M, Lewandowska AA, Pawlak Ł. Anti-Inflammatory and Antiviral Effects of Cannabinoids in Inhibiting and Preventing SARS-CoV-2 Infection. Int J Mol Sci 2022;23(8):4170. doi:10.3390/ijms23084170, PMID:35456990.
[130] Sionov RV, Steinberg D. Anti-Microbial Activity of Phytocannabinoids and Endocannabinoids in the Light of Their Physiological and Pathophysiological Roles. Biomedicines 2022;10(3):631. doi:10.3390/biomedicines10030631, PMID:35327432.
[131] Munjal M, ElSohly MA, Repka MA. Chemical stabilization of a Delta9-tetrahydrocannabinol prodrug in polymeric matrix systems produced by a hot-melt method: role of microenvironment pH. AAPS PharmSciTech 2006;7(3):71. doi:10.1208/pt070371, PMID:17025251.
[132] Kumari A, Yadav SK, Pakade YB, Singh B, Yadav SC. Development of biodegradable nanoparticles for delivery of quercetin. Colloids Surf B Biointerfaces 2010;80(2):184–192. doi:10.1016/j.colsurfb.2010.06.002, PMID:20598513.
[133] Fraguas-Sánchez AI, Fernández-Carballido A, Martin-Sabroso C, Torres-Suárez AI. Stability characteristics of cannabidiol for the design of pharmacological, biochemical and pharmaceutical studies. J Chromatogr B Analyt Technol Biomed Life Sci 2020;1150:122188. doi:10.1016/j.jchromb.2020.122188, PMID:32506012.

Journal of Exploratory Research in Pharmacology **2023** vol. 8(2) | 131–139
DOI: 10.14218/JERP.2022.00066

Review Article

Emerging Pharmacological Targets for Treatment of Dry Age-related Macular Degeneration and Geographical Atrophy

Miteshkumar Maurya[1*], Renuka Munshi[1], Sanket Thakur[2] and Sachin Zambare[3]

[1]Department of Clinical Pharmacology, Topiwala National Medical College & B. Y. L. Nair Charitable Hospital, Mumbai, India; [2]Pediatric Critical Care, Royal Manchester Children's hospital, Manchester, United Kingdom; [3]Department of Nephrology, Sterling Hospital, Vadodara, Gujarat, India

Received: August 09, 2022 | **Revised:** September 05, 2022 | **Accepted:** October 19, 2022 | **Published online:** December 21, 2022

Abstract

Age-related macular degeneration (AMD) is difficult to treat and causes visual impairment worldwide, especially for dry AMD. The aging phenomenon can affect macular function, manifesting as blurred central vision. There are two types of AMD: dry and wet. By 2040, some variants of AMD are estimated to affect 288 million people globally. Although wet (exudative) AMD accounts for 10% of all AMD cases, it also contributes to 90% of the cases of patients with vision loss. Therapeutic options for wet age-related macular degeneration have expanded during the last few years. The therapeutic strategies mainly rely on anti-vascular endothelial growth factor (anti-VEGF) drugs and photodynamic therapy (PDT), though the treatment approaches for dry AMD are limited to dietary supplementation to delay progression. Moreover, clinical trials with potential candidate molecules for wet AMD exceed those for dry AMD. Although the disease is not rare, there are few therapeutic targets in the pipeline for dry AMD, and these targets may serve as promising pharmacotherapeutic options in the future. The current review sheds light on successes and failures of the existing novel drug molecules and potential targets for treating dry AMD in clinical trials registered at the Clinical Trials.gov registry run by the United States Food and Drug Administration (U.S. FDA) some of which are published in relevant journals.

Introduction

Age-related macular degeneration (AMD) is one of the critical causes of vision loss and visual disability in the elderly population in developed countries.[1,2] Dry AMD contributes to 10% of vision loss cases and is categorized into early, intermediate, and late stages, depending on the presence of hyper or hypopigmentation with drusen within the macula.[3] Late dry AMD, also known as geographical atrophy, and wet AMD, characterized by choroidal neovascularization, are both advanced forms of age-related macular degeneration (AMD). Geographical atrophy or advanced/late-stage of dry AMD has been named due to the appearance of map-like lesions in the macula on performing the ocular examination. The macular retinal lesions develop due to the degeneration of photoreceptor cells and supporting retinal pigment epithelial tissues, which may take years to develop, and the patient may appear asymptomatic. However, at the late stage of geographical atrophy, the patients develop sudden and severe visual disabilities.[4] The pathophysiology behind the dry AMD is drusen formation (insoluble lipid-laden cellular debris deposits between Bruch's membrane and Retinal Pigment Epithelium, RPE), a post-inflammatory process. During the process, complement and cytokines are involved, leading to atrophy in the macular retinal pigment epithelium, usually associated with the degeneration of the photoreceptors that clinically manifest as central blurring of vision in the affected eye.[5,6] Once dry AMD progresses to the advanced or late stage (geographical atrophy), there is no effective treatment to prevent vision loss or repair damaged photoreceptors. The existing treatment targeting the inflammatory complement and cytokine pathways may benefit patients by delaying the disease pro-

Keywords: Age related macular degeneration; Geographical atrophy; Choroidal neovascularization; Photoreceptors; Retinal Pigment Epithelium; Pipeline drugs; Clinical trials.

Abbreviations: A2E, N-retinylidene-N-retinylethanolamine; AAV2, adeno-associated viral vector; ADMSC, adipose tissue derived mesenchymal stem cells; ARMD/AMD, age-related macular degeneration; ATP, Adenosine Tri Phosphate; BCVA, best corrected visual acuity; CF1, complement factor 1; CTNF, ciliary neurotrophic factor; Da, Daltons; DDS, drug delivery system; DHA, docosahexanoic acid; ECT, encapsulated cell technology; FAF, fundus autofluorescence photography; GA, geographical atrophy; HESC, human embryonic stem cells; HT1A, hydroxytryptamine 1A receptor; IOP, intra ocular pressure; LCPUFA, long chain poly-unsaturated fatty acid; LDL, low-density lipoprotein; mf-ERG, modified Electro-retinogram; MIRA-1, Multicenter investigation of Rheopheresis for Age-related macular degeneration; OCT, optical coherence tomography; PBM, photobiomodulation therapy; PLGA, Poly Lactic-co-Glycolic Acid; RBP, retinol binding protein; RCT, randomised controlled trials; RPE, retinal pigment epithelium; VEGF, vascular endothelial growth factor.

[*]**Correspondence to:** Miteshkumar Maurya, Department of Clinical Pharmacology, Topiwala National Medical College & B. Y. L. Nair Charitable Hospital, Mumbai 400008, India. ORCID: https://orcid.org/0000-0001-6328-4731. Tel: +91-9167612373, E-mail: mitesh.maurya4@gmail.com

How to cite this article: Maurya M, Munshi R, Thakur S, Zambare S. Emerging Pharmacological Targets for Treatment of Dry Age-related Macular Degeneration and Geographical Atrophy. *J Explor Res Pharmacol* 2023;8(2):131–139. doi: 10.14218/JERP.2022.00066.

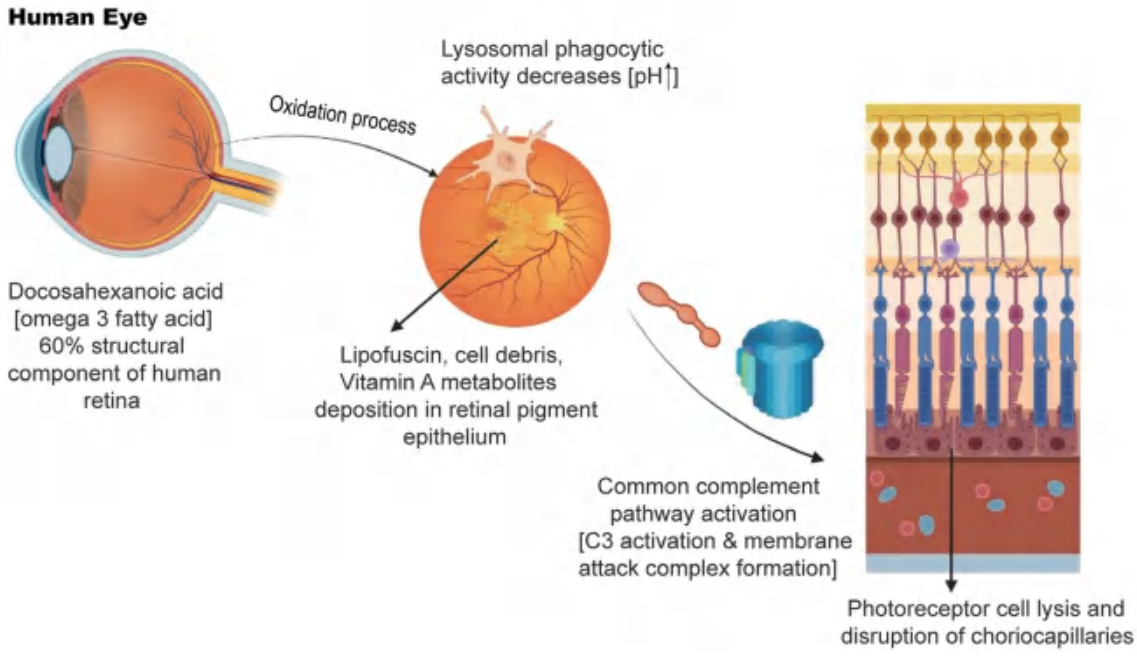

Fig. 1. Pathogenesis of dry age related macular degeneration and geographical atrophy. A2E, N-retinylidene-N-retinylethanolamine; GA, geographical atrophy; RPE, retinal pigment epithelium (created with www.BioRender.com).

gression.[7] Our review mainly focuses on all pipeline drugs tested under clinical trials registered at the U.S. FDA-run Clinical Trials.gov registry some of which are published in the relevant journals to understand the potential therapeutic targets and their mechanisms for treating dry AMD or Geographical Atrophy.

Pathogenesis of dry AMD

The pathogenesis of dry AMD is mediated by cytokines and complement pathway activation. However, various unexplained trigger factors contribute to the disease development and need further evaluation. Docosahexaenoic acid (DHA) constitutes almost 60% polyunsaturated fatty acid of the structural framework of the human retina, especially in the RPE, and is involved in the pathogenesis of dry AMD.[8] Human retina is the ocular interface exposed constantly most of the time to light and oxygen due to excess oxygen demand by RPE cells. Peroxidation of DHA leads to the formation of lipofuscin (yellow-brown pigment) that tends to accumulate in the RPE, which is non-degradable in the RPE cellular lysosomes.[9] Therefore, an increase in the lysosomal pH impairs the phagosomal activity of lysosomal enzymes in the RPE. Subsequently, there is deposition of cellular debris, lipofuscin, and vitamin A metabolites (A2-E) in the RPE layer of the retina, which activates the complement pathway to activate complement C3.[10] C3 protein, an essential component for amplification of the complement pathways, is cleaved to membrane attack complex (cytotoxic component) that induces cell lysis and subsequently destroys photoreceptors and choriocapillaries progressing to GA. GA is a chronic progressive macular degeneration and can manifest as late-stage dry AMD.[11] Diagrammatic representation of the AMD and GA pathogenesis and pharmacological intervention is provided in Figures 1 and 2 respectively. Recent studies in a mouse macular degeneration model have shown that immunotherapies targeting the beta-amyloid plaques in Alzheimer's disease can improve the clearance of amyloid deposited in the retina and electroretinogram deficits, suggesting that beta amyloids deposits are crucial for the pathogenesis of dry AMD.[12]

Pipeline drugs for dry AMD

The treatment armamentarium for wet AMD is exhaustive.[13] There is no approved drug for treating dry AMD or GA globally, and there remains an unmet need for developing drugs in this therapeutic area. Few drugs in the pipeline are undergoing clinical trials that have shown promising results in delaying the progression of dry AMD by their neuroprotective effect on photoreceptors and RPE.[14] Hence, understanding and exploring more therapeutic targets for treating dry AMD and GA is vital.

The treatment of dry AMD is based on two disease-modifying agents: 1) Neuroprotectants for photoreceptors and RPE cells and antioxidant agents. 2) Anti-inflammatory agents, like corticosteroids and agents targeting complement activation (Fig. 2).

Neuroprotective agents

Ciliary Neurotrophic Factor (CNTF, NT-501) (Neurotech Pharmaceuticals)

CNTF has been tried and tested as a treatment for dry AMD and GA. CNTF can retard further damage to the photoreceptor cells in degenerative macular diseases, such as AMD and retinitis pigmentosa. Delivering drugs from the systemic circulation across the blood-retinal barrier is a big challenge to reaching the neurosensory retina. With the advent of Encapsulated Cell Technology (ECT), sustained release of therapeutic agents across the blood-retinal barrier has become convenient. However, the dose-dependent increase in retinal thickness has been observed by optical coherence tomography (OCT) over four months. CTNF delivered by encapsulated cell technology effectively delayed the progression of GA, especially for those with 20/63 or bet-

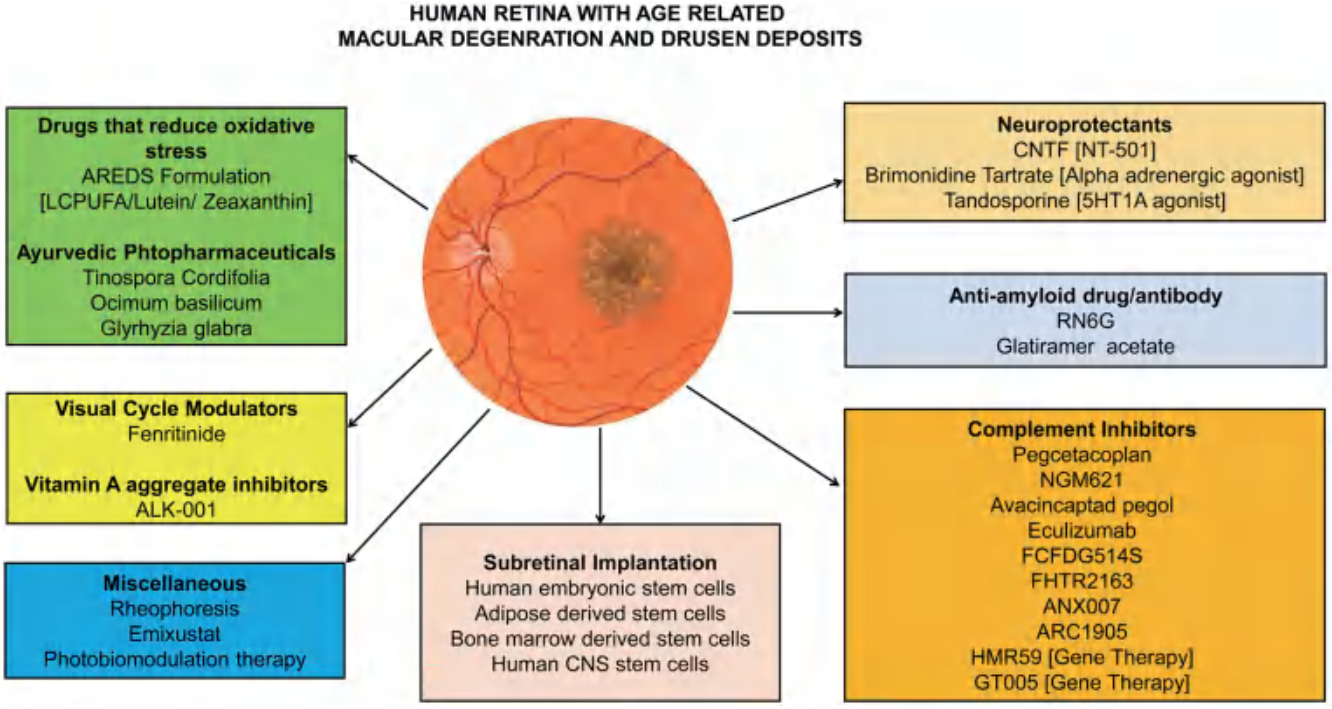

Fig. 2. Pipeline investigational drugs for dry age related macular degeneration and geographical atrophy. 5HT1A, Serotonin receptor agonist; AREDS, age related eye disease studies; CNS, central nervous system; CNTF, Ciliary Neurotropic Factors; LCPUFA, long chain polyunsaturated fatty acid.

ter vision at baseline. However, the study failed to demonstrate any improvement in macular lesion size in GA cases.[15–18]

Brimonidine Tartrate (Allergan, Inc)

Brimonidine has neuroprotective action due to its alpha-adrenergic activity and has been shown to retard retinal degeneration and protect RPE and photoreceptors in rodent studies. A phase IIA study has reported that brimonidine can lower intraocular pressure (IOP) when injected into the eye (through Ozurdex-like intravitreal implant) and inhibit the progression of GA in dry AMD. Brimonidine is implanted through pars plana in the vitreous humor of GA patients every six months, reducing the frequency of injections and maintaining therapeutic drug levels in the retina. Like the Ozurdex dexamethasone implant, brimonidine can be delivered by the Novadur solid polymer drug delivery system made of PLGA intravitreal solid polymer matrix that slowly degrades to lactic acid and glycolic acid with no residues left in the eye. The trial used first-generation brimonidine DDS tartrate in 22-gauge implants at doses of 132 and 264 micrometers. At the end of 12 months, there was a 19% and 28% reduction in the lesion growth rate compared with the placebo. The BEACON Phase IIB trial is ongoing and tests the second generation of brimonidine DDS that delivers more drug to the retina, i.e., a dose of 400 micrometers of free base brimonidine in a 25 gauge implant.[19,20]

Tandospirone (Alcon Laboratories, Inc.)

Tandospirone (AL-8309B) is a serotonin receptor (5-HT1A) agonist and has been approved for the treatment of depressive illness. However, it also possesses a neuroprotective effect on the photoreceptor and retinal pigment cells. The GATE study is a randomized phase III, multicenter clinical trial (N = 768) to investigate the safety and efficacy of Tandospirone in patients with GA secondary to AMD. The patients were treated with AL-8309B ophthalmic solution at varying concentration i.e 1.0%, 1.75%, or a vehicle control as topical eye drops twice daily for 30–36 months. Unfortunately, AL-8309B treatment did not significantly change the annualized GA lesion size (1.73, 1.76, and 1.71 mm^2 for the AL-8309B 1.0%, 1.75%, and vehicle group, respectively, though not associated with any safety concern.[21]

Anti-amyloid beta antibody

Glatiramer acetate (Copaxone, Teva Pharmaceuticals, Israel)

Glatiramer acetate has been used to treat multiple sclerosis due to its immunomodulatory action. This drug can suppress T cells and reduce retinal microglial cytotoxicity induced by beta-amyloid plaques. It has been shown to reduce the drusen area in patients with dry AMD compared to the sham treatment.[22–24]

RN6G (Pfizer, Inc, USA)

RN6G is a humanized monoclonal antibody against beta-amyloid plaques and disseminates the amyloid concentration in the periphery of the retina, reducing macular toxicity. In rodent models of AMD, treatment with RN6G decreases amyloid plaque deposits in the retina. However, the trial of RN6G (NCT01577381) was terminated for lack of efficacy, and the trial of GSK933776 also failed to show any benefit of treatment.[25]

Reducing oxidative stress

AREDS (Age-Related Eye Disease Studies) formulation (Bausch & Lomb, Inc.)

In AREDS2 cognition function testing RCT (factorial design),

there was no significant difference in the scores observed in participants treated with long-chain poly-unsaturated fatty acid supplements (LCPUFA) 1 gram or lutein (10 mg)/zeaxanthin (2 mg) when compared with those treated with standard of care only. All study participants were provided standard care therapy as a micronutrient formulation containing zinc, vitamin C, vitamin E, and beta carotene. Although it reduced the risk of vision loss by 19% in patients with pre-existing intermittent/ advanced AMD, it failed to show any apparent benefit in early AMD. The lutein and zeaxanthin components of the formulation are known to have anti-inflammatory and antioxidant properties and hence may exert a neuroprotective effect on the retinal pigment epithelium.[26,27]

Visual cycle modulators

Fenretinide (ReVision Therapeutics)

A synthetic retinoid can be used orally as a chemoprotective drug against prostate cancer and in women at risk of developing breast cancer. It also has antineoplastic, chemoprotective, pro-apoptotic, anti-inflammatory, and anti-angiogenic properties, and its side effects include mild to moderate drying of mucosal membranes with a delay in dark adaptation. Fenretinide can reduce the accumulation of lipofuscin and retinol-derived toxins in an animal model of Stargardt disease. Fenretinide reduces the circulating levels of retinol and its carrier protein, retinol-binding protein (RBP). As A2E and related toxins are derived from retinol, reducing circulating RBP-retinol levels can decrease retinol-derived toxins in the eye.[28,29] A phase 2 study with 100 and 300 mg of fenretinide was investigated. The interim results revealed that at 24 months, the 300 mg fenretinide group exhibited approximately 40% reduction in the progression of GA compared to the placebo group.[30,31]

Subretinal implantation of stem cells derived from different sources

Human Embryonic Stem Cells (HESC)

Stem cell therapy may provide a safe and promising treatment for retinal diseases. The technology to derive RPEs from hESCs has been developed. A Phase I/IIa clinical study in patients diagnosed with advanced dry AMD and GA (NCT02286089) by subretinal injection of 50–200 k OpRegen cells with immunosuppressive therapy for three months post-implantation. Based on interim Phase I/IIa results of 3 cohorts of 12 patients each, the therapy was well tolerated. Adverse events included the formation of mild epiretinal membranes (ERM), with one being successfully peeled two months after therapy while one patient experienced retinal detachment. OCT confirmed the continued presence of retinal pigment cells transplanted. Dosing in cohort 4 is still ongoing.[32,33]

Adipose-derived stem cell implantation

There are case reports to evaluate the safety of subretinal implantation with adipose tissue-derived mesenchymal stem cell (ADMSC) in advanced stages of retinitis pigmentosa (RP), with one out of 11 patients experiencing choroidal neovascular membrane and five patients having epiretinal membrane at and around the implantation site, respectively. Many studies have investigated the efficacy of this intervention in different types of degenerative macular diseases. Among the published prospective case series, one of the Phase 2 studies assessed the safety and efficacy of suprachoroidal Adipose Tissue-Derived Mesenchymal Stem Cell (ADMSC) in patients suffering from dry AMD and observed an improvement in visual acuity and visual field.[34,35]

Bone marrow-derived stem cell implantation

Few studies have evaluated the role of bone marrow-derived stem cells in treating advanced dry AMD using multifocal electroretinogram (mf-ERG) and fundus autofluorescence imaging. There is no significant improvement in median log MAR BCVA between the test and control groups at the 6-month follow-up. Multifocal Electroretinogram, however, revealed significant improvement in amplitude and implicit time in the intervention group, while there was a significant decrease noted in the greatest linear dimension (GLD) of GA in the eyes receiving stem cells (6.78 ± 2.60 mm at baseline to 6.56 ± 2.59 mm at six months, $p = 0.021$) while there was no such improvement noticed in the control group.[36]

Human CNS stem cells (Hu CNS-SC)

The Phase 1/2 study by StemCells, Inc. United States (NCT01632527) tested the efficacy of surgical implantation with human CNS Stem cells (Hu CNS-SC) in the subretinal space of patients with GA without choroidal neovascularization. However, this study did not report the results yet.[37]

Potential drugs and gene therapies targeting the complement system

The details of drugs affecting the various components of the complement pathway and route of administration are provided in Table 1.

C3 complement system inhibitors

Pegcetacoplan (Apellis Pharmaceuticals)

It is a protein drug approved to treat paroxysmal nocturnal hemoglobinuria in adults. Pegcetacoplan functions and acts as a pegylated C3 inhibitor. In the Phase 2 FILLY study, intravitreal injections with 15 mg pegcetacoplan monthly for 12 months significantly inhibited the growth rate of GA lesions by 29% compared with the sham therapy. This was further confirmed by the Phase 3 OAKS study (N = 637 patients) that revealed that monthly injections with 15 mg/0.1 mL pegcetacoplan for 12 months significantly reduced GA lesion growth by 22% compared with the sham therapy. Treatment with the same dose of pegcetacoplan every other month significantly reduced GA lesion growth by 16%. Another confirmatory Phase 3 study of DERBY (621 patients) did not meet the primary endpoint. In the pooled analysis of all Phase 3 trials, pegcetacoplan has a greater effect on eyes with extrafoveal lesions at baseline, decreasing GA lesion growth by 26% for monthly regimen and 23% with every-other-month injections with accepted tolerability profile. However, the pooled safety data of these Phase 3 trials have shown three cases with infectious endophthalmitis (0.047% risk per injection), 13 cases with intraocular inflammation (0.21% risk per injection), and no retinal vasculitis or vascular occlusion. The pooled data also revealed that pegcetacoplan treatment was associated with a dose-dependent increase in new-onset wet AMD with a rate of 6.0% in the monthly cohort, 4.1% in the every-other-month cohort, and 2.4% in the sham group.[38,39]

NGM621 (NGM Biopharmaceuticals)

NGM621 is a humanized IgG1 antibody and can inhibit the enzymatic cleavage of C3. Unlike the other complement-targeting ther-

Table 1. Novel Therapies targeting complement pathway for Geographical atrophy and dry AMD

Study Drug [Pharmaceutical company name]	Complement Target	Delivery method	Current trial phase	Most Recent Trials	Study Status
Pegcetacoplan [Apellis]	C3	Intra vitreal implant [IVI]	III	OAKS, DERBY	Active, Not recruiting
NGM621 [NGM Biopharmaceuticals]	C3	Intra vitreal implant [IVI]	II	CATALINA	Active, Not recruiting
Avacincaptad pegol/Zimura [Iveric Bio]	C5	Intra vitreal implant [IVI]	III	GATHER II	Active, Not recruiting
ANX007 [Hemera]	C1q	Intra vitreal implant [IVI]	II	ARCHER	Recruiting
HMR59 [Hemera]	C9	Intra vitreal implant [IVI]	I	HMR-1001	Completed
GT005 [Gyroscope Therapeutics]	Complement Factor I	Subretinal	I/II and II	FOCUS, EXPLORE, HORIZON	Recruiting

AMD, Age related Macular Degeneration; C, Complement factor; IVI, Intravitreal injection. Clinical trials name: OAKS, DERBY, GATHER II, ARCHER, HMR-1001, FOCUS, EXPLORE, HORIZON.

apeutics for GA, NGM621 is not pegylated. In the Phase 1 trial, the agent was well tolerated with no drug-related adverse events. The Phase 2 CATALINA trial is ongoing, with approximately 320 patients enrolled. The study is designed to randomly assign patients to receive intravitreal injections of 15 mg versus sham therapy (2:1 ratio) every 4 or 8 weeks for a total of 52 weeks. The primary efficacy endpoint is the rate of change in GA lesion area measured by fundus autofluorescence (FAF) for 52 weeks.[40]

POT-4 (Potentia Pharmaceuticals, USA)

When injected intravitreally, the drug is released gradually, and it binds to C3 protein, the central component of the complement pathways known to trigger the inflammatory process.[41]

Avacincaptad pegol (Zimura, Iveric Bio)

Avacincaptad pegol is a specific inhibitor of C5 and can slow down the progression of retinal cell degeneration. Treatment with 2 mg or 4 mg Avacincaptad pegol for 12 months can reduce GA lesion growth by approximately 27% in the (Phase III GATHER 1, N = 286) clinical trial. This drug selectively inhibits C5 and has additional safety advantages. A confirmatory pivotal trial (GATHER II) is underway to evaluate the efficacy and safety of this drug.[42,43]

Eculizumab (Soliris, Alexion Pharmaceuticals, USA)

Eculizumab is a humanized IgG monoclonal antibody against C5 that prevents its cleavage into C5a and C5b during the process of complement activation. The strategic blockade of the C5 cleavage prevents the release of the downstream anaphylatoxin C5a and the formation of the cytolytic membrane attack complex (MAC). Currently, a phase II study (COMPLETE trial) is testing the efficacy and safety of intravenous infusion with eculizumab for patients with dry AMD/GA.[44]

ARC 1905 (Opthotech Corp, USA)

This aptamer selectively inhibits C5. Currently, there is an undergoing Phase 1 study (NCT 00950638).[45]

Gene therapy

HMR59 (Hemera Biosciences)

HMR59 carries the soluble form of CD59 gene in a recombinant adeno-associated viral (AAV2) vector. CD59 is a glycosylphosphatidylinositol-anchored membrane inhibitor of the membrane attack complex. Functionally, HMR59 treatment can prevent the recruitment of complement C9. The membrane attack complex is the terminal step of an activated complement cascade. A completed Phase 1 study of HMR59 investigated the dose-escalating safety and tolerability of a single intravitreal injection for GA with a total of 17 patients. There were no systemic or severe adverse events associated with HMR59 injections. Mild ocular inflammation occurred in three patients' treated eyes, including two eyes that developed vitreous inflammation that resolved after six weeks of observation and one eye that developed anterior chamber and vitreous inflammation that resolved with topical corticosteroids. Not a single patient converted to wet AMD during the 18-month follow-up period.[46]

GT005 (Gyroscope Therapeutics)

GT005 is a recombinant adenovirus-associated vector 2 (AAV2) that contains a nucleotide sequence encoding complement factor I (CFI). Subretinal injection with GT005 was designed to enable cellular transduction and induce CFI expression and secretion.

While low serum CFI levels are associated with a much higher risk of AMD, an increase in intraocular CFI levels can dampen an over-activated alternative complement pathway and potentially reduce AMD progression.[47] The Phase 1/2 FOCUS study has evaluated the safety and tolerability of subretinal delivery of GT005 in patients with GA. Dose escalation in cohorts 1 to 3 have completed dosing *via* transvitreal delivery, while in the dose expansion in cohort 4, recruitment is still ongoing. Cohorts 5 to 7 will receive gene therapy through the Orbit Subretinal Delivery System (Gyroscope Therapeutics).[47] Interim results from cohorts 1 to 4 revealed that GT005 subretinal delivery was well tolerated. Compared with the baseline, there was an average increase in CFI levels by 146%. The first patient who received GT005 had a sustainable CFI increase at 84 weeks post-treatment. In addition, reductions in downstream complement biomarkers were detected. Two Phase 2 studies, EXPLORE and HORIZON, actively enroll patients to evaluate the safety and efficacy of two doses of GT005 administered as a single subretinal injection, with GA lesion growth measured by Fundus Autofluorescence Photography (FAF) at 48 weeks post-treatment as the primary efficacy endpoint.[48,49]

Factor D protein inhibition in the alterative complement pathway

FCFD4514S (Genentech Inc, USA)

FCFD4514S is a humanized monoclonal antibody against factor D protein in the alternative complement pathway and is also undergoing phase 1 study (NCT 00973011).[50]

C1Q protein inhibition of the complement pathway

ANX007 (Annexon Biosciences)

ANX007 is an antigen-binding fragment of a humanized recombinant monoclonal antibody. ANX007 can bind to the C1q component to block the downstream signaling of the classical complement cascade. Safety and efficacy data from two Phase 1 studies in primary open-angle glaucoma patients are promising. The Phase 2 ARCHER (NCT04656561) study is active and investigating the efficacy of intravitreal injections with ANX007 for GA patients. The sample size for this study is 240 individuals randomly assigned to monthly or every-other-month intravitreal injections with 5 mg ANX007 or sham therapy for 12 months, followed by 6 months in the off-treatment phase. The primary efficacy endpoint is the change in the GA lesion area.[51,52]

High-temperature requirement A1 (HTRA1) inhibition

FHTR2163 (Genentech)

FHTR2163 is an antigen-binding fragment of a humanized monoclonal antibody against the A1 protein. A single nucleotide polymorphism is associated with increased levels of HTRA1 protein, which confers a risk of dry AMD by 49.3%. In the Phase 1 study, the drug molecule was tolerated well with no dose-limiting toxicity, while currently, the Phase 2 GALLEGO study is underway to evaluate the efficacy of intravitreal injections with 20 mg FHTR2163 every 4 or 8 weeks over 76 weeks. The primary efficacy endpoint measures the GA lesion growth area from baseline to 72 weeks using fundus autofluorescence imaging.[53]

Vitamin A aggregates formation inhibitors

ALK-001 (Alkeus Pharmaceuticals)

ALK-001 is a chemically modified vitamin A and can prevent the formation of toxic vitamin A aggregates, reducing the accumulation of debris in the RPE. The results of the Phase III study are awaited and will help us to evaluate the efficacy of this potential drug molecule in inhibiting the growth rate of GA lesions.[31,54,55]

Miscellaneous therapies

Photobiomodulation therapy (PBM)

PBM is a light-based technology that stimulates bioenergetic output in targeted tissues. Selected wavelengths of light in the far red to near-infrared spectrum (500–1,000 nm) can modulate biological function through direct and indirect cellular effects on mitochondrial respiratory chain components. PBM activation of photoacceptors in the mitochondria improves the generation of adenosine triphosphate (ATP), modulates the production of intracellular signaling molecules, such as reactive oxygen species and nitric oxide, and triggers secondary effects that produce sustainable changes in cell function and viability. The beneficial cellular effects can be observed only with the appropriate selection of wavelength, dose, timing, and delivery of PBM treatment.[56]

Emixustat (ACU-4429, Acucela Inc.)

Emixustat is a small molecule visual cycle modulator formulated as emixustat hydrochloride. This is the first oral drug that delays the retinal disease process. Emixustat was developed by British-American chemist Ian L. Scott and is undergoing Phase 3 trials for dry AMD. The toxic byproduct, N-retinylidene-N-retinylethanolamine (A2E), is a major chromophore in lipofuscin, formed from the release of all-trans-retinol within the outer segment of human photoreceptors. A2E leads to the formation of singlet oxygen radicals on exposure to high-energy light and oxygen. Emixustat hydrochloride is a synthetic small molecule non-retinoid designed to stop the visual cycle by inhibiting the formation of 11-cis-retinal. Emixustat hydrochloride binds to RPE-65 and prevents the isomerohydrolase reaction. Without 11-cis-retinal, the rod photoreceptor cells do not produce all-trans-retinol and A2E. A placebo-controlled Phase 1b RCT has shown the safety and tolerability of treatment with emixustat (5, 10, 20, 30, or 40 mg) daily for 14 days in healthy volunteers.[57,58]

Rheopheresis

AMD is considered to be mediated by the disturbance in the micro-circulation of the retina at a cellular and molecular level. Rheopheresis is a type of therapeutic plasmapheresis-like procedure that is safe and effective in treating retinal microcirculatory disorders of the retina. Rheopheresis can eliminate high molecular weight proteins from human plasma of a defined spectrum. These include many components in the blood (>25 nm or >500 kDa) that are pathophysiologically related to AMD, such as fibrinogen, LDL cholesterol, immune complexes, IgM, von Willebrand factor, and alpha 2 & beta 2 macroglobulin that are associated with increased blood viscosity. The increase in blood viscosity reduces blood flow, especially micro-circulation, with more propensity for blood erythrocytes and thrombocytes to aggregate. A series of Rheopheresis procedures at definite intervals can improve the microcirculation of the retina and help in faster recovery of retinal function. Though it is as yet an unproven therapeutic option under investigation, it has been tested in clinical trials. The most extensive study to assess the effectiveness of Rheopheresis in dry AMD is the Multicenter Investigation of Rheopheresis for

AMD (MIRA-1) trial, which leads the results. Moreover, a larger proportion of treated subjects experienced adverse events that required intervention (24.0%) compared to those receiving placebo (5.8%).[59,60]

Ayurvedic phytopharmaceuticals

Many Rasayana medicines, such as *Tinospora Cordifolia, Cantella Asiatica, Bacopa monnieri, Convolvulus pluricaulis, Ocimum basilicum L., Curcuma Longa L., Acorus Calamus, Glycyrrhiza glabra L*. mentioned in Ayurvedic literature may have a potential role in the age-related degenerative process in cells by telomere lengthening and preventing DNA damage.[61] However, their effect needs to be explored in AMD-related clinical trials.

Strengths and limitations

Our review covers all the unapproved pipeline therapies for dry AMD under investigation. The study discusses the published clinical trial results/interim results related to dry AMD. However, the study has a few limitations. Some of the interventions to treat dry AMD are still under investigation, and results are not updated in the public domain. Hence, we have not discussed these results in detail, although their mechanisms are well described as an investigational therapy. BVCA is the most common primary endpoint used in many clinical trials, but it may fail to diagnose foveal-sparing GA. Moreover, the review mainly narrates the clinical development phase, and describing all the pre-clinical development part of a new molecular/chemical entity does not fall under the scope of this review.

Future directions

GA is an irreversible or decompensated stage of dry AMD and has no successful treatment. Stem cell-based therapy (embryonic stem cell-derived and induced pluripotent stem cells) remains under investigation to rejuvenate the degraded photoreceptor cells, but it faces challenges such as immune rejection, non-desired cellular differentiation, and tumor formation. BCVA is a gold standard measure to evaluate the visual function and most accepted endpoints to test the efficacy of treatment. However, fovea-sparing GA is often missed in the early stages. Recent technologies to assess visual function, like microperimetry, color fundus photography, fundus autofluorescence, optical coherence tomography, multifocal electroretinography, low luminance visual acuity, reading speed, and contrast sensitivity, are the most sensitive methods to check the visual function, even in a patient with foveal sparing GA using the preserved BCVA. With advancing drug delivery technology, disease progression monitoring, and better safety and efficacious treatment, the treatment of armamentarium for dry AMD will expand.

Conclusions

There is a need to explore promising therapeutic targets and treatment options for dry AMD or GA. Furthermore, early and accurate diagnosis may aid in initiating treatment before disease progression. Genetics and environmental factors may also help researchers better understand the pathogenesis of dry AMD.

Acknowledgments

None.

Funding

None.

Conflict of interest

The authors have no conflicts of interest related to this publication.

Author contributions

Conceptualization, review of literature, and manuscript drafting (MM, RM, SZ, and ST); manuscript editing and reviewing (RM). All authors have made a significant contribution to this study and have approved the submission of the final manuscript (MM, RM, SZ, and ST).

References

[1] Gehrs KM, Anderson DH, Johnson LV, Hageman GS. Age-related macular degeneration—emerging pathogenetic and therapeutic concepts. Ann Med 2006;38(7):450–471. doi:10.1080/07853890600946724, PMID:17101537.

[2] Ayoub T, Patel N. Age-related macular degeneration. J R Soc Med 2009;102(2):56–61. doi:10.1258/jrsm.2009.080298, PMID:19208869.

[3] Ferris FL 3rd, Fine SL, Hyman L. Age-related macular degeneration and blindness due to neovascular maculopathy. Arch Ophthalmol 1984;102(11):1640–1642. doi:10.1001/archopht.1984.01040031330019, PMID:6208888.

[4] Schmitz-Valckenberg S, Sadda S, Staurenghi G, Chew EY, Fleckenstein M, Holz FG, *et al*. GEOGRAPHIC ATROPHY: Semantic Considerations and Literature Review. Retina 2016;36(12):2250–2264. doi:10.1097/IAE.0000000000001258, PMID:27552292.

[5] Boyer DS, Schmidt-Erfurth U, van Lookeren Campagne M, Henry EC, Brittain C. THE PATHOPHYSIOLOGY OF GEOGRAPHIC ATROPHY SECONDARY TO AGE-RELATED MACULAR DEGENERATION AND THE COMPLEMENT PATHWAY AS A THERAPEUTIC TARGET. Retina 2017;37(5):819–835. doi:10.1097/IAE.0000000000001392, PMID:27902638.

[6] Tezel TH, Bora NS, Kaplan HJ. Pathogenesis of age-related macular degeneration. Trends Mol Med 2004;10(9):417–420. doi:10.1016/j.molmed.2004.07.004, PMID:15350892.

[7] Fleckenstein M, Mitchell P, Freund KB, Sadda S, Holz FG, Brittain C, *et al*. The Progression of Geographic Atrophy Secondary to Age-Related Macular Degeneration. Ophthalmology 2018;125(3):369–390. doi:10.1016/j.ophtha.2017.08.038, PMID:29110945.

[8] Fliesler SJ, Anderson RE. Chemistry and metabolism of lipids in the vertebrate retina. Prog Lipid Res 1983;22(2):79–131. doi:10.1016/0163-7827(83)90004-8, PMID:6348799.

[9] Zarbin MA. Current concepts in the pathogenesis of age-related macular degeneration. Arch Ophthalmol 2004;122(4):598–614. doi:10.1001/archopht.122.4.598, PMID:15078679.

[10] Holz FG, Bellman C, Staudt S, Schütt F, Völcker HE. Fundus autofluorescence and development of geographic atrophy in age-related macular degeneration. Invest Ophthalmol Vis Sci 2001;42(5):1051–1056. PMID:11274085.

[11] Radu RA, Hu J, Yuan Q, Welch DL, Makshanoff J, Lloyd M, *et al*. Complement system dysregulation and inflammation in the retinal pigment epithelium of a mouse model for Stargardt macular degeneration. J Biol Chem 2011;286(21):18593–18601. doi:10.1074/jbc.M110.191866, PMID:21464132.

[12] Ding JD, Lin J, Mace BE, Herrmann R, Sullivan P, Bowes Rickman C. Targeting age-related macular degeneration with Alzheimer's disease based immunotherapies: anti-amyloid-beta antibody attenuates pathologies in an age-related macular degeneration mouse model. Vision Res 2008;48(3):339–345. doi:10.1016/j.visres.2007.07.025, PMID:17888483.

[13] Baumal CR. Wet age-related macular degeneration: treatment advances to reduce the injection burden. Am J Manag Care 2020;26(5 Suppl):S103–S111. doi:10.37765/ajmc.2020.43435, PMID:32479026.

[14] Damico FM, Gasparin F, Scolari MR, Pedral LS, Takahashi BS. New approaches and potential treatments for dry age-related macular degeneration. Arq Bras Oftalmol 2012;75(1):71–76. doi:10.1590/s0004-27492012000100016, PMID:22552424.
[15] Faktorovich EG, Steinberg RH, Yasumura D, Matthes MT, LaVail MM. Photoreceptor degeneration in inherited retinal dystrophy delayed by basic fibroblast growth factor. Nature 1990;347(6288):83–86. doi:10.1038/347083a0, PMID:2168521.
[16] LaVail MM, Yasumura D, Matthes MT, Lau-Villacorta C, Unoki K, Sung CH, Steinberg RH. Protection of mouse photoreceptors by survival factors in retinal degenerations. Invest Ophthalmol Vis Sci 1998;39(3):592–602. PMID:9501871.
[17] Tao W, Wen R, Goddard MB, Sherman SD, O'Rourke PJ, Stabila PF, *et al*. Encapsulated cell-based delivery of CNTF reduces photoreceptor degeneration in animal models of retinitis pigmentosa. Invest Ophthalmol Vis Sci 2002;43(10):3292–3298. PMID:12356837.
[18] LaVail MM, Unoki K, Yasumura D, Matthes MT, Yancopoulos GD, Steinberg RH. Multiple growth factors, cytokines, and neurotrophins rescue photoreceptors from the damaging effects of constant light. Proc Natl Acad Sci U S A 1992;89(23):11249–11253. doi:10.1073/pnas.89.23.11249, PMID:1454803.
[19] Tatton W, Chen D, Chalmers-Redman R, Wheeler L, Nixon R, Tatton N. Hypothesis for a common basis for neuroprotection in glaucoma and Alzheimer's disease: anti-apoptosis by alpha-2-adrenergic receptor activation. Surv Ophthalmol 2003;48(Suppl 1):S25–S37. doi:10.1016/s0039-6257(03)00005-5, PMID:12852432.
[20] Donello JE, Padillo EU, Webster ML, Wheeler LA, Gil DW. alpha(2)-Adrenoceptor agonists inhibit vitreal glutamate and aspartate accumulation and preserve retinal function after transient ischemia. J Pharmacol Exp Ther 2001;296(1):216–223. PMID:11123383.
[21] Collier RJ, Wang Y, Smith SS, Martin E, Ornberg R, Rhoades K, *et al*. Complement deposition and microglial activation in the outer retina in light-induced retinopathy: inhibition by a 5-HT1A agonist. Invest Ophthalmol Vis Sci 2011;52(11):8108–8116. doi:10.1167/iovs.10-6418, PMID:21467172.
[22] Yong VW. Differential mechanisms of action of interferon-beta and glatiramer aetate in MS. Neurology 2002;59(6):802–808. doi:10.1212/wnl.59.6.802, PMID:12349849.
[23] Landa G, Butovsky O, Shoshani J, Schwartz M, Pollack A. Weekly vaccination with Copaxone (glatiramer acetate) as a potential therapy for dry age-related macular degeneration. Curr Eye Res 2008;33(11):1011–1013. doi:10.1080/02713680802484637, PMID:19085384.
[24] Landa G, Rosen RB, Patel A, Lima VC, Tai KW, Perez VR, *et al*. Qualitative spectral OCT/SLO analysis of drusen change in dry age-related macular degeneration patients treated with Copaxone. J Ocul Pharmacol Ther 2011;27(1):77–82. doi:10.1089/jop.2010.0109, PMID:21254921.
[25] Ding JD, Johnson LV, Herrmann R, Farsiu S, Smith SG, Groelle M, *et al*. Anti-amyloid therapy protects against retinal pigmented epithelium damage and vision loss in a model of age-related macular degeneration. Proc Natl Acad Sci U S A 2011;108(28):E279–E287. doi:10.1073/pnas.1100901108, PMID:21690377.
[26] Chew EY, Clemons TE, Agrón E, Launer LJ, Grodstein F, Bernstein PS, *et al*. Effect of Omega-3 Fatty Acids, Lutein/Zeaxanthin, or Other Nutrient Supplementation on Cognitive Function: The AREDS2 Randomized Clinical Trial. JAMA 2015;314(8):791–801. doi:10.1001/jama.2015.9677, PMID:26305649.
[27] Chew EY, Clemons T, SanGiovanni JP, Danis R, Domalpally A, McBee W, *et al*. The Age-Related Eye Disease Study 2 (AREDS2): study design and baseline characteristics (AREDS2 report number 1). Ophthalmology 2012;119(11):2282–2289. doi:10.1016/j.ophtha.2012.05.027, PMID:22840421.
[28] Bavik C, Henry SH, Zhang Y, Mitts K, McGinn T, Budzynski E, *et al*. Visual Cycle Modulation as an Approach toward Preservation of Retinal Integrity. PLoS One 2015;10(5):e0124940. doi:10.1371/journal.pone.0124940, PMID:25970164.
[29] Di Paolo D, Pastorino F, Zuccari G, Caffa I, Loi M, Marimpietri D, *et al*. Enhanced anti-tumor and anti-angiogenic efficacy of a novel liposomal fenretinide on human neuroblastoma. J Control Release 2013;170(3):445–451. doi:10.1016/j.jconrel.2013.06.015, PMID:23792118.
[30] Mata NL, Lichter JB, Vogel R, Han Y, Bui TV, Singerman LJ. Investigation of oral fenretinide for treatment of geographic atrophy in age-related macular degeneration. Retina 2013;33(3):498–507. doi:10.1097/IAE.0b013e318265801d, PMID:23023528.
[31] Cabral de Guimaraes TA, Daich Varela M, Georgiou M, Michaelides M. Treatments for dry age-related macular degeneration: therapeutic avenues, clinical trials and future directions. Br J Ophthalmol 2022;106(3):297–304. doi:10.1136/bjophthalmol-2020-318452, PMID:33741584.
[32] Banin E, Barak A, Boyer DS, Do DV, Ehrlich R, Jaouni T, *et al*. Phase I/IIa Clinical Trial of Human Embryonic Stem Cell (hESC)-Derived Retinal Pigmented Epithelium (RPE, OpRegen) Transplantation in Advanced Dry Form Age-Related Macular Degeneration (AMD): Interim Results. Invest Ophthalmol Vis Sci 2019;60(9):6402.
[33] Cho SM, Lee J, Lee HB, Choi HJ, Ryu JE, Lee HJ, *et al*. Subretinal transplantation of human embryonic stem cell-derived retinal pigment epithelium (MA09-hRPE): A safety and tolerability evaluation in minipigs. Regul Toxicol Pharmacol 2019;106:7–14. doi:10.1016/j.yrtph.2019.04.006, PMID:31009651.
[34] Oner A, Gonen ZB, Sevim DG, Smim Kahraman N, Unlu M. Suprachoroidal Adipose Tissue-Derived Mesenchymal Stem Cell Implantation in Patients with Dry-Type Age-Related Macular Degeneration and Stargardt's Macular Dystrophy: 6-Month Follow-Up Results of a Phase 2 Study. Cell Reprogram 2018;20(6):329–336. doi:10.1089/cell.2018.0045, PMID:31251672.
[35] Kahraman NS, Gonen ZB, Sevim DG, Oner A. First Year Results of Suprachoroidal Adipose Tissue Derived Mesenchymal Stem Cell Implantation in Degenerative Macular Diseases. Int J Stem Cells 2021;14(1):47–57. doi:10.15283/ijsc20025, PMID:33122468.
[36] Kumar A, Midha N, Mohanty S, Chohan A, Seth T, Gogia V, *et al*. Evaluating role of bone marrow-derived stem cells in dry age-related macular degeneration using multifocal electroretinogram and fundus autofluorescence imaging. Int J Ophthalmol 2017;10(10):1552–1558. doi:10.18240/ijo.2017.10.12, PMID:29062775.
[37] Mead B, Berry M, Logan A, Scott RA, Leadbeater W, Scheven BA. Stem cell treatment of degenerative eye disease. Stem Cell Res 2015;14(3):243–257. doi:10.1016/j.scr.2015.02.003, PMID:25752437.
[38] Liao DS, Metapally R, Joshi P. Pegcetacoplan treatment for geographic atrophy due to age-related macular degeneration: a plain language summary of the FILLY study. Immunotherapy 2022;14(13):995–1006. doi:10.2217/imt-2022-0078, PMID:35860926.
[39] Liao DS, Grossi FV, El Mehdi D, Gerber MR, Brown DM, Heier JS, *et al*. Complement C3 Inhibitor Pegcetacoplan for Geographic Atrophy Secondary to Age-Related Macular Degeneration: A Randomized Phase 2 Trial. Ophthalmology 2020;127(2):186–195. doi:10.1016/j.ophtha.2019.07.011, PMID:31474439.
[40] Qin S, Dong N, Yang M, Wang J, Feng X, Wang Y. Complement Inhibitors in Age-Related Macular Degeneration: A Potential Therapeutic Option. J Immunol Res 2021;2021:9945725. doi:10.1155/2021/9945725, PMID:34368372.
[41] Ricklin D, Lambris JD. Complement-targeted therapeutics. Nat Biotechnol 2007;Nov25(11):1265–1275. doi:10.1038/nbt1342, PMID:17989689.
[42] Jaffe GJ, Westby K, Csaky KG, Monés J, Pearlman JA, Patel SS, *et al*. C5 Inhibitor Avacincaptad Pegol for Geographic Atrophy Due to Age-Related Macular Degeneration: A Randomized Pivotal Phase 2/3 Trial. Ophthalmology 2021;128(4):576–586. doi:10.1016/j.ophtha.2020.08.027, PMID:32882310.
[43] Armento A, Ueffing M, Clark SJ. The complement system in age-related macular degeneration. Cell Mol Life Sci 2021;78(10):4487–4505. doi:10.1007/s00018-021-03796-9, PMID:33751148.
[44] Yehoshua Z, de Amorim Garcia Filho CA, Nunes RP, Gregori G, Penha FM, Moshfeghi AA, *et al*. Systemic complement inhibition with eculizumab for geographic atrophy in age-related macular degeneration: the COMPLETE study. Ophthalmology 2014;121(3):693–701. doi:10.1016/j.ophtha.2013.09.044, PMID:24289920.
[45] Taskintuna I, Elsayed ME, Schatz P. Update on Clinical Trials in Dry Age-related Macular Degeneration. Middle East Afr J Ophthalmol 2016;23(1):13–26. doi:10.4103/0974-9233.173134, PMID:26957835.
[46] Ramlogan-Steel CA, Murali A, Andrzejewski S, Dhungel B, Steel

JC, Layton CJ. Gene therapy and the adeno-associated virus in the treatment of genetic and acquired ophthalmic diseases in humans: Trials, future directions and safety considerations. Clin Exp Ophthalmol 2019;47(4):521–536. doi:10.1111/ceo.13416, PMID: 30345694.

[47] clinicaltrials.gov [Internet]. First in human study to evaluate the safety and efficacy of GT005 administered in subjects with dry AMD. Available from: https://clinicaltrials.gov/ct2/show/NCT03846193. Accessed July 1, 2022.

[48] clinicaltrials.gov [Internet]. EXPLORE: a phase II study to evaluate the safety and efficacy of two doses of GT005 (EXPLORE). ClinicalTrials.gov. Available from: https://clinicaltrials.gov/ct2/show/NCT04437368. Accessed July 1, 2022.

[49] clinicaltrials.gov [Internet]. HORIZON: a phase II study to evaluate the safety and efficacy of two doses of GT005. ClinicalTrials.gov. Available from: https://clinicaltrials.gov/ct2/show/NCT04566445. Accessed July 1, 2022.

[50] Katschke KJ Jr, Wu P, Ganesan R, Kelley RF, Mathieu MA, Hass PE, *et al*. Inhibiting alternative pathway complement activation by targeting the factor D exosite. J Biol Chem 2012;287(16):12886–12892. doi:10.1074/jbc.M112.345082, PMID:22362762.

[51] Kawa MP, Machalinska A, Roginska D, Machalinski B. Complement system in pathogenesis of AMD: dual player in degeneration and protection of retinal tissue. J Immunol Res 2014;2014:483960. doi:10.1155/2014/483960, PMID:25276841.

[52] Desai D, Dugel PU. Complement cascade inhibition in geographic atrophy: a review. Eye (Lond) 2022;36(2):294–302. doi:10.1038/s41433-021-01765-x, PMID:34999723.

[53] Khanani AM, Hershberger VS, Pieramici DJ, Khurana RN, Brunstein F, Ma L, *et al*. Phase 1 Study of the Anti-HtrA1 Antibody-binding Fragment FHTR2163 in Geographic Atrophy Secondary to Age-related Macular Degeneration. Am J Ophthalmol 2021;232:49–57. doi:10.1016/j.ajo.2021.06.017, PMID:34214452.

[54] Zhang D, Mihai DM, Washington I. Vitamin A cycle byproducts explain retinal damage and molecular changes thought to initiate retinal degeneration. Biol Open 2021;10(11):bio058600. doi:10.1242/bio.058600, PMID:34842275.

[55] Rubner R, Li KV, Canto-Soler MV. Progress of clinical therapies for dry age-related macular degeneration. Int J Ophthalmol 2022;15(1):157–166. doi:10.18240/ijo.2022.01.23, PMID:35047371.

[56] Merry GF, Munk MR, Dotson RS, Walker MG, Devenyi RG. Photobiomodulation reduces drusen volume and improves visual acuity and contrast sensitivity in dry age-related macular degeneration. Acta Ophthalmol 2017;95(4):e270–e277. doi:10.1111/aos.13354, PMID: 27989012.

[57] Dugel PU, Novack RL, Csaky KG, Richmond PP, Birch DG, Kubota R. Phase ii, randomized, placebo-controlled, 90-day study of emixustat hydrochloride in geographic atrophy associated with dry age-related macular degeneration. Retina 2015;35(6):1173–1183. doi:10.1097/IAE.0000000000000606, PMID:25932553.

[58] Rosenfeld PJ, Dugel PU, Holz FG, Heier JS, Pearlman JA, Novack RL, *et al*. Emixustat Hydrochloride for Geographic Atrophy Secondary to Age-Related Macular Degeneration: A Randomized Clinical Trial. Ophthalmology 2018;125(10):1556–1567. doi:10.1016/j.ophtha.2018.03.059, PMID:29716784.

[59] Koss MJ, Kurz P, Tsobanelis T, Lehmacher W, Fassbender C, Klingel R, *et al*. Prospective, randomized, controlled clinical study evaluating the efficacy of Rheopheresis for dry age-related macular degeneration. Dry AMD treatment with Rheopheresis Trial-ART. Graefes Arch Clin Exp Ophthalmol 2009;247(10):1297–1306. doi:10.1007/s00417-009-1113-7, PMID:19629514.

[60] Pulido J, Sanders D, Winters JL, Klingel R. Clinical outcomes and mechanism of action for rheopheresis treatment of age-related macular degeneration (AMD). J Clin Apher 2005;20(3):185–194. doi:10.1002/jca.20047, PMID:15892078.

[61] Sharma R, Martins N. Telomeres, DNA Damage and Ageing: Potential Leads from Ayurvedic Rasayana (Anti-Ageing) Drugs. J Clin Med 2020;9(8):E2544. doi:10.3390/jcm9082544, PMID:32781627.

Journal of Exploratory Research in Pharmacology **2023** vol. 8(2) | 140–154
DOI: 10.14218/JERP.2022.00043

Original Article

Generic Solving of Physiologically-based Kinetic Models in Support of Next Generation Risk Assessment Due to Chemicals

Sandrine Charles[1*], Ophelia Gestin[1,2,3], Jérémie Bruset[1], Dominique Lamonica[1], Virgile Baudrot[4], Arnaud Chaumot[2], Olivier Geffard[2], Thomas Lacoue-Labarthe[3] and Christelle Lopes[1]

[1]University of Lyon, University Lyon 1, UMR CNRS 5558, Villeurbanne, France; [2]INRAE, Riverly, Ecotoxicology, Lyon, France; [3]University of La Rochelle, UMRi 7266, La Rochelle, France; [4]Qonfluens, Rdpt Benjamin Franklin, Montpellier, France

Received: May 16, 2022 | **Revised:** June 19, 2022 | **Accepted:** July 06, 2022 | **Published online:** September 29, 2022

Abstract

Background and objectives: Increasing confidence in using *in vitro* and *in silico* model-based data to aid the chemical risk assessment process is one of the most significant challenges faced by regulatory authorities. A crucial concern is taking full advantage of scientifically valid physiologically-based kinetic (PBK) models. The present study aims to present a very innovative solution of a fully generic PBK model written as a set of ordinary differential equations (ODE).

Methods: This study proposes an innovative and unified modeling framework for writing PBK equations as matrix ODE and their solutions, expressed with matrix products. This generic PBK solution considers as many state variables as needed to quantify chemical absorption, distribution, metabolism, and excretion processes within living organisms when exposed to chemical substances.

Results: We first introduce our PBK modeling framework, with all the intermediate steps from the matrix ODE to the exact solution. Then we apply this framework to bioaccumulation testing before illustrating its concrete use through complementary case studies regarding species, compounds, and model complexity.

Conclusions: This generic PBK model makes it possible for any compartmentalization to be considered, as well as all appropriate interconnections between compartments and with the external medium.

Introduction

Physiologically-based kinetic (PBK) models encompass both physiologically-based pharmaco-kinetic and physiologically-based (eco-) toxico-kinetic models depending on the context.[1,2] Hence, PBK models can refer either to therapeutic drug development[3] or environmental risk assessment.[4–6] All PBK models are compartment models employing ordinary differential equations (ODE) to quantify chemical absorption, distribution, metabolism (*i.e.*, biotransformation), and excretion processes within living organisms when exposed to chemical substances.[7,8] One fundamental aspect of PBK model complexity is the degree of compartmentalization (*i.e.*, differentiation of an organism into various tissues or organs).[9,10] This complexity translates into a high number of parameters usually valued from literature information or expert knowledge. Consequently, most PBK models have purely predictive usages, for example, for human health assessments where novel experiments are very limited, even impossible.[11] Nevertheless, recent advances

Keywords: Pharmacokinetics; Toxicokinetics; General unified modelling framework; Bioaccumulation; Chemical exposure.

Abbreviations: As, arsenic; Cd, cadmium; ODE, ordinary differential equation; PBK model, physiologically-based kinetic model; t_c, duration of the accumulation phase.

***Correspondence to:** Sandrine Charles, University of Lyon, University Lyon 1, UMR CNRS 5558, Villeurbanne 69100, France. ORCID: https://orcid.org/0000-0003-4604-0166. Tel: +33 (0)4 7243 2900, E-mail: sandrine.charles@univ-lyon1.fr

How to cite this article: Charles S, Gestin O, Bruset J, Lamonica D, Baudrot V, Chaumot A, *et al*. Generic Solving of Physiologically-based Kinetic Models in Support of Next Generation Risk Assessment Due to Chemicals. *J Explor Res Pharmacol* 2023;8(2):140–154. doi: 10.14218/JERP.2022.00043.

in the development of Bayesian inference tools make it possible to deal with complex models[12–15] even with sparse data sets, which opens up new possibilities for PBK models to obtain parameter estimates associated with their uncertainties and to propagate this information to model-informed predictions. Also, as part of new approach methodologies , PBK models as well as *in vitro-in vivo* extrapolation approaches can be combined with bioactivity data, all of this helping prioritize thousands of "data poor" chemicals in human health risk assessment.[10,16]

Relying *a priori* on the anatomical and physiological structure of the body, PBK model compartments usually correspond to target organs or tissues, possibly all interconnected and related to the external exposure medium. However, many PBK models only relate organs or tissues to blood or lymph, with only one or two organs or tissues linked to the external medium.[17,18] Unfortunately, such simplifications of PBK models are often justified based on technical bases rather than physiological ones. All PBK models are written as coupled ODE whose parameters correspond to fluxes between compartments, for which information is partly available in the scientific literature. The general tendency to develop more complex models to include as many physiological processes as possible, and the current computational capacities, may give the impression that the most complex models will be the most efficient. Nevertheless, with increasing parameters to calibrate, such complex models may be avoided in favor of balancing complexity and simplicity. Current regulatory documents for assessing the bioaccumulation of chemicals in organisms usually only require simple one-compartment models,[19–23] even if it is now recognized that it is necessary to also consider internal concentrations within target organs in order to fully capture the chemical bioaccumulation behavior, the specific role of organs, and the dynamics of toxic effects.[24]

Multi-compartment models sometimes reveal the necessary, for example, to finely decipher the internal contamination routes of specific chemical compounds causing damage to only specific organs.[25–27] Additionally, PBK models can be crucial to predicting organ-level concentration-time profiles in a situation where animal testing is now prohibited, using PBK model information from one chemical substance to inform the development or evaluation of a PBK model for a similar chemical substance.[3] In the perspective to enlarge and facilitate the use of PBK models, namely to include more compartments, to better estimate parameter values from data, and to better support a fine deciphering of underlying contamination processes after chemical exposure, there is today a clear need for user-friendly tools. From an automatized implementation, fully transparent and reproducible, such tools should simplify the use of any PBK models, preventing users from investing in technicalities, whatever the required number of compartments to consider physiologically, whatever the number of connections to account for between compartments in pairs or between compartments and the external medium, and whatever the species-compound combination of interest. Such tools seem the only way to gradually achieve greater acceptability of complex PBK models, even in a regulatory context.[10,28]

Capitalizing on recent publications on TK models,[15,22] we present in this paper a very innovative solution of a fully generic PBK model written as a set of ODE. Benefiting from an exact solution is a tremendous advantage in numerical implementation. Indeed, it avoids discretizing ODE as there is no more numerical approximation. The solution is directly used for the inference process and the subsequent simulations. The gain in calculation time is enormous (more than 100-fold), associated with fair use of computer resources. Moreover, the new modeling framework we propose makes it possible to account for an infinite number of compartments, with all possible connections between pairs of compartments and between compartments and the exposure medium, independently of the investigated species or chemical substance. Indeed, we found a particularly condensed way to write a linear ODE system, which is typical of PBK models, thus allowing us to fully and exactly solve the ODE system to write an exact generic solution. This exact solution is fascinating when estimating many parameters related to many state variables, for which experimental data may be sparse, with few replicates and high variability.

In the methods, we first detail our generic modeling framework, together with notations of parameters and variables, providing the generic solution at the end of section 2. Then, the generic modeling framework is applied to the particular context of bioaccumulating chemical substances within organisms. We detail how to write the ODE system for both accumulation and depuration phases of standard bioaccumulation tests and then how to get the final generic solution to simulate internal concentrations over time from parameter estimates. Results presents four different situations where simulations were useful to predict what happens within organs and/or tissues according to the species under consideration and the chemical substance to which it is exposed. These case studies were chosen from the literature to be diverse and complementary in terms of questions that a PBK model can help to investigate. We thus present two case studies for the species *Gammarus fossarum* exposed to cadmium, for which internal concentrations have been measured within four organs: one case study with one-compartment PBK models for each organ considered separately; the other case study with a four-compartment PBK model. These case studies illustrate the added value of considering one single four-compartment model rather than four one-compartment models for each organ. The third case study concerns the sea cucumber exposed to six different antibiotics. Furthermore, the fourth case study concerns the species *Danio rerio* exposed to arsenic, whose bioaccumulation process is described with a six organ-based compartment PBK model.

Materials and methods

Generic modeling framework

Biologists often expect an exhaustive description of the phenomenon they are studying. In the same way, mathematicians will want to use the most sophisticated methods they know. However, all models are inherently wrong; only some of them will prove helpful.[29] As a consequence, the modeler should position between these two points of view to be efficient. Such a position is known as the *parsimony principle* by which the simplest model that adequately explains the data should be used; it was proposed in the 14th century by William of Ockam, an English Franciscan friar, scholastic philosopher, and theologian.[30] In its general form, the parsimony principle, also referred to as Occam's Razor, states that the simplest of competing explanations is the most likely to be correct. In model fitting, the simplest model providing a good fit will be preferred over a more complex one. The compromise is thus between the good description of the observed data and simplicity.

In this spirit, the most generic PBK models will rely on simplifying hypotheses to decipher enough internal mechanisms under chemical exposure and remain mathematically reasonable to be easily manipulated. Below is a non-prioritized short list of the most current hypotheses: (i) the exposure concentra-

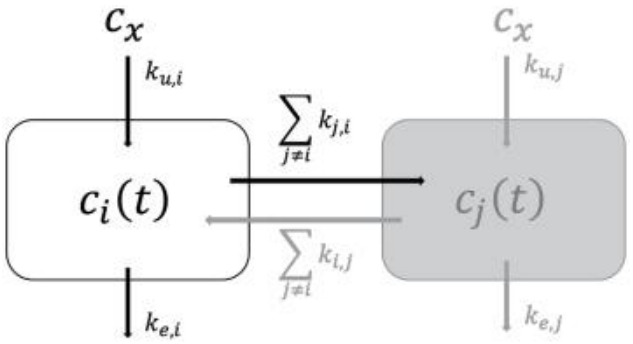

Fig. 1. Generic scheme of a multi-compartments physiologically-based kinetic model connecting *n* compartments two-by-two and each of them to the external medium at exposure concentration c_x ($i, j \in [1;n]$). Refer to Table 1 for names, meanings, and units of variables and parameters.

tion is assumed constant over time; (ii) there can be any number of compartments in direct relation with any number of tissues and organs that are needed to consider on a biological point of view; (iii) all compartments can be connected two-by-two to all the others; (iv) the exposure contaminant can enter within each compartment; and additionally, (v) all compartments can be theoretically connected to the external medium, the final choice to be based on biological expertise.

From these hypotheses, Figure 1 gives the general schematic representation of exchanges between the external medium and compartments and between compartments themselves. Table 1 gathers all variables and parameters involved in the generic writing of the PBK model and is used in Figure 1.

Mathematical equations of the PBK model

From Figure 1, we can derive the entire system of the ODE describing the dynamics of the multi-compartments model when organisms are exposed to an external constant concentration c_x:

$$\frac{dc_i(t)}{dt} = k_{u,i}c_x - k_{e,i}c_i(t) + \sum_{j\neq i} k_{i,j}C_j(t) - \sum_{j\neq i} k_{j,i}c_i(t) \quad \forall i, j \in [1;n] \tag{1}$$

Names, meanings, and units of variables and parameters are provided in Table 1.

This full system of ODE for *n* compartments all related by pairs (Equation 1) can equivalently be written in a matrix way as follows:

$$\frac{d\mathbf{C}(t)}{dt} = \mathbf{U}c_x + \mathbf{E}\mathbf{C}(t) \tag{2}$$

where vector C(t) gathers all internal concentrations in compartments i at time t, $i \in [1;n]$:

$$\mathbf{C}(t) = \left(c_1(t) \quad c_2(t) \quad \dots \quad c_n(t)\right)^T \tag{3}$$

Vector U contains all uptake rates from the external medium at exposure concentration c_x:

$$\mathbf{U} = \left(k_{u,1} \quad k_{u,2} \quad \dots \quad k_{u,n}\right)^T \tag{4}$$

Matrix **E** gathers both input and output rates between compartments two-by-two, together with the elimination rates from each compartment i, $i \in [1;n]$:

$$\mathbf{E} = \left[e_{ij}\right]_{i,j\in[1;n]} \quad \text{with} \quad \begin{cases} e_{ii} = -k_{e,i} - \sum_{j\neq i} k_{j,i} \\ e_{ij} = k_{i,j} \end{cases} \tag{5}$$

Equation (2) is a matrix ODE system, which is linear with a second member. It can be solved in two steps, as detailed below.

Generic solving the PBK model

The first step is to solve the matrix system (2) without its second member. Then, the second step consists in finding the final general solution using the method of the variation of constant.

Solving the ODE system without the second member

Removing the second member from the matrix ODE system (2) leads to the following system to solve:

$$\frac{d\mathbf{C}_{\mathbf{wosm}}(t)}{dt} = \mathbf{E}\mathbf{C}_{\mathbf{wosm}}(t) \tag{6}$$

With $C_{wosm}(t)$ the desired solution of Equation (6) without a second member (abbreviated by index *wosm*). Using matrix exponential immediately provides the solution:

$$\mathbf{C}_{\mathbf{wosm}}(t) = e^{t\mathbf{E}}\Omega_1 \tag{7}$$

With Ω_1 a vector integration constant ($\in \mathbb{R}^n$), and the following

Table 1. Variable and parameter names, meanings, and units used within the generic PBK model all along this paper

Names	Meaning	Unit
t	time	[t]
n	total number of compartments	#
i, j	Compartment numbers	$i, j \in [1;n]$
c_x	exposure concentration in the external medium	mass per volume
$c_i(t)$	internal concentration in compartment i at time t	mass per weight
$k_{u,i}$	uptake rate from the external medium to compartment i	$[t]^{-1}$
$k_{e,i}$	elimination rate from compartment i to the external medium	$[t]^{-1}$
$k_{i,j}$	input rate from compartment j to compartment i	$[t]^{-1}$
$k_{j,i}$	output rate from compartment j to compartment j	$[t]^{-1}$

The symbol # means dimensionless; [t] stands for a time unit.

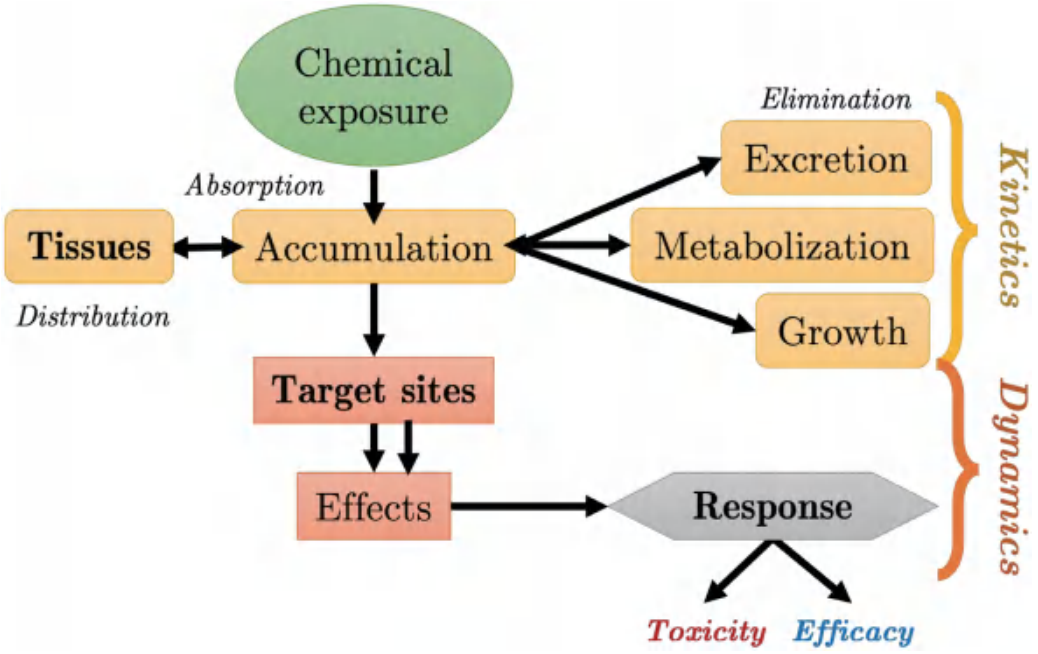

Fig. 2. Absorption, distribution, metabolism, and excretion processes and their relationships with effects and responses within living organisms, leading to toxicity or efficacy depending on the chemical substance they are exposed to.

definition for the matrix exponential:

$$e^{t\mathbf{E}} = \sum_{k=0}^{\infty} \frac{1}{k!} (t\mathbf{E})^k \quad (8)$$

Getting the generic solution for the ODE system

For the second step, including the second member, we used the method of the variation of the constant, starting from the assumption that the final general solution with the second member (abbreviated by index *wsm*) can be written as follows:

$$\mathbf{C}_{\mathbf{wosm}} = e^{t\mathbf{E}} \Omega_1(t) \quad (9)$$

with a vector function $\Omega_1(t)$ to be determined.

Given that the exposure concentration is assumed constant (equal to c_x) in this paper, deriving Equation (9) and replacing terms in Equation (2) leads to the following result:

$$\frac{d\Omega_1(t)}{dt} = e^{-t\mathbf{E}} \mathbf{U} c_x \Leftrightarrow \Omega_1(t) = \left(\int_0^t e^{-\tau\mathbf{E}} d\tau \right) \mathbf{U} c_x + \Omega_2 \quad (10)$$

The final generic solution of Equation (2) will thus write as:

$$\mathbf{C}_{\mathbf{wsm}}(t) = \left(\int_0^t e^{(t-\tau)\mathbf{E}} d\tau \right) \mathbf{U} c_x + e^{t\mathbf{E}} \mathbf{\Omega_2} \quad (11)$$

With $\Omega_2 \in \mathbb{R}^n$ a constant to be determined.

From an initial condition $C_{wsm}(t = 0) = C_0$, we finally get $\Omega_2 = C_0$, which leads to the following final particular solution of Equation (2):

$$\mathbf{C}_{\mathbf{wsm}}(t) = \left(\int_0^t e^{(t-\tau)\mathbf{E}} d\tau \right) \mathbf{U} c_x + e^{t\mathbf{E}} \mathbf{C_0} \quad (12)$$

It remains to calculate the matrix integral to achieve the final solution of the matrix ODE system (2).

Final expression of the PBK solution

As detailed in the Supplementary File 1, and using the definition of a matrix exponential from Equation (8), the matrix integral in Equation (12) can be calculated with the following expression:

$$\int_0^t e^{(t-\tau)\mathbf{E}} d\tau = \left(e^{t\mathbf{E}} - \mathbf{I} \right) \mathbf{E}^{-1} \quad (13)$$

where matrix I is the identity matrix, *i.e.* the ($n \times n$) square matrix with ones on the main diagonal and zeros elsewhere, and $\mathbf{E}^{-1}$ the inverse matrix of **E**.

It can immediately be deduced that the final solution of Equation (12) simplifies as follows:

$$\mathbf{C}_{\mathbf{wsm}}(t) = e^{t\mathbf{E}} \left(\mathbf{E}^{-1} \mathbf{U} c_x + \mathbf{C_0} \right) - \mathbf{E}^{-1} \mathbf{U} c_x \quad (14)$$

In the following sections, we employed this generic expression to go beyond and build generic physiologically-based kinetic models that we applied to different case-studies in the field of toxicology.

Application to bioaccumulation testing

Accumulation and depuration phases

Bioaccumulation is defined as an increase in contaminant concentrations inside living organisms following uptake from the surrounding medium (living media, food, even workplace for humans). Bioaccumulation results from dynamical processes of uptake and elimination that can be modeled with the above ODE system (Equation (2)). The extent to which bioaccumulation occurs within a given species determines the subsequent toxic effects. Hence, a better knowledge of bioaccumulation enables us to assess the risk of exposure to chemicals and to evaluate our ability to control their use and emissions in the field.[31] Bioaccumulation is thus the net result of all uptake and elimination processes by egestion, passive diffusion, metabolization, excretion, and maternal transfer. Concomitantly, the organism's growth modulates the bioaccumulation by diluting

chemical quantities in increasing body or organ mass (Fig. 2).

Bioaccumulation tests are usually mid-to-long term laboratory experiments designed to identify all the potential uptake pathways, including food and waterborne exposure routes.[32] Bioaccumulation tests commonly comprise an accumulation phase followed by a depuration phase.[33] During the accumulation phase, organisms are exposed to a chemical substance of interest. After a specific time (for $t \in [0;t_c]$), with t_c fixed by the experimental design, organisms are transferred to a clean medium for the depuration phase (for $t > t_c$). The concentration of the chemical substance (and of its potential metabolites) within organisms is then measured internally at regular time points during both phases. From an ERA perspective, such data can be used finely to estimate bioaccumulation metrics.[22]

If the bioaccumulation within organisms is widely studied for humans and large animals, namely, fish, birds, and farm animals,[34,35] this is less the case for invertebrates.[36] However, it is equally essential to decipher internal processes at the target organ level in invertebrates. Indeed, profoundly unraveling internal routes of chemical substances between organs after they enter the body is of great interest to better understand mechanisms implied in the subsequent effects on fitness, a phenomenon known as organotropism.[37–39] Among invertebrate species of interest, crustacean amphipods are already recognized as particularly relevant as aquatic biomonitors of trace metals.[36,40–43]

Generic modeling of bioaccumulation

Within this context, the generic ODE system (Equation (2)) may be fully applied to describe, simulate and predict what happens within organs (in terms of internal concentration over time) and between organs (in terms of uptake, elimination, and exchange rates) when an organism is exposed to a given chemical substance. To this end, each organ can be associated with one model compartment, leading to the following equations for both accumulation and depuration phases:

$$\frac{d\mathbf{C_A}(t)}{dt} = \mathbf{U}c_x + \mathbf{E}\mathbf{C_A}(t) \tag{15}$$

Equation (15) is identical to Equation (2), denoting $C_A(t)$ the internal concentration at time t during the accumulation phase.

$$\frac{d\mathbf{C_D}(t)}{dt} = \mathbf{E}\mathbf{C_D}(t) \tag{16}$$

Variable $C_D(t)$ is the internal concentration at time t during the depuration phase. Parameters and variables have the same meaning as given in Table 1.

Regarding the accumulation phase, Equation (15) has a solution directly given by Equation (14), whatever the initial condition equal to $C_A(t = 0) = C_0$.

As a consequence, the generic solution for the accumulation phase writes as follows:

$$\mathbf{C_A}(t) = \left(e^{t\mathbf{E}} - \mathbf{I}\right)\mathbf{E}^{-1}\mathbf{U}c_x + e^{t\mathbf{E}}C_0 \tag{17}$$

Regarding the depuration phase, Equation (16) is similar to Equation (6), with the corresponding generic solution given by Equation (7). The constant vector Ω_1 can be determined from the initial condition of the depuration phase that corresponds to the internal concentration reached at $t = t_c$ at the end of the accumulation phase. We must therefore solve the following equation:

$$\mathbf{C_A}(t_c) = \mathbf{C_D}(t_c) \tag{18}$$

Given solutions from Equations (14) and (7), we get:

$$\mathbf{C_A}(t_c) = \left(e^{t_c\mathbf{E}} - \mathbf{I}\right)\mathbf{E}^{-1}\mathbf{U}c_x + e^{t_c\mathbf{E}}C_0 \quad \text{and} \quad \mathbf{C_D}(t_c) = e^{t_c\mathbf{E}}\Omega_1 \tag{19}$$

Hence, the constant vector Ω_1 derives from the following equation:

$$\begin{aligned}\left(e^{t_c\mathbf{E}} - \mathrm{I}\right)\mathrm{E}^{-1}\mathrm{U}c_x + e^{t\mathbf{E}}C_0 = e^{t_c\mathbf{E}}\Omega_1 \\ \Leftrightarrow \Omega_1 = \left(\mathrm{I} - e^{-t_c\mathbf{E}}\right)\mathrm{E}^{-1}\mathrm{U}c_x + C_0\end{aligned} \tag{20}$$

The generic solution for the depuration phase then writes as follows:

$$\mathbf{C_D}(t) = \left(e^{t\mathbf{E}} - e^{(t-t_c)\mathbf{E}}\right)\mathbf{E}^{-1}\mathbf{U}c_x + e^{t\mathbf{E}}C_0 \tag{21}$$

Results

This section presents four case studies with different numbers of compartments. Two case studies concern the species *Gammarus fossarum* exposed to cadmium (Cd).[27,44] The third one concerns *Apostichopus japonicus* sea cucumber exposed to six different antibiotics;[45] the fourth one concerns species *Danio rerio* exposed to arsenic (As).[46] Gestin and colleagues[27,44] used several one-compartment PBK models compared with one four-compartment PBK model to gain knowledge on the accumulation and fate dynamic of Cd in and between gammarids' organs. Subsections give the generic solutions with median parameter values for this particular case study (Table 2).

Case study with one compartment

Applying Equation (2) with only one compartment leads to two single equations:

$$\begin{cases}\dfrac{dc_{A,i}(t)}{dt} = k_{u,1}c_x - k_{e,1}c_{A,i}(t) \\ \quad \text{when} \quad 0 \leqslant t \leqslant t_c \quad \text{(accumulation phase)} \quad \text{(a)} \\ \dfrac{dc_{D,i}(t)}{dt} = -k_{e,1}c_{D,i}(t) \\ \quad \text{when} \quad t > t_c \quad \text{(depuration phase)} \quad \text{(b)}\end{cases} \tag{22}$$

System of Equations (22a) and (22b) can easily be solved with

Table 2. Medians of parameters estimated by Bayesian inference from TK one-compartment models separately fitted to each organ of *Gammarus fossarum* exposed to dissolved Cd at 11.1 $\mu g \cdot L^{-1}$ for seven days before being placed for 14 days under depuration conditions

Process	Organ	Parameter	Median value (in $[t]^{-1}$)
Uptake	Intestines	$k_{u,1}$	1917
	Caeca	$k_{u,2}$	1571
	Cephalons	$k_{u,3}$	91.1
	Remaining tissues	$k_{u,4}$	135
Elimination	Intestines	$k_{e,1}$	0.506
	Caeca	$k_{e,2}$	0.053
	Cephalons	$k_{e,3}$	0.060
	Remaining tissues	$k_{e,4}$	0.026

Cd, Cadmium; TK, toxicokinetics.

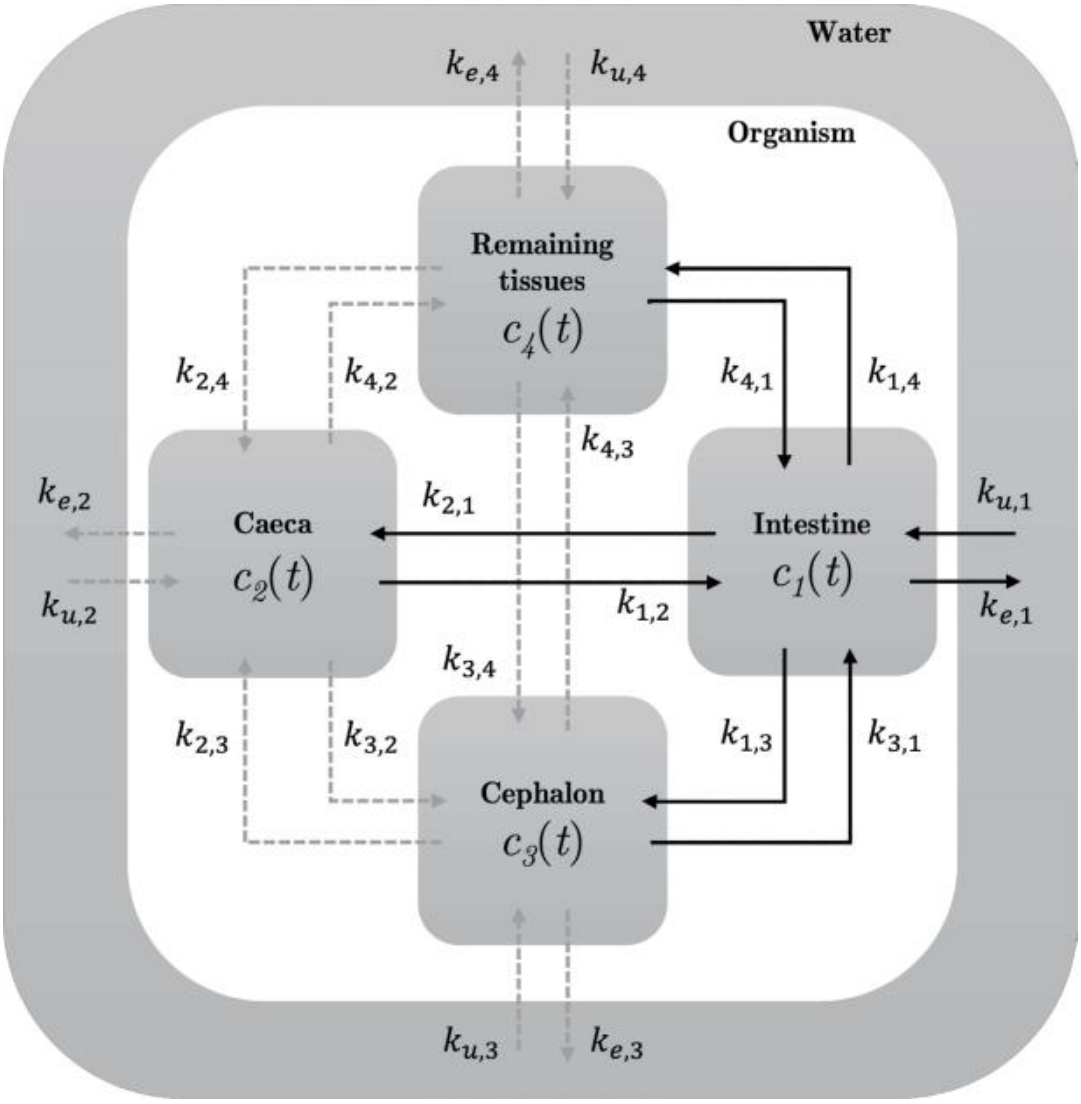

Fig. 3. General scheme of the multi-compartment physiologically-based kinetic model used by [1] at the initial modeling stage when all compartments were connected to each other. Parameter values as given in Table 3.

the method of the separation of variables (also known as the Fourier method), leading to the following system of solutions for both accumulation and depuration phases:

$$\begin{cases} c_{A,i}(t) = \dfrac{k_{u,i}}{k_{e,i}} c_x \left(1 - e^{-k_{e,i}t}\right) \\ \quad \text{when} \quad 0 \leqslant t \leqslant t_c \quad \text{(accumulation phase)} \quad \text{(a)} \\ c_{D,i}(t) = \dfrac{k_{u,i}}{k_{e,i}} c_x \left(e^{k_{e,i}(t_c - t)} - e^{-k_{e,i}t}\right) \\ \quad \text{when} \quad t > t_c \quad \text{(depuration phase)} \quad \text{(b)} \end{cases} \tag{23}$$

Getting the set of solutions (23) directly from the generic expressions given by the combination of both Equations (17) and (21) leads precisely to the same result. Indeed, with one compartment, matrix $\mathbf{E} = -k_{e,i}$ and vector $\mathbf{U} = k_{u,i}$.

Inspired from Gestin *et al*.,[27,44] when considering only solid black arrows, Figure 3 highlights the target organs that can correspond to one compartment according to *i*: intestine ($i = 1$); cephalon ($i = 2$); caeca ($i = 3$); remaining tissues ($i = 4$). Each compartment has its own parameter pair for uptake ($k_{u,i}$) and elimination ($k_{e,i}$) rates (Table 2). Model parameters were estimated under a unified Bayesian framework.[20] In particular, parameters of PBK one-compartment models were fitted separately for each organ of *G. fossarum* exposed to dissolved Cd at 11.1 $\mu g \cdot L^{-1}$ for seven days before being placed for 14 days under depuration conditions. Getting median parameter values as given in Table 2 allows simulating what happens within the intestines when it is connected to all other organs, for example (see Supplementary File 1 for more details).

Case study with four compartments

Applying the general matrix ODE system given by the set of Equations (15) and (16) to the particular case of four compartments connected by pairs (Fig. 3) leads to the following writing:

$$\begin{cases} \dfrac{d\mathbf{C_A}(t)}{dt} = \mathbf{U}c_x + \mathbf{E}\mathbf{C_A}(t) \\ \quad \text{when} \quad 0 \leqslant t \leqslant t_c \quad \text{(accumulation phase)} \quad \text{(a)} \\ \dfrac{d\mathbf{C_D}(t)}{dt} = \mathbf{E}\mathbf{C_D}(t) \\ \quad \text{when} \quad t > t_c \quad \text{(depuration phase)} \quad \text{(b)} \end{cases} \tag{24}$$

with vectors and matrices defined as follows:

$$\mathbf{C_A}(t) = \mathbf{C_D}(t) = \begin{pmatrix} c_1(t) \\ c_2(t) \\ c_3(t) \\ c_4(t) \\ c_5(t) \end{pmatrix} \quad \mathbf{U} = \begin{pmatrix} k_{u,1} \\ k_{u,2} \\ k_{u,3} \\ k_{u,4} \\ k_{u,5} \end{pmatrix}$$

$$\mathbf{E} = \begin{pmatrix} e_{1,1} & k_{1,2} & k_{1,3} & k_{1,4} & k_{1,5} \\ k_{2,1} & e_{2,2} & k_{2,3} & k_{2,4} & k_{2,5} \\ k_{3,1} & k_{3,2} & e_{3,3} & k_{3,4} & k_{3,5} \\ k_{4,1} & k_{4,2} & k_{4,3} & e_{4,4} & k_{4,5} \\ k_{5,1} & k_{5,2} & k_{5,3} & e_{5,4} & e_{5,5} \end{pmatrix} \tag{25}$$

and diagonal elements of matrix **E** defined by:

$$\begin{cases} e_{1,1} = -k_{e,1} - \left(k_{2,1} + k_{3,1} + k_{4,1}\right) & \text{(a)} \\ e_{2,2} = -k_{e,2} - \left(k_{1,2} + k_{3,2} + k_{4,2}\right) & \text{(b)} \\ e_{3,3} = -k_{e,3} - \left(k_{1,3} + k_{2,3} + k_{4,3}\right) & \text{(c)} \\ e_{4,4} = -k_{e,4} - \left(k_{1,4} + k_{2,4} + k_{3,4}\right) & \text{(d)} \end{cases} \tag{26}$$

The exact solution of the matrix ODE system (24) can be directly deduced from Equations (17) and (21):

$$\begin{cases} \mathbf{C_A}(t) = \left(e^{t\mathbf{E}} - \mathbf{I}\right)\mathbf{E}^{-1}\mathbf{U}c_x \\ \quad \text{when} \quad 0 \leqslant t \leqslant t_c \quad \text{(accumulation phase)} \quad \text{(a)} \\ \mathbf{C_D}(t) = \left(e^{t\mathbf{E}} - e^{(t-t_c)\mathbf{E}}\right)\mathbf{E}^{-1}\mathbf{U}c_x \\ \quad \text{when} \quad t > t_c \quad \text{(depuration phase)} \quad \text{(b)} \end{cases} \tag{27}$$

Developing the matrix Equations (27a) and (27b) finally provides the following sets of four equations for both accumulation and depuration phases:

For the accumulation phase ($0 \leqslant t \leqslant t_c$):

$$\begin{cases} \dfrac{dc_1(t)}{dt} = k_{u,1}c_x - k_{e,1}c_1(t) + k_{1,2}c_2(t) + k_{1,3}c_3(t) \\ \quad + k_{1,4}c_4(t) - \left(k_{2,1} + k_{3,1} + k_{4,1}\right)c_1(t) & \text{(a)} \\ \dfrac{dc_2(t)}{dt} = k_{u,2}c_x - k_{e,2}c_2(t) + k_{2,1}c_1(t) + k_{2,3}c_3(t) \\ \quad + k_{2,4}c_4(t) - \left(k_{1,2} + k_{3,2} + k_{4,2}\right)c_2(t) & \text{(b)} \\ \dfrac{dc_3(t)}{dt} = k_{u,3}c_x - k_{e,3}c_3(t) + k_{3,1}c_1(t) + k_{3,2}c_2(t) \\ \quad + k_{3,4}c_4(t) - \left(k_{1,3} + k_{2,3} + k_{4,3}\right)c_3(t) & \text{(c)} \\ \dfrac{dc_4(t)}{dt} = k_{u,4}c_x - k_{e,4}c_4(t) + k_{4,1}c_1(t) + k_{4,2}c_2(t) \\ \quad + k_{4,3}c_3(t) - \left(k_{1,4} + k_{2,4} + k_{3,4}\right)c_4(t) & \text{(d)} \end{cases} \tag{28}$$

For the depuration phase ($t > t_c$):

$$\begin{cases} \dfrac{dc_1(t)}{dt} = -k_{e,1}c_1(t) + k_{1,2}c_2(t) + k_{1,3}c_3(t) \\ \quad + k_{1,4}c_4(t) - \left(k_{2,1} + k_{3,1} + k_{4,1}\right)c_1(t) & \text{(a)} \\ \dfrac{dc_2(t)}{dt} = -k_{e,2}c_2(t) + k_{2,1}c_1(t) + k_{2,3}c_3(t) \\ \quad + k_{2,4}c_4(t) - \left(k_{1,2} + k_{3,2} + k_{4,2}\right)c_2(t) & \text{(b)} \\ \dfrac{dc_3(t)}{dt} = -k_{e,3}c_3(t) + k_{3,1}c_1(t) + k_{3,2}c_2(t) \\ \quad + k_{3,4}c_4(t) - \left(k_{1,3} + k_{2,3} + k_{4,3}\right)c_3(t) & \text{(c)} \\ \dfrac{dc_4(t)}{dt} = -k_{e,4}c_4(t) + k_{4,1}c_1(t) + k_{4,2}c_2(t) \\ \quad + k_{4,3}c_3(t) - \left(k_{1,4} + k_{2,4} + k_{3,4}\right)c_4(t) & \text{(d)} \end{cases} \tag{29}$$

The four-compartment model in Equations (27a) and (27b) based on the matrix ODE system in Equations (24a) and (24b), with its exact solution in (28) and (29), assumes that all compartments are connected to each other by pairs and with the external medium (Fig. 3). This means that the model is considering all incoming and outgoing arrows from all compartments. This model comprises a total of 20 parameters, plus the c_x value for the exposure concentration. As given in Table 3, median parameter values were used to simulate what happens within each organ in terms of internal concentration dynamic and compared to the previous results with the four independent one-compartment PBK models. See Supplementary File 1 for details.

As illustrated above, our generic modeling framework allows simulating complex situations involving several compartments, their connections in pairs and/or with the exposure media. Let us now relate what we did for simulations of four one-compartment models for each organ of *G. fossarum* exposed to Cd – with the four-compartment model developed by Gestion *et al*.[27] Indeed, they showed that *G. fossarum* takes up and eliminates Cd rather quickly, with the intestines and the caeca accumulating and depurating the most compared to the cephalon and the remaining tissues. Gestin *et al*. also proved that a four-compartment model better describes the Cd internal contamination route than the single one-compartment model for each organ. Furthermore, they finally highlighted that the most parsimonious multi-compartments model corresponds to the solid black arrows in Figure 3.

Such a situation corresponds to a nested model within the four-compartment ODE system as given by Equations (24a) and (24b). This model thus comprises only 12 parameters whose values are listed in Table 3. Figure 4 shows the simulated kinetics within the four organs. Our four curves exactly superimpose to the four median curves provided in Figure 3 by Gestin *et al*. Benefiting from this exact match between our exact generic solution and what was numerically integrated by these authors before the implementation of their inference process ultimately strengthens both approaches: the numerical integration (a basic Euler integration scheme with a time-step equal to 1/10 day); and the curve plotting from the exact solution. Nevertheless, to infer parameter values from observed data, there is absolutely no doubt that the exact solution will provide much better computational performance for implementing the Monte Carlo Markov Chain simulations needed to use Bayesian inference. Readers who would like to convince themselves of this added value of our generic solving can refer to our dedicated R-package named

Table 3. Parameter estimates (expressed as medians and 95% uncertainty intervals) of the four-compartment model corresponding to solid black arrows in Figure 3 as provided by[1] in Table S6

Organ-Connection	Parameter	Median	$Q_{2.5\%}$	$Q_{97.5\%}$
Intestines (uptake)	$k_{u,1}$	3342	2720	3707
Intestines (elimination)	$k_{e,1}$	0.54	0.415	1.402
Intestines-Caeca	k_{21}	0.873	0.603	1.739
Caeca-Intestines	k_{12}	0.218	0.132	0.376
Intestines-Cephalons	k_{31}	0.059	0.034	0.124
Cephalons-Intestines	k_{13}	0.262	0.124	0.871
Intestines-remaining tissues	k_{41}	0.069	0.049	0.126
Remaining tissues-Intestines	k_{14}	0.14	0.086	0.238
Intestines	σ_1	8.974	6.469	15.28
Caeca	σ_2	17.94	13.07	26.84
Cephalons	σ_3	1.223	0.863	1.818
Remaining tissues	σ_4	1.468	1.06	2.242

The first column stands for connected organs, either to water or to the other organs; the second column is for parameter names; the following three columns are for medians, lower and upper quantiles of parameter estimates when *G. fossarum* was exposed to Cd = 11.1 $\mu g \cdot L^{-1}$.

'rPBK,' officially available from the official R CRAN website (https://CRAN.R-project.org/package=rPBK) together with a very recent related paper.[47] Thanks to the R-package 'rPBK', we already experienced that using this exact generic solution divided at least by 100 the computation time of the whole process. Our first inference implementation required numerically integrating the original ODE system and running the MCMC algorithm to fit the numerical solution to the accumulation-depuration data sets corresponding to the different organs and tissues. The numerical integration step was highly computationally demanding. Avoiding this numerical step much faster now delivers relevant and precise parameter estimates.

Case study with five compartments

Zhu and colleagues[45] studied the effect of six different antibiotics on the sea cucumber *Apostichopus japonicus*: sulfadiazine, tri-

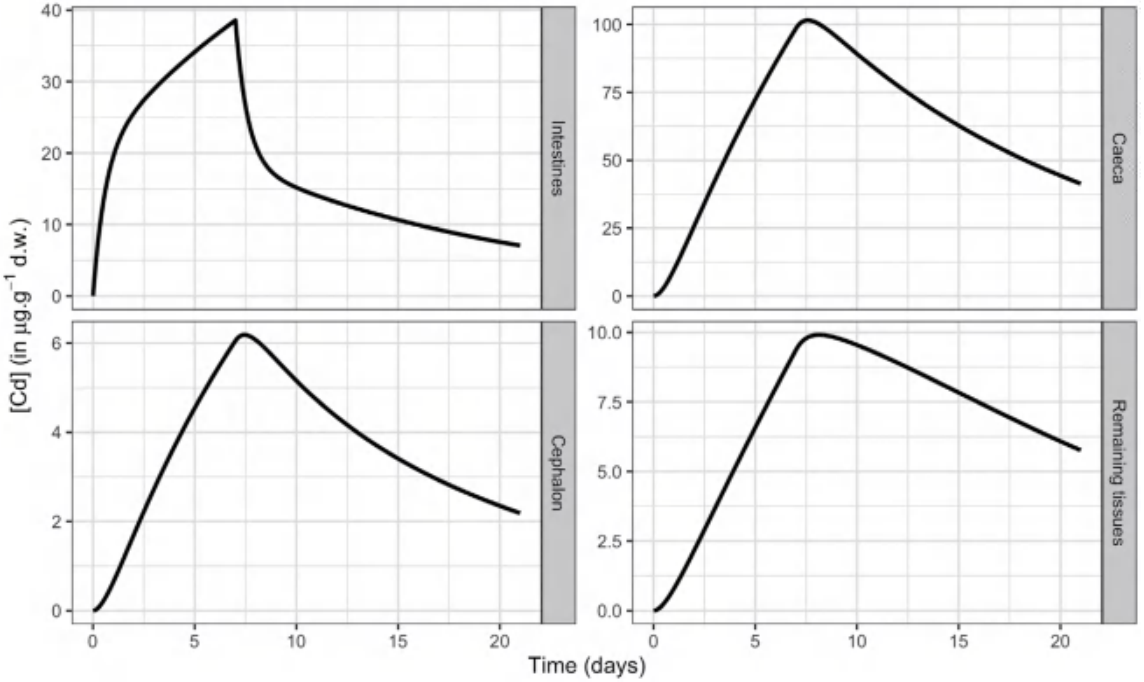

Fig. 4. Simulations of the internal concentrations within the different organs or tissues of *Gammarus fossarum* when exposed to an external cadmium concentration equal to 11.1 $\mu g \cdot L^{-1}$. The four-compartment PBK solution used for simulations is given in Equation (27). Parameter values are those given in Table 2.

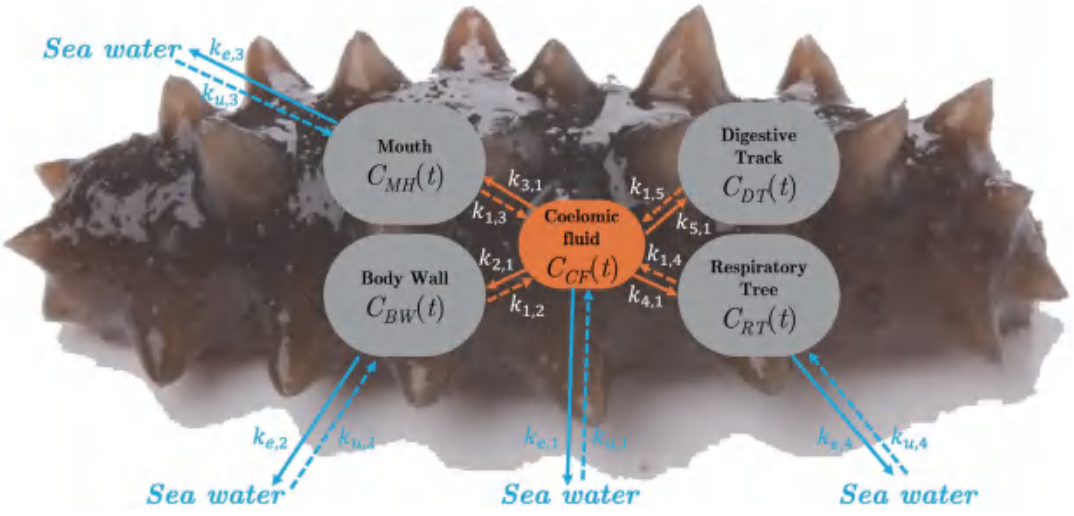

Fig. 5. Schematic representation of the five-compartment kinetic model used to simulate the effects of waterborne antibiotics in sea cucumbers: the coleomic fluid (*CF*), the body wall (*BW*), the mouth (*MH*), the respiratory tree (*RT*) and the digestive tract (*DT*). Parameters $k_{u,i}$ and $k_{e,i}$, $\forall i = 1,4$, stand for uptake and elimination rates from or towards seawater, respectively; parameters $k_{i,j}$ represent from and back exchanges between compartments *i* and *j*, $\forall i, j = 1,5$.

methoprim, enrofloxacin, ofloxacin, clarithromycin, and azithromycin. All compartments (blood or organs) are internally related to the coelomic fluid. Except for the digestive tract, all compartments are externally related to seawater (Fig. 5). Based on the original paper,[45] biological parameter values were extracted to calculate the model's coefficients used for the simulations. All these parameters are provided in Table 4.

Below are the model equations written within our new generic mathematical formalism, with the following correspondence between index *i* and the different compartments: coleomic fluid (*CF*, $i = 1$); the body wall (*BW*, $i = 2$), the mouth (*MH*, $i = 3$), the respiratory tree (*RT*, $i = 4$) and the digestive tract (*DT*, $i = 5$).

Table 4. Parameter values for the five-compartment physiologically-based kinetic model on sea cucumbers, after recalculation from the initial parameters as given by[45] in their supplementary information

Parameter	Sulfadiazine	Trimethoprim	Enrofloxacin	Ofloxacin	Clarithromycin	Azithromycin
$k_{u,1}$	68.73	68.73	68.73	68.73	68.73	68.73
$k_{e,1}$	68.73	5.61	4.01	4.89	5.35	5.64
$k_{u,2}$	0.53	34.97	21.10	36.77	24.10	24.10
$k_{e,12}$	0.06	285.76	234.84	229.46	177.87	209.72
$k_{u,3}$	2.86	0.00	0.00	0.00	0.00	0.00
$k_{e,3}$	0.45	68.73	68.73	68.73	68.73	68.73
$k_{u,4}$	19.51	0.11	0.07	0.13	0.07	0.04
$k_{e,4}$	4.11	0.51	0.59	0.88	0.22	0.14
$k_{u,5}$	0.00	3.88	11.91	8.44	1.98	1.55
$k_{e,t}$	0.00	0.00	0.00	0.00	0.00	0.00
$k_{1,2}$	0.06	0.08	0.09	0.11	0.07	0.04
$k_{2,1}$	0.50	0.40	0.92	0.70	0.26	0.20
$k_{1,3}$	0.43	3.27	10.75	9.29	2.20	1.93
$k_{3,1}$	2.70	0.40	1.16	1.06	0.48	0.25
$k_{1,4}$	4.11	4.00	4.94	4.17	5.52	5.50
$k_{4,1}$	19.51	27.22	32.72	29.37	28.15	35.42
$k_{1,5}$	0.48	241.35	211.96	252.56	198.06	261.31
$k_{5,1}$	2.46	29.69	29.03	26.96	25.34	25.65

Mathematical relationships between initial and recalculated parameters are detailed in the main text.

$$\begin{cases} \dfrac{d\mathbf{C_A}(t)}{dt} = \mathbf{U}c_x + \mathbf{E}\mathbf{C_A}(t) \\ \quad \text{when} \quad 0 \leqslant t \leqslant t_c \quad \text{(accumulation phase)} \quad \text{(a)} \\ \dfrac{d\mathbf{C_D}(t)}{dt} = \mathbf{E}\mathbf{C_D}(t) \\ \quad \text{when} \quad t > t_c \quad \text{(depuration phase)} \quad \text{(b)} \end{cases} \tag{30}$$

with vectors and matrices defined as follows:

$$\mathbf{C_A}(t) = \mathbf{C_D}(t) = \begin{pmatrix} c_1(t) \\ c_2(t) \\ c_3(t) \\ c_4(t) \\ c_5(t) \end{pmatrix} \quad \mathbf{U} = \begin{pmatrix} k_{u,1} \\ k_{u,2} \\ k_{u,3} \\ k_{u,4} \\ k_{u,5} \end{pmatrix}$$

$$\mathbf{E} = \begin{pmatrix} e_{1,1} & k_{1,2} & k_{1,3} & k_{1,4} & k_{1,5} \\ k_{2,1} & e_{2,2} & k_{2,3} & k_{2,4} & k_{2,5} \\ k_{3,1} & k_{3,2} & e_{3,3} & k_{3,4} & k_{3,5} \\ k_{4,1} & k_{4,2} & k_{4,3} & e_{4,4} & k_{4,5} \\ k_{5,1} & k_{5,2} & k_{5,3} & e_{5,4} & e_{5,5} \end{pmatrix} \tag{31}$$

and diagonal elements of matrix **E** defined by:

$$\begin{cases} e_{1,1} = -k_{e,1} - \left(k_{2,1} + k_{3,1} + k_{4,1} + k_{5,1}\right) & \text{(a)} \\ e_{2,2} = -k_{e,2} - k_{1,2} & \text{(b)} \\ e_{3,3} = -k_{e,3} - k_{1,3} & \text{(c)} \\ e_{4,4} = -k_{e,4} - k_{1,4} & \text{(d)} \\ e_{5,5} = -k_{1,5} & \text{(e)} \end{cases} \tag{32}$$

The exact solution of the matrix ODE system (30) can be directly deduced from Equations (17) and (21):

$$\begin{cases} \mathbf{C_A}(t) = \left(e^{t\mathbf{E}} - \mathbf{I}\right)\mathbf{E}^{-1}\mathbf{U}c_x \\ \quad \text{when} \quad 0 \leqslant t \leqslant t_c \quad \text{(accumulation phase)} \quad \text{(a)} \\ \mathbf{C_D}(t) = \left(e^{t\mathbf{E}} - e^{(t-t_c)\mathbf{E}}\right)\mathbf{E}^{-1}\mathbf{U}c_x \\ \quad \text{when} \quad t > t_c \quad \text{(depuration phase)} \quad \text{(b)} \end{cases} \tag{33}$$

The relationships between the initial and the recalculated parameters are the following, with the index *SW* referring to seawater:

$$k_{u,i} = \frac{D_{i,SW}}{V_i} \text{ and } k_{e,i} = \frac{D_{i,SW}}{V_i P_{i,SW}} \quad \forall i \in CF, BW, MH, RT, DT$$

$$k_{CF,i} = \frac{D_{CF,i}}{V_{CF}} \text{ and } k_{i,CF} = \frac{D_{CF,i}}{V_{CF} P_{i,CF}} \quad \forall i \in BW, MH, RT, DT$$

This leads to the first ODE of the five-compartment system for the sea cucumber:

$$\frac{dC_{CF}(t)}{dt} = k_{u,CF} c_w - \left(k_{e,CF} + \sum_{i \neq CF} k_{i,CF}\right) C_{CF}(t) + \sum_{i \neq CF} \left(k_{CF,i} C_i(t)\right) \quad \forall i \in BW, MH, RT, DT \tag{34}$$

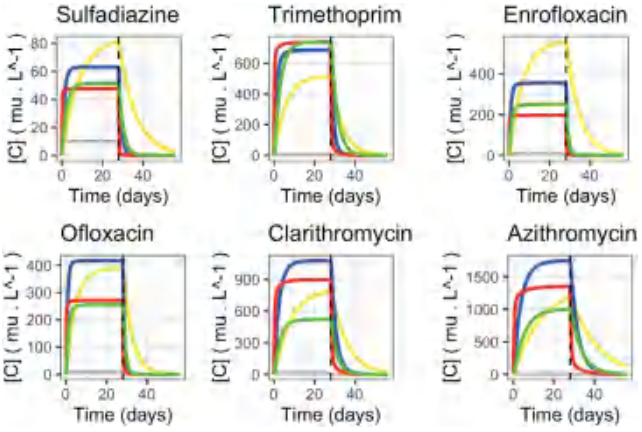

Fig. 6. Predicted time course of the median internal concentrations in antibiotics (given on the top legend of each graph) under a constant exposure concentration of 10 *μg·L*$^{-1}$: in yellow the body wall (*BW*), in blue the mouth (*MH*), in red the respiratory tree (*RT*) and in green the digestive tract (*DT*).

with $c_w = 10\ \mu g \cdot L^{-1}$ the concentration in the seawater to which they are exposed.

$$k_{CF,i} = \frac{D_{CF,i}}{V_i P_{i,CF}} \text{ and } k_{i,CF} = \frac{D_{CF,i}}{V_j} \quad \forall i \in BW, MH, RT, DT$$

Finally, we get the four complementary equations of the system for the sea cucumber:

$$\frac{dC_i(t)}{dt} = k_{u,i} c_w - \left(k_{e,i} + k_{CF,i}\right) C_i(t) + k_{i,CF} C_{CF}(t) \tag{35}$$

Given parameter values in Table 4, we performed simulations over time for the six antibiotics and the four internal organs. As shown in Figure 6, we reproduced the same median curves as those of[45] in Figure S10 of their supplementary information.

Case study with six compartments

Here is a final illustration of the usefulness of our generic solution to simulate any PBK model. We identically reproduced all the simulations provided by[46] concerning exposure of zebrafish (*Danio rerio*) to arsenic (As). To this end, Zhang *et al*.[46] proposed a six-compartments model with five compartments corresponding to organs: gills (i = 2), intestine (i = 3), liver (i = 4), head (i = 5) and carcass (i = 6). The sixth compartment corresponds to blood (i = 1). The five organs were connected to blood, while the gills and intestines were also connected to the external medium (contaminated water). These assumptions are translated in Figure 7, together with the different parameters used for the corresponding PBK model (Table 5).

From the generic matrix form of a PBK model we present in this paper, the model writes as follows:

$$\frac{d\mathbf{C}(t)}{dt} = \mathbf{U}c_x + \mathbf{E}\mathbf{C}(t) \tag{36}$$

with vectors and matrices defined as follows:

$$\mathbf{C}(t) = \begin{pmatrix} c_1(t) & c_2(t) & c_3(t) & c_4(t) & c_5(t) & c_6(t) \end{pmatrix}^T \tag{37}$$

where $c_i(t)$, $\forall i$ = 1,6, are the variables corresponding to internal concentrations to be simulated. Variables $c_i(t)$ are equal to $\overline{w}_i C_i(t)$,

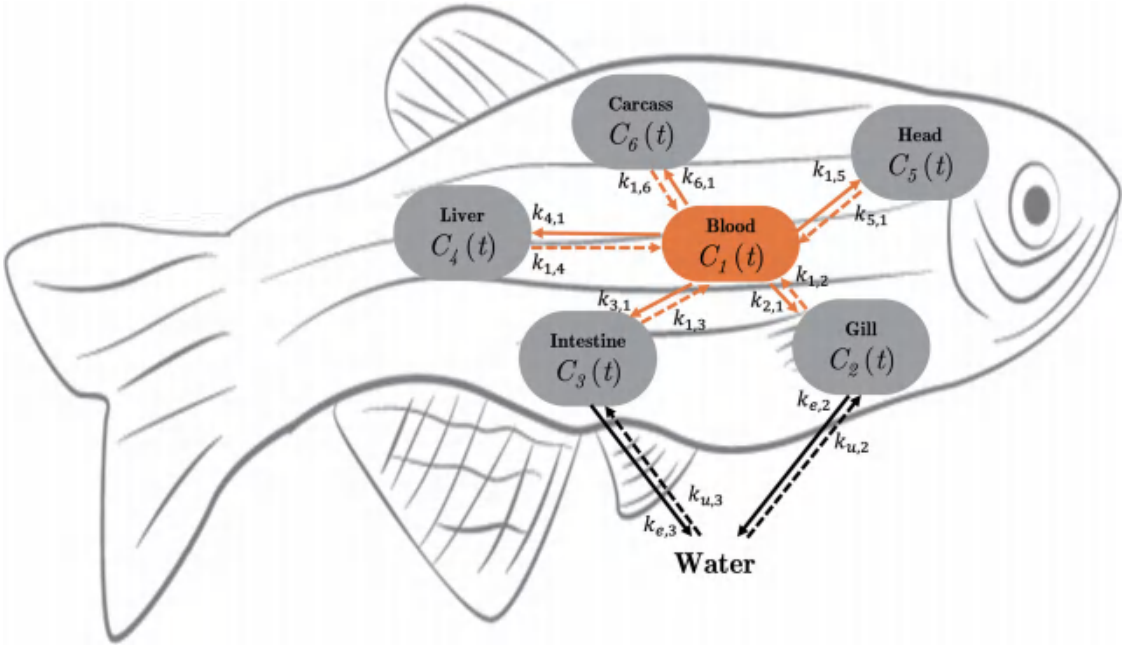

Fig. 7. General scheme of the six-compartment kinetic model for zebrafish exposed to arsenic (Adapted from [3]). Parameters, between-organ and/or with-water connections, numerical values, and units are given in Table 5.

$\forall i$ = 1,6, with $\overline{w}_i$ the mean wet weight of blood volume (when i = 1) or fish organs ($\forall i$ = 2,6). Variables $Ci(t)$ are the measured concentrations of As in fish organs ($\forall i$ = 2,6, expressed in $\mu g \cdot L^{-1}$) at time t (in days). Variable c_x is the exposure concentration of As in water (expressed in $\mu g \cdot L^{-1}$), assumed to be constant over time.

From concentrations within organs, the concentration for the whole organism can be deduced as follows:

$$C_{whole}(t) = \frac{1}{\sum_{i=1}^{6} \overline{w}_i} \left(\sum_{i=1}^{6} \overline{w}_i c_i(t) \right) \tag{38}$$

According to our mathematical formalism, uptake parameters from water are included in the following vector:

$$\mathbf{U} = \begin{pmatrix} 0 & k_{u2} & k_{u3} & 0 & 0 & 0 \end{pmatrix}^T \tag{39}$$

while elimination parameters towards the water, as well as parameters corresponding to organ-organ connections, are gathered together within the following matrix:

$$\mathbf{E} = \begin{pmatrix} -\sum_{j=2}^{6} k_{j,1} & k_{1,2} & k_{1,3} & k_{1,4} & k_{1,5} & k_{1,6} \\ k_{2,1} & -k_{e,2} - k_{1,2} & 0 & 0 & 0 & 0 \\ k_{3,1} & 0 & -k_{e,3} - k_{1,3} & 0 & 0 & 0 \\ k_{4,1} & 0 & 0 & -k_{1,4} & 0 & 0 \\ k_{5,1} & 0 & 0 & 0 & -k_{1,5} & 0 \\ k_{6,1} & 0 & 0 & 0 & 0 & -k_{1,6} \end{pmatrix} \tag{40}$$

The matrix ODE system (36) finally leads to the following exact solution:

$$\mathbf{C}(t) = \left(e^{t\mathbf{E}} - \mathbf{I} \right) \mathbf{E}^{-1} \mathbf{U} c_x \tag{41}$$

where c_x is the exposure concentration in water.

The above matrix solution (41) can then be developed in order to retrieve the six-compartment PBK model as constructed by

Table 5. Parameter estimates for arsenic distribution in zebrafish (from[46])

Connection	$\mathcal{ML}$	Value	Unit	Connection	$\mathcal{ML}$	Value	Unit
Water to gills	$k_{u,2}$	5.28 10^{-5}	L.d^{-1}	Gill to water	$k_{e,2}$	0.152	d^{-1}
Water to intestine	$k_{u,2}$	1.52 10^{-4}	L.d^{-1}	Intestine to water	$k_{e,2}$	0.672	d^{-1}
Blood to gills	$k_{2,1}$	76.0	d^{-1}	Gill to blood	$k_{1,2}$	58.2	d^{-1}
Blood to intestine	$k_{3,1}$	27.8	d^{-1}	Intestine to blood	$k_{1,3}$	3.94	d^{-1}
Blood to liver	$k_{4,1}$	38.5	d^{-1}	Liver to blood	$k_{1,4}$	23.6	d^{-1}
Blood to head	$k_{5,1}$	97.5	d^{-1}	head to blood	$k_{1,5}$	8.48	d^{-1}
Blood to carcass	$k_{6,1}$	7.20	d^{-1}	Carcass to blood	$k_{1,6}$	0.317	d^{-1}

Notation $\mathcal{ML}$ stands for the estimated maximum likelihood value of the parameter.

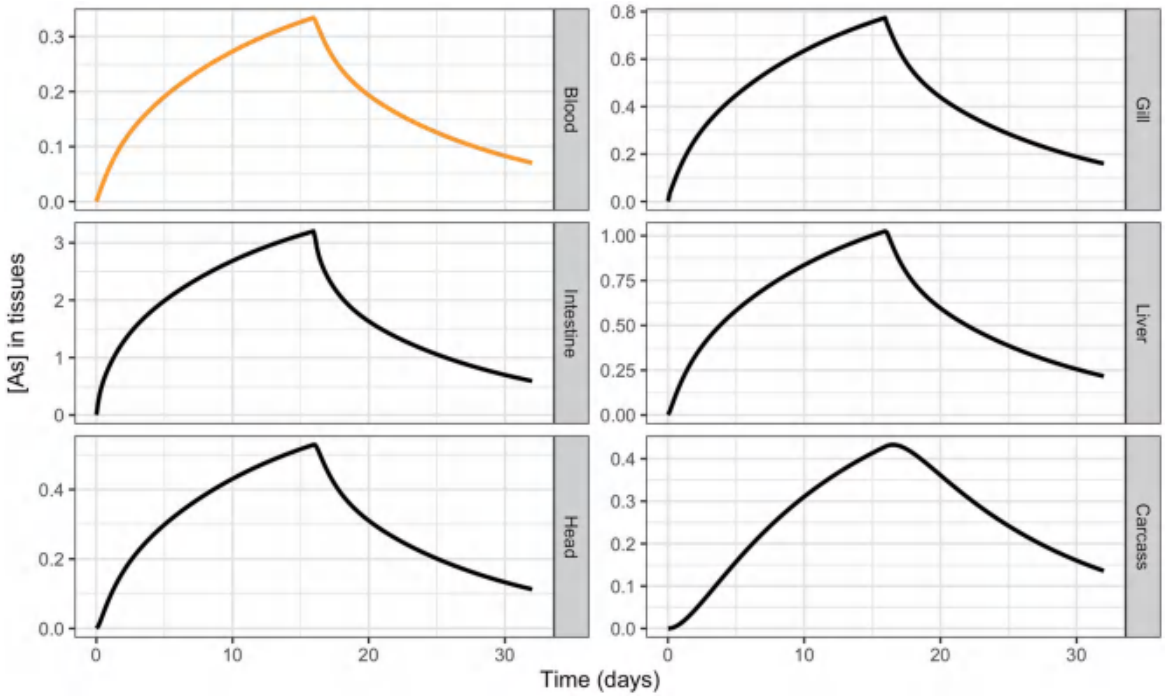

Fig. 8. Simulation of the total arsenic concentration in fish tissues and blood during the accumulation phase of 16 days (exposure concentration equal to 400 $\mu g \cdot L^{-1}$) and the subsequent 16 days of depuration in a clean medium. The PBK model used for simulations is given as a matrix solution in Equation (41) with parameter values from Table 5.

Zhang *et al*.[46] Denoting the exposure concentration in water (variable c_x in our modeling) by C_{water}, we ultimately get:

$$\begin{cases} \overline{w_1}\dfrac{dC_1(t)}{dt} = \sum_{j=2}^{7} k_{1,j} C_j(t)\overline{w_i} - \left(\sum_{j=2}^{7} k_{j,1}\right) C_1(t)\overline{w_1} & \text{(a)} \\ \overline{w_2}\dfrac{dC_2(t)}{dt} = k_{u,2} C_{water} + k_{2,1} C_1(t)\overline{w_1} - \left(k_{e,2} + k_{1,2}\right) C_2(t)\overline{w_2} & \text{(b)} \\ \overline{w_3}\dfrac{dC_3(t)}{dt} = k_{u,3} C_{water} + k_{3,1} C_1(t)\overline{w_1} - \left(k_{e,3} + k_{1,3}\right) C_3(t)\overline{w_3} & \text{(c)} \\ \overline{w_4}\dfrac{dC_4(t)}{dt} = k_{4,1} C_1(t)\overline{w_1} - k_{1,4} C_4(t)\overline{w_4} & \text{(d)} \\ \overline{w_5}\dfrac{dC_5(t)}{dt} = k_{5,1} C_1(t)\overline{w_1} - k_{1,5} C_5(t)\overline{w_5} & \text{(e)} \\ \overline{w_6}\dfrac{dC_6(t)}{dt} = k_{6,1} C_1(t)\overline{w_1} - k_{1,6} C_6(t)\overline{w_6} & \text{(f)} \end{cases} \quad (42)$$

Zhang *et al*. measured internal concentrations over time in each organ and blood during both accumulation and depuration phases. This data allowed them to estimate all their parameters. Using a Bayesian inference framework also provided them with quantifying the uncertainty of these parameters. Then they deliver parameter estimates as maximum likelihood ($\mathcal{ML}$) values associated with a 95% credible interval, as partly reported in Table 5.

Based on parameter $\mathcal{ML}$ values in Table 5, using the fresh weight of the different organs as provided in Table S2 from Zhang *et al*.,[46] we performed simulations of the internal concentrations within each of the five organs as well as in blood (variables $c_i(t)$, $\forall i$ = 1,6). As shown in Figure 8, our generic solved PBK model (see Equation (41)) again exactly reproduce the median curves provided by Zhang *et al*. in Figure 1 (solid blue lines). Such an exact match between our curves and the authors' ones again provides a complete check of the mathematical writing of our generic solution, together with the fact that it produces identical median curves. These results again reinforce the possibility of using this exact generic solution for the further implementation of inference processes with the guarantee of obtaining the parameter estimates much faster, avoiding the time-consuming step of the numerical integration of the ODE system.

Discussion and future directions

Benefiting from the generic solution of a PBK model allows us now to envisage the continuation of this work with confidence, in particular the implementation of a Bayesian inference framework to get parameter estimates quickly and efficiently, based on a fully harmonized methodology. The next step will thus be to make freely and easily accessible this generic modeling framework, innovative both in the writing of the PBK model and in its exact resolution and the implementation of the fitting and simulation tools. Most users, who are not necessarily modeling specialists, would be willing to use more complex PBK models, especially if necessity dictates and sufficient input data is available.

Unfortunately, turnkey tools are still rare today. In line with the MOSAIC platform spirit (https://mosaic.univ-lyon1.fr), we have already started to build a new prototype that will facilitate the use of PBK models, also for beginners, with a step-by-step workflow to first upload data and select the model to fit. By default, the complete PBK model will be automatically proposed from which users can deselect either compartment and/or exchanges between the compartment and/or with the external medium according to prior physiological knowledge. Then the user can try nested models and

finally identify the most appropriate model for the question. Users will be accompanied to run the fitting process, get the results (parameter estimates and fitting plots), look at the goodness-of-fit criteria (with guidance on their interpretation), and use the model comparison criteria in case several models would have been tested. Once this calibration step is achieved, users can run simulations, compare with additional data, or plan further experiments. In the end, all expected features of a convenient help-decision service could be offered, with particular attention to further supporting the next generation tiered PBK modeling framework that could become the new paradigm in human and environmental risk assessment. Once our generic PBK modeling framework is firmly anchored in practice, we should be in the right place to consider its coupling with mechanistic models to build an utterly general modeling framework from exposure (pharmaco/toxico-kinetics) to effects (pharmaco/toxico-dynamics) on life history traits, hence defining a unifying PBKD modeling framework.

Conclusions

Our generic solving of any full PBK model comprising as many compartments as physiologically needed, as well as all potential connections between compartments and with the external medium, revealed particularly efficient in simulating diverse situations in terms of species, compounds, and purpose. The four-compartment PBK model for *G. fossarum* exposed to Cd highlighted the dynamic transfer of Cd among the different organs. The six-compartment PBK model for *D. rerio* exposed to As showed that intestines were the leading uptake site for waterborne As, instead of gills as the authors expected. Several other examples have complementary been tested (results not shown). Nevertheless, the genericity of the solution we proposed here could still be further extended in order to account for simultaneous but different routes of exposure (via water, food, sediment and/or pore water, for example), as well as several elimination processes, among which the dilution by growth would allow to be more realistic for long-lived species. Moreover, accounting for the metabolization of the parent compound could also be of great interest to better deal with organic compounds.

Supporting information

Supplementary material for this article is available at https://doi.org/10.14218/JERP.2022.00043.

Supplementary File 1. Generic solving of a multi-compartment physiologically-based kinetic model.

Acknowledgments

A large part of the work benefited from the French GDR "Aquatic Ecotoxicology" framework, which aims to foster stimulating scientific discussions and collaborations for more integrative approaches. The authors would like to express their sincere gratitude to Julie KLEINE-SCHULTJANN as part of a training course during her 5th year study at the National Institute of Applied Sciences (INSA) in Lyon (France). At last, the work presented in this paper was performed using the computing facilities of the CC LBBE/PRABI.

Funding

The authors would like to thank the BioEEnViS research federation (Biodiversity, Water, Environment, City, Health) for its financial support for collaboratively achieving this study. Moreover, this work is part of the ANR project APPROve (ANR-18-CE34-0013) for an integrated approach to propose proteomics for biomonitoring: accumulation, fate, and multi-markers (https://anr.fr/Projet-ANR-18-CE34-0013).

Conflict of interest

The authors have no conflicts of interest related to this publication.

Author contributions

SC resolved the full generic PBK model, wrote the manuscript, and coordinated all discussions around this paper. OGes, AC, OGef, TLL, and CL were strongly involved in the *G. fossarum* case study in close collaboration with OGes's PhD supervision, who led all the underlying experimental work. JB, DL, and VB paid particular attention to the model equation writing. VB wrote the R source code, which generated simulation curves; this R code was also checked by SC, JB, DL, and CL. All authors contributed to and agreed on the final version of the manuscript.

References

[1] Paini A, Leonard JA, Kliment T, Tan YM, Worth A. Investigating the state of physiologically based kinetic modelling practices and challenges associated with gaining regulatory acceptance of model applications. Regul Toxicol Pharmacol 2017;90:104–115. doi:10.1016/j.yrtph.2017.08.019, PMID:28866268.

[2] Madden JC, Pawar G, Cronin MTD, Webb S, Tan YM, Painie A. In silico resources to assist in the development and evaluation of physiologically based kinetic models. Computational Toxicology 2019;11:33–49. doi:10.1016/j.comtox.2019.03.001.

[3] Thompson CV, Firman JW, Goldsmith MR, Grulke CM, Tan YM, Paini A, *et al*. A Systematic Review of Published Physiologically-based Kinetic Models and an Assessment of their Chemical Space Coverage. Altern Lab Anim 2021;49(5):197–208. doi:10.1177/02611929211060264, PMID:34836462.

[4] Grech A, Brochot C, Dorne JL, Quignot N, Bois FY, Beaudouin R. Toxicokinetic models and related tools in environmental risk assessment of chemicals. Sci Total Environ 2017;578:1–15. doi:10.1016/j.scitotenv.2016.10.146, PMID:27842969.

[5] Tebby C, van der Voet H, de Sousa G, Rorije E, Kumar V, de Boer W, *et al*. A generic PBTK model implemented in the MCRA platform: Predictive performance and uses in risk assessment of chemicals. Food Chem Toxicol 2020;142:111440. doi:10.1016/j.fct.2020.111440, PMID:32473292.

[6] Mit C, Bado-Nilles A, Daniele G, Giroud B, Vulliet E, Beaudouin R. The toxicokinetics of bisphenol A and its metabolites in fish elucidated by a PBTK model. Aquat Toxicol 2022;247:106174. doi:10.1016/j.aquatox.2022.106174, PMID:35462154.

[7] Wang WX, Rainbow PS. Comparative approaches to understand metal bioaccumulation in aquatic animals. Comp Biochem Physiol C Toxicol Pharmacol 2008;148(4):315–323. doi:10.1016/j.cbpc.2008.04.003, PMID:18502695.

[8] Lautz LS, Oldenkamp R, Dorne JL, Ragas AMJ. Physiologically based kinetic models for farm animals: Critical review of published models and future perspectives for their use in chemical risk assessment. Toxicol In Vitro 2019;60:61–70. doi:10.1016/j.tiv.2019.05.002, PMID:31075317.

[9] Zhao P, Zhang L, Grillo JA, Liu Q, Bullock JM, Moon YJ, *et al*. Applications of physiologically based pharmacokinetic (PBPK) modeling and simulation during regulatory review. Clin Pharmacol Ther 2011;89(2):259–267. doi:10.1038/clpt.2010.298, PMID:21191381.

[10] Armitage JM, Hughes L, Sangion A, Arnot JA. Development and intercomparison of single and multicompartment physiologically-based toxicokinetic models: Implications for model selection and tiered modeling frameworks. Environ Int 2021;154:106557. doi:10.1016/j.envint.2021.106557, PMID:33892222.
[11] Paini A, Tan YM, Sachana M, Worth A. Gaining acceptance in next generation PBK modelling approaches for regulatory assessments - An OECD international effort. Comput Toxicol 2021;18:100163. doi:10.1016/j.comtox.2021.100163, PMID:34027244.
[12] Fransson MN, Barregard L, Sallsten G, Akerstrom M, Johanson G. Physiologically-based toxicokinetic model for cadmium using Markov-chain Monte Carlo analysis of concentrations in blood, urine, and kidney cortex from living kidney donors. Toxicol Sci 2014;141(2):365–376. doi:10.1093/toxsci/kfu129, PMID:25015660.
[13] Sweeney LM, MacCalman L, Haber LT, Kuempel ED, Tran CL. Bayesian evaluation of a physiologically-based pharmacokinetic (PBPK) model of long-term kinetics of metal nanoparticles in rats. Regul Toxicol Pharmacol 2015;73(1):151–163. doi:10.1016/j.yrtph.2015.06.019, PMID:26145831.
[14] Testai E, Bechaux C, Buratti FM, Darney K, Consiglio E, Kasteel EEJ, *et al*. Modelling human variability in toxicokinetic and toxicodynamic processes using Bayesian meta-analysis, physiologically based modelling and in vitro systems. EFSA Journal 2021;18(4):EN-6504. doi:10.2903/sp.efsa.2021.EN-6504.
[15] Charles S, Ratier A, Lopes C. Generic Solving of One-compartment Toxicokinetic Models. J Explor Res Pharmacol 2021;6(4):158–167. doi:10.14218/JERP.2021.00024.
[16] Breen M, Ring CL, Kreutz A, Goldsmith MR, Wambaugh JF. High-throughput PBTK models for *in vitro* to *in vivo* extrapolation. Expert Opin Drug Metab Toxicol 2021;17(8):903–921. doi:10.1080/17425255.2021.1935867, PMID:34056988.
[17] Zhang Y, Feng J, Gao Y, Liu X, Qu L, Zhu L. Physiologically based toxicokinetic and toxicodynamic (PBTK-TD) modelling of Cd and Pb exposure in adult zebrafish Danio rerio: Accumulation and toxicity. Environ Pollut 2019;249:959–968. doi:10.1016/j.envpol.2019.03.115, PMID:30965548.
[18] Zhang S, Wang Z, Chen J, Xie Q, Zhu M, Han W. Tissue-Specific Accumulation, Biotransformation, and Physiologically Based Toxicokinetic Modeling of Benzotriazole Ultraviolet Stabilizers in Zebrafish (*Danio rerio*). Environ Sci Technol 2021;55(17):11874–11884. doi:10.1021/acs.est.1c02861.10.1021/acs.est.1c02861, PMID:34488350.
[19] Organisation for Economic Cooperation and Development (OECD). OECD Guidelines for the Testing of Chemicals - Test No. 211: Daphnia magna Reproduction test. Paris: OECD Publishing; 2012. doi:10.1787/9789264185203-en.
[20] Ratier A, Lopes C, Labadie P, Budzinski H, Delorme N, Quéau H, *et al*. A Bayesian framework for estimating parameters of a generic toxicokinetic model for the bioaccumulation of organic chemicals by benthic invertebrates: Proof of concept with PCB153 and two freshwater species. Ecotoxicol Environ Saf 2019;180:33–42. doi:10.1016/j.ecoenv.2019.04.080, PMID:31059905.
[21] Ratier A, Lopes C, Geffard O, Babut M. The added value of Bayesian inference for estimating biotransformation rates of organic contaminants in aquatic invertebrates. Aquat Toxicol 2021;234:105811. doi:10.1016/j.aquatox.2021.105811.10.1016/j.aquatox.2021.105811, PMID:33812312.
[22] Ratier A, Lopes C, Multari G, Mazerolles V, Carpentier P, Charles S. New perspectives on the calculation of bioaccumulation metrics for active substances in living organisms. Integr Environ Assess Manag 2022;18(1):10–18. doi:10.1002/ieam.4439, PMID:33982382.
[23] Charles S, Ratier A, Baudrot V, Multari G, Siberchicot A, Wu D, *et al*. Taking full advantage of modelling to better assess environmental risk due to xenobiotics-the all-in-one facility MOSAIC. Environ Sci Pollut Res Int 2022;29(20):29244–29257. doi:10.1007/s11356-021-15042-7, PMID:34255258.
[24] Vijver MG, Van Gestel CA, Lanno RP, Van Straalen NM, Peijnenburg WJ. Internal metal sequestration and its ecotoxicological relevance: a review. Environ Sci Technol 2004;38(18):4705–4712. doi:10.1021/es040354g, PMID:15487776.
[25] Brinkmann M, Eichbaum K, Kammann U, Hudjetz S, Cofalla C, Buchinger S, *et al*. Physiologically-based toxicokinetic models help identifying the key factors affecting contaminant uptake during flood events. Aquat Toxicol 2014;152:38–46. doi:10.1016/j.aquatox.2014.03.021, PMID:24727214.
[26] Allen GJP, Weihrauch D. Exploring the versatility of the perfused crustacean gill as a model for transbranchial transport processes. Comp Biochem Physiol B Biochem Mol Biol 2021;254:110572. doi:10.1016/j.cbpb.2021.110572, PMID:33556621.
[27] Gestin O, Lacoue-Labarthe T, Coquery M, Delorme N, Garnero L, Dherret L, *et al*. One and multi-compartments toxico-kinetic modeling to understand metals' organotropism and fate in Gammarus fossarum. Environ Int 2021;156:106625. doi:10.1016/j.envint.2021.106625, PMID:34010754.
[28] Paini A, Leonard JA, Joossens E, Bessems JGM, Desalegn A, Dorne JL, *et al*. Next generation physiologically based kinetic (NG-PBK) models in support of regulatory decision making. Comput Toxicol 2019;9:61–72. doi:10.1016/j.comtox.2018.11.002, PMID:31008414.
[29] Box GEP. Science and statistics. J Am Stat Assoc 1976;71(356):791–799. doi:10.1080/01621459.1976.10480949.
[30] Green JW, Springer TA, Holbech H. Statistical Analysis of Ecotoxicity Studies. John Wiley & Sons; 2018. doi:10.1002/9781119488798.refs.
[31] Chojnacka K, Mikulewicz M. Bioaccumulation. Encyclopedia of Toxicology (3rd Edition). Elsevier; 2014:456–460. doi:10.1016/B978-0-12-386454-3.01039-3.
[32] Marigomez I. Environmental risk assessment, marine. Encyclopedia of Toxicology (3rd Edition). Elsevier; 2014:398–401. doi:10.1016/B978-0-12-386454-3.00556-X.
[33] Ratier A, Charles S. Accumulation-depuration data collection in support of toxicokinetic modelling. Sci Data 2022;9(1):130. doi:10.1038/s41597-022-01248-y, PMID:35354827.
[34] Gobas FA, Burkhard LP, Doucette WJ, Sappington KG, Verbruggen EM, Hope BK, *et al*. Review of existing terrestrial bioaccumulation models and terrestrial bioaccumulation modeling needs for organic chemicals. Integr Environ Assess Manag 2016;12(1):123–134. doi:10.1002/ieam.1690, PMID:26272325.
[35] Grech A, Tebby C, Brochot C, Bois FY, Bado-Nilles A, Dorne JL, *et al*. Generic physiologically-based toxicokinetic modelling for fish: Integration of environmental factors and species variability. Sci Total Environ 2019;651(Pt 1):516–531. doi:10.1016/j.scitotenv.2018.09.163, PMID:30243171.
[36] Amyot M, Pinel-Alloul B, Campbell PGC, Désy JC. Total metal burdens in the freshwater amphipod *Gammarus fasciatus*: Contribution of various body parts and influence of gut contents. Freshwater Biology 1996;35:363–373. doi:10.1046/j.1365-2427.1996.00493.x.
[37] Ju YR, Chen WY, Singh S, Liao CM. Trade-offs between elimination and detoxification in rainbow trout and common bivalve molluscs exposed to metal stressors. Chemosphere 2011;85(6):1048–1056. doi:10.1016/j.chemosphere.2011.07.033, PMID:21840032.
[38] Chen W, Hoffmann AD, Liu H, Liu X. Organotropism: new insights into molecular mechanisms of breast cancer metastasis. NPJ Precis Oncol 2018;2(1):4. doi:10.1038/s41698-018-0047-0, PMID:29872722.
[39] Rocha TL, Gomes T, Pinheiro JP, Sousa VS, Nunes LM, Teixeira MR, *et al*. Toxicokinetics and tissue distribution of cadmium-based Quantum Dots in the marine mussel Mytilus galloprovincialis. Environ Pollut 2015;204:207–214. doi:10.1016/j.envpol.2015.05.008, PMID:25982546.
[40] Gust KA, Fleeger JW. Exposure-related effects on Cd bioaccumulation explain toxicity of Cd-phenanthrene mixtures in Hyalella azteca. Environ Toxicol Chem 2005;24(11):2918–2926. doi:10.1897/05-005r.1, PMID:16398129.
[41] Ingersoll CG, Brunson EL, Dwyer FJ, Ankley GT, Benoit DA, Norberg-King TJ, *et al*. Toxicity and bioaccumulation of sediment-associated contaminants using freshwater invertebrates: a review of methods and applications. Environmental Toxicology & Chemistry 1995;14(11):1885–1894. doi:10.1002/etc.5620141110.
[42] Van Geest JL, Poirier DG, Sibley PK, Solomon KR. Measuring bioaccumulation of contaminants from field-collected sediment in freshwater organisms: a critical review of laboratory methods. Environ Toxicol Chem 2010;29(11):2391–2401. doi:10.1002/etc.326, PMID:20886499.
[43] Kuehr S, Kaegi R, Maletzki D, Schlechtriem C. Testing the bioaccumulation potential of manufactured nanomaterials in the fresh-

water amphipod Hyalella azteca. Chemosphere 2021;263:127961. doi:10.1016/j.chemosphere.2020.127961, PMID:32829223.
[44] Gestin O, Lopes C, Delorme N, Garnero L, Geffard O, Lacoue-Labarthe T. Organ-specific accumulation of cadmium and zinc in Gammarus fossarum exposed to environmentally relevant metal concentrations. Environ Pollut 2022;308:119625. doi:10.1016/j.envpol.2022.119625, PMID:35714792.
[45] Zhu M, Wang Z, Chen J, Xie H, Zhao H, Yuan X. Bioaccumulation, Biotransformation, and Multicompartmental Toxicokinetic Model of Antibiotics in Sea Cucumber (*Apostichopus japonicus*). Environ Sci Technol 2020;54(20):13175–13185. doi:10.1021/acs.est.0c04421, PMID:32985863.
[46] Zhang J, Tan QG, Huang L, Ye Z, Wang X, Xiao T, *et al*. Intestinal uptake and low transformation increase the bioaccumulation of inorganic arsenic in freshwater zebrafish. J Hazard Mater 2022;434:128904. doi:10.1016/j.jhazmat.2022.128904, PMID:35452982.
[47] Ratier A, Baudrot V, Kaag M, Siberchicot A, Lopes C, Charles S. rbioacc: An R-package to analyze toxicokinetic data. Ecotoxicol Environ Saf 2022;242:113875. doi:10.1016/j.ecoenv.2022.113875, PMID: 35843108.

Journal of Exploratory Research in Pharmacology **2023** vol. 8(2) | 155–163
DOI: 10.14218/JERP.2022.00065

Review Article

Primary and Secondary Prevention in Delusional Disorder

Alexandre González-Rodríguez[1] and Mary V. Seeman[2*]

[1]*Department of Mental Health, Mutua Terrassa University Hospital, Fundació Docència i Recerca Mutua Terrassa, University of Barcelona (UB), Centro de Investigación Biomédica en Red de Salud Mental (CIBERSAM), Terrassa, Spain;* [2]*Department of Psychiatry, University of Toronto, Toronto, Canada*

Received: August 08, 2022 | **Revised:** September 05, 2022 | **Accepted:** October 25, 2022 | **Published online:** June 20, 2023

Abstract

Delusional disorder (DD), once entrenched, responds poorly to currently available treatment. This calls for community and individual preventive measures. Our goal was to conduct a literature review exploring the possibilities of prevention. This narrative review was based on a search of the PubMed database from its inception until July 2022. While not specific to DD, the search found evidence for primary and secondary strategies used to protect against or ameliorate psychotic illness characterized by prominent delusions. Community preventive strategies included addressing socioeconomic disadvantage and mental health stigma, improving mental health service accessibility, screening for and treating potential precursors to DD, such as sensory and cognitive deficits, and psychiatric symptoms, like depression, anxiety, sleep disturbance, and substance abuse. Secondary community prevention relied on early detection programs and specialized services for early treatment of DD symptoms and their co-morbidities. Individual forms of secondary prevention were interventions geared toward illness denial, treatment nonresponse and antipsychotic refusal. Effective secondary prevention reduced symptom intensity and diminished the risk of fatal outcomes such as suicide. Based mostly on the evidence from related disorders, the implementation of preventive and early treatment strategies held promise for reducing morbidity and facilitating the recovery of patients with DD.

Introduction

Delusional disorder (DD) is a schizophrenia-related disorder characterized by the presence of monosymptomatic delusions and distinguished from schizophrenia by a relative absence of hallucinations and negative symptoms such as apathy, anhedonia, and avolition. Importantly, DD first occurs in middle to late age. In addition to prominent delusional symptoms, its presentation most often includes significant depressive symptoms and relatively intact global functioning.[1] DD has traditionally been considered difficult to cure. In large part, this has been because patients did not believe that they were ill and, therefore, did not adhere to long-term treatment.[2]

DD is currently classified into subtypes according to its main delusional theme, e.g., persecutory, erotomanic, jealous, grandiose, somatic, mixed, and unspecified.[1,3] Although the current Diagnostic and Statistical Manual of Mental Disorders, Fifth Edition (DSM-5)[1] does not report on its demographics, DD is more prevalent in women than men, and the mean age at onset is approximately 45 years, which would correspond to the beginning of the decline of estrogen, or pre-menopause in women. Men with DD are more likely than women to be unmarried, and women, to be widowed.[3]

The etiology of DD is essentially unknown. Molecular genetic investigations have been limited to small association studies of dopamine receptor (DR) polymorphisms.[4] Because DD is a late-occurring condition, large family studies have not been feasible. Morimoto *et al*. examined the plasma levels of homovanillic acid (pHVA) and DR genes and their synthesizing enzyme, tyrosine hydroxylase (TH) in patients with DD and schizophrenia, as well as in healthy controls.[4] The conclusion of their study was that DD, especially the persecutory type, was a hyperdopaminergic psychosis

Keywords: Delusional disorder; Prevention; Psychosis; Treatment; Pharmacotherapy; Psychosocial management.

Abbreviations: AMDP, Manual for Assessment and Documentation of Psychopathology; AP, antipsychotics or antipsychotic medication; AUDIT, Alcohol Use Disorders Identification Test; BPRS, Brief Psychiatric Rating Scale; CBT, Cognitive Behavioral Therapy; CNV, copy number variation; CPAP, continuous positive airway pressure; DD, delusional disorder; DI, delusional infestation; DR, dopamine receptor; DSM-5, Diagnostic and Statistical Manual of Mental Disorders, Fifth Edition; DSM-IV-TR, Diagnostic and Statistical Manual of Mental Disorders, Fourth Edition, Text Revision; DUP, duration of untreated psychosis; FDA, Food and Drug Administration; GAF, Global Assessment of Functioning Scale; GMV, gray matter volume; HADES, Halle Delusional Syndromes Study; HLA, human leukocyte antigen; LOI, long-acting injectable antipsychotics; LSD, lysergic acid diethylamide; MDMA, 3,4-methylenedioxymethamphetamine; OSA, obstructive sleep apnea; pHVA, plasma homovanillic acid; SAD, social anxiety disorder; SNP, single-nucleotide polymorphism; SNV, single-nucleotide variant; SSRI, selective serotonin reuptake inhibitor; TH, tyrosine hydroxylase; WHO, World Health Organization.

[*]**Correspondence to:** Mary V. Seeman, Department of Psychiatry, University of Toronto, Toronto, ON M5T 1R8, Canada. ORCID: https://orcid.org/0000-0001-6797-3382, Tel: 1-416-486-3456, E-mail: mary.seeman@utoronto.ca

How to cite this article: González-Rodríguez A, Seeman MV. Primary and Secondary Prevention in Delusional Disorder. *J Explor Res Pharmacol* 2023;8(2):155–163. doi: 10.14218/JERP.2022.00065.

in which polymorphisms of dopamine receptors D2 and D3 played a part. Likewise, a study by Debnath *et al*.[5] confirmed the importance of human leukocyte antigen (HLA) genes in DD and emphasized the evidence for the shared nature of etiological mechanisms in this disorder and schizophrenia. Neurotransmitter abnormalities similar to those in schizophrenia (dopamine dysregulation and elevated dopamine synthesis) have also been found in DD.[6] In addition, rare copy number variations (CNVs), rare single-nucleotide variants (SNVs), and commonly found single-nucleotide polymorphisms (SNPs) are currently being investigated in schizophrenia and its several related disorders.[7] CNVs tend to be expressed in the developing brain, and they could predispose to a variety of psychiatric disorders with little diagnostic specificity. It has also been found that major psychiatric disorders share common genetic variations in neuronal, immune, and histone pathways.[7] This is consistent with clinical trials that show the symptoms of all major psychotic disorders to be responsive to the same antipsychotic medications (AP).[8]

A variety of structural brain abnormalities (relative to healthy controls) have been noted in the paranoid type of DD by Wolf *et al*.[9] They found aberrant gray matter volume (GMV) in right prefrontal regions implicated in the emotions of fear and anxiety, and in circumstances of threat. Brain abnormalities in the medial frontal and anterior cingulate cortex were also found in DD.[10] Prefrontal, parietal, temporal, thalamic, and striatal dysfunctions have been reported in delusional infestation (DI), whereas white matter volume dysfunctions were seen in patients with accompanying organic lesions.[9,11] Additionally, cerebellar dysfunctions have been specifically reported in somatic type DD.[12]

The standard treatment of DD is AP with, sometimes, adjunct antidepressants.[13] As is the case for psychotic disorders in general, current evidence favors treatment in the community as opposed to treatment in hospital[14] although a combination of both has often been necessary.[15] Furthermore, community care has been reported to significantly reduce relapses and hospital admissions, to improve medication adherence, and to result in clinical improvement more often than hospital care.[16] Community care allows for multidisciplinary psychosocial interventions, such as patient and family psychoeducation, cognitive therapy, and social skills training. Interventions such as these reduce self-stigma and are known to improve treatment effectiveness in related disorders. Family support, provision of employment opportunities, and a variety of rehabilitative strategies are offered in many community services for psychosis; they improve global functioning and aid subjectively defined recovery.[14]

Primary prevention measures, when offered to all members of a community, aim at suspected causes and known risk factors for mental illness.[17] Alternatively, specific preventive strategies are directed at groups at high risk for specific disorders. Secondary prevention addresses early detection and early intervention after symptom onset.

As in all psychiatric disorders, biological causes interact with exposures and responses to life stress. Genes and environment interact, so that modifying the environment can prevent the expression of disorder-determining genes.[18,19] Results of a recent study support the effectiveness of such preventive measures.[20]

Thus, the aim of this narrative review was to summarize the literature that examined:

1. Community level preventive strategies in DD, especially those targeting demographically vulnerable populations.
2. Individual level primary preventive strategies in DD, i.e., pharmacological and psychosocial treatment of pre-delusional psychiatric symptoms (mood, anxiety, sleep disturbance, and substance abuse), as well as potentially pre-delusional medical symptoms (sensory and cognitive deficits).
3. Secondary prevention at the community level, i.e., early detection, and at the individual level, i.e., early intensive and comprehensive treatment of the symptoms, both pharmacological and psychosocial.
4. Additional secondary strategies on an individual level, i.e., intervention directed at illness denial, treatment resistance, and AP refusal.

We conducted the review by searching the PubMed database from its inception until July 2022. Search terms were "delusional disorder" OR "delusional psychosis", AND "prevention," OR "early detection," OR "early treatment." The literature was sparse; we cite all the papers we found that addressed prevention in delusional syndromes.

Primary and secondary preventive strategies at the community level.

The World Health Organization (WHO) has defined health as "a state of complete physical, mental, and social well-being and not merely the absence of disease or infirmity".[21] This definition is based on the understanding that many precursors to mental ill health, such as socioeconomic disadvantage, air and water pollution, discrimination and stigmatization, are, in theory, preventable. Therefore, the WHO has promoted comprehensive strategies for mental health prevention.[21] Determinants of mental health go beyond the individual; they include the social, cultural, economic, and environmental milieu in which a person lives. The WHO has also acknowledged special vulnerability factors in specific populations, e.g., the physically or intellectually disabled, the frail elderly, or persons living in poverty, suffering chronic health conditions, or belonging to stigmatized minority groups.[21]

Mental and physical health are considered inseparable. Mental disabilities are disproportionally accompanied by comorbid malignancies and cardiovascular diseases. Additionally, mortality rates are high among the mentally ill because of increases in physical ill health, but also because of high rates of suicide, which is one of the leading causes of premature death in patients suffering from persistent delusions.[22] Moreover, a significant association has been found between positive psychotic symptoms (delusions and hallucinations) and suicidal ideation.[23] Nevertheless, this can be prevented by prompt treatment of psychotic symptoms with effective doses of AP. It is well known that mental illness often leads to unhealthy life choices - poor nutrition, poor hygiene, excessive alcohol and drug use, lack of sufficient physical, mental, or social activity, all of which contribute to poor health and poor quality of life. In this sense, preventive intervention, such as exercise programs, have been investigated and found effective as secondary prevention in the first episodes of psychosis.[24] Moderate exercise training was found to induce changes in the markers of oxidative stress and antioxidant concentration, with subsequent improvements in psychotic symptoms. One example of a primary prevention strategy is community infection control. It has been shown that SARS-CoV2 infection is able to induce psychosis,[25] thus implying that promotion of hygiene measures could potentially reduce the incidence of disorders such as DD.

The WHO's Comprehensive Mental Health Action Plan 2013–2030 has focused on the promotion and protection of mental health, and the prevention of mental disorders.[21] This is based on six principles and approaches: 1) universal health coverage, 2) hu-

man rights, 3) evidence-based-practice, 4) a life-course approach, 5) a multisectoral approach, and 6) empowerment of persons with mental disorders and psychosocial disabilities.

Evidence-based practice recognizes the need for robust trial methodology and reproducibility of results. The life-course approach recognizes that risk and protective factors for mental illness vary across the different life stages.

In the context of DD, a study carried out by Tizon *et al*. investigated two cohorts of patients from two different neighborhoods in Barcelona, Spain.[26] The objective of the study was to compare the prevalence, socio-demographic, and clinical factors in a catchment area consisting of 103,615 inhabitants in two neighborhoods that differed with respect to socioeconomic level and degree of psychosocial risk factors for mental illness. Tizon *et al*.[26] found that the prevalence of DD was higher in the less advantaged neighborhood. This implied that eradicating inequities in social capital could reduce the risk of DD. The study concluded by highlighting the political feasibility of such intervention and its vital importance to public health.

Wustmann *et al*.[27] conducted a project called the Halle Delusional Syndromes (HADES) study, a cross-sectional and longitudinal study investigating a sample of patients with DD, in order to determine prevalence, socio-demographics, and clinical features. Forty-three patients were recruited who fulfilled the International Classification of Diseases, Tenth Revision (ICD-10) and DSM-IV criteria for a DD diagnosis. The Brief Psychiatric Rating Scale (BPRS) and the Manual for Assessment and Documentation of Psychopathology (AMPD system) were used to evaluate symptoms, and the Global Assessment of Functioning Scale (GAF) was used to assess function. The study found some gender differences. Men tended to be single, had a history of more frequent perinatal and developmental disturbances, and came more often from lower socioeconomic classes. These findings implied that DD prevention needs to take gender into account.

Routine community screening programs for conditions that predispose to DD, such as neurological or sensory impairment, form part of primary prevention. Early detection and treatment of sensory impairments were shown to prevent not only DD, but also depressive illness and dementia in a psychiatric outpatient clinic in Ghana.[28] The paranoid subtype of DD was found in this study to be positively associated with both blindness and deafness and to be more common in women than in men.[28] More recent studies have also investigated the prevalence of vision and hearing loss in DD.[29] In a sample of 1,452 patients fulfilling DSM-5 DD criteria, 7.4% were found to have sensory deficits: vision loss (3.5%) and hearing loss (3.9%). These findings were in line with previous reports from de Portugal *et al*. who found a 5.7% prevalence of sensory deficits in DD.[30] A recent systematic review and meta-analysis also confirmed an increased risk of psychosis in patients with hearing impairment.[31] Likewise, loneliness, diminished ability to place oneself in another's shoes (impairment in the theory of mind), and disturbances of source monitoring (memory errors where the source of a memory is misattributed) were all found to be potential mechanisms underlying the association between psychosis and hearing loss.[31]

In addition, sensory impairment is known to be intimately connected with low socioeconomic status,[32] thereby doubling the risk for psychotic disorder. Effective treatment of vision and hearing loss has thus served as a potential primary preventive measure against DD. Vision rehabilitation in a general population of visually impaired adults was recently shown to improve quality of life.[33] However, no similar studies have been done in DD patients.

An important and prevalent community preventive mental health measure is the attempt to reduce mental health stigma among the public at large, in the healthcare sector, and in the workplace.[21] This strategy has shown beneficial effects in the context of severe mental illness.[34] A systematic review carried out by Hanisch *et al*. investigated the effectiveness of interventions targeting the stigma of mental illness in the workplace.[35] Employee knowledge and supportive behavior were targeted, and the results were judged successful.

The WHO's Comprehensive Mental Health Plan 2013–2030 included strategies for combating stigma in schools and in the workplace.[21] In contrast to other psychotic disorders, such as schizophrenia where patients are often too disabled to hold jobs, DD patients are very frequently employed, so that combating workplace stigma becomes particularly important.[36]

Suicidal preoccupation, which occurs in DD in 8–21% of cases[37] is critical to prevent. Cutting suicide rates by one third has, for instance, been a prime WHO target.[21] Nonetheless, the SARS-CoV-2 pandemic has increased suicide attempts in DD. Weise *et al*. reported the case of a 60-year-old woman whose first psychiatric admission was caused by an attempted suicide during the COVID pandemic.[38] The pandemic was, and continues to be, known for its potential to aggravate mental health symptoms. This implies that community level preventive measures (use of digital monitoring systems and distress phone lines), when put into effect, are able, to some extent, to reduce suicide rates. Older patients, postmenopausal women in particular, are at special risk and require extra monitoring.[39]

Another potential community strategy to prevent the development of severe mental illness such as DD is to institute programs for family psychoeducation, in order to help family members address delusional beliefs.[40] A recent review pointed out that some family responses to psychiatric symptoms appear to be more constructive than others. Stigmatization of delusional beliefs, guilt, withdrawal, anger, and fear were found counterproductive,[41] whereas calm and empathic understanding of the affect behind the delusion prevented the crystallization of delusions. It was also important for families to become acquainted with the mental health system, so that they could access the appropriate services promptly. Hence, organizing educational family group sessions relevant to mental health is considered a useful community intervention, as it is in schizophrenia.[42]

In summary, numerous community preventive strategies are possible in this population (Table 1). Combating socioeconomic disadvantage, reducing mental illness stigma, routinely screening for sensory impairment, instituting community suicide prevention, and family psychoeducation programs have been shown to be relevant preventive measures for disorders such as DD.

Primary and secondary preventive strategies on an individual level

Many of the same measures apply to individuals determined to be at risk for psychotic illness. Helping to attenuate the disadvantages of poverty by providing at-risk individuals with educational bursaries, skills training and supported employment opportunities form part of comprehensive social services. Referral to ophthalmology and otolaryngology whenever sensory impairment are suspected is standard medical practice. One study of 104 outpatients with chronic schizophrenia-spectrum disorders (which included DD) examined the factors that contributed to self-stigma, such as coping styles and symptom severity.[43] A significant positive associa-

Table 1. Community-level and individual-level strategies for prevention of delusional disorder

Target	*Strategies*
Community level	
Socioeconomic disadvantage	Subsidized skills training, supportive employment, affordable housing, disability benefits, and health insurance.[21]
Stigmatization of mental illness	Mental health advocacy, combating stigma in schools, workplaces, health system, and the general public.[34,36]
Health screening	Screening programs for sensory impairment and provision of treatment.[29]
Suicide prevention	Distress phone lines and public health announcements.[37,38]
Individual level	
Physical health	Early treatment of all physical illnesses, especially sensory and neurological that contribute to delusion formation.[32]
Suicide prevention	Close monitoring, liaison with family, recognition of warning signs, and access to immediate care for persons at risk.[37]
Life Style	Intervention and promotion (nutrition, alcohol and drug use, physical activity, and meaningful occupation).[42]
Family interventions	Family liaison and psychoeducation.[40]

tion was found between self-stigma and disorder severity, thus inferring that the effective treatment of psychotic symptoms reduced patients' tendencies to be ashamed of and blame themselves for their illness.

Treating pre-existing psychiatric conditions is an important component of prevention. Several study results have shown that patients with DD often experience a variety of non-psychotic psychiatric symptoms before they are diagnosed with DD. These were pre-morbidities whose treatment serves as primary prevention of DD. When they occur alongside DD, their early treatment serves as secondary prevention of DD severity and primary prevention of fatal outcomes such as suicide.

Early researchers who investigated this topic were Opjordsmoen and Retterstöll who, in 1993, compared clinical outcomes in two cohorts of 72 first-admission patients with DD. The first cohort was hospitalized between 1946 and 1948 (called the long-term group); the second was admitted between 1958 and 1961 (the short-term group).[44] The second group, treated in hospital with antidepressants and AP, showed no improvement in outcome over that of the first group, whose hospitalizations predated the introduction of either of these classes of drugs. These findings implied that patients with DD were not better off when treated with AP + antidepressants. However, it is possible that treatment non-adherence – usually considered particularly high in DD - could have influenced these results.

The coexistence of mood disorders occurs in approximately half of all DD patients according to a study conducted by Marino *et al*.[45] This study also found a familial risk for both DD and mood disorder and reported that mood symptoms, when present, preceded DD about half the time. This is important clinical information that can serve preventive ends.

Furthermore, in a cohort of 64 DD patients, Maina *et al*.[46] found that 72% suffered from at least one comorbid psychiatric disorder. In their study, comorbid affective disorders only preceded the onset of DD in younger patients with relatively early DD onset. Likewise, de Portugal *et al*.[47] found that, out of 86 DD outpatients, 46% presented with signs of depression or anxiety. Patients with comorbidity had more somatic delusions, non-prominent hallucinations, and exhibited a higher suicide risk than those without comorbidity.[47] The implication was that active treatment of comorbidity could reduce psychotic symptom severity and, perhaps, lower the risk of suicide.

González-Rodríguez *et al*. carried out a cross-sectional study of 44 patients with DD who fulfilled DSM-IV-TR criteria.[48] From the total sample, 15 patients (34.1%) presented with comorbid depressive symptoms, 14 (31.8%) showed suicidal ideation, and seven (15.9%) showed recent (within the prior two years) suicidal behavior. Patients with comorbid depression had an earlier age at onset and suffered a greater intensity of suicidal ideation, again implying that early treatment of depression could reduce the risk of suicide. The results of a recent review were also consistent with these findings.[49]

Veras *et al*. reported four cases of patients first diagnosed with social anxiety disorder (SAD) that was followed, after a period of time, by a diagnosis of DD.[50] SAD, in some cases, can be a prodromal form of DD.

Panic attacks have also been associated with psychoticism,[51] but this possibility has not been systematically addressed in DD. Gupta and Kulhara[52] reported one case of a woman who first presented with a history of panic attacks, and subsequently developed persecutory delusions that fulfilled the DD criteria. The patient suffered from anticipatory anxiety and systematized persecutory delusions and received a diagnosis of a DD persecutory type with comorbid panic attacks, which remitted with AP treatment. While this was only one case, it was consistent with other studies that pointed to anxiety disorders in general as being potentially a premorbid manifestation of DD.

Substance use disorder is a further important co-morbidity that, when treated, could prevent or reduce the severity of DD, as was demonstrated in patients with first-episode psychosis.[53] de Portugal *et al*., using DSM-IV-TR criteria, carried out a cross-sectional study of 86 DD outpatients with and without pre-morbid substance use disorder.[3] They found that men had a significantly higher frequency of premorbid substance use than women (30.3%

Table 2. Early detection of non-psychotic psychiatric comorbidities

	Hypotheses	Strategies
Affective comorbidities		
Affective symptoms prior to the onset of DD	Could increase risk of DD and self-injury or suicide.[49]	Early antidepressant Rx to reduce symptoms and suicide risk.[48]
Affective symptoms after the onset of DD	Early Rx, especially in somatic DD, can reduce the severity of symptoms.[77]	Early Rx to prevent poor outcomes.[44]
Anxiety comorbidities		
Social anxiety disorder (SAD)	SAD could lead to delusions.[50]	CBT for SAD.[50]
Panic attacks	Anticipatory anxiety and panic could lead to DD.[52]	CBT for panic.[52]
Sleep disorders		
Insomnia	Insomnia can worsen DD symptoms.[62,63]	Rx of insomnia improves outcome.[62]
Sleep apnea (OSA)	OSA can increase symptom severity, especially negative symptoms.[60]	Screening and Rx for OSA.[60]
Substance use disorders		
Alcohol and other drug use disorders	Substance use can worsen DD symptoms.[55,57]	Early detection of substance use, esp. targeting men, and prompt Rx.[55]

CBT, cognitive behavioral therapy; DD, delusional disorder.

vs. 11.3%). This confirmed the results of Román-Avezuela *et al*.[54] who, in a study of 50 inpatients with DD, also showed that men far more often than women were diagnosed with comorbid substance use disorders (40.9% *vs.* 3.6%). This was true for alcohol (22.7% *vs.* 3.6%) and for cannabis (22.7% *vs.* 0%), thus indicating that prevention and early treatment of substance abuse could be an effective risk management technique in men.

Kulkarni *et al*. investigated a cohort of 445 patients with persistent DD (men: 236, women: 219) from a tertiary center in India.[55] Men more often than women presented with comorbid substance use disorders (24.1% *vs.* 1.8%). The most common psychotic content in the context of this comorbidity was the delusional convictions of partner infidelity or Othello syndrome, which has long been associated with alcohol use disorders.[56] These findings were consistent with the results of a cross-sectional study of patients with first-episode of psychosis from Northern India.[42] A semi-structured interview was used in this latter research to assess clinical variables as well as information regarding the use of substances: age at first consumption, type of substance used, and duration and pattern of substance use. Cannabis use was assessed by urine testing, whereas alcohol use was evaluated using the Alcohol Use Disorder Identification Test (AUDIT). In accordance with the studies listed previously, men were significantly more frequently diagnosed than women with alcohol use disorders. Treating substance abuse early can also prevent medical sequelae secondary to an excessive intake of alcohol.[57] Substance use treatment should also be able to increase adherence to DD management.

Another frequent premorbid as well as comorbid condition in psychotic disorders is sleep disorder[58] and its treatment has been shown to reduce the severity of psychosis.[59] Moreover, insomnia and nightmares have been called out as potential risk factors for the onset and persistence of psychotic symptoms.[60] Kasanova *et al*.[61] investigated the temporal relationship between sleep disturbances, sleep quality and occurrence of paranoid ideation in 42 acutely paranoid and 32 non-paranoid individuals, and 41 further study participants with schizotypal traits. Poor subjective sleep quality at night was associated with greater paranoid ideation the following morning.[61] Sleep disturbances specifically in DD have not been investigated but a review conducted by our team[62] has recommended early identification and treatment of sleep problems because of the link not only with paranoid ideation but also with cognitive impairment and suicidal ideation.

As has been previously mentioned, DD usually begins at middle age, which, in women, corresponds to the period of menopausal transition. This period, and the postmenopausal stage that follows, are associated with a significant increase in sleep disturbances such as sleep apnea, insomnia and restless leg syndrome, all of which impact quality of life, health, and social and personal functioning.[63] During perimenopause, insomnia is the most frequently experienced and treatable sleep disorder.[64] Effective treatment of pre-existing sleep problems could prevent the onset of psychotic thinking and can reduce symptom severity if diagnosed after the onset of psychosis[65] although this has not yet been specifically studied in DD.

In summary, treating associated psychiatric disorders early, whether they precede or are comorbid with DD, could serve as a protective measure (Table 2).

Benefits of starting DD treatment early

The early identification and treatment of psychotic symptoms have been widely considered to benefit patients suffering from psychotic disorders. Several studies have reported that early intervention services are superior to standard care in terms of remission rates, hospitalization rates, and social and personal functioning.[66] These studies, however, have usually been done in early onset schizophrenia with patients who were adolescents or young adults. Very few studies had addressed the potential benefits of treating DD patients (usually middle aged and elderly adults) as early as possible after the onset of psychotic symptoms.

Age is an important variable. A case register study of 236 patients with delusional infestation who attended four special-

Table 3. Management of treatment-resistant DD and antipsychotic refusal

Clinical scenario	Hypotheses	Strategies
Treatment-resistant DD	Drugs with affinity for multiple receptors may overcome resistance.[8]	Check adherence. Motivate adherence. Try clozapine. Try LAIs.[74]
Antipsychotic refusal	Denial of illness and intolerance of side-effects can result in drug refusal.[77]	Explain the wide application of APs. Try antidepressants[8] and psychoRx.[73]

APs, Antipsychotics; LAI, long-acting injectables; DD, delusional disorder.

ized clinics in the United Kingdom, Italy, and Russia[67] described clinical outcomes and compared them with those of previous cohort studies. A total of 189 patients were followed longitudinally and classified according to age: <55 years, 56–75 years, and >75 years. Younger age was associated with better clinical outcomes. A longer duration of untreated psychosis (DUP) correlated positively with worse outcomes, which suggested that early detection and treatment of DD could improve prognosis, at least for the delusional infestation form of the disorder. These findings were consistent with previous studies in delusional parasitosis,[68] notably with those from specialty clinics in Austria.[69] Two recent studies also confirmed that later age at onset and longer DUP in delusional infestation was associated with poor outcome.[70,71]

In summary, the very scant available literature suggests that early AP intervention in DD can produce several benefits. Early treatment with antidepressants, as noted earlier, reduces suicidal ideation.

What can be done for treatment resistance or antipsychotic refusal?

Approximately one third of patients with schizophrenia are treatment resistant, meaning that positive symptoms persist despite two or more trials of an adequate dose and duration of AP (with documented adherence).[72] Strong evidence does not exist for DD, but the mode of action of AP has been deemed analogous in the two conditions, which would make treatment resistance equally likely. An observational registry cohort study from Sweden compared the effectiveness of various pharmacotherapies in the prevention of hospitalization and work disability in DD populations.[73] The results showed that the use of clozapine and a long-acting injectable (LOA) AP was associated with the lowest risk of hospitalization. The use of both LOA and oral aripiprazole correlated positively with the lowest risk of work disability. The relatively superior performance of LOAs suggests that a lack of adherence could explain a large part of the failure to respond to treatment. The reason for the superiority of clozapine over other AP still remains unknown but several hypotheses exist, such as clozapine's affinity for the serotonin receptor (5-HT2R), for the dopamine 1 receptor (D1), for the adrenoreceptor (α2c), and for muscarinic receptors (M1-M4).[74]

In addition, there is evidence that many DD patients refuse AP treatment, chiefly because they do not consider themselves 'psychotic,' but also because they cannot tolerate the side effects.[73] Brownstone *et al*.[75] have provided some tips on how best to address the issue of AP refusal in the context of delusional parasitosis, sometimes referred to as delusional infestation (DI). They recommend introducing the use of an AP by explaining that medications are often used for symptoms and not necessarily for their original indication. They stated that: "One way to get the patient to accept AP treatment is to offer a medication that has no US Food and Drug Administration (FDA) psychiatric indication because DI patients are universally opposed to taking medications involving mental illness." Because the AP, pimozide, is only FDA indicated for Tourette's syndrome and not psychosis they reported being able to convince their patients to take it.

In the same spirit, clinicians offer antidepressants instead of AP because many patients with DD readily admit that they are depressed. Though the available evidence for antidepressant effectiveness in most cases of DD is weak, there are reports of the efficacy of clomipramine and other antidepressants in the treatment of the somatic subtype (Table 3).[8,76,77]

Previous studies have reported that cognitive-behavioral therapy (CBT) is effective in treating delusional symptoms in schizophrenia patients, as well as in DD.[72,78] One trial compared patients with DD who received CBT with a placebo-control group who received an equal amount of medical attention. The results showed that CBT had a higher impact than placebo on the affect relating to delusional belief, strength of conviction, and on proneness to act on delusional beliefs.[78] This suggests that secondary prevention in the form of psychotherapy, when added to pharmacological treatment, might shorten the duration of symptoms and prevent negative sequelae.

Discussion

The goal of primary prevention in mental health is to reduce incidence by intervening prior to the onset of illness.[79] Through early detection and prompt treatment, secondary prevention aims to reduce severity and disability, as well as prevent recurrence and, thus, reduce prevalence.[80] Poor mental health in a community is a concern because it leads to widespread disability and mortality; it is also an economic concern[81] as well as a cause of major personal and family distress. Prevention, therefore, addresses public health as well as individual health and quality of life.[80]

Delusional disorder (DD) is considered a schizophrenia-related disorder, and, by implication, a severe mental illness associated with disability and suicide, sometimes homicide.[81] It is an understudied disorder, which is why we chose to review the literature pertaining to its primary and secondary prevention.

To address our three aims, we examined the literature on community and individual opportunities for preventive interventions. In considering the establishment of a clinical service to prevent psychosis, Salazar de Pablo *et al*.[82] systematically reviewed the relevant prevention literature. Although the evidence came mostly from the field of schizophrenia, especially first episode schizophrenia, the conclusions of the review were that clinical monitoring, psychoeducation, antidepressants, psychosocial support, and family intervention were the most effective prevention strategies. Less effective but still recommended measures were anxiolytics, mood stabilizers, and physical health interventions. The authors recommended a multidisciplinary approach, a rapid response to referrals, and flexibility with regard to assessment times and settings (e.g. possibility of home visits after office hours). They also supported a transdiagnostic approach.[83] A transdiagnostic approach is consistent with our findings that DD can follow from prior mood

and anxiety dysregulation or substance abuse, or sleep disturbance, or sensory impairment.

At the individual level, the literature emphasizes that lifestyle issues are important in prevention - healthy living, diet, exercise, social activity, solid relationships, social and personal functioning and occupation. Exploring personal stress reduction techniques is also relevant.[84] Greater accessibility to mental health and social services to rural communities, impoverished and immigrant communities, patients with physical disabilities, women with childcare responsibilities, and workers unable to take time off work are also vital.[85]

The literature has described modifiable and nonmodifiable risk factors and primary prevention strategies for major depressive disorders and for suicidal patients and for elderly psychiatric patients.[86] These strategies apply to DD patients.

Comorbidities (depression, anxiety, sleep disturbance, substance abuse, and sensory impairment) are often present in DD and their early and comprehensive treatment reduces DD symptoms and prevents sequelae such as injury to self and other.[68]

Demographic factors, such as age, gender, minority status, employment, marriage, parental, or immigrant status require specially tailored and targeted interventions.[86,87]

Future directions

Because delusional disorder (DD) is a less well-recognized disorder than schizophrenia or depression or dementia, preventive clinical services have not been devoted to this disorder, or the age group most at risk for this disorder, the same way that has been done[82,86] for more prevalent forms of psychiatric disease. Similar preventive measures apply – psychoeducation, screening, early intervention and psychosocial support for individuals most at risk. Telepsychiatry and outreach to remote communities is the way of the future and has already begun. With respect to improved early treatment effectiveness, genotyping and matching patient to a personally effective therapeutic drug is now underway in many medical specialties. Psychiatric disorders are more complex, but psychiatry will, in the near future, also become the beneficiary of precision medicine.

Conclusions

Because DD is universally considered a relatively treatment-resistant disorder, it is important to prevent this disorder whenever possible by vigorously screening for and treating delusion-inducing medical and psychiatric conditions. Once the disorder has been diagnosed, antipsychotic medication is the treatment of choice. Patients, however, often do not perceive themselves as ill and, therefore refuse psychiatric intervention. Psychosocial treatments are more readily accepted. Although the literature is sparse, the evidence for the success of preventive measures is growing.

Acknowledgments

None.

Funding

No funding has been received for this manuscript.

Conflict of interest

AGR received registration for congresses and travel funds for them from Janssen-Cilag, Lundbeck-Otsuka, Angelini, and Pfizer.

Author contributions

AGR and MVS wrote parts of the first draft of the manuscript and worked together to improve the subsequent versions. Both authors approved the final version of the manuscript.

References

[1] American Psychiatric Association. Diagnostic and Statistical Manual of Mental Disorders: DSM-5. 5th edition. Arlington, VA: American Psychiatric Publishing; 2013. doi:10.1176/appi.books.9780890425596.

[2] González-Rodríguez A, Esteve M, Álvarez A, Guàrdia A, Monreal JA, Palao D, *et al*. What we know and still need to know about gender aspects of delusional disorder: A narrative review of recent work. J Psychiatry Brain Sci 2019;4(3):e190009. doi:10.20900/jpbs.20190009.

[3] de Portugal E, González N, Miriam V, Haro JM, Usall J, Cervilla JA. Gender differences in delusional disorder: Evidence from an outpatient sample. Psychiatry Res 2010;177(1-2):235–239.

[4] Morimoto K, Miyatake R, Nakamura M, Watanabe T, Hirao T, Suwaki H. Delusional disorder: molecular genetic evidence for dopamine psychosis. Neuropsychopharmacology 2002;26(6):794–801. doi:10.1016/S0893-133X(01)00421-3, PMID:12007750.

[5] Debnath M, Das SK, Bera NK, Nayak CR, Chaudhuri TK. Genetic associations between delusional disorder and paranoid schizophrenia: A novel etiologic approach. Can J Psychiatry 2006;51(6):342–349. doi:10.1177/070674370605100602, PMID:16786814.

[6] Cheng PWC, Chang WC, Lo GG, Chan KWS, Lee HME, Hui LMC, *et al*. The role of dopamine dysregulation and evidence for the transdiagnostic nature of elevated dopamine synthesis in psychosis: a positron emission tomography (PET) study comparing schizophrenia, delusional disorder, and other psychotic disorders. Neuropsychopharmacology 2020;45(11):1870–1876. doi:10.1038/s41386-020-0740-x, PMID:32612207.

[7] Kato H, Kimura H, Kushima I, Takahashi N, Aleksic B, Ozaki N. The genetic architecture of schizophrenia: review of large-scale genetic studies. J Hum Genet 2022. doi:10.1038/s10038-022-01059-4, PMID:35821406.

[8] Guàrdia A, González-Rodríguez A, Seeman MV, Álvarez A, Estrada F, Acebillo S, *et al*. Dopamine, serotonin, and structure/function brain defects as biological bases for treatment response in delusional disorder: a systematic review of cases and cohort studies. Behav Sci (Basel) 2021;11(10):141. doi:10.3390/bs11100141, PMID:34677234.

[9] Wolf RC, Hildebrandt V, Schmitgen MM, Pycha R, Kirchler E, Macina C, *et al*. Aberrant gray matter volume and cortical surface in paranoid-type delusional disorder. Neuropsychobiology 2020;79(4-5):335–344. doi:10.1159/000505601, PMID:32160619.

[10] Vicens V, Radua J, Salvador R, Anguera-Camós M, Canales-Rodríguez EJ, Sarró S, *et al*. Structural and functional brain changes in delusional disorder. Br J Psychiatry 2016;208(2):153–159. doi:10.1192/bjp.bp.114.159087, PMID:26382955.

[11] Wolf RC, Huber M, Depping MS, Thomann PA, Karner M, Lepping P, *et al*. Abnormal gray and white matter volume in delusional infestation. Prog Neuropsychopharmacol Biol Psychiatry 2013;46:19–24. doi:10.1016/j.pnpbp.2013.06.004, PMID:23791615.

[12] Krämer J, Huber M, Mundinger C, Schmitgen MM, Pycha R, Kirchler E, *et al*. Abnormal cerebellar volume in somatic vs. non-somatic delusional disorders. Cerebellum Ataxias 2020;7:2. doi:10.1186/s40673-020-0111-8, PMID:31993210.

[13] Manschreck TC, Khan NL. Recent advances in the treatment of delusional disorder. Can J Psychiatry 2006;51(2):114–119. doi:10.1177/070674370605100207, PMID:16989110.

[14] Thornicroft G, Deb T, Henderson C. Community mental health care worldwide: current status and further developments. World Psychiatry 2016;15(3):276–286. doi:10.1002/wps.20349, PMID:27717265.

[15] Thornicroft G, Tansella M. The balanced care model for global mental health. Psychol Med 2013;43(4):849–863. doi:10.1017/S0033291712001420, PMID:22785067.

[16] Armijo J, Méndez E, Morales R, Schilling S, Castro A, Alvarado R, *et al*.

Efficacy of community treatments for schizophrenia and other psychotic disorders: a literature review. Front Psychiatry 2013;4:116. doi:10.3389/fpsyt.2013.00116, PMID:24130534.
[17] Min JA, Lee CU, Lee C. Mental health promotion and illness prevention: a challenge for psychiatrists. Psychiatry Investig 2013;10(4):307–316. doi:10.4306/pi.2013.10.4.307, PMID:24474978.
[18] Jaffee SR, Price TS. Gene-environment correlations: a review of the evidence and implications for prevention of mental illness. Mol Psychiatry 2007;12(5):432–442. doi:10.1038/sj.mp.4001950, PMID:17453060.
[19] Jaffee SR, Price TS. The implications of genotype-environment correlation for establishing causal processes in psychopathology. Dev Psychopathol 2012;24(4):1253–1264. doi:10.1017/S0954579412000685, PMID:23062295.
[20] DeRosse P, Barber AD. Overlapping neurobiological substrates for early-life stress and resilience to psychosis. Biol Psychiatry Cogn Neurosci Neuroimaging 2021;6(2):144–153. doi:10.1016/j.bpsc.2020.09.003, PMID:33097471.
[21] WHO. Comprehensive mental health action plan 2013-2030. Geneva: World Health Organization; 2021.
[22] Freeman D, Bold E, Chadwick E, Taylor KM, Collett N, Diamond R, *et al*. Suicidal ideation and behaviour in patients with persecutory delusions: Prevalence, symptom associations, and psychological correlates. Compr Psychiatry 2019;93:41–47. doi:10.1016/j.comppsych.2019.07.001, PMID:31319194.
[23] Bornheimer LA, Jaccard J. Symptoms of depression, positive symptoms of psychosis, and suicidal ideation among adults diagnosed with schizophrenia within the clinical antipsychotic trials of intervention effectiveness. Arch Suicide Res 2017;21(4):633–645. doi:10.1080/13811118.2016.1224990, PMID:27552340.
[24] Fisher E, Wood SJ, Elsworthy RJ, Upthegrove R, Aldred S. Exercise as a protective mechanism against the negative effects of oxidative stress in first-episode psychosis: a biomarker-led study. Transl Psychiatry 2020;10(1):254. doi:10.1038/s41398-020-00927-x, PMID:32709912.
[25] Postolache TT, Benros ME, Brenner LA. Targetable biological mechanisms implicated in emergent psychiatric conditions associated with SARS-CoV-2 infection. JAMA Psychiatry 2021;78(4):353–354. doi:10.1001/jamapsychiatry.2020.2795, PMID:32735332.
[26] Tizón J, Morales N, Artigue J, Quijada Y, Pérez C, Pareja F, *et al*. Delusional disorders: Prevalence in two socially differentiated neighborhoods of Barcelona. Psychosis 2014;6(2):107–116. doi:10.1080/17522439.2013.773364.
[27] Wustmann T, Pillmann F, Friedemann J, Piro J, Schmeil A, Marneros A. The clinical and sociodemographic profile of persistent delusional disorder. Psychopathology 2012;45(3):200–202. doi:10.1159/000332004, PMID:22441422.
[28] Turkson SN, Asamoah V. Common psychiatric disorders among the elderly attending a general psychiatric out patient clinic in Accra, Ghana: a five year retrospective study (1989-1993). West Afr J Med 1997;16(3):146–149. PMID:9329282.
[29] Porras-Segovia A, Guerrero Jiménez M, Carrillo de Albornoz Calahorro C, Cervilla J. Comorbidity between delusional disorder and sensory deficits. Results from the deliranda case register. Eur Psychiatry 2016;33(Suppl):S144–S145. doi:10.1016/j.eurpsy.2016.01.249.
[30] de Portugal E, González N, del Amo V, Haro JM, Díaz-Caneja CM, Luna del Castillo Jde D, *et al*. Empirical redefinition of delusional disorder and its phenomenology: the DELIREMP study. Compr Psychiatry 2013;54(3):243–255. doi:10.1016/j.comppsych.2012.08.002, PMID:23021895.
[31] Linszen MM, Brouwer RM, Heringa SM, Sommer IE. Increased risk of psychosis in patients with hearing impairment: Review and meta-analyses. Neurosci Biobehav Rev 2016;62:1–20. doi:10.1016/j.neubiorev.2015.12.012, PMID:26743858.
[32] Demmin DL, Silverstein SM. Visual impairment and mental health: unmet needs and treatment options. Clin Ophthalmol 2020;14:4229–4251. doi:10.2147/OPTH.S258783, PMID:33299297.
[33] van Nispen RM, Virgili G, Hoeben M, Langelaan M, Klevering J, Keunen JE, *et al*. Low vision rehabilitation for better quality of life in visually impaired adults. Cochrane Database Syst Rev 2020;1(1):CD006543. doi:10.1002/14651858.CD006543.pub2, PMID:31985055.
[34] Taghva A, Farsi Z, Javanmard Y, Atashi A, Hajebi A, Noorbala AA. Strategies to reduce the stigma toward people with mental disorders in Iran: stakeholders' perspectives. BMC Psychiatry 2017;17(1):17. doi:10.1186/s12888-016-1169-y, PMID:28088199.
[35] Hanisch SE, Twomey CD, Szeto AC, Birner UW, Nowak D, Sabariego C. The effectiveness of interventions targeting the stigma of mental illness at the workplace: a systematic review. BMC Psychiatry 2016;16:1. doi:10.1186/s12888-015-0706-4, PMID:26739960.
[36] Hampson ME, Watt BD, Hicks RE. Impacts of stigma and discrimination in the workplace on people living with psychosis. BMC Psychiatry 2020;20(1):288. doi:10.1186/s12888-020-02614-z, PMID:32513133.
[37] González-Rodríguez A, Molina-Andreu O, Navarro Odriozola V, Gastó Ferrer C, Penadés R, Catalán R. Suicidal ideation and suicidal behaviour in delusional disorder: a clinical overview. Psychiatry J 2014;2014:834901. doi:10.1155/2014/834901, PMID:24829903.
[38] Weise J, Schomerus G, Speerforck S. [The SARS-CoV-2 pandemic and an attempted suicide of a patient with delusional disorder]. Psychiatr Prax 2020;47(4):218–220. doi:10.1055/a-1158-1745, PMID:32340051.
[39] González-Rodríguez A, Seeman MV, Izquierdo E, Natividad M, Guàrdia A, Román E, *et al*. Delusional disorder in old age: a hypothesis-driven review of recent work focusing on epidemiology, clinical aspects, and outcomes. Int J Environ Res Public Health 2022;19(13):7911. doi:10.3390/ijerph19137911, PMID:35805570.
[40] González-Rodríguez A, Seeman MV. Addressing delusions in women and men with delusional disorder: key points for clinical management. Int J Environ Res Public Health 2020;17(12):4583. doi:10.3390/ijerph17124583, PMID:32630566.
[41] Menculini G, Balducci PM, Moretti P, Tortorella A. 'Come share my world' of 'madness': a systematic review of clinical, diagnostic and therapeutic aspects of folie à deux. Int Rev Psychiatry 2020;32(5-6):412–423. doi:10.1080/09540261.2020.1756754, PMID:32363956.
[42] Banyal N, Bhattacharyya D, Yadav P. Study to determine the prevalance of substance use and factors associated with it, in first-episode of psychosis. Ind Psychiatry J 2018;27(2):264–270. doi:10.4103/ipj.ipj_86_18, PMID:31359982.
[43] Holubova M, Prasko J, Hruby R, Latalova K, Kamaradova D, Marackova M, *et al*. Coping strategies and self-stigma in patients with schizophrenia-spectrum disorders. Patient Prefer Adherence 2016;10:1151–1158. doi:10.2147/PPA.S106437, PMID:27445463.
[44] Opjordsmoen S, Retterstöl N. Outcome in delusional disorder in different periods of time. Possible implications for treatment with neuroleptics. Psychopathology 1993;26(2):90–94. doi:10.1159/000284805, PMID:8100636.
[45] Marino C, Nobile M, Bellodi L, Smeraldi E. Delusional disorder and mood disorder: can they coexist? Psychopathology 1993;26(2):53–61. doi:10.1159/000284800, PMID:8321893.
[46] Maina G, Albert U, Badà A, Bogetto F. Occurrence and clinical correlates of psychiatric co-morbidity in delusional disorder. Eur Psychiatry 2001;16(4):222–228. doi:10.1016/s0924-9338(01)00568-5, PMID:11418272.
[47] de Portugal E, Martínez C, González N, del Amo V, Haro JM, Cervilla JA. Clinical and cognitive correlates of psychiatric comorbidity in delusional disorder outpatients. Aust N Z J Psychiatry 2011;45(5):416–425. doi:10.3109/00048674.2010.551279, PMID:21417554.
[48] González-Rodríguez A, Molina-Andreu O, Penadés Rubio R, Catalán Campos R, Bernardo Arroyo M. [Clinical significance of suicidal behaviour in delusional disorder: a 44 case-series descriptive study]. Med Clin (Barc) 2014;142(7):299–302. doi:10.1016/j.medcli.2013.04.029, PMID:23768464.
[49] Guàrdia A, González-Rodríguez A, Álvarez A, Betriu M, Estrada F, Parra I, *et al*. Systematic review of the prevalence of suicidal ideation and suicidal behavior in delusional disorder. Eur Psychiatry 2019;56S:S1–S900.
[50] Veras AB, Souza TG, Ricci TG, de Souza CP, Moryiama MC, Nardi AE, *et al*. Paranoid delusional disorder follows social anxiety disorder in a long-term case series: evolutionary perspective. J Nerv Ment Dis 2015;203(6):477–479. doi:10.1097/NMD.0000000000000311, PMID:26034873.
[51] Goodwin RD, Fergusson DM, Horwood LJ. Panic attacks and psychoticism. Am J Psychiatry 2004;161(1):88–92. doi:10.1176/appi.ajp.161.1.88, PMID:14702255.
[52] Gupta N, KuLhara P. Co-occurrence of panic attacks in delusional disorder. Psychiatry Clin Neurosci 2001;55(6):653. doi:10.1046/j.1440-1819.2001.00920_55_6.x, PMID:11737801.
[53] Herman Y, Norouzian N, MacKenzie LE. An integrated substance use

treatment model for young adults with first-episode psychosis: A naturalistic pilot evaluation. Early Interv Psychiatry 2022. doi:10.1111/eip.13337, PMID:35932200.
[54] Román Avezuela N, Esteve Díaz N, Domarco Manrique L, Domínguez Longás A, Miguélez Fernández C, de Portugal E. Gender differences in delusional disorder. Rev Asoc Esp Neuropsiq 2015;35(125):37–51. doi:10.4321/S0211-57352015000100004.
[55] Kulkarni KR, Arasappa R, Prasad MK, Zutshi A, Chand PK, Murthy P, *et al*. Gender differences in persistent delusional disorder. Indian J Psychol Med 2017;39(2):216–217. doi:10.4103/0253-7176.203123, PMID:28515568.
[56] Graff-Radford J, Whitwell JL, Geda YE, Josephs KA. Clinical and imaging features of Othello's syndrome. Eur J Neurol 2012;19(1):38–46. doi:10.1111/j.1468-1331.2011.03412.x, PMID:21518145.
[57] Gaughran F, Stahl D, Patel A, Ismail K, Smith S, Greenwood K, *et al*. A health promotion intervention to improve lifestyle choices and health outcomes in people with psychosis: a research programme including the IMPaCT RCT. Southampton (UK): NIHR Journals Library; 2020. PMID:31999410.
[58] Schennach R, Feige B, Riemann D, Heuser J, Voderholzer U. Pre- to post-inpatient treatment of subjective sleep quality in 5,481 patients with mental disorders: A longitudinal analysis. J Sleep Res 2019;28(4):e12842. doi:10.1111/jsr.12842, PMID:30907038.
[59] Freeman D, Sheaves B, Waite F, Harvey AG, Harrison PJ. Sleep disturbance and psychiatric disorders. Lancet Psychiatry 2020;7(7):628–637. doi:10.1016/S2215-0366(20)30136-X, PMID:32563308.
[60] Waite F, Sheaves B, Isham L, Reeve S, Freeman D. Sleep and schizophrenia: From epiphenomenon to treatable causal target. Schizophr Res 2020;221:44–56. doi:10.1016/j.schres.2019.11.014, PMID:31831262.
[61] Kasanova Z, Hajdúk M, Thewissen V, Myin-Germeys I. Temporal associations between sleep quality and paranoia across the paranoia continuum: An experience sampling study. J Abnorm Psychol 2020;129(1):122–130. doi:10.1037/abn0000453, PMID:31343182.
[62] González-Rodríguez A, Labad J, Seeman MV. Sleep disturbances in patients with persistent delusions: Prevalence, clinical associations, and therapeutic strategies. Clocks Sleep 2020;2(4):399–415. doi:10.3390/clockssleep2040030, PMID:33118525.
[63] Schaedel Z, Holloway D, Bruce D, Rymer J. Management of sleep disorders in the menopausal transition. Post Reprod Health 2021;27(4):209–214. doi:10.1177/20533691211039151, PMID:34748453.
[64] Caretto M, Giannini A, Simoncini T. An integrated approach to diagnosing and managing sleep disorders in menopausal women. Maturitas 2019;128:1–3. doi:10.1016/j.maturitas.2019.06.008, PMID:31561815.
[65] Myles H, Myles N, Coetzer CLC, Adams R, Chandratilleke M, Liu D, *et al*. Cognition in schizophrenia improves with treatment of severe obstructive sleep apnoea: A pilot study. Schizophr Res Cogn 2019;15:14–20. doi:10.1016/j.scog.2018.09.001, PMID:30450286.
[66] Malla A, McGorry P. Early intervention in psychosis in young people: A population and public health perspective. Am J Public Health 2019;109(S3):S181–S184. doi:10.2105/AJPH.2019.305018, PMID:31242015.
[67] Romanov DV, Lepping P, Bewley A, Huber M, Freudenmann RW, Lvov A, *et al*. Longer duration of untreated psychosis is associated with poorer outcomes for patients with delusional infestation. Acta Derm Venereol 2018;98(9):848–854. doi:10.2340/00015555-2888, PMID:29362814.
[68] Rodríguez-Alonso B, Álvarez-Artero E, Martínez-Goñi R, Almeida H, Casado-Espada NM, Jaén-Sánchez N, *et al*. Delusional parasitosis. A multicenter retrospective study in Spanish infectious disease services. Enferm Infecc Microbiol Clin (Engl Ed) 2021;39(5):223–228. doi:10.1016/j.eimc.2020.07.009, PMID:33010962.
[69] Musalek M, Bach M, Gestberger K, Lesch OM, Passweg V, Wancata J, *et al*. Zur pharmakotherapie des dermatozoenwahns. Wien Med Wochenschr 1989;139:297–302.
[70] Lepping P, Aboalkaz S, Squire SB, Romanov DV, Bewley A, Huber M, *et al*. Later age of onset and longer duration of untreated psychosis are associated with poorer outcome in delusional infestation. Acta Derm Venereol 2020;100(16):adv00261. doi:10.2340/00015555-3625, PMID:32852560.
[71] Linder D. Delusional Infestation - Importance of Early Treatment. Acta Derm Venereol 2020;100(16):adv00262. doi:10.2340/00015555-3626, PMID:32964940.
[72] Skelton M, Khokhar WA, Thacker SP. Treatments for Delusional Disorder. Schizophr Bull 2015;41(5):1010–1012. doi:10.1093/schbul/sbv080, PMID:26209547.
[73] Lähteenvuo M, Taipale H, Tanskanen A, Mittendorfer-Rutz E, Tiihonen J. Effectiveness of pharmacotherapies for delusional disorder in a Swedish national cohort of 9076 patients. Schizophr Res 2021;228:367–372. doi:10.1016/j.schres.2021.01.015, PMID:33548837.
[74] de Bartolomeis A, Vellucci L, Barone A, Manchia M, De Luca V, Iasevoli F, *et al*. Clozapine's multiple cellular mechanisms: What do we know after more than fifty years? A systematic review and critical assessment of translational mechanisms relevant for innovative strategies in treatment-resistant schizophrenia. Pharmacol Ther 2022;236:108236. doi:10.1016/j.pharmthera.2022.108236, PMID:35764175.
[75] Brownstone N, Howard J, Koo J. Management of delusions of parasitosis: an interview with experts in psychodermatology. Int J Womens Dermatol 2022;8(3):e035. doi:10.1097/JW9.0000000000000035, PMID:35822193.
[76] Delgado L, González-Rodríguez A, Pedrero AA, Guàrdia A, Fucho GF, Seeman MV, *et al*. Successful treatment of primary delusional parasitosis with paroxetine: A case report and narrative review. Eur Psychiatry 2021;64(Suppl 1):S317. doi:10.1192/j.eurpsy.2021.851.
[77] Dimopoulos NP, Mitsonis CI, Psarra VV. Delusional disorder, somatic type treated with aripiprazole—mirtazapine combination. J Psychopharmacol 2008;22(7):812–814. doi:10.1177/0269881107082905, PMID:18308798.
[78] O'Connor K, Stip E, Pélissier MC, Aardema F, Guay S, Gaudette G, *et al*. Treating delusional disorder: a comparison of cognitive-behavioural therapy and attention placebo control. Can J Psychiatry 2007;52(3):182–190. doi:10.1177/070674370705200310, PMID:17479527.
[79] McDaid D, Park AL, Wahlbeck K. The economic case for the prevention of mental illness. Annu Rev Public Health 2019;40:373–389. doi:10.1146/annurev-publhealth-040617-013629, PMID:30601725.
[80] Brenner R, Madhusoodanan S, Puttichanda S, Chandra P. Primary prevention in psychiatry—adult populations. Ann Clin Psychiatry 2010;22(4):239–248.
[81] Provoost E, Raymond S, Gasman I. Homicides committed by delusional patients in the early 20th and 21st centuries: A study conducted in a French secure unit. J Forensic Sci 2022;67(1):265–274. doi:10.1111/1556-4029.14892, PMID:34634145.
[82] Salazar de Pablo G, Estradé A, Cutroni M, Andlauer O, Fusar-Poli P. Establishing a clinical service to prevent psychosis: What, how and when? Systematic review. Transl Psychiatry 2021;11(1):43. doi:10.1038/s41398-020-01165-x, PMID:33441556.
[83] Fusar-Poli P, Solmi M, Brondino N, Davies C, Chae C, Politi P, *et al*. Transdiagnostic psychiatry: a systematic review. World Psychiatry 2019;18(2):192–207. doi:10.1002/wps.20631, PMID:31059629.
[84] Maj M, van Os J, De Hert M, Gaebel W, Galderisi S, Green MF, *et al*. The clinical characterization of the patient with primary psychosis aimed at personalization of management. World Psychiatry 2021;20(1):4–33. doi:10.1002/wps.20809, PMID:33432763.
[85] Alegría M, Zhen-Duan J, O'Malley IS, DiMarzio K. A new agenda for optimizing investments in community mental health and reducing disparities. Am J Psychiatry 2022;179(6):402–416. doi:10.1176/appi.ajp.21100970, PMID:35599537.
[86] Madhusoodanan S, Ibrahim FA, Malik A. Primary prevention in geriatric psychiatry. Ann Clin Psychiatry 2010;22(4):249–261. PMID:21180656.
[87] González-Rodríguez A, Molina-Andreu O, Penadés R, Garriga M, Pons A, Catalán R, *et al*. Delusional disorder over the reproductive life span: The potential influence of menopause on the clinical course. Schizophr Res Treatment 2015;2015:979605. doi:10.1155/2015/979605, PMID:26600949.

Journal of Exploratory Research in Pharmacology **2023** vol. 8(2) | 164–171
DOI: 10.14218/JERP.2022.00078

Review Article

Therapeutic Potential of Extracellular Vesicles as Vehicles to Deliver Druggable Molecules for Hepatocellular Carcinoma

Yudan Wang[1], Mei Wang[2], Ning Lin[3], Chunjie Ni[4] and Yi Xu[1,2,3,4,5,6,7,8*]

[1]Department of Pathology, Li Ka Shing Faculty of Medicine, The University of Hong Kong, Hong Kong SAR, China; [2]Key Laboratory of Basic Pharmacology of Ministry of Education, Zunyi Medical University, Zunyi, China; [3]Key Laboratory of Functional and Clinical Translational Medicine, Fujian Province University, Xiamen Medical College, Xiamen, China; [4]Department of Hepatopancreatobiliary Surgery, Second Affiliated Hospital of Harbin Medical University, Harbin, China; [5]Jiangsu Province Engineering Research Center of Tumor Targeted Nano Diagnostic and Therapeutic Materials, Yancheng Teachers University, Yancheng, China; [6]Key Laboratory of Biomarkers and In Vitro Diagnosis Translation of Zhejiang province, Hangzhou, China; [7]Key Laboratory of Gastrointestinal Cancer (Fujian Medical University), Ministry of Education, School of Basic Medical Sciences, Fujian Medical University, Fuzhou, China; [8]Key Laboratory of Myocardial Ischemia, Ministry of Education, Harbin Medical University, Harbin, China

Received: October 03, 2022 | **Revised:** December 14, 2022 | **Accepted:** December 27, 2022 | **Published online:** January 31, 2023

Abstract

Hepatocellular carcinoma (HCC) is the most common type of primary liver cancer and a leading cause of cancer-related deaths. Standard treatments, such as surgery, chemotherapy, and radiotherapy, frequently fail to produce positive therapeutic outcomes. Thus, it is essential to identify new treatment modalities with improved survival rates. Extracellular vesicles (EVs) are nanosized lipid bilayer vesicles secreted by cells that mediate intercellular communication. EVs have been used to deliver several non-coding RNAs (ncRNAs), including miRNA, circRNA, and lncRNA. These ncRNAs demonstrate excellent tumor-suppressive effects and serve as new therapeutic candidates for HCC. EVs possess several characteristics, including high biocompatibility, enhanced stability, and limited cytotoxicity, making them promising drug-delivery vehicles. Although these characteristics make them better drug carriers than traditional synthetic delivery vehicles, translating engineered EVs into clinical practice has been challenging. In this review, we summarise the tumor-suppressive roles of ncRNAs, the recent progress of EV-associated ncRNAs in HCC treatment, unique features of EVs relevant to drug delivery, and current challenges in the clinical translation of EVs.

Introduction

Hepatocellular carcinoma (HCC) is one of the main causes of cancer-related deaths globally and is the most common type of primary liver cancer, accounting for 70–90% of all cases.[1] Hepatic resection and liver transplantation are the most effective curative treatments for HCC. Nonetheless, HCC resection in patients with non-cirrhotic livers has a mortality rate as high as 20%; furthermore, the outcome of liver transplantation is unsatisfactory, with a 10-year survival rate of only 50%. Moreover, hepatic resection is associated with a high recurrence rate of 70% at five years, even in patients with tumor sizes as small as ≤2 cm.[2] Although the recurrence rate following liver transplantation is relatively low, the waiting period for transplantation has been increasing over the years owing to organ shortages, resulting in high patient dropout rates. Finding new treatment modalities with better prognoses is essential for physicians and researchers.

Extracellular vesicles (EVs) are small particles released by almost all cell types in the human body. Numerous names exist across the literature, referring to EVs of various origins, natures, and features.[3] EVs are classified into two major subtypes, microvesicles (MVs) and exosomes. These subtypes have different origins; MVs are formed by budding off the plasma membrane, whereas exosomes are derived from endosomal compartments.[4] Studies have shown that EVs are more than just waste carriers; they are essential in mediating cell-cell communication. EVs carry a variety of components ranging from nucleic acids to proteins, lipids, and metabolites.[5] Notably, cancer cells induce phenotypic

Keywords: Hepatocellular carcinoma; Extracellular vesicles; Exosome; Non-coding RNAs; Drug delivery.

Abbreviations: CAF, cancer-associated fibroblasts; circRNAs, circular RNAs; ECM, extracellular matrix; EVs, extracellular vesicles; HCC, hepatocellular carcinoma; lncRNAs, long ncRNAs; MSCs, mesenchymal stem cells; miRNAs, microRNAs; MVs, microvesicles; ncRNAs, non-coding RNAs; RBPs, RNA-binding proteins.

***Correspondence to:** Yi Xu, Department of Hepatopancreatobiliary Surgery, Second Affiliated Hospital of Harbin Medical University, No. 246, Xuefu Road, Nangang District, Harbin, Heilongjiang 150086, China. ORCID: https://orcid.org/0000-0003-2720-0005. Tel: +86-451-86605113, Fax: +86-451-86605356, E-mail: xuyihrb@pathology.hku.hk

How to cite this article: Wang Y, Wang M, Lin N, Ni C, Xu Y. Therapeutic Potential of Extracellular Vesicles as Vehicles to Deliver Druggable Molecules for Hepatocellular Carcinoma. *J Explor Res Pharmacol* 2023;8(2):164–171. doi: 10.14218/JERP.2022.00078.

reprogramming of recipient cells by transferring molecules contained in EVs. The tumor microenvironment can also be altered by EVs, thereby promoting tumor cell proliferation, invasion, and metastasis.[6,7] The secretion and uptake of EVs involve several steps, from the budding of the donor cell plasma membrane to docking and fusion at the recipient cell surface. Through this process, EV cargoes can enter the recipient cell and subsequently activate signaling pathways that result in various physiological changes.[8] The detailed mechanisms of secretion and uptake of EVs are reviewed elsewhere.[9,10] To date, a substantial amount of literature has reported the secretion of EVs by cancer cells. However, few studies have investigated the uptake of EVs by cancer cells. Pi et al. modified exosomes with folate to enhance their binding to cancer cells with overexpression of folate receptors. The engineered exosomes successfully delivered siRNAs to cancer cells, with a significant suppressive effect on cancer progression.[11] Other studies successfully incorporated miRNA inhibitors (anti-miR-9[12] and anti-miR-214[13]) into EVs to overcome the drug resistance of cancer cells. These findings highlight the feasibility and effectiveness of EVs for drug delivery to cancer cells.

Non-coding RNAs (ncRNAs) are a subtype of RNA not involved in protein-coding. They account for more than 90% of the RNAs made from the human genome and regulate gene expression.[14] Studies have consistently demonstrated that EVs contain several ncRNA species, including microRNAs (miRNAs), circular RNAs (circRNAs), and long ncRNAs (lncRNAs). Furthermore, exosomal ncRNAs participate in cancer regulation.[15–18] Adams et al. showed that *miR-34a* is a tumor-suppressive miRNA that inhibits cancer cell proliferation and invasion and is a direct downstream target of p53.[15] In a large-scale analysis of miRNA profiles from samples, including lung, breast, stomach, prostate, colon, and pancreatic tumors, several miRNAs were significantly downregulated in cancer cells.[16] Lu et al. showed that the tumor-suppressive lncRNA *MEG3* was significantly downregulated in lung cancer cells, subsequently suppressing p53 expression that induces increased cell proliferation.[17] *In vivo* experimental evidence identified *GAS5* as another tumor-suppressive lncRNA that is downregulated in breast cancers.[18] In this review, we discuss the tumor-suppressive functions of ncRNAs and summarise the recent progress in developing EVs as ncRNA delivery vehicles in treating HCC. Additionally, we present the unique features of EVs that make them a good candidate for cancer therapeutics and highlight the current understanding of the challenges associated with the clinical translation of EVs.

Functions of non-coding RNAs in HCC

LncRNAs act as miRNA sponges

Certain lncRNAs interact with miRNAs to act as molecular sponges. They sequester and inhibit the activity of miRNAs, thereby allowing the re-expression of miRNA target genes, which may include important tumor-suppressor genes.[19] Therefore, lncRNAs indirectly regulate cell fate. Zhuang et al. found that *miR-92b* promotes HCC cell proliferation and metastasis by upregulating β-catenin signaling. They further found that Smad7, a direct target of *miR-92b*, was downregulated in HCC cells and that re-expression of Smad7 significantly suppressed *miR-92b*-induced cell proliferation and metastasis. Notably, the lncRNA *XIST* was found to act as a miRNA sponge and inhibit HCC tumourigenesis by targeting *miR-92b.*[20] Wang et al. showed that the lncRNA *SENP3-EIF4A1* acts as a molecular sponge of *miR-9-5p* to protect the expression of the target gene *ZFP36*. Inhibition of *miR-9-5p* subsequently reverses HCC tumourigenesis by inducing apoptosis and reducing the invasiveness and metastatic potential of HCC cells.[21] These studies support the tumor-suppressive role of lncRNAs and their function as miRNA sponges.

lncRNAs in protein regulation and interaction

lncRNAs can associate with proteins to modify their properties and functions. The tumor suppressor p53 is degraded by MDM2 via E3 ubiquitin ligase activity. Zhou et al. found that the p53-MDM2 interaction was decreased in the *lncRNA-PRAL*-overexpressing HCC cells, with a corresponding increase in the HSP90-p53 interaction and p53-induced HCC apoptosis. p53 utilizes HSP90 for its efficient translocation into the nucleus. The interactions of *lncRNA-PRAL* with HSP90 and HSP90 with p53 were confirmed via co-immunoprecipitation, followed by Western blotting. These results revealed that *lncRNA-PRAL* promotes the interaction between HSP90 and p53 and hence, competitively inhibits p53 ubiquitination by MDM2, thereby promoting HCC cell apoptosis.[22] Similarly, Qin et al. found that the lncRNA *PSTAR* could bind to the hnRNP K protein to strengthen its interaction with p53, thereby competitively blocking MDM2-dependent p53 ubiquitination and preventing HCC cells.[23] These studies suggest that lncRNAs act as tumor suppressors by interacting with proteins and modulating their function.

circRNAs act as miRNA sponges

A substantial amount of literature suggests that certain circRNAs have multiple binding sites for miRNAs, indicating that circRNAs can act as miRNA sponges to reverse miRNA-mediated gene degradation.[24] Zhang et al. found that *circTRIM33–12* eliminates the suppression of TET1 by sponging *miR-191*, and the knockdown of TET1 results in HCC cell proliferation, invasion, and migration. The TET1 protein can induce DNA demethylation, thus playing an important role in tumor suppression.[25] Similarly, another group found that *circMTO1* acts as a *miR-9* sponge in HCC cells to liberate downstream p21 expression. Silencing of *circMTO1* in HCC can lead to the downregulation of p21, thereby promoting HCC cell proliferation and invasion.[26] Many other circRNAs (*circ_0091570*, *circ_0014717*, and *circRNA_101505*) were also downregulated in HCC, and they all function as miRNA sponges.[27–29]

circRNAs in protein regulation and interaction

Specific circRNAs can interact with proteins. RNA-binding proteins (RBPs) are necessary for the post-transcriptional modulation of RNAs and the promotion of mRNA stability, localization, and translation. Zhu et al. found that *circZKSCAN1* can act as an RBP (FMRP) sponge rather than a miRNA sponge to inhibit multiple malignant behaviors by suppressing HCC cell stemness. FMRP can bind to the mRNA of its target gene, *CCAR1*, which participates in the Wnt/β-catenin signaling pathway to upregulate cell stemness. *circZKSCAN1* acts as an RBP sponge and blocks the binding between *CCAR1* mRNA and FMRP, thus preventing the transcriptional activity of Wnt/β-catenin signaling.[30] Similarly, Liu et al. found that *circDLC1* can bind to the RBP HuR and prevent its interaction with *MMP1* mRNAs, inhibiting the expression of *MMP1* and preventing HCC progression.[31] On the other hand, Shi et al. identified the role of circRNAs as protein scaffolds. Research has suggested that smaller circRNAs act as scaffolds to facilitate protein binding and interactions that are otherwise physically separated. It was found that *circPABPC1* inhibits HCC cell adhesion and migration by directly binding to and downregulating

oncogenic ITGB1, a key molecule involved in HCC metastasis. *circPABPC1* acts as a bridge to facilitate the interaction between ITGB1 and the proteasome in HCC cells, thus promoting proteasome degradation.[32] Taken together, these studies suggest that circRNAs elicit tumor-suppressive functions by interacting with other proteins.

miRNAs in cell cycle control

Several miRNAs regulate cell cycle progression. Xu et al. found that *miR-195* was significantly downregulated in HCC cells. Overexpression of *miR-195* blocked G1/S transition and suppressed cancer cell proliferation. In terms of molecular mechanisms, *miR-195* directly inhibited cyclin D1 and CDK6, which are required to initiate Rb phosphorylation. Phosphorylated Rb suppresses the inhibition of E2F, which promotes the upregulation of proteins involved in the S-phase entry. Hence, *miR-195* may inhibit HCC progression by repressing Rb-E2F signaling that mediates the G1/S transition.[33] Similarly, Kota et al. found that HCC cells exhibit reduced *miR-26a* expression. *miR-26a* expression induces G1 arrest by directly targeting cyclin D2 and E2, which are essential for the G1/S transition. Overexpression of *miR-26a in vivo* resulted in the inhibition of HCC cell proliferation, induction of apoptosis, and inhibition of cancer progression.[34] The above studies showed that miRNAs play a tumor-suppressive role by inhibiting cell cycle progression in HCC cells.

miRNAs in the regulation of angiogenesis and metastasis

miRNAs are also involved in metastasis and angiogenesis. Tsai et al. found that *miR-122* was significantly downregulated in metastatic HCC. Subsequently, ADAM17 was identified as a direct downstream target of *miR-122*, and its knockdown significantly reduced tumor migration, angiogenesis, and local invasion. This is likely due to the role of ADAM17 in activating certain EGF receptor ligands and modifying integrin signaling during cell adhesion and migration.[35] Fang et al. also found that *miR-29b*-overexpressed HCC cells exhibited a substantial decrease in microvessel density and metastatic potential. *miR-29b* inhibits angiogenesis and metastasis by downregulating MMP2, which assists the migration and proliferation of cancer cells by facilitating the remodeling of the extracellular matrix (ECM) and the release of ECM growth factors.[36] Alpini et al. found that decreased *miR-125b* expression contributed to the invasive phenotype of HCC cells. *miR-125b* suppresses cancer cell survival and tumor angiogenesis by targeting PGF, which may promote the recruitment of circulating hematopoietic progenitor cells and macrophages that contribute to tumor angiogenesis.[37] Taken together, these studies show that miRNAs prevent HCC progression by inhibiting angiogenesis and metastasis (Fig. 1).

EVs loaded with non-coding RNAs as a therapy approach for HCC

EVs can be loaded with therapeutic cargoes such as ncRNAs and delivered to target tumor cells. Several studies have demonstrated that delivering tumor-suppressive ncRNAs via EVs successfully modifies cancer cell activities.[38–43] Various methods have been used to load ncRNAs into EVs. These can be divided into two main categories: endogenous and exogenous. Endogenous loading involves the direct addition of the donor cell ncRNA into EVs before shedding, whereas exogenous loading refers to the loading of the ncRNA into EVs once they are isolated and purified.[38] After loading, the donor and recipient cells are co-cultured to transfer EVs from donor to recipient HCC cells.

MVs derived from mesenchymal stem cells (MSCs) can induce the reprogramming of cancer cells upon the active transfer of ncRNAs. HCC cells treated with MSC-derived MVs showed reduced proliferation and an increased number of cells in the G0-G1 phase. Consistently, increased cell cycle inhibitors were observed in these cells, suggesting that a block in the cell cycle progression led to the observed inhibition of HCC cell proliferation. However, the authors did not further investigate the tumor-suppressive molecules present in these MVs.[39] Alzahrani et al. identified *miR-122* as a liver-specific miRNA downregulated in HCC cells. They reported an increase in the apoptosis of HCC cells following the injection of MSC-derived exosomes loaded with *miR-122*.[40] Similarly, Fonsato et al. showed that the uptake of human liver stem cell-derived MVs by HCC cells resulted in a substantial decrease in tumor cell proliferation and an increase in apoptosis. Several tumor-suppressive miRNAs in MVs have been reported, including *miR451*, *miR223*, *miR24*, *miR125b*, *miR31*, and *miR122*. Notably, proteins essential for cell cycle regulation were downregulated in HCC cells treated with MV, and these proteins are the downstream targets of the antitumor miRNAs present in MV.[41]

Additionally, cancer-associated fibroblasts (CAFs) are essential elements of the tumor microenvironment, which communicate with HCC cells and are, therefore, crucial for HCC therapy. Zhang et al. reported reduced *miR-320a* expression in CAF-derived exosomes. Further investigations suggested that *miR-320a* plays an important tumor-suppressive role by binding to PBX3, suppressing the activation of the MAPK pathway that promotes cell proliferation and metastasis.[42] In another study, Yugawa et al. suggested that CAFs may promote HCC progression via the production of interleukins, chemokines, and other growth factors. Based on this hypothesis, they found that *miR-150-3p* is significantly downregulated in CAF-derived exosomes. Overexpression of *miR-150-3p* in these exosomes significantly inhibited HCC cell migration and invasion. Immunofluorescence further confirmed that *miR-150-3p* was transferred from the CAFs to the HCC cells.[43]

Most studies have identified exosomal miRNAs with antitumor functions; however, other ncRNAs, such as circRNAs and lncRNAs, may also be important. Chen et al. found that patients with HCC exhibit lower *circ-0051443* expression in plasma exosomes than healthy individuals. Transfecting HCC cells with *circ-0051443*-expressing plasmid significantly inhibited the proliferation of cancer cells. The proposed regulatory mechanism is that *circ-0051443* acts as a 'sponge' to sequester *miR-331-3p*, resulting in downstream BAK1 gene transcription, which is important for cell death regulation and mitochondria-mediated apoptosis.[44] Wang et al. identified *lncRNA SENP3*-EIF4A1 as a molecular sponge of *miR-9-5p*, and its expression was significantly reduced in patients with HCC compared to healthy controls. When exosomal *SENP3*-EIF4A1 was transferred from healthy liver cells to HCC cells, apoptosis was increased, and the invasiveness and metastatic potential of HCC cells were decreased.[21] These studies provide evidence for the use of EVs to deliver antitumor ncRNAs in HCC therapy.

Advantages of EV-based drug-delivery system

Safety profiles

Unlike synthetic drug-delivery systems, EVs are relatively safe and minimally reactive to the immune system because of their endogenous origin and high biocompatibility (Table 1). Synthetic

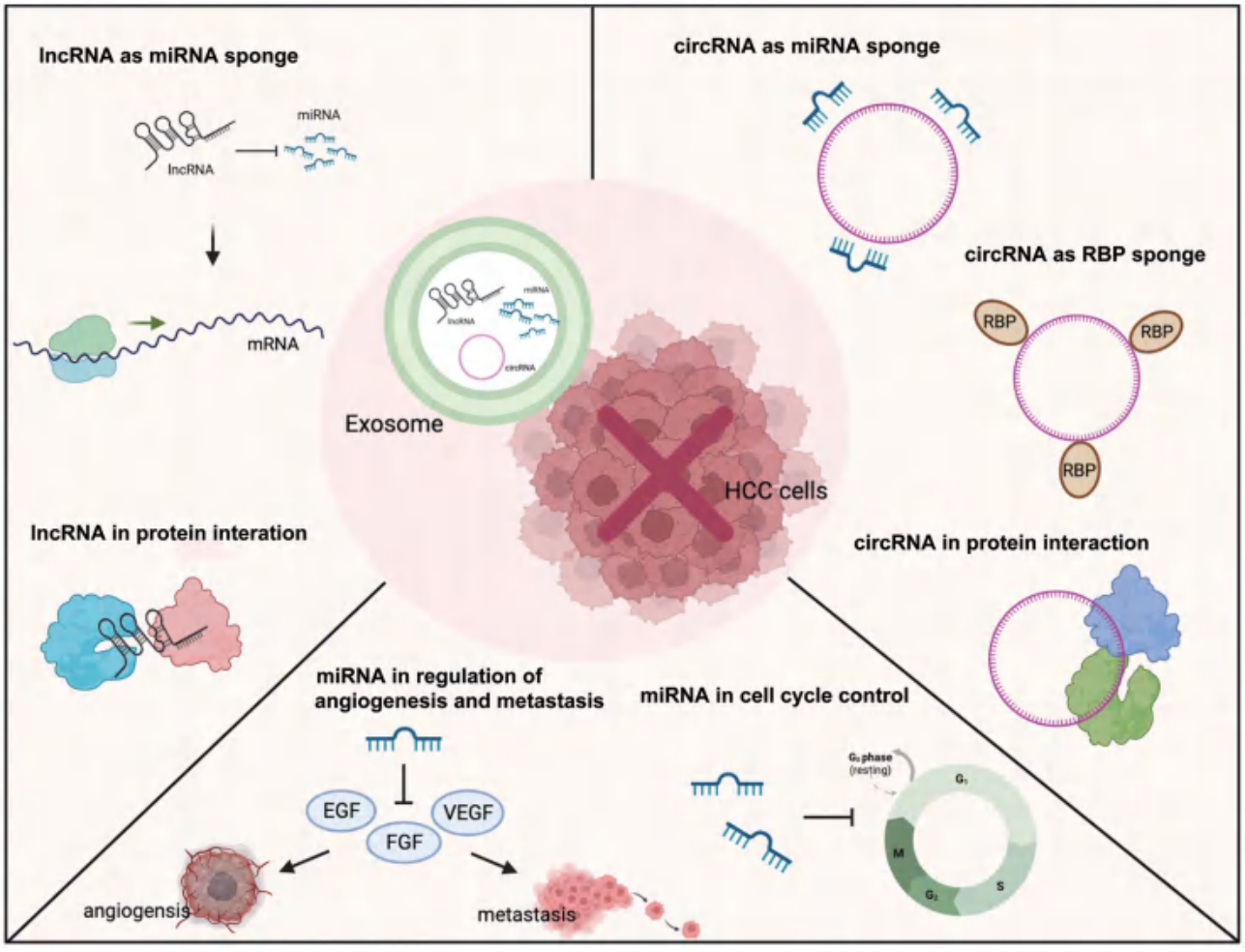

Fig. 1. Exosomes can be used as a drug-delivery vehicle for delivering tumor-suppressive non-coding RNAs (long non-coding RNAs, circular RNAs, and micro RNAs) to HCC cells. HCC, hepatocellular carcinoma; RBP, RNA-binding proteins; circRNA, circular RNAs; lncRNA, long ncRNAs; miRNA, microRNAs.

lipid nanoparticles (such as liposomes) have demonstrated enormous potential for the delivery of nucleic acids, including RNAs. Nevertheless, adverse effects and safety concerns associated with the clinical application of synthetic lipid nanoparticles continue to exist. For instance, poly(ethylene glycol) (PEG), a commonly used hydrophilic polymer coating for drug-delivery vehicles to prevent opsonization and enhance water solubility, is associated with potential side effects. PEG-coated liposomes may induce hypersensitivity reactions, produce toxic side products, and change pharmacokinetic behavior by altering the circulation time of the enclosed

Table 1. Advantages and disadvantages of EV-based different drug-delivery systems

	Advantages	***Disadvantages***
Synthetic lipid nanoparticles	Easy to be modified, controllable size and shape	PEG-coated nanolipids may induce toxic side effects and alter drug pharmacokinetic behavior
	High scalability and reproducibility, easy for quality control	Accumulation of lipids in the liver and spleen may cause pathological changes
	Low manufacturing cost	Not easily targetable
EV-based drug-delivery system	Low immunogenicity	Low scalability and reproducibility, difficult for quality control
	Relatively low cytotoxicity when externally modified	Low drug loading efficiency
	High delivery efficiency due to membrane proteins and lipids that can bind specifically to receptors on target cells	Lack of development in modification techniques

EV, extracellular vesicle; PEG, poly(ethylene glycol).

Table 2. Passive and active loading methods to enhance tumor-targeting ability and drug-delivery efficiency

Strategies	Methods	Description	Advantages	Disadvantages
Passive loading	Simple incubation	EVs are co-incubated with drugs at room temperature	Simple and straightforward	Limited by the volume of EVs and small membrane pore size
Active loading	Electroporation	Uses electrical current to increase the permeability of EV membranes to allow rapid drug entry	High loading efficiency; Ability to load large molecules	Disruption of EV membrane integrity; EV aggregation
	Sonication	Ultrasound probe with different amplitude is used to permeabilize the EV membrane	High loading efficiency	Disruption of EV membrane integrity
	Extrusion	An extruder is used to squeeze the cells co-cultured with the drug to complete drug loading	High loading efficiency; Short duration	Disruption of EV membrane integrity
	Freeze-thaw cycle	Formation of temporary pores on EV membrane through several rapid freeze-thaw cycles	No change in the EV surface charge	Low loading efficiency due to EV aggregation
	Saponin	Form pores on EV membrane through interactions with cholesterol	Higher loading efficiency	Disruption of EV membrane integrity

EV, extracellular vesicle.

drugs.[45] Additionally, it has been noted that synthetic lipid nanoparticles might induce toxic immune responses *in vivo*, causing liver injury in rodents. This might be explained by the cytotoxicity of the lipid materials and their ability to induce a dramatic proinflammatory response.[46] In contrast, Kamerkar et al. showed that exosomes were better siRNA-delivering vehicles than liposomes, as they suppressed KRAS-mutated cancers without inducing any obvious adverse immune responses. Moreover, plasma membrane-like phospholipids and membrane proteins of exosomes may prevent them from being quickly eliminated from circulation.[47] More importantly, no detectable toxicity or inflammatory response was noted, even when exosomes were externally modified with ligands to enhance delivery and uptake.[48] Although some studies have suggested that nanoparticles, including EVs, tend to accumulate in the liver *in vivo*, Saleh et al. confirmed that EVs induced minimal hepatotoxicity and immunogenicity, as the uptake of EVs into HepG2 cells did not show notable changes in histopathology, proinflammatory cytokine levels, or liver transaminases.[49] These findings showed that EVs are generally well-tolerated and may be better candidates than other synthetic drug-delivery systems.

Enhanced drug delivery with modification

EVs can be modified using various strategies to improve their tumor-targeting ability and drug-delivery efficiency. Passive or active loading methods are used to enhance the loading of exogenous cargo. Passive loading refers to the incubation of EVs with therapeutic drugs. This method generally does not damage the structure of EVs and is highly effective for hydrophobic drugs with poor solubility. Active loading refers to loading therapeutic drugs into EVs, mainly by electroporation, sonication, extrusion, freeze-thaw cycles, and saponins. The details of these methods are listed in Table 2. Kim et al. compared different drug loading methods and showed that all active loading methods achieved higher loading efficiencies than passive loading, especially sonication.[50] However, the most appropriate loading method depends on the chemical and physical properties of the cargo. For instance, small and hydrophobic molecules can easily cross the hydrophobic membrane of EVs; hence, coincubation would be suitable in this case. Electroporation and sonication are the best approaches for small RNAs (siRNA and miRNA) that require higher loading efficiencies.[51,52] To facilitate specific binding and uptake by cancer cells, EV surfaces are modified using either covalent or non-covalent methods. Covalent modifications mainly involve chemical conjugation, attaching ligands to the EV surfaces. This method generally does not affect the structural integrity of EVs; however, it depends on carefully controlling the modification conditions (such as temperature, pressure, and pH) to avoid denaturing them.[53] Non-covalent modification involves electrostatic and ligand-receptor interactions. The EV surfaces are negatively charged, thereby allowing the binding of positively charged molecules via electrostatic interactions. Zhan et al. showed that attaching a cationic lipid-sensitive endosomolytic peptide, L17E, to the EVs surface enhanced miRNA release and strongly suppressed tumor progression without apparent adverse effects.[54] In contrast, hydrophobic ligands can be integrated into the EV membranes via hydrophobic interactions. Cheng et al. showed that integrating nuclear localization signal peptides to the EV surfaces greatly enhanced the nuclear delivery of cargo, thus inhibiting tumor growth.[55] Taken together, EVs can be modified using several bioengineering methods to achieve enhanced targetability and drug-delivery efficiency.

Challenges of EV-based drug delivery

Although *in vivo* studies have shown promising progress in EV-based drug delivery, several challenges may hinder the clinical translation and application of EVs. First, a major bottleneck is the massive production of engineered clinical-grade EVs. This refers to the sterile production of EVs in large batches sufficient for clinical testing without batch-to-batch variation and decreased effectiveness. Currently, no viable approach satisfies the desired standards for large-scale EV production. Traditional methods, such as ultracentrifugation, have limitations, including low production yield, non-exosomal contaminants, and poor reproducibility. Large-scale manufacturing of sterile EVs can be achieved using a bioreactor-based culture system and developing a streamline-based microfluidic filtration device for efficient purification.[56,57] Second, achieving a higher drug loading efficiency for EVs is needed. Vader et al. suggested that the loading efficiency of EVs is relatively low compared to that of synthetic liposomes.[58] This may be because EVs develop a high proportion of parental ma-

terials during their formation, leaving a limited loading space for exogenous drugs. Additionally, the loading capacity of EVs may be affected by their various chemical and lipid components; hence, it is important to choose an appropriate method for optimizing the loading efficiency of EVs. The characteristics of each loading method are presented in Table 2. Third, more comprehensive preclinical examinations should be conducted to prevent potential adverse effects, particularly those related to pharmacokinetics, pharmacodynamics, toxicity, and dosage. Some researchers have argued that EVs produced from immortalized cell lines may carry oncogenic materials. However, different immortalized cell lines have been commonly used for EV production owing to their infinite supply and high proliferation rate. As a safe drug carrier, EVs are minimally reactive to the host immune system and are derived from healthy human cells. For example, Zhu et al. showed that administering EVs derived from human embryonic kidney cells to mice for three weeks induced no adverse side effects. The engineered type of EVs showed notable clinical benefits, as the loaded *miR-199a-3p* significantly reduced the proliferation of CD44-positive HCC but not wild types.[59] Moreover, modification and engineering may alter the composition and content of EVs, reducing their effectiveness and immunogenicity. These potential adverse effects should be considered when developing new methods for EV modifications.

Future perspectives

Future studies should explore the therapeutic effects of EVs as ncRNA carriers for targeting HCC cells. To optimize EV use, it is important to understand the underlying mechanisms involved in the cellular sorting of cargoes, which may provide valuable insights into the loading of ncRNAs into EVs. Moreover, EVs from various cell origins may interact differently with the same type of recipient cell; thus, a better understanding of this variation in EV transfer and uptake could improve therapeutic efficacy. Finally, understanding the components of the EV membranes and selecting appropriate modification techniques are essential for EV modifications. This would avoid structural changes to the EV membranes and preserve their physicochemical stability.

Conclusions

EVs have enormous potential as drug-delivery vehicles for cancer therapeutics. In this review, we identified several ncRNAs (miRNAs, circRNAs, and lncRNAs) that play a crucial role in tumor suppression. Several studies have successfully introduced ncRNAs into engineered EVs, significantly inhibiting HCC progression. Targets such as β-catenin, which are not readily targetable by small molecules, can be targeted using siRNA or miRNA; hence, the RNA-targeting approach is an attractive strategy for the modulation of gene expression. Despite all the challenges and questions to be addressed, EVs may still provide hope for developing new treatment modalities against the deadly HCC.

Acknowledgments

None.

Funding

This work was supported by Hong Kong Scholars Program (Grant No. XJ2020012), National Natural Science Foundation of China (Grant No. 81902431), Excellent Young Scientists Project of Natural Science Foundation of Heilongjiang Province (Grant No. YQ2019H007), Special Project of China Postdoctoral Science Foundation (Grant No. 2019T120279), Special Project of Heilongjiang Postdoctoral Science Foundation (Grant No. LBH-TZ1016), Strengthening and Enhancing the Efficiency Plan of the Dominant and Characteristic Disciplines of Harbin Medical University (Grant No. HMUMIF-22008), China Postdoctoral Science Foundation (Grant No. 2018M641849), Heilongjiang Postdoctoral Science Foundation (Grant No. LBH-Z18107), Beijing Xisike Clinical Oncology Research Foundation (Grant No. Y-Young2022-0188), Medjaden Academy & Research Foundation for Young Scientists (Grant No. MJR20220903), Opening Project of Key Laboratory of Basic Pharmacology of Ministry of Education, Zunyi Medicial University (Grant No. 2022-449), Opening Research Fund of Key Laboratory of Gastrointestinal Cancer, Fujian Medical University, Ministry of Education (Grant No. FMUGIC-202203), Opening Project of Key Laboratory of Environment and Health, Ministry of Education (Grant No. 2022GWK-FJJ01), Opening Project of Key Laboratory of Functional and Clinical Translational Medicine, Fujian Province University (Grant No. XMMC-FCTM202205), Opening Project of Guangxi Laboratory of Enhanced Recovery after Surgery for Gastrointestinal Cancer (Grant No. GXEKL202204), Opening Project of Key Laboratory of Biomarkers and In Vitro Diagnosis Translation of Zhejiang Province (Grant No. KFJJ-2022002), Opening Project of Jiangsu Province Engineering Research Center of Tumor Targeted Nano Diagnostic and Therapeutic Materials (Grant No. JETNM202210).

Conflict of interest

The authors declare no conflict of interest in the publication of this work.

Author contributions

Writing – review & editing: WM, LN; Contributed to the figure and table design: NC; Performed the literature search and data analysis: WM, LN, NC; Funding acquisition: XY.

References

[1] Torre LA, Bray F, Siegel RL, Ferlay J, Lortet-Tieulent J, Jemal A. Global cancer statistics, 2012. CA Cancer J Clin 2015;65(2):87–108. doi:10.3322/caac.21262, PMID:25651787.

[2] Llovet JM, Kelley RK, Villanueva A, Singal AG, Pikarsky E, Roayaie S, *et al*. Hepatocellular carcinoma. Nat Rev Dis Primers 2021;7(1):6. doi:10.1038/s41572-020-00240-3, PMID:33479224.

[3] Colombo M, Raposo G, Thery C. Biogenesis, secretion, and intercellular interactions of exosomes and other extracellular vesicles. Annu Rev Cell Dev Biol 2014;30:255–289. doi:10.1146/annurev-cellbio-101512-122326, PMID:25288114.

[4] Murphy DE, de Jong OG, Brouwer M, Wood MJ, Lavieu G, Schiffelers RM, *et al*. Extracellular vesicle-based therapeutics: natural versus engineered targeting and trafficking. Exp Mol Med 2019;51(3):1–12. doi:10.1038/s12276-019-0223-5, PMID:30872574.

[5] Xavier CPR, Caires HR, Barbosa MAG, Bergantim R, Guimaraes JE, Vasconcelos MH. The Role of Extracellular Vesicles in the Hallmarks of Cancer and Drug Resistance. Cells 2020;9(5):1141. doi:10.3390/cells9051141, PMID:32384712.

[6] Fang T, Lv H, Lv G, Li T, Wang C, Han Q, *et al*. Tumor-derived exosomal miR-1247-3p induces cancer-associated fibroblast activation to foster lung metastasis of liver cancer. Nat Commun 2018;9(1):191.

doi:10.1038/s41467-017-02583-0, PMID:29335551.
[7] Peinado H, Aleckovic M, Lavotshkin S, Matei I, Costa-Silva B, Moreno-Bueno G, *et al*. Melanoma exosomes educate bone marrow progenitor cells toward a pro-metastatic phenotype through MET. Nat Med 2012;18(6):883–891. doi:10.1038/nm.2753, PMID:22635005.
[8] Pitt JM, Kroemer G, Zitvogel L. Extracellular vesicles: masters of intercellular communication and potential clinical interventions. J Clin Invest 2016;126(4):1139–1143. doi:10.1172/JCI87316, PMID: 27035805.
[9] van Niel G, D'Angelo G, Raposo G. Shedding light on the cell biology of extracellular vesicles. Nat Rev Mol Cell Biol 2018;19(4):213–228. doi:10.1038/nrm.2017.125, PMID:29339798.
[10] Mathieu M, Martin-Jaular L, Lavieu G, Thery C. Specificities of secretion and uptake of exosomes and other extracellular vesicles for cell-to-cell communication. Nat Cell Biol 2019;21(1):9–17. doi:10.1038/s41556-018-0250-9, PMID:30602770.
[11] Zheng Z, Li Z, Xu C, Guo B, Guo P. Folate-displaying exosome mediated cytosolic delivery of siRNA avoiding endosome trapping. J Control Release 2019;311-312:43–49. doi:10.1016/j.jconrel.2019.08.021, PMID:31446085.
[12] Munoz JL, Bliss SA, Greco SJ, Ramkissoon SH, Ligon KL, Rameshwar P. Delivery of Functional Anti-miR-9 by Mesenchymal Stem Cell-derived Exosomes to Glioblastoma Multiforme Cells Conferred Chemosensitivity. Mol Ther Nucleic Acids 2013;2:e126. doi:10.1038/mtna.2013.60, PMID:24084846.
[13] Wang X, Zhang H, Bai M, Ning T, Ge S, Deng T, *et al*. Exosomes Serve as Nanoparticles to Deliver Anti-miR-214 to Reverse Chemoresistance to Cisplatin in Gastric Cancer. Mol Ther 2018;26(3):774–783. doi:10.1016/j.ymthe.2018.01.001, PMID:29456019.
[14] Slack FJ, Chinnaiyan AM. The Role of Non-coding RNAs in Oncology. Cell 2019;179(5):1033–1055. doi:10.1016/j.cell.2019.10.017, PMID:31730848.
[15] Adams BD, Parsons C, Slack FJ. The tumor-suppressive and potential therapeutic functions of miR-34a in epithelial carcinomas. Expert Opin Ther Targets 2016;20(6):737–753. doi:10.1517/14728222.2016.1114102, PMID:26652031.
[16] Volinia S, Calin GA, Liu CG, Ambs S, Cimmino A, Petrocca F, *et al*. A microRNA expression signature of human solid tumors defines cancer gene targets. Proc Natl Acad Sci U S A 2006;103(7):2257–2261. doi:10.1073/pnas.0510565103, PMID:16461460.
[17] Lu KH, Li W, Liu XH, Sun M, Zhang ML, Wu WQ, *et al*. Long non-coding RNA MEG3 inhibits NSCLC cells proliferation and induces apoptosis by affecting p53 expression. BMC Cancer 2013;13:461. doi:10.1186/1471-2407-13-461, PMID:24098911.
[18] Zhang Z, Zhu Z, Watabe K, Zhang X, Bai C, Xu M, *et al*. Negative regulation of lncRNA GAS5 by miR-21. Cell Death Differ 2013;20(11):1558–1568. doi:10.1038/cdd.2013.110, PMID:23933812.
[19] Huang Z, Zhou JK, Peng Y, He W, Huang C. The role of long noncoding RNAs in hepatocellular carcinoma. Mol Cancer 2020;19(1):77. doi:10.1186/s12943-020-01188-4, PMID:32295598.
[20] Zhuang LK, Yang YT, Ma X, Han B, Wang ZS, Zhao QY, *et al*. MicroRNA-92b promotes hepatocellular carcinoma progression by targeting Smad7 and is mediated by long non-coding RNA XIST. Cell Death Dis 2016;7:e2203. doi:10.1038/cddis.2016.100, PMID:27100897.
[21] Wang J, Pu J, Zhang Y, Yao T, Luo Z, Li W, *et al*. Exosome-transmitted long non-coding RNA SENP3-EIF4A1 suppresses the progression of hepatocellular carcinoma. Aging (Albany NY) 2020;12(12):11550–11567. doi:10.18632/aging.103302, PMID:32602848.
[22] Zhou CC, Yang F, Yuan SX, Ma JZ, Liu F, Yuan JH, *et al*. Systemic genome screening identifies the outcome associated focal loss of long noncoding RNA PRAL in hepatocellular carcinoma. Hepatology 2016;63(3):850–863. doi:10.1002/hep.28393, PMID:26663434.
[23] Qin G, Tu X, Li H, Cao P, Chen X, Song J, *et al*. Long Noncoding RNA p53-Stabilizing and Activating RNA Promotes p53 Signaling by Inhibiting Heterogeneous Nuclear Ribonucleoprotein K deSUMOylation and Suppresses Hepatocellular Carcinoma. Hepatology 2020;71(1):112–129. doi:10.1002/hep.30793, PMID:31148184.
[24] Zhang Y, Wang Y. Circular RNAs in Hepatocellular Carcinoma: Emerging Functions to Clinical Significances. Front Oncol 2021;11:667428. doi:10.3389/fonc.2021.667428, PMID:34055634.
[25] Zhang PF, Wei CY, Huang XY, Peng R, Yang X, Lu JC, *et al*. Circular RNA circTRIM33-12 acts as the sponge of MicroRNA-191 to suppress hepatocellular carcinoma progression. Mol Cancer 2019;18(1):105. doi:10.1186/s12943-019-1031-1, PMID:31153371.
[26] Han D, Li J, Wang H, Su X, Hou J, Gu Y, *et al*. Circular RNA circMTO1 acts as the sponge of microRNA-9 to suppress hepatocellular carcinoma progression. Hepatology 2017;66(4):1151–1164. doi:10.1002/hep.29270, PMID:28520103.
[27] Wang YG, Wang T, Ding M, Xiang SH, Shi M, Zhai B. hsa_circ_0091570 acts as a ceRNA to suppress hepatocellular cancer progression by sponging hsa-miR-1307. Cancer Lett 2019;460:128–138. doi:10.1016/j.canlet.2019.06.007, PMID:31207319.
[28] Ma H, Huang C, Huang Q, Li G, Li J, Huang B, *et al*. Circular RNA circ_0014717 Suppresses Hepatocellular Carcinoma Tumorigenesis Through Regulating miR-668-3p/BTG2 Axis. Front Oncol 2020;10:592884. doi:10.3389/fonc.2020.592884, PMID:33598424.
[29] Luo Y, Fu Y, Huang R, Gao M, Liu F, Gui R, *et al*. CircRNA_101505 sensitizes hepatocellular carcinoma cells to cisplatin by sponging miR-103 and promotes oxidored-nitro domain-containing protein 1 expression. Cell Death Discov 2019;5:121. doi:10.1038/s41420-019-0202-6, PMID:31372241.
[30] Zhu YJ, Zheng B, Luo GJ, Ma XK, Lu XY, Lin XM, *et al*. Circular RNAs negatively regulate cancer stem cells by physically binding FMRP against CCAR1 complex in hepatocellular carcinoma. Theranostics 2019;9(12):3526–3540. doi:10.7150/thno.32796, PMID:31281495.
[31] Liu H, Lan T, Li H, Xu L, Chen X, Liao H, *et al*. Circular RNA circDLC1 inhibits MMP1-mediated liver cancer progression via interaction with HuR. Theranostics 2021;11(3):1396–1411. doi:10.7150/thno.53227, PMID:33391541.
[32] Shi L, Liu B, Shen DD, Yan P, Zhang Y, Tian Y, *et al*. A tumor-suppressive circular RNA mediates uncanonical integrin degradation by the proteasome in liver cancer. Sci Adv 2021;7(13):abe5043. doi:10.1126/sciadv.abe5043, PMID:33762338.
[33] Xu T, Zhu Y, Xiong Y, Ge YY, Yun JP, Zhuang SM. MicroRNA-195 suppresses tumorigenicity and regulates G1/S transition of human hepatocellular carcinoma cells. Hepatology 2009;50(1):113–121. doi:10.1002/hep.22919, PMID:19441017.
[34] Kota J, Chivukula RR, O'Donnell KA, Wentzel EA, Montgomery CL, Hwang HW, *et al*. Therapeutic microRNA delivery suppresses tumorigenesis in a murine liver cancer model. Cell 2009;137(6):1005–1017. doi:10.1016/j.cell.2009.04.021, PMID:19524505.
[35] Tsai WC, Hsu PW, Lai TC, Chau GY, Lin CW, Chen CM, *et al*. MicroRNA-122, a tumor suppressor microRNA that regulates intrahepatic metastasis of hepatocellular carcinoma. Hepatology 2009;49(5):1571–1582. doi:10.1002/hep.22806, PMID:19296470.
[36] Fang JH, Zhou HC, Zeng C, Yang J, Liu Y, Huang X, *et al*. MicroRNA-29b suppresses tumor angiogenesis, invasion, and metastasis by regulating matrix metalloproteinase 2 expression. Hepatology 2011;54(5):1729–1740. doi:10.1002/hep.24577, PMID:21793034.
[37] Alpini G, Glaser SS, Zhang JP, Francis H, Han Y, Gong J, *et al*. Regulation of placenta growth factor by microRNA-125b in hepatocellular cancer. J Hepatol 2011;55(6):1339–1345. doi:10.1016/j.jhep.2011.04.015, PMID:21703189.
[38] Sutaria DS, Badawi M, Phelps MA, Schmittgen TD. Achieving the Promise of Therapeutic Extracellular Vesicles: The Devil is in Details of Therapeutic Loading. Pharm Res 2017;34(5):1053–1066. doi:10.1007/s11095-017-2123-5, PMID:28315083.
[39] Bruno S, Collino F, Deregibus MC, Grange C, Tetta C, Camussi G. Microvesicles derived from human bone marrow mesenchymal stem cells inhibit tumor growth. Stem Cells Dev 2013;22(5):758–771. doi:10.1089/scd.2012.0304, PMID:23034046.
[40] Alzahrani FA, El-Magd MA, Abdelfattah-Hassan A, Saleh AA, Saadeldin IM, El-Shetry ES, *et al*. Potential Effect of Exosomes Derived from Cancer Stem Cells and MSCs on Progression of DEN-Induced HCC in Rats. Stem Cells Int 2018;2018:8058979. doi:10.1155/2018/8058979, PMID:30224923.
[41] Fonsato V, Collino F, Herrera MB, Cavallari C, Deregibus MC, Cisterna B, *et al*. Human liver stem cell-derived microvesicles inhibit hepatoma growth in SCID mice by delivering antitumor microRNAs. Stem Cells 2012;30(9):1985–1998. doi:10.1002/stem.1161, PMID:22736596.
[42] Zhang Z, Li X, Sun W, Yue S, Yang J, Li J, *et al*. Loss of exosomal miR-320a from cancer-associated fibroblasts contributes to HCC prolif-

eration and metastasis. Cancer Lett 2017;397:33–42. doi:10.1016/j.canlet.2017.03.004, PMID:28288874.
[43] Yugawa K, Yoshizumi T, Mano Y, Itoh S, Harada N, Ikegami T, *et al*. Cancer-associated fibroblasts promote hepatocellular carcinoma progression through downregulation of exosomal miR-150-3p. Eur J Surg Oncol 2021;47(2):384–393. doi:10.1016/j.ejso.2020.08.002, PMID:32883551.
[44] Chen W, Quan Y, Fan S, Wang H, Liang J, Huang L, *et al*. Exosome-transmitted circular RNA hsa_circ_0051443 suppresses hepatocellular carcinoma progression. Cancer Lett 2020;475:119–128. doi:10.1016/j.canlet.2020.01.022, PMID:32014458.
[45] Knop K, Hoogenboom R, Fischer D, Schubert US. Poly(ethylene glycol) in drug delivery: pros and cons as well as potential alternatives. Angew Chem Int Ed Engl 2010;49(36):6288–6308. doi:10.1002/anie.200902672, PMID:20648499.
[46] Kedmi R, Ben-Arie N, Peer D. The systemic toxicity of positively charged lipid nanoparticles and the role of Toll-like receptor 4 in immune activation. Biomaterials 2010;31(26):6867–6875. doi:10.1016/j.biomaterials.2010.05.027, PMID:20541799.
[47] Kamerkar S, LeBleu VS, Sugimoto H, Yang S, Ruivo CF, Melo SA, *et al*. Exosomes facilitate therapeutic targeting of oncogenic KRAS in pancreatic cancer. Nature 2017;546(7659):498–503. doi:10.1038/nature22341, PMID:28607485.
[48] Gao X, Ran N, Dong X, Zuo B, Yang R, Zhou Q, *et al*. Anchor peptide captures, targets, and loads exosomes of diverse origins for diagnostics and therapy. Sci Transl Med 2018;10(444):aat0195. doi:10.1126/scitranslmed.aat0195, PMID:29875202.
[49] Saleh AF, Lazaro-Ibanez E, Forsgard MA, Shatnyeva O, Osteikoetxea X, Karlsson F, *et al*. Extracellular vesicles induce minimal hepatotoxicity and immunogenicity. Nanoscale 2019;11(14):6990–7001. doi:10.1039/c8nr08720b, PMID:30916672.
[50] Kim MS, Haney MJ, Zhao Y, Mahajan V, Deygen I, Klyachko NL, *et al*. Development of exosome-encapsulated paclitaxel to overcome MDR in cancer cells. Nanomedicine 2016;12(3):655–664. doi:10.1016/j.nano.2015.10.012, PMID:26586551.
[51] Lamichhane TN, Jeyaram A, Patel DB, Parajuli B, Livingston NK, Arumugasaamy N, *et al*. Oncogene Knockdown via Active Loading of Small RNAs into Extracellular Vesicles by Sonication. Cell Mol Bioeng 2016;9(3):315–324. doi:10.1007/s12195-016-0457-4, PMID:27800035.
[52] Lamichhane TN, Raiker RS, Jay SM. Exogenous DNA Loading into Extracellular Vesicles via Electroporation is Size-Dependent and Enables Limited Gene Delivery. Mol Pharm 2015;12(10):3650–3657. doi:10.1021/acs.molpharmaceut.5b00364, PMID:26376343.
[53] Zhang F, Guo J, Zhang Z, Duan M, Wang G, Qian Y, *et al*. Application of engineered extracellular vesicles for targeted tumor therapy. J Biomed Sci 2022;29(1):14. doi:10.1186/s12929-022-00798-y, PMID:35189894.
[54] Zhan Q, Yi K, Qi H, Li S, Li X, Wang Q, *et al*. Engineering blood exosomes for tumor-targeting efficient gene/chemo combination therapy. Theranostics 2020;10(17):7889–7905. doi:10.7150/thno.45028, PMID:32685027.
[55] Cheng H, Fan JH, Zhao LP, Fan GL, Zheng RR, Qiu XZ, *et al*. Chimeric peptide engineered exosomes for dual-stage light guided plasma membrane and nucleus targeted photodynamic therapy. Biomaterials 2019;211:14–24. doi:10.1016/j.biomaterials.2019.05.004, PMID:31078049.
[56] Mendt M, Kamerkar S, Sugimoto H, McAndrews KM, Wu CC, Gagea M, *et al*. Generation and testing of clinical-grade exosomes for pancreatic cancer. JCI Insight 2018;3(8):e99263. doi:10.1172/jci.insight.99263, PMID:29669940.
[57] Zhang X, Zhang H, Gu J, Zhang J, Shi H, Qian H, *et al*. Engineered Extracellular Vesicles for Cancer Therapy. Adv Mater 2021;33(14):e2005709. doi:10.1002/adma.202005709, PMID:33644908.
[58] Vader P, Mol EA, Pasterkamp G, Schiffelers RM. Extracellular vesicles for drug delivery. Adv Drug Deliv Rev 2016;106(Pt A):148–156. doi:10.1016/j.addr.2016.02.006, PMID:26928656.
[59] Zhu X, Badawi M, Pomeroy S, Sutaria DS, Xie Z, Baek A, *et al*. Comprehensive toxicity and immunogenicity studies reveal minimal effects in mice following sustained dosing of extracellular vesicles derived from HEK293T cells. J Extracell Vesicles 2017;6(1):1324730. doi:10.1080/20013078.2017.1324730, PMID:28717420.

Journal of Exploratory Research in Pharmacology **2023** vol. 8(2) | 172–179
DOI: 10.14218/JERP.2022.00063

Review Article

Future Prospects of Insulin Mutants, Biosimilars, Bioconjugates, and Newer Insulin-delivery Devices in Diabetes Mellitus

Ankit Bhardwaj[1*], Hara Prasad Mishra[2] and Ayush Goel[1]

[1]*Department of Pharmacology, University College of Medical Sciences, Delhi, India;* [2]*All India Institute of Medical Sciences, Delhi, India*

Received: July 27, 2022 | **Revised:** October 20, 2022 | **Accepted:** November 10, 2022 | **Published online:** January 12, 2023

Abstract

Insulin is the cornerstone of type 1 diabetes therapy and a crucial component for controlling type 2 diabetes. Despite significant advancements in insulin therapy research, including the creation of innovative insulin formulations and delivery systems, there are still numerous difficulties and unknowns surrounding insulin therapy. The main issues with more recent pharmacological and technological methods are biocompatibility, degradation/clearance of delivery materials, immunogenicity, stability, the precision of dosing, reproducibility of an effect similar to that of endogenous insulin, predictability of performance, and safety over time. In order to achieve a protracted, flatter profile, with fewer instances of hypoglycemia and an improvement in postprandial glucose level, more recent insulin mutants have been developed. The "meal" (glucose-responsive) insulins, which are supplied in accordance with an endogenous glucose-sensing feedback mechanism, best represent the future generation of insulin treatment. Insulin delivery methods with novel jet injectors, smart pens, patch pumps, and other needle-free tools for subcutaneous doses are another area of ongoing advancements. Digital health has significantly advanced treatments in recent years. As such, insulin treatments should become more scalable and potentially more cost-effective.

Introduction

Diabetes is one of the world's fastest-growing non-communicable chronic disorders. In 1980 a total of 108 million people worldwide had diabetes, and this number grew to 422 million in 2014.[1] Based on a report by the International Diabetes Federation (IDF) an estimated 700 million adults will have diabetes by 2045.[2] China has the highest number of diabetic patients worldwide (116 million), followed by India (77 million) and then the United States (31 million).[3]

A global study found that roughly 63 million people with type 2 diabetes need insulin treatment, while about 9 million people with type 1 diabetes mellistus (T1DM) depend on it for survival. Natural insulin, a polypeptide hormone produced by the pancreatic islets of Langerhans beta cells, largely controls how fat and glucose are metabolized, making it a vital and significant drug.[3] Frederick Banting and Charles Best initially identified the therapeutic applications of insulin in the year 1921, which was a significant turning point for contemporary medicine. Insulin thereafter took over as the cornerstone of T1DM treatment and a crucial supplement for the care of other kinds of diabetes and diabetic emergencies.[4,5]

Exogenous insulin formulations have made considerable advances, however, there are still several obstacles. The possible downsides that need to be addressed include immunogenicity, biocompatibility, degradation/clearance of the delivery substance, stability, dosage accuracy, repeatability, performance predictability, and safety over time. New formulations and delivery methods also need to be affordable and easily available in addition to having a good safety profile.

Novel insulin formulations that speed up the rate of rapid-acting insulin absorption and lengthen and flatten the action of basal insulins were developed to address these treatment-related difficulties (Table 1).[6–21,23a31a] The rate of insulin conversion can be altered, and its absorption from the injection site can be reduced using one of three main strategies: 1) changing the amino acid sequence of

Keywords: Insulin mutants; Biosimilar; Bioconjugates; Insulin-delivery devices; Diabetes mellitus.

Abbreviations: AI, artificial intelligence; BCLIS, bio chaperone lispro insulin; CGM, continuous glucose monitoring; ConA, concanavalin A; DNA, deoxyribonucleic acid; EDE, experimental device exemption; FDA, Food and Drug Administration; GBPs, glucose binding proteins; GOx, glucose oxidase; GRI, glucose responsive insulin; HbA1c, haemoglobin A1c; IDF, international diabetes federation; NPH, neutral protamine hagedorn; PBAs, phenylboronic acids; PK/PD, pharmacokinetics/pharmacodynamics; r-DNA, recombinant depxyribonucleic acid; T1DM, type 1 diabetes mellitous; T2DM, type 2 diabetes mellitous; TMR, transparency market research; URLi, ultra rapid lispro insulin.

[*]**Correspondence to:** Ankit Bhardwaj, Department of Pharmacology, University College of Medical Sciences, Delhi 110095, India. ORCID: https://orcid.org/0000-0001-6750-8405. Tel: +918076118430, E-mail: drankitbhardwaj25@gmail.com

How to cite this article: Bhardwaj A, Mishra HP, Goel A. Future Prospects of Insulin Mutants, Biosimilars, Bioconjugates, and Newer Insulin-delivery Devices in Diabetes Mellitus. *J Explor Res Pharmacol* 2023;8(2):172–179. doi: 10.14218/JERP.2022.00063.

Table 1. Types of insulin preparation, uses, adverse effects and contraindications

Types of Insulin	Trade Name of Biosimilar	Uses	Adverse drug reactions	Contraindications	References
Insulin lispro	LY900014 (URLi)	ultra-rapid insulin	Hypoglycemia; Injection site reactions; Weight gain	Hypoglycemia. In patients who are hypersensitive to insulin lispro or to any of the excipients.	6–11
Insulin lispro	BioChaperone	ultra-rapid insulin	Hypoglycemia; skin rash, itching, redness,	Hypoglycemia. In patients who are hypersensitive to insulin lispro or to any of the excipients	12–14
Insulin aspart	AT247	Short-acting insulin	low potassium; swelling in your hands and feet; skin rash, itching, redness, or swelling;	Hypoglycemia. In patients who are hypersensitive to insulin aspart or to any of the excipients	15–17
Insulin glargine	ADMELOG	long-acting type of insulin	Severe hypoglycemia; Lipodystrophy; Weight gain; Peripheral Edema; Infusion site erythema and infusion site reaction	Hypoglycemia. In patients who are hypersensitive to insulin glargine or to any of the excipients.	18,19
Insulin aspart	Kixelle	Short-acting insulin	Hypoglycemia; Urticaria, rash, eruptions; Refraction disorders, diabetic retinopathy; Lipodystrophy; Injection site reactions, oedema; Peripheral neuropathy (painful neuropathy)	Hypoglycemia. In patients who are hypersensitive to insulin aspart or to any of the excipients.	20
Insulin glargine	Basaglar	long-acting type of insulin	Hypoglycemia; Urticaria, rash, eruptions; Lipodystrophy	Hypoglycemia. In patients who are hypersensitive to insulin glargine or to any of the excipients	21,22
Insulin glargine	SEMGLEE	long-acting type of insulin	Hypoglycemia; Lipodystrophy; Injection site reactions, oedema	Hypoglycemia. In patients who are hypersensitive to insulin glargine or to any of the excipients	22,23
Insulin glargine	REZVOGLAR™	long-acting type of insulin	Hypoglycemia; Lipodystrophy; Injection site reactions, oedema	Hypoglycemia. In patients who are hypersensitive to insulin glargine or to any of the excipients	24
Insulin glargine	Glaritus	long-acting type of insulin	Hypoglycemia; Injection site reactions, oedema	Hypoglycemia. In patients who are hypersensitive to insulin glargine or to any of the excipients	25–27
Glucose responsive insulin	MK-2640		Hypoglycemia; Lipodystrophy; Injection site reactions, oedema	Hypoglycemia.	28–31

insulin, 2) adding fatty acid components that change the link between insulin hexamers and affect their binding with albumin in the bloodstream, or 3) using additives that affect the insulin absorption rate. At the same time, researchers are looking at other possible treatments, including different insulin delivery methods that avoid conventional subcutaneous absorption and closed-loop technologies that dynamically regulate insulin supply depending on *in vivo* glucose levels.[5] This article analyzes future prospects and emphasizes current developments in insulin treatment.

Progress in insulin mutants: the link between structure and function

In a healthy person, insulin levels reach their peak 1 hour after eating a meal and then begin to fall within the next 2 hours. For diabetic patients, on the other hand, achieving a normal blood sugar profile and preventing nocturnal hypoglycemia requires a precise insulin peak timing and duration of action.[32] The single zinc ion that holds the insulin hexamer molecules together dissociates, releasing dimers and monomers into the circulation. By swapping one or two amino acid residues in the insulin molecule, recombinant DNA technology can create formulations of rapid-acting insulin. The ProB28 and LysB29 residues on the C-terminal end of the B-chain of the lispros homologue can be switched to LysB28 and ProB29 (Fig. 1).[33] Position 28 on the B-chain of aspart insulin has an aspartic acid substitution for proline.[34] Insulin with a speedier onset of action is produced via the alteration of aspartamine, which results in an increase in charge repulsion. Because protamine, a little nuclear protein rich in arginine, is present in neutral protamine hagedorn (NPH), the absorption rates are reduced. Protamine also prolongs the duration of insulin action and delays its beginning. By including zinc in its formulation, Lente does the same.

Meal insulin

Insulin can be given as a meal or a bolus to reduce the postprandial hyperglycemic peak that occurs after eating. The optimal meal insulin should enter the circulation quickly in order to replicate the natural physiological insulin prandial production. Since the devel-

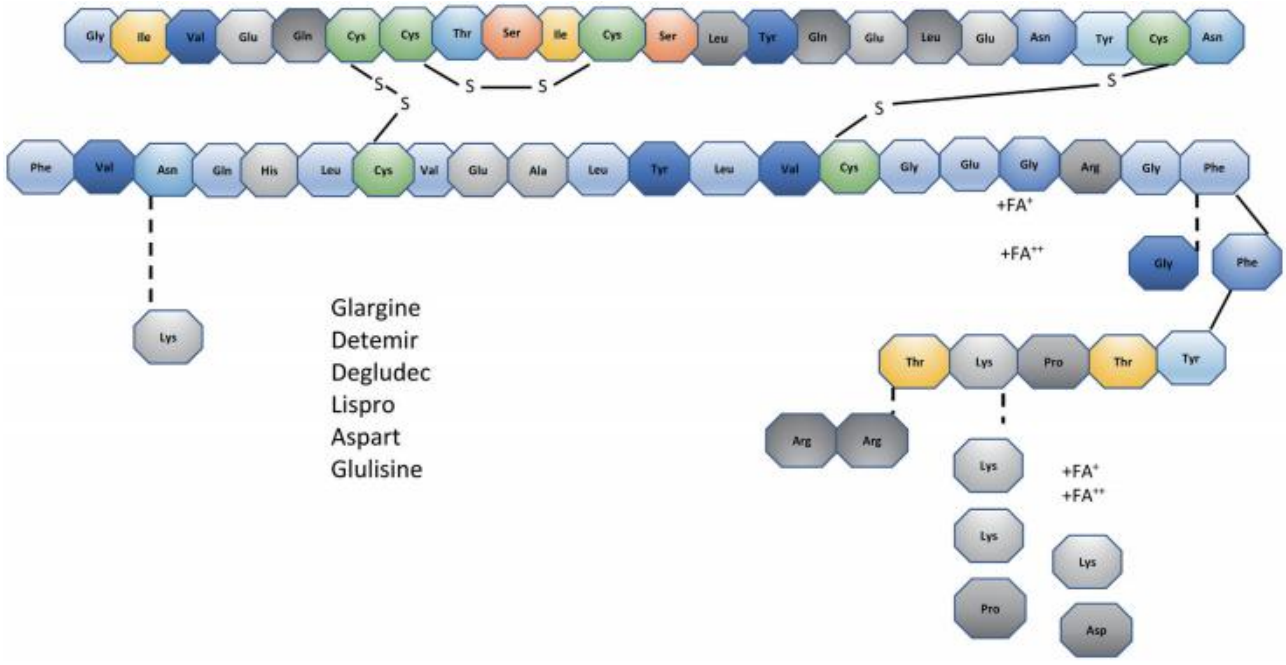

Fig. 1. Schematic representation of human insulin polypeptide and insulin analog showing the amino acid sequences of the two chains (A-chain and B-chain) linked by two disulfide bridges and changes in amino acid sequences in selected insulin analogues. *FA, fatty acid; **FA, fatty acid linked to lysine through a glutamic acid linker.

opment of a rapid-acting analogue, regular insulin has been seen as a less desirable alternative to meal insulin because of its delayed onset and prolonged duration compared to endogenous insulin in response to meals.

By altering one or two amino acids in the primary structure of the insulin molecule, it is possible to weaken the self-association of insulin monomers and create formulations with a quicker onset and shorter duration of action. This was done to overcome the slow onset and prolonged duration of regular insulin.[35]

These rapid-acting analogues showed a slight favourable effect in clinical tests on reducing HbA1c in T1DM patients, although a decreased incidence of hypoglycemia was noted compared to ordinary human insulin.[36] Patients with type 2 diabetes mellitus (T2DM) show less evidence of this therapeutic benefit.[37] Additionally, using rapid insulin right before meals rather than normal insulin (30–45 minutes beforehand) may increase adherence.

LY900014 lispro

The new ultrarapid formulation of insulin lispro, known as LY900014 (URLi), is intended to enhance glycemic control in individuals with T1DM and T2DM. It was created to lower HBA1c levels and hasten insulin absorption in circulation.

The effectiveness and safety of 1222 in comparison to lispro were reported in a double-blind, treat-to-target 26-week study of T2DM patients. The experiment showed a non-inferiority of 1222 with regard to HBA1c changes.[6] The frequency of severe hypoglycemia did not decrease much. URLi showed lower hypoglycemia rates 4 hours after a meal and better glucose excursions at 1 and 2 hours after on a meal test. With this insulin, there were no noted variations in tolerability.[7–11]

BioChaperone lispro insulin

Adocia created two ultra-rapid versions of the insulin analogue lispro, BioChaperone® Lispro U100 and BioChaperone® Lispro U200, to address the need for ultra-rapid insulin. For quicker absorption, BioChaperone® Lispro incorporates a unique excipient called BioChaperone BC222, a modified oligosaccharide molecule. The area under the curve for the 1 and 2 hour postprandial glucose excursions was 31% smaller with BCLIS than lispro in a different trial including T1DM patients who self-administered BCLIS at the beginning of a mixed meal test.[12] Adocia is a long-acting/short-acting combination formulation that combines BCLIS and insulin glargine with BioChaperone147, a polyanionic amphiphilic polymer. In T2DM patients who ingested a substantial mixed meal, this combination product demonstrated modest improvements in postprandial parameters compared with NPH/lispro mixed insulin and separate injections of glargine and lispro.[13,14] With this insulin, there have been no documented changes in local tolerability.

"Superfast" insulin aspart

AT247 (Arecor Limited Little Chester-ford, UK) is a new insulin aspartamine formulation that uses excipients with metal ion binding ability. It is intended to deliver an improved time-action profile following subcutaneous injection. Insulin's excipient component binds to calcium ions. By temporarily disrupting calcium-dependent cell adhesion at the injection site through reversible interactions with the calcium-cadherin complex on the cell surface, this increases tissue permeability and speeds up the absorption rate.[15–17] AT247 has been shown to dramatically improve postprandial glucose control in T1DM patients in a newly published European Phase I clinical investigation, and it was reported to prevent episodes of both hypoglycemia and hyperglycemia.

Admelog

Admelog is the first short-acting insulin that has been authorised

for use as a "follow-on" medication, which is given right before meals to regulate blood sugar levels after meal consumption. They can also be used in conjunction with insulin pumps to accommodate both the pre-meal and post-meal insulin requirements.

Admelog was authorised under the 505(b)(2) route, a streamlined approval process under the Federal Food, Drug, and Cosmetic Act. In accordance with this method, the Food and Drug Administration's (FDA's) assessment of the safety and efficacy of a newer drug application or published research supporting the safety and/or effectiveness of the proposed product may be used to approve the application. Because of these shortened drug development processes, patients may get medications for less cost.

Hypoglycemia, itching, and rash were the most frequently reported adverse medication responses during the clinical trial. Injection site responses, allergic reactions, and thickening or thinning of the adipose tissue at the injection site were among the other negative side effects (lipodystrophy).[18,19]

Kixelle (MYL 1601D)

The human insulin analogue Kixelle, developed by Biocon as a biosimilar of Novo Nordisk's NovoRapid/Novolog (insulin aspart), is made using recombinant DNA technology and Pichia pastoris (yeast). Except for the substitution of an aspartic acid residue for a single proline amino acid at position 28 in the C-terminal region of the insulin B-chain, the main structure is comparable to that of endogenous insulin.

Compared to regular human insulin, MYL-1601D starts working faster and wears out faster. Insulin aspart, a fast-acting counterpart of insulin, is the ingredient that makes MYL-1601D active. Lower blood glucose levels result from insulin aspart's facilitation of glucose absorption in muscle and fat cells and concurrent reduction of glucose production from the liver.

MYL-1601D was given approval because it exhibits similar clinical efficacy to NovoLog® (NovoLog), which the US has licenced, and NovoRapid® (NovoRapid), which the EU has authorized, in terms of physicochemical properties, biological activity, phramacokinetic and pharmacodynamic (PK/PD), safety, and efficacy, including immunogenicity. Other effectiveness endpoints, including the treatment-emergent antibody response (TEAR), were similar in both groups.[20,38]

Basaglar

An analogue of human insulin called Basaglar is created using recombinant DNA technology and a particular strain of E. coli. It is intended to be more predictable and to have fewer hypoglycemic spells, particularly at night. Its structural makeup is based on that of human insulin and insulin glargine, where two more amino acids, arginine at the C and B chains, are added and glycine replaces aspartic acid at position 21 at the C end of the A chain. Glycine with a neutral charge at the C terminus of the A chain stabilizes insulin glargine and inhibits the generation of deamination products. Basaglar was also authorized under the Federal Food, Drug, and Cosmetic Act through a shortened approval process known as the 505(b)(2) pathway. Its use is recommended for adults with T2DM and pediatric patients with T1DM to maintain better glycemic control. The solubility of insulin glargine is decreased after subcutaneous injection, generating a tiny precipitate that is progressively broken down into monomers and released into the circulation because the pH value (7.4) of tissue fluid is near the isoelectric point of insulin glargine. Its baseline insulin released throughout the day is comparable to that of healthy individuals and can have a consistent and long-lasting effect.[39,40]

Insulin biosimilar products

A biological product is considered to be biosimilar if it is extremely comparable to another biological product that has already received FDA approval (also known as the reference product) and is not significantly different in any other clinical aspects.[21] This implies that a biosimilar produce will provide the same level of safety and efficacy as the reference product. Similar to how generic pharmaceuticals have cut prices, biosimilar and interchangeable biosimilar goods have the potential to lower health care expenses. The first list costs of biosimilars sold in the United States were generally 15% to 35% less expensive than the comparable list prices of the reference drugs.[22]

SEMGLEE (insulin glargine-yfgn)

Exogenous insulin is injected subcutaneously after a delayed absorption to maintain 24 hour stable blood insulin levels. Initially, this effect was produced by the insulin molecule's isoelectric point changing, which reduces solubility at the injection site and encourages delayed absorption. Its reference product Lantus (insulin glargine), a long-acting insulin analogue, is interchangeable with SEMGLEE (insulin glargine-yfgn), the first biosimilar. SEMGLEE can be expected to produce the same clinical outcome as Lantus in any given patient, according to its clinical trials, and switching between SEMGLEE and Lantus carries no additional risk over simply using Lantus without switching. In the US, SEMGLEE is 64% less expensive than Lantus based on its wholesale purchase cost, which is around 22% less than Lantus. Hypoglycemia, life-threatening allergic responses, hypokalemia, and heart failure are just a few of the dangerous adverse effects associated with SEMGLEE. Oedema (fluid retention), lipodystrophy (pitting at the injection site), weight gain, and allergic responses, such as injection site reactions, rash, redness, discomfort, and severe itching, are the most frequent adverse effects associated with insulin glargine products other than hypoglycemia.[22,23]

REZVOGLAR™

A biosimilar of Lantus is REZVOGLAR™ (insulin glargine). Its mechanism of action is extremely similar to that of insulin glargine because it is a biosimilar of insulin glargine-aglr. Although Rezvoglar can be taken in place of Lantus, patients require a prescription written expressly for Rezvoglar, as the two medications are not interchangeable. Rezvoglar, like Lantus, cannot be used to manage diabetic ketoacidosis. The recognized major adverse effects of Rezvoglar include hypoglycemia, severe allergic responses, hypokalemia, and heart failure.[24]

Glaritus®

Wockhardt created Glaritus®, a biosimilar of insulin glargine. Glaritus® is administered as an injection of 100 IU/mL insulin glargine generated from r-DNA. Glaritus® and Lantus® have contrasting effects in both T1DM and T2DM patients, as well as healthy volunteers. Glaritus® and Lantus are bioequivalent, according to research involving healthy volunteers.[25] In a 12-week trial of adult patients with T1DM, Glaritus®, a biosimilar insulin glargine, was found to have glycemic control that was on par with Lantus®.[26,27]

Insulin bioconjugates

The majority of glucose-responsive insulin (GRI) devices employ polymeric biomaterials with embedded insulin. This polymeric substance contains glucose-responsive components, including glucose-binding proteins (GBPs), glucose oxidase (GOx), and phenylboronic acids (PBAs), which control the release of insulin

by degrading the polymer, altering the structure of the matrix, or competing with glucose for binding.[41] The most popular GBP utilized in polymeric materials for insulin administration is concanavalin A (ConA). ConA is employed as a crosslinker for the production of glucose-containing biopolymers because it possesses four high-affinity glucose binding sites.[42] Free glucose competes with bound glucose for binding sites as blood sugar levels rise, breaking the polymer bond and causing the release of insulin. As a catalyst, enzyme GOx transforms glucose into gluconic acid and produces hydrogen peroxide. When GOx is incorporated into the polymer matrix, acid-sensitive groups induce a glucose-triggered reaction (volume change or matrix disintegration), which causes the matrices to release insulin. PBAs, a subclass of tiny molecules, combine with 1,2- or 1,3-cis diols to create a complex that is negatively charged. Because PBAs may bind to glucose and other sugar sources, they are frequently used in cross-linked polymeric matrices. They swell and combine with glucose to produce a negatively charged complex, which triggers the release of insulin.[43] All of these methods for delivering insulin required either administration tools (such as microneedles) or matrices to encapsulate the insulin that will be released when blood glucose levels are raised. However, a few bioconjugation techniques are accessible that do not impair insulin's bioactivity due to its tiny size.[44,45] The most recent four methods to achieve glucose responsiveness using modified insulin molecules without the need for exogenous matrices are PBA-Modified Aliphatic Insulin Conjugate, Red Blood Cell-Bound Insulin Conjugate, PBA-Modified Aliphatic Insulin Conjugate, and Glucose-Responsive Insulin Through Mannose Receptor Interactions.

MK-2640 as a future novel GRI bioconjugate

The most advanced GRI bioconjugate is the Merck candidate, MK-2640. The findings of a phase 1 study released in 2018[28] implied that careful consideration should be given before clinical administration of GRI bioconjugates that are created through adding partners such as mannose receptors, albumin, and red blood cells. Designing new GRI bioconjugates presents a number of challenges, but the main one is the method for detecting glucose. The only minor molecule other than sugar currently employed in GRI designs is PBA. Although PBA's glucose interaction fits serum glucose levels well, its poor selectivity (10-fold greater affinity to fructose than glucose) raises questions. However, one potential future approach to overcome this issue is to employ bidentate PBA as a selective glucose sensor.[29,30] Utilizing *de novo* glucose sensors to produce GRIs - lectin molecules that bind selectively to glucose - is another tactic to address this low glucose selectivity.[31] A patent application on glucose-sensitive hydrazone reactions was recently published by Jensen *et al* (Glucose-sensitive peptide hormones, WO2018115462A1). They noticed that the hydrazone dissociation characteristic was glucose dependent. For GRI designs, these hydrazone linkers might be linked onto insulin molecules.

Newer devices in the diabetes therapy area

According to a recent industry report by Transparency Market Research (TMR), there are different companies worldwide manufacturing global digital therapy devices, and there is fierce competition between them. This market of digital therapy devices is growing daily, as more and more people use technology to treat their medical conditions. The availability of knowledgeable consumers who are aware that technologically cutting-edge items are available to cure a medical condition, as well as greater disposable income that enables them to choose these products, promote the market for digital therapeutic devices. As more medical device companies enter this market with their technological prowess, the competitive environment is likely to intensify. By the end of 2025, the digital therapy device market is expected to generate $2,082.3 million in revenue.

A collaboration between Danish pharmaceutical giant Novo Nordisk and a Taiwanese chronic disease company Health2Sync will enable patients receiving insulin therapy to wirelessly transmit dose logs to a mobile health app. Field comms can now synchronize patient dose logs, including the time and dose of each injection. Because of this connectivity, patients can view their insulin data on the patient management platform, while doctors can view their insulin readings and analysis along with other health data on the Health2Sync app. The Alliance is also launching a patient support initiative that will develop age-appropriate, customized educational materials for T1DM patients. These materials include information about their condition, how to use insulin, what to look out for with the changing seasons, how to manage adverse health conditions, and stories from other T1DM patients.[46]

By the mid-2000s, technology had progressed to continuous glucose monitor-driven predictive insulin suspension that reduced severe hypoglycemic episodes by 83%. The year 2016 saw the launch of the hybrid closed-loop algorithm (MiniMedTM 670G) for automated basal insulin administration. The 670G study improved time in range (70–180 mg/dL) and decreased time under range (70 and 50 mg/dL) in a clinical trial. The MiniMedTM 780G*, an advanced hybrid closed-loop system, provided even better glycemic control and minimized post-meal hyperglycemia brought on by missing, delayed, or underestimated meal boluses by providing a lower glucose goal and autocorrection boluses administered every five minutes.

The FDA has approved DreaMed Advisor Pro, an artificial intelligence (AI)-based diabetes treatment decision support tool that is intended to help medical professionals manage persons with T1DM who use insulin pumps and continuous glucose monitoring (CGM). DreaMed Advisor Pro, a cloud-based digital tool, analyzes data from an insulin pump, a CGM, and blood glucose self-monitoring to offer suggestions for administering insulin. The system, according to DreaMed, employs event-driven learning to better understand each individual before recommending adjustments to the patient's basal rate, carbohydrate ratio, and insulin pump correction factor. The FDA's decision supports what we consider to be an important step in forging a deeper bond between healthcare professionals and their T1DM patients. The *de novo* request for the DreaMed Advisor Pro is the most recent illustration of how AI is reshaping the diabetes sector. The FDA has granted a start-up company Beta Bionics an Experimental Device Exemption (EDE), enabling Beta Bionics to enroll patients in home trials of the iLet Bionic Pancreas System in its insulin-only configuration. The business uses AI and glucose monitoring to design the system.[46]

The US FDA produced Insulia, a thoroughly proven digital therapeutic solution that has CE approval for numerous international markets. Diabetes patients may self-manage their condition with Insulia, and healthcare companies can remotely monitor changes. Insulia is the first regulatory-approved digital therapeutic to offer automatic titration for all types of basal insulins.[47]

Future perspectives

Due to the expanding variety of insulin therapy options, diabetes

care is transitioning from a one-size-fits-all approach to customized treatment regimens suited to the patient's needs. Proper dose titration is essential to achieve glycemic goals. In practice, doctors and people with diabetes often disregard recommendations for optimal titration because they find them very stressful. If fasting blood glucose is the determining factor, a digital therapeutic platform for diabetes management could develop an immediate feedback system that encourages patients to follow their treatment recommendations. An observational study illustrates the potential use of a digital diabetes management platform for the self-management needed by insulin-treated users, including their daily use and maintaining behavioural changes.[48]

Digital health-aided treatments have the potential to be a cost-effective, scalable, and effective for treating T2DM patients in underserved groups. Telemedicine education programs for diabetes in primary care are reasonably priced in the short term, while additional long-term research is required. The majority of behavioural or community health treatments for T2DM need a sizable commitment from participants as well as staff in terms of time, money, and effort. As a result, these methods only succeeded in reaching 1% of their intended viewers. Finding ways to integrate real-time participant feedback, device-free remote participant monitoring, and coaching via the phone and SMS can not only address some of these difficulties but also raise participant engagement and self-efficacy. Additionally, personalization can help treat diabetes by removing some obstacles. Motivational interviewing and health coaching are used to assist patients in creating SMART goals–specific, measurable, achievable, relevant, and time-based—that are catered to the patients' particular requirements and circumstances. It should be noted, though, that studies on diabetes health coaching have yielded different levels of positive clinical effects.[49]

Demand for telemedicine and home care is growing rapidly around the world, and several healthcare systems are now offering reimbursements to individuals who qualify for such services. Voluntis is developing digital medicines that enable people with chronic illnesses to take control of their daily care to improve outcomes. Voluntis solutions combines mobile and online apps to give the patient and care team personalized advice, such as changing medication dosage, controlling side effects, or monitoring symptoms. These instant suggestions are based on digitized clinical algorithms. Using its Theraxium technology platform, Voluntis has developed and managed a range of digital therapies, particularly in the areas of oncology and diabetes.

AI will be essential to accomplish the ultimate dual objectives of near-normal glycemia and decreased burden. It is important to control diabetes mentally, and this cannot be stressed enough. Patients who are constantly faced with choices may get overwhelmed, abandoning even the greatest technologies. Multiple dosing decisions must be made by meals, exercise, and other activities under the current methods. By encouraging pharmaco-adherence and offering individualized care, incorporating AI through a frequently updated "digital twin" could mitigated daily obstacles to self-care. Machine learning can interact with the digital twin using physiologic and/or activity sensors built into smartphones or wearables to give individualized therapy that improves glycaemia while reducing load. For instance, geolocation on a smartphone can give the proper insulin dose before the meal and forecast the contents of an upcoming meal based on historical behavior. The amount of food consumed, as well as the start and end of the meal, can be determined using hand gesture sensing.

Fitness trackers can measure the duration, intensity, and glycemic response of exercise so that insulin supply can be modified as necessary. By maximizing glycaemic control through individualized medication, iteratively updating algorithms put us on the verge of creating a real artificial pancreas.

Conclusions

This review highlights the various types of insulin and recent development in insulin therapy. Additionally, this review focuses on various difficulties and challenges faced by diabetes patients and tries to identify possible solutions for them. Due importance has been given to recent developments in the space of AI and machine learning in diabetes therapy and digital therapeutics. With fast technological development and research in diabetes space, reversal of diabetes, precision and integrative medicine could significantly benefit patient in the near future.

Acknowledgments

None.

Funding

No funding was received for this review article.

Conflict of interest

The authors declare no conflict of interest.

Author contributions

AB proposed the review aim. AB, HP, and AG collected and organized literature and data. AB and HP drafted the manuscript. HP and AG advised on the structure and the content of the manuscript. AB and HP revised the manuscript. All authors have read the manuscript and approved the final manuscript.

References

[1] NCD Risk Factor Collaboration (NCD-RisC). Worldwide trends in diabetes since 1980: a pooled analysis of 751 population-based studies with 4.4 million participants. Lancet 2016;387(10027):1513–1530. doi:10.1016/S0140-6736(16)00618-8, PMID:27061677.

[2] Saeedi P, Petersohn I, Salpea P, Malanda B, Karuranga S, Unwin N, *et al*. Global and regional diabetes prevalence estimates for 2019 and projections for 2030 and 2045: Results from the International Diabetes Federation Diabetes Atlas, 9th ed. Diabetes Res Clin Pract 2019;157:107843. doi:10.1016/j.diabres.2019.107843, PMID:31518657.

[3] Pradeepa R, Mohan V. Epidemiology of type 2 diabetes in India. Indian J Ophthalmol 2021;69(11):2932–2938. doi:10.4103/ijo.IJO_1627_21, PMID:34708726.

[4] Vecchio I, Tornali C, Bragazzi NL, Martini M. The Discovery of Insulin: An Important Milestone in the History of Medicine. Front Endocrinol (Lausanne) 2018;9:613. doi:10.3389/fendo.2018.00613, PMID:30405529.

[5] Bekiari E, Kitsios K, Thabit H, Tauschmann M, Athanasiadou E, Karagiannis T, *et al*. Artificial pancreas treatment for outpatients with type 1 diabetes: systematic review and meta-analysis. BMJ 2018;361:k1310. doi:10.1136/bmj.k1310, PMID:29669716.

[6] Blevins T, Zhang Q, Frias JP, *et al*. Ultra Rapid Lispro improves postprandial glucose control vs. humalog (lispro) in patients with type 2 diabetes: PRONTO-T2D. American Diabetes Associations 79th Scientific Sessions; June 7–11, 2019; San Francisco, CA.

[7] Bode BW, Cao D, Liu R, Hardy T, Bue-Valleskey JM. Ultra Rapid Lispro

improves postprandial glucose control and time in range in T1D compared with Humalog (lispro): PRONTO-T1D continuous glucose monitoring (CGM) Substudy. Diabetes 2019;68(Supplement_1):1089–P. doi:10.2337/db19-1089-P.
[8] Leohr J, Dellva MA, Coutant DE, Labell ES, Reddy S, Heise T, *et al*. Ultra Rapid Lispro accelerates insulin lispro absorption and insulin action vs. Humalog (lispro) in patients with T2D. Diabetes 2019;68 (S1):1100–P. doi:10.2337/db19-1100-P.
[9] Linnebjerg H, Zhang Q, Labell ES, Reddy S, Coutant DE, Hoevelmann U, *et al*. Ultra Rapid Lispro accelerates insulin lispro absorption and insulin action vs. Humalog (lispro) in patients with T1D. Diabetes 2019; 68(S1):1107–P. doi:10.2337/db19-1107-P.
[10] Heise T, Linnebjerg H, Cao D, Coutant DE, Labell ES, Reddy S, *et al*. Ultra Rapid Lispro lowers postprandial glucose and more closely matches normal physiological glucose response compared with other rapid insulin analogs. Canadian Journal of Diabetes 2019;43(7):S36). doi:10.1016/j.jcjd.2019.07.105.
[11] Bhattacharyya A, Bhattacharya I, Deshmukh V, Mohan V, Spaepen E. Efficacy and Safety of Ultra-Rapid Lispro Versus Lispro in Patients with Type 1 and 2 Diabetes: Indian Subpopulation Analyses of the PRONTO-T1D and PRONTO-T2D Trials. Indian J Endocrinol Metab 2022; 26(2):186–188. doi:10.4103/ijem.ijem_459_21, PMID:35873944.
[12] Andersen G, Meiffren G, Lamers D, DeVries JH, Ranson A, Seroussi C, *et al*. Ultra-rapid BioChaperone Lispro improves postprandial blood glucose excursions vs insulin lispro in a 14-day crossover treatment study in people with type 1 diabetes. Diabetes Obes Metab 2018;20(11):2627–2632. doi:10.1111/dom.13442, PMID:29923294.
[13] Meiffren G, Herbrand T, Anastassiadis E, Klein O, DeVries JH, Heise T, *et al*. Better glycaemic control with BioChaperone glargine lispro co-formulation than with insulin lispro Mix25 or separate glargine and lispro administrations after a test meal in people with type 2 diabetes. Diabetes Obes Metab 2019;21(7):1570–1575. doi:10.1111/dom.13685, PMID:30828929.
[14] Handeslman Y. Concentrated Rapid-Acting Insulin Preparations. Endocrine Practice 2017;23(S1):18–23. doi:10.1016/S1530-891X(20)43536-0.
[15] Pieber TR, Howell SJ, Jezek J, Gerring DJ. Pharmacokinetic and pharmacodynamic properties of a novel "superfast" insulin aspart formulation. Diabetes 2018;67(S1):95–LB. doi:10.2337/db18-95-LB.
[16] Hompesch M, Lawrence FJ, Jezek J, Gerring DJ, Pieber T. 805-P: Double-Blind Crossover Study of Ultra-Rapid AT247 Compared with NovoLog and Fiasp during Continuous Subcutaneous Infusion (CSII) Assessed by a Hyperinsulinemic Euglycemic Clamp. Diabetes 2023;;72(Supplement_1):805P. doi:10.2337/db23-805-P.
[17] Svehlikova E, Mursic I, Augustin T, Magnes C, Gerring D, Jezek J, *et al*. Pharmacokinetics and Pharmacodynamics of Three Different Formulations of Insulin Aspart: A Randomized, Double-Blind, Crossover Study in Men with Type 1 Diabetes. Diabetes Care 2021;44(2):448–455. doi:10.2337/dc20-1017, PMID:33328285.
[18] White J, Goldman J. Biosimilar and Follow-on Insulin: The Ins, Outs, and Interchangeability. J Pharm Technol 2019;35(1):25–35. doi:10.1177/8755122518802268, PMID:34861004.
[19] Zhang RM, Puri R, McGill JB. Update on Biosimilar Insulins: A US Perspective. BioDrugs 2020;34(4):505–512. doi:10.1007/s40259-020-00431-0, PMID:32681425.
[20] European Commission. Annex I: Summary of Product Characteristics. Available from: https://ec.europa.eu/health/documents/community-register/2021/20210205150468/anx_150468_en.pdf. Accessed July 4, 2022.
[21] Weise M, Bielsky MC, De Smet K, Ehmann F, Ekman N, Narayanan G, *et al*. Biosimilars-why terminology matters. Nat Biotechnol 2011;29(8):690–693. doi:10.1038/nbt.1936, PMID:21822237.
[22] Matli MC, Wilson AB, Rappsilber LM, Sheffield FP, Farlow ML, Johnson JL. The First Interchangeable Biosimilar Insulin: Insulin Glargine-yfgn. J Diabetes Sci Technol 2023;Mar17(2):490–494. doi: 10.1177/19322968211067511.
[23] Joshi SR, Mittra S, Raj P, Suvarna VR, Athalye SN. Biosimilars and interchangeable biosimilars: facts every prescriber, payor, and patient should know. Insulins perspective. Expert Opin Biol Ther 2022;doi:10.1080/14712598.2022.2112664, PMID:35993301.
[24] US Food and Drug Administration (FDA). Highlights of Prescribing Information to Use Rezvoglar Safely and Effectively. Available from: https://www.accessdata.fda.gov/drugsatfda_docs/label/2021/761215s000lbl.pdf. Accessed July 4 2022.
[25] Puppalwar G, Sawant S, Silgiri B, Shukla K, Barkate H. Evaluation of Safety and Efficacy of Glaritus® versus Lantus® in Combination with Insulin Lispro among Adults with Type 1 Diabetes Mellitus-Phase IV Study. Open J Endocr Metab Dis 2017;7:111–125. doi:10.4236/ojemd.2017.74011.
[26] Bhatia A, Tawade S, Mastim M, Kitabi EN, Gopalakrishnan M, Shah M, *et al*. Comparative evaluation of pharmacokinetics and pharmacodynamics of insulin glargine (Glaritus®) and Lantus® in healthy subjects: a double-blind, randomized clamp study. ActaDiabetol 2018;55:461–468. doi:10.1007/s00592-018-1113-3, PMID:29453671.
[27] Janež A, Guja C, Mitrakou A, Lalic N, Tankova T, Czupryniak L, *et al*. Insulin Therapy in Adults with Type 1 Diabetes Mellitus: a Narrative Review. Diabetes Ther 2020;11(2):387–409. doi:10.1007/s13300-019-00743-7, PMID:31902063.
[28] James TD, Sandanayake KRAS, Shinkai S. A glucose-selective molecular fluorescence sensor. Angew Chem Int Edit 1994;33(21):2207–2209. doi:10.1002/anie.199422071.
[29] Yang W, He H, Drueckhammer DG. Computer-Guided Design in Molecular Recognition: Design and Synthesis of a Glucopyranose Receptor This work was supported by the National Institutes of Health (grant DK5523402). Angew Chem Int Ed Engl 2001;40(9):1714–1718. PMID:11353489.
[30] Ke C, Destecroix H, Crump MP, Davis AP. A simple and accessible synthetic lectin for glucose recognition and sensing. Nat Chem 2012;4(9):718–723. doi:10.1038/nchem.1409, PMID:22914192.
[31] Kaarsholm NC, Lin S, Yan L, Kelly T, van Heek M, Mu J, *et al*. Engineering Glucose Responsiveness Into Insulin. Diabetes 2018;67(2):299–308. doi:10.2337/db17-0577, PMID:29097375.
[32] Ahmad K. Insulin sources and types: a review of insulin in terms of its mode on diabetes mellitus. J Tradit Chin Med 2014;34(2):234–237. doi:10.1016/s0254-6272(14)60084-4, PMID:24783939.
[33] Howey DC, Bowsher RR, Brunelle RL, Woodworth JR. [Lys(B28), Pro(B29)]-human insulin. A rapidly absorbed analogue of human insulin. Diabetes 1994;43(3):396–402. doi:10.2337/diab.43.3.396, PMID: 8314011.
[34] Mudaliar SR, Lindberg FA, Joyce M, Beerdsen P, Strange P, Lin A, *et al*. Insulin aspart (B28 asp-insulin): a fast-acting analog of human insulin: absorption kinetics and action profile compared with regular human insulin in healthy nondiabetic subjects. Diabetes Care 1999;22(9):1501–1506. doi:10.2337/diacare.22.9.1501, PMID:10480516.
[35] Hirsch IB, Juneja R, Beals JM, Antalis CJ, Wright EE. The Evolution of Insulin and How it Informs Therapy and Treatment Choices. Endocr Rev 2020;41(5):733–755. doi:10.1210/endrev/bnaa015, PMID: 32396624.
[36] Brunelle BL, Llewelyn J, Anderson JH Jr, Gale EA, Koivisto VA. Meta-analysis of the effect of insulin lispro on severe hypoglycemia in patients with type 1 diabetes. Diabetes Care 1998;21(10):1726–1731. doi:10.2337/diacare.21.10.1726, PMID:9773738.
[37] Fullerton B, Siebenhofer A, Jeitler K, Horvath K, Semlitsch T, Berghold A, *et al*. Short-acting insulin analogues versus regular human insulin for adult, non-pregnant persons with type 2 diabetes mellitus. Cochrane Database Syst Rev 2018;12(12):CD013228. doi:10.1002/14651858.CD013228, PMID:30556900.
[38] Blevins TC, Raiter Y, Sun B, Donnelly C, Shapiro R, Chullikana A, *et al*. Immunogenicity, Efficacy, and Safety of Biosimilar Insulin Aspart (MYL-1601D) Compared with Originator Insulin Aspart (Novolog(®)) in Patients with Type 1 Diabetes After 24 Weeks: A Randomized Open-Label Study. BioDrugs 2022;36(6):761–772. doi:10.1007/s40259-022-00554-6, PMID:36114990.
[39] Lindauer K, Becker R. Insulin depot absorption modeling and pharmacokinetic simulation with insulin glargine 300 U/mL. Int J Clin Pharmacol Ther 2019;57(1):1–10. doi:10.5414/CP203269, PMID:30369394.
[40] AlRuthia Y, Bahari OH, Alghnam S, Alrumaih AM, Asiri H, Alshammari M, *et al*. Real-World Impact of Switching From Insulin Glargine (Lantus(®)) to Basaglar(®) and Potential Cost Saving in a Large Public Healthcare System in Saudi Arabia. Front Public Health 2022;10:852721. doi:10.3389/fpubh.2022.852721, PMID:35769787.

[41] Rege NK, Phillips NFB, Weiss MA. Development of glucose-responsive 'smart' insulin systems. Curr Opin Endocrinol Diabetes Obes 2017;24(4):267–278. doi:10.1097/MED.0000000000000345, PMID:28509691.
[42] Zion TC, Zarur A, Ying JY. Massachusetts Institute of Technology, assignee. Stimuli-responsive systems for controlled drug delivery. US Patent US7531191B2. May 12, 2009.
[43] Matsumoto A, Ishii T, Nishida J, Matsumoto H, Kataoka K, Miyahara Y. A synthetic approach toward a self-regulated insulin delivery system. Angew Chem Int Ed Engl 2012;51(9):2124–2128. doi:10.1002/anie.201106252, PMID:22162189.
[44] Mayer JP, Zhang F, DiMarchi RD. Insulin structure and function. Biopolymers 2007;88(5):687–713. doi:10.1002/bip.20734, PMID:17410596.
[45] Krug AW, Visser SAG, Tsai K, Kandala B, Fancourt C, Thornton B, *et al*. Clinical Evaluation of MK-2640: An Insulin Analog With Glucose-Responsive Properties. Clin Pharmacol Ther 2019;105(2):417–425. doi:10.1002/cpt.1215, PMID:30125349.
[46] Polonsky WH, Arsenault J, Fisher L, Kushner P, Miller EM, Pearson TL, *et al*. Initiating insulin: How to help people with type 2 diabetes start and continue insulin successfully. Int J Clin Pract 2017;71(8):e12973. doi:10.1111/ijcp.12973, PMID:28735508.
[47] Dang A, Arora D, Rane P. Role of digital therapeutics and the changing future of healthcare. J Family Med Prim Care 2020;9(5):2207–2213. doi:10.4103/jfmpc.jfmpc_105_20, PMID:32754475.
[48] Azelton KR, Crowley AP, Vence N, Underwood K, Morris G, Kelly J, *et al*. Digital Health Coaching for Type 2 Diabetes: Randomized Controlled Trial of Healthy at Home. Front Digit Health 2021;3:764735. doi:10.3389/fdgth.2021.764735, PMID:34901926.
[49] Simmons LA, Wolever RQ. Integrative Health Coaching and Motivational interviewing: Synergistic Approaches to Behavior Change in Healthcare. Glob Adv Health Med 2013;2(4):28–35. doi:10.7453/gahmj.2013.037, PMID:24416683.

Published by Xia & He Publishing Inc.
14090 Southwest Freeway, Suite 300, Sugar Land, Texas, 77478, USA
Telephone: +1-409-420-2868
E-mail: service@xiahepublishing.com
Website: www.xiahepublishing.com